



University of Benghazi,  
Faculty of Science, Department of Earth Sciences,  
Benghazi - Libya

**Lithofacies Identification and Reservoir Quality Variation of  
the Lower Acacus Formation, Concession NC100, Ghadames  
Basin, NW Libya.**

A thesis is submitted to the Department of Earth Sciences as  
partial fulfillment of the requirements for the degree of master of  
sciences (M.Sc) in geology.

Submitted by  
NAJM EDEEN IDREES ELRAHEL

Supervised by  
Dr. OMAR B. ELFIGIH

Academic year. 2016-2017

Copyright © 2018.All rights reserved , no part of this thesis may be reproduced in any form, electronic or mechanical, including photocopy , recording scanning , or any information , without the permission in writhing from the author or the Directorate of Graduate Studies and Training university of Benghazi .

حقوق الطبع 2018 محفوظة ، لا يسمح اخذ اى معلومة من اى جزء من هذه الرسالة على هيئة نسخة الكترونية او ميكانيكية بطريقة التصوير او التسجيل او المسح من دون الحصول على اذن كتابي من المؤلف أو إدارة الدراسات العليا والتدريب جامعة بنغازي

## ABSTRACT

By viewing and describing the available 215ft of cores cut in Lower Acacus Formation from five wells in the study area (concession NC100), Ghadames Basin, NW Libya, the Lower Acacus Formation is divided into five lithofacies types including; 1) Bioturbated marine silty shale lithofacies, 2) Reworked marine sandstone lithofacies, 3) Distal delta front silty sandstone lithofacies, 4) Proximal delta front – coastal sandstone lithofacies, 5) Fluvial channel sandstone lithofacies. Furthermore, on the basis of GR-log motifs these identified lithofacies were grouped into four major categories, which are: 1) 1<sup>st</sup> category represented by bell shape GR-log motif corresponds with the fluvial channel lithofacies, 2) 2<sup>nd</sup> category of funnel shape GR-log motif corresponds with the gradational sequence of the shaly siltstone of distal delta front at the base to proximal delta front-coastal lithofacies at the top, 3) 3<sup>rd</sup> category of spiky shale GR-log motif corresponds to reworked marine sandstone lithofacies and 4) 4<sup>th</sup> category of thinly serrated to smooth “featureless” GR-log motif corresponds to bioturbated marine shale lithofacies. Suits of wireline logs were used to construct stratigraphic cross sections to reveal the paleogeography of the study area “concession NC100” and to examine the lateral relationships between sandstone units or lithofacies packages identified in cores.

The petrographic analysis of 18 thin sections obtained from selected sandstones units of Lower Acacus Formation from five wells, allowed the identification of primary composition and diagenetic constituents of the Lower Acacus Formation in concession NC100. The original detrital compositions included sublitharenites with quartzarenites and rarely litharenites. The main diagenetic processes observed were: compaction of framework grains, silica cement by pressure solution and precipitation of quartz overgrowths, feldspar grains dissolution, calcite/dolomite cementation, partial and total dissolution of labile grains and calcite/dolomite cements during progressive burial, and the development of secondary porosity which partially or totally filled by clay matrix.

Cross plots of core plug porosity ( $\phi_c$ ) versus permeability (k) for the identified lithofacies of Lower Acacus Formation have showed that the plotted samples have negative relationship and are relatively heterogeneous, since sample points deviated and can be extremely tenuous due to large scatter in the data between lithofacies. However, linear relationship and positive correlation have been found to exist between core plug porosity ( $\phi_c$ ) and permeability (k) of the same lithofacies which have similar rock properties. Other good linear positive relationships between thin section macro porosity ( $\phi_{T.S}$ ) and

permeability (k), and between core plug total porosity ( $\phi_c$ ) versus thin section macro porosity ( $\phi_{T.S}$ ) has been established for the various studied lithofacies points.

The identified lithofacies of the Lower Acacus Formation in concession NC100 were also defined and grouped into three quality assessment grades: average, reduced, low and very low reservoir quality. The good quality was assessed as average reservoir quality and characterized by average core plug total porosity of 18% and permeability of 204md, associated with the proximal delta front-coastal sandstone lithofacies, the reduced quality shows average of core plug total porosity of 14% and of average permeability 12md, associated with the reworked marine sandstone lithofacies, whereas the low quality shows average of core plug total porosity of 7% and of average permeability 2md, associated with the fluvial channel sandstone lithofacies, and very low-quality by reduced presents average core plug total porosity of 12% and of average permeability 0.025md characterizing distal delta front silty sandstone. Overall, the obtained assessed results of reservoir quality indicate some possible physical and diagenetic processes associated with lithofacies types and reservoir sandstones and could effect hydrocarbons accommodation in the studied structures in concession NC100.

Integration of all geological exploration components including depositional structures, stratigraphic maps, lithofacies patterns, sandstone textures, primary composition, diagenetic processes and products, and pore types, help to generate some basic steps (1-8) to be used for the establishment of better understanding of the future exploration strategy in concession NC100.

## **ACKNOWLEDGEMENTS**

I would like to express my sincere thanks and appreciation to my supervisor, Dr. Omar B. Elfigih, Earth Sciences Department, Benghazi University for his continuous guidance, encouragement, wisdom, constructive criticism, and insight motivated me to earn my degree. He was helpful, supportive, patient, and available at all times.

I am grateful to AGOCO management for their generous help for providing me with unlimited access to the core storage facility, Technical Data Library (TDL), and their continuous support throughout this study.

To all who helped me, in whatever capacity in preparing this thesis, I express my sincere thanks and appreciation.

This thesis is dedicated to my father (IDREES), and my son (MOHAMED) whose unsurpassable encouragement, patient and moral support made all this possible.

## CONTENTES

<b>ABSTRACT</b> .....	i
<b>ACKNOWLEDGEMENTS</b> .....	iii
<b>LIST OF FIGURES</b> .....	vi
<b>LIST OF TABELS</b> .....	xiv
<b>1. INTRODUCTION</b> .....	1
<b>1.1 Research Problems</b> .....	4
1.2 Objectives.....	5
1.3 Scope of the study.....	5
<b>2. REGIONAL GEOLOGY OF GHADAMES BASIN</b> .....	6
2.1 Tectonic and structures.....	6
2.2 Stratigraphy.....	12
<b>3. MATERIALS AND METHODS</b> .....	19
<b>4. LITHOFACIES TYPES OF LOWER ACACUS FORMATION</b> .....	32
4.1 Core descriptions.....	32
4.2 Wireline-log characterization.....	57
<b>5. TRENDS OF DEPOSITIONAL SYSTEM OF THE LOWER ACACUS FORMATION IN CONCESSION NC100</b> .....	59
5.1 Cross section construction.....	59
5.2 Geological maps.....	64
1- Structural maps.....	64
2 - Isopach maps.....	69
3- Lithofacies maps.....	78
<b>6. PETROGRAPHY</b> .....	84
A) – Rock texture.....	85
B) – Detrital composition.....	85
C) – Cement types and matrix.....	95
D) – Digenetic constitutes.....	103
E) – Pore types.....	104
<b>7. RESERVOIR CHARACTERIZATION</b> .....	105
1- Diagenetic impact on reservoir properties.....	105
2- Reservoir quality variation.....	107

3- Assessment of the reservoir quality of Lower Acacus Formation.....	112
<b>8. EXPLORATION STRATEGY OF LOWER ACACUS FORMATION IN CONCESSION NC100.....</b>	<b>116</b>
<b>9. CONCLUSIONS.....</b>	<b>121</b>
<b>REFERENCES.....</b>	<b>123</b>
<b>ENCLOSURES (1 and 2)</b>	

## LIST OF FIGURES

Figure 1. Location Map showing Concession NC100, NW part of Ghadames Basin.....	2
Figure 2. Location map of the study area (concession NC100), showing drilled wells in Concession NC100, Ghadames Basin NW Libya.....	3
Figure 3. Main structural elements of Ghadames basin and location of concession NC100.....	6
Figure 4. Post Pan-African (Caledonian NW-SE) structural trends in Libya.....	8
Figure 5. Hercynian structural trends, in Libya.....	9
Figure 6. N-S Structural cross-section illustrates configuration of the Palaeozoic succession in Ghadames Basin, and the effect of the Hercynian unconformity.....	10
Figure 7. NNW-SSE Structural Section, Ghadames Basin, NW Libya.....	11
Figure 8. Generalized stratigraphic type section of Ghadames Basin, NW Libya.....	13
Figure 9. Sketch showing the progradation and variation in sand/shale of the Silurian and Devonian sequences in SE-NW trend.....	15
Figure 10. Total thickness map of the Lower Acacus Formation, Concession NC100, Ghadames Basin, NW Libya.....	16
Figure 11. Sand content (percentage) of Lower Acacus Formation.....	17
Figure 12. Base map of Concession NC100, showing wells distribution, and lines of stratigraphic cross-section (A-A', B-B') used in this study. Ghadames Basin NW Libya .....	20
Figure 13. Core description sheet used for describing core samples.....	30
Figure 14. Petrographic description sheet used for model analysis of thin sections in the study area, concession NC100.....	31
Figure 15. Showing wells location, cored intervals, and GR-log motifs of the identified lithofacies of Lower Acacus Formation, Concession NC100, Ghadames Basin NW Libya.....	34



Figure 16. Graphic log of core samples cut in the bioturbation marine silty shale and reworked marine sandstone lithofacies of Lower Acacus Formation in well C2-NC100, core # (2), concession NC100, Ghadames Basin, NW Libya.....35

Figure 17. Cores samples (core #2), cut in Lower Acacus Formation, well C2-NC100, concession NC100, Ghadames Basin, NW Libya.....36

Figure 18. Core samples showing: (a) - Bioturbated marine silty shale lithofacies @ 9431.5ft, (b)- Reworked marine sandstone lithofacies @9418.2ft, well C2-NC100, Lower Acacus Formation, core (2), concession NC100, Ghadames Basin.....38

Figure 19. Graphic log of core samples cut in the bioturbated marine silty shale, distal delta front silty sandstone, and proximal delta front and costal sandstone lithofacies of Lower Acacus Formation in well Q1-NC100, core #1, concession NC100, Ghadames Basin, NW Libya.....40

Figure 20. Core samples, (core #1), cut in Lower Acacus Formation, well Q1-NC100, concession NC100, Ghadames Basin, NW Libya.....41

Figure 21. Core samples showing: (a)- Alternating siltstone and shale, @10481.5ft. (b)- Distal delta front silty sandstone lithofacies @10469.4ft, (c)- Proximal delta front lithofacies @ 10469.8ft, .....42

Figure 22. Graphic log of core samples cut in the bioturbated marine silty shale, distal delta front silty sandstone, and proximal delta front and coastal sandstone, and reworked marine sandstone lithofacies of Lower Acacus Formation in well Q1-NC100, concession NC100, Ghadames Basin, NW Libya.....43

Figure 23. Core samples, core #3, cut in Lower Acacus Formation, well Q1-NC100, concession NC100, Ghadames Basin, NW Libya.....44

Figure 24. Core samples showing: (a)–Distal delta front silty sandstone lithofacies @10598.3ft, (b)- Proximal delta front-coastal sandstone lithofacies @10569.8ft, (c)- Proximal delta front-coastal silty sandstone lithofacies @10565.8ft.....46

Figure 25. Graphic log of core samples cut in the proximal delta front-coastal sandstone and reworked marine sandstone lithofacies of Lower Acacus Formation in well L3-NC100, core #2 and 3, concession NC100, Ghadames Basin, NW Libya.....47

Figure 26. Core samples, core #2, cut in Lower Acacus Formation, well L3-NC100, concession NC100, Ghadames Basin, NW Libya.....48

Figure 27. Core samples showing: (a)- proximal delta front and coastal sandstone lithofacies @ 9334ft, well L3-NC100, Lower Acacus Formation, core #2.....49

Figure 28. Graphic log of core samples, core #1, cut in the fluvial channel sandstone lithofacies of Lower Acacus Formation in well Z1-NC100, concession NC100, Ghadames Basin, NW Libya.....51

Figure 29. Partially recovered core samples, core #1, from the fluvial channel sandstone lithofacies of the Lower Acacus Formation in well Z1-NC100, concession NC100, Ghadames Basin, NW Libya.....52

Figure 30. Core samples of fluvial channel sandstone lithofacies, well Z1-NC100, Lower Acacus Formation, core #1, concession NC100, Ghadames Basin, NW Libya .....53

Figure 31. Graphic log of core samples core #3, cut in the fluvial channel sandstone lithofacies of Lower Acacus Formation in well Z3-NC100, concession NC100, Ghadames Basin, NW Libya.....54

Figure 32. Core samples, core #3, cut in Lower Acacus Formation, well Z3-NC100, concession NC100, Ghadames Basin, NW Libya.....55

Figure 33. GR-log motifs for the identified lithofacies in some studied wells drilled in the Lower Acacus Formation, concession NC100, Ghadames Basin, NW Libya.....58

Figure 34. L3-NC100 type well, showing signature of well log (GR, SP, R), depositional cycles(sequences), and regional time stratigraphic markers (TS, and MFS), concession NC100, Ghadames basin, NW Libya.....61

Figure 35. South – North (A-A’) stratigraphic cross section of Lower Acacus Formation, concession NC-100, NW of Ghadames Basin, NW Libya.....62

Figure 36. East – West (B-B’) stratigraphic cross section of Lower Acacus Formation, crossing concession NC-100 and neighbor area (A1-NC118 area), Ghadames Basin, NW Libya.....	63
Figure 37. Time structural map on top of the Memouniat Formation, concession NC100, Ghadames Basin, NW Libya.....	66
Figure 38. Structural contour map on top of the Tanezzuft Formation, concession NC100, Ghadames Basin, NW Libya.....	67
Figure 39. Structural contour map on top of the Lower Acacus Formation, concession NC100, Ghadames Basin, NW Libya.....	68
Figure 40. Total isopach map of the Lower Acacus Formation, concession NC100, Ghadames Basin, NW Libya.....	70
Figure 41. Isopach map of unit Lf2 of the Lower Acacus Formation, concession NC100, Ghadames Basin, NW Libya.....	71
Figure 42. Isopach map of unit A6 of the Lower Acacus Formation, concession NC100, Ghadames Basin, NW Libya.....	72
Figure 43. Isopach map of unit A7 of the Lower Acacus Formation, concession NC100, Ghadames Basin, NW Libya.....	73
Figure 44. Isopach map of unit A9 of the Lower Acacus Formation, concession NC100, Ghadames Basin, NW Libya.....	76
Figure 45. Isopach map of unit A11 of the Lower Acacus Formation, concession NC100, Ghadames Basin, NW Libya.....	77
Figure 46. Lithofacies map of Lf2 sandstone unit and its equivalent of the Lower Acacus Formation, concession NC100, Ghadames Basin, NW Libya.....	79
Figure 47. Lithofacies map of A6 sandstone unit and its equivalent of the Lower Acacus Formation, concession NC100, Ghadames Basin, NW Libya.....	80
Figure 48. Lithofacies map of A7 sandstone unit and its equivalent of the Lower Acacus Formation, concession NC100, Ghadames Basin, NW Libya.....	81

Figure 49. Lithofacies map of A9 sandstone unit and its equivalent of the Lower Acacus Formation, concession NC100, Ghadames Basin, NW Libya.....82

Figure 50. Lithofacies map of A11 sandstone unit and its equivalent of the Lower Acacus Formation, concession NC100, Ghadames Basin, NW Libya.....83

Figure 51a. Thin section photomicrograph of sublitharenite, fine-medium grained, sub angular to sub rounded, in fluvial channel lithofacies of Lower Acacus Formation, core #3 @11716.2ft, well Z1-NC100, concession NC100, Ghadames basin, NW Libya, (PPL).....86

Figure 51b. Thin section photomicrograph of sublitharenite, fine-medium grained, sub angular to sub rounded, in fluvial channel lithofacies of Lower Acacus Formation, core #3 @11716.2ft, well Z1-NC100, concession NC100, Ghadames basin, NW Libya, (XPL).....86

Figure 52. Thin section photomicrograph of Quartzarenite, in fluvial channel sandstone lithofacies, core #1 @ 11688.6ft, well Z1-NC-100, concession NC100, Ghadames basin, NW Libya .....87

Figure 53. Thin section photomicrograph of sublitharenite in proximal delta front-costal sandstone lithofacies of Lower Acacus Formation, core #3 @ 9312ft, well L3-NC-100, concession NC100, Ghadames basin, NW Libya.....88

Figure 54. Detrital plot of various sandstone lithofacies in the Lower Acacus Formation, Concession NC100, Ghadames Basin, NW Libya.....89

Figure 55. Summary histogram for each constituent identified in the sandstone lithofacies of Lower Acacus Formation concession NC100, Ghadames basin, NW Libya.....90

Figure 56a. Thin section photomicrograph of sublitharenite in fluvial sandstone lithofacies of Lower Acacus Formation, core #1, @ 11694.3ft well Z1-NC100, concession NC100, Ghadames basin, NW Libya, (PPL).....93

Figure 56b. Thin section photomicrograph of sublitharenite in fluvial sandstone lithofacies of Lower Acacus Formation, core #1, @ 11694.3ft well Z1-NC100, concession NC100, Ghadames basin, NW Libya (XPL).....93

Figure 57a. Thin section photomicrograph in fluvial channel sandstone lithofacies of Lower Acacus Formation, core #3, @ 11746.3ft, well Z3-NC100, concession NC100, Ghadames basin, NW Libya, (PPL).....	94
Figure 57b. Thin section photomicrograph in fluvial channel sandstone lithofacies of Lower Acacus Formation, core #3, @ 11746.3ft, well Z3-NC100, concession NC100, Ghadames basin, NW Libya, (XPL).....	94
Figure 58. Thin section photomicrograph of quartzarenite, in fluvial channel sandstone lithofacies, core #1, @ 11688.6ft well Z1-NC100, concession NC100, Ghadames basin, NW Libya .....	95
Figure 59a. Thin section photomicrograph delta front-coastal sandstone lithofacies (A4), core #3, @ 10587.3ft, well Q1-NC100, concession NC100, Ghadames basin, NW Libya, (PPL).....	97
Figure 60. Thin section photomicrograph in fluvial channel sandstone lithofacies of Lower Acacus Formation, core #3 @ 11730.3ft well Z3-NC100, concession NC100, Ghadames basin, NW Libya.....	98
Figure 61. Thin section photomicrograph in fluvial channel sandstone lithofacies of Lower Acacus Formation, core #3 @ 11716.2ft, well Z3-NC100, concession NC100, Ghadames basin, NW Libya.....	98
Figure 62. Thin section photomicrograph of delta front-coastal sandstone lithofacies, core #2, @ 9334.8ft, well L3-NC100, concession NC100, Ghadames basin, NW Libya.....	99
Figure 63. Thin section photomicrograph distal delta silty sandstone lithofacies, core #1, @ 10490.7ft, well Q1-NC100, concession NC100, Ghadames basin, NW Libya.....	100
Figure 64. Thin section photomicrograph of proximal delta front-coastal sandstone lithofacies, core #1, @ 10465.4ft, well Q1-NC100, concession NC100, Ghadames basin, NW Libya.....	101

Figure 65. Thin section photomicrograph of reworked marine sandstone lithofacies, core #2, @ 9412.2ft, well C2-NC100, concession NC100, Ghadames basin, NW Libya .....	101
Figure 66. Thin section photomicrograph of distal delta front silty sandstone lithofacies, core #1, @ 10491.4ft, well Q1-NC100, concession NC100, Ghadames basin, NW Libya.....	102
Figure 67. Thin section photomicrograph of reworked marine sandstone lithofacies, core #3, @ 10559.5ft, well Q1-NC100, concession NC100, Ghadames basin, NW Libya.....	102
Figure 68. Paragenetic sequence showing diagenetic events in the studied Lower Acacus sandstone in concession NC100.....	104
Figure 69. Core plug porosity versus permeability data of all studied lithofacies of Lower Acacus Formation, concession NC100, Ghadames Basin, NW Libya.....	110
Figure 70. Core plug porosity versus permeability data of all studied lithofacies of Lower Acacus Formation, showing linear relationship between porosity ( $\emptyset$ )-permeability (k) readings of the same lithofacies type, concession NC100, Ghadames Basin, NW Libya.....	110
Figure 71. Thin section (macro porosity) versus permeability data of all studied lithofacies of Lower Acacus Formation, concession NC100, Ghadames Basin, NW Libya.....	111
Figure 72. Core plug (total porosity) versus thin section (macro porosity) data of all studied lithofacies samples of Lower Acacus Formation, concession NC100, Ghadames Basin, NW Libya.....	112
Figure 73. Summary histogram of average total porosity and permeability readings from all lithofacies of Lower Acacus Formation, concession NC100, Ghadames basin, NW Libya.....	113
Figure 74. Composite lithofacies log map, showing discrete zones and distribution of GR-log patterns tied in to a lithofacies scheme of some selected sandstone units of Lower Acacus Formation, concession NC100, Ghadames Basin, NW Libya.....	115
Figure 75. Undrilled structures and drilled structures pools on the level of Lower Acacus Formation concession NC100, Ghadames Basin, NW Libya.....	117

Figure 76. A superimposed map achieved by overlapping the composite lithofacies map on the leads-hydrocarbon pools map of concession NC100, Ghadames Basin, NW Libya.....118

## LIST OF TABLES

Table 1. List of drilled wells and their status in the study area concession NC100 ,Ghadames Basin, NW Libya.....	21
Table 2. Digitized well-log formation tops (drilling depth, and subsurface depth) of the Tanezzuft, Lower Acacus and Middle Acacus Formations as picked from studied wells in concession NC100, Ghadames Basin, NW Libya.....	22
Table 3. Core intervals (depths) in the Lower Acacus Formation, concession NC100, Ghadames Basin, NW Libya.....	29
Table 4. The available cores cut in the Lower Acacus Formation in some drilled wells of concession NC100, Ghadames Basin.....	33
Table 5. Thickness variation of Lower Acacus Formation (Total and unit thickness) in studied wells of concession NC100, Ghadames Basin, NW Libya.....	65
Table 6. Average mineral framework composition, cement types, and thin section porosity, in percent, for the various sandstone units of the Lower Acacus Formation, concession NC100, Ghadames Basin, NW Libya.....	84
Table 7. Classification of hydrocarbon reservoir according to permeability and porosity.....	107
Table 8. Thin section macro porosity ( $\phi_{T.S}$ ) estimation and routine core plug total porosity ( $\phi_c$ ) and permeability (k) measurement for some selected units of Lower Acacus Formation, concession NC100, Ghadames Basin, NW Libya.....	108



## 1. INTRODUCTION

The interplay between facies change and stratigraphy architecture of Lower Acacus reservoir sandstones exerts an important influence on hydrocarbon distribution and production within the Ghadames Basin in general and concession NC100 in particular.

This study will be dealing with the subsurface facies identification and reservoir quality variation of upper Silurian, Lower Acacus Formation in Concession NC100 of Ghadames Basin, NW Libya (Fig. 1).

The concession NC100 is located in the NNW part of Ghadames Basin, some 250Km SW of Tripoli (Fig. 2). It is bounded by the latitudes 31°48' N to 30° 50' N and longitudes 10°20' E to 11°00' E, and covering an area of about 3250 km<sup>2</sup>. The Block lies on the northern truncated Palaeozoic flank of Ghadames Basin which is an interior sag basin filled with clastic dominated Palaeozoic and Mesozoic sediments (internal company report, AGOCO, 2008).

Three petroleum systems can be distinguished within the Basin: (i) Tanezzuft - Acacus system to the north; (ii) Tanezzuft - Tadrart system to the south; and (iii) Tanezzuft - Acacus/Tadrart system in the centre, with some leakage into overlying Devonian and Carboniferous sandstones locally and number of sub-systems, such as the long range migration of oil into the Triassic reservoir in the Ghadames area (Don Hallett, 2002).

The Acacus Formation, particularly the lower Acacus portion, has proved to contain prolific reservoirs, producing mainly oil in the northwestern part of the Libyan portion of the Ghadames Basin (Concessions NC100, NC2, NC1, 23 and 61), where Caledonian erosion is minor, net gross values are at its maximum and effective intraformational seals are highly developed in this part in Ghadames Basin, (K. Echikh, 1998).

The principal traps of this system are structural and consist of small-sizes anticlines of Hercynian age. These structures are rather limited in vertical closure, which implies that a relatively small amount of hydrocarbon reserves is usually found. (Francesco Bertello, Claudio, Walter 2003).

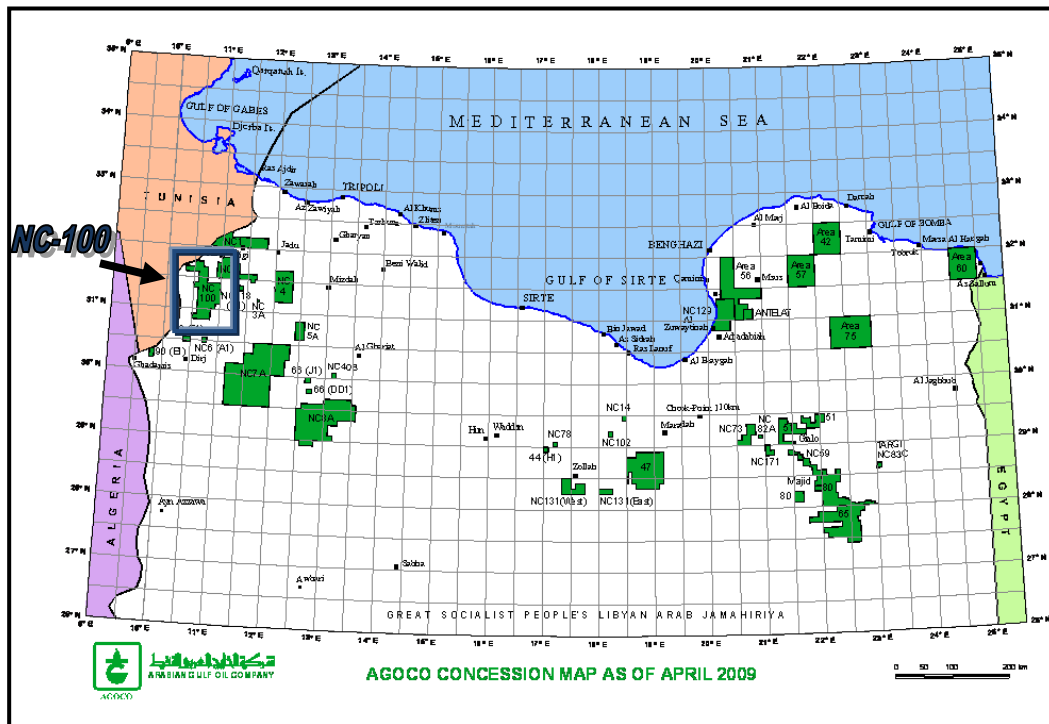


Figure 1. Location Map showing Concession NC100, NW part of Ghadames Basin. (AGOCO Concession map, 2009).

### Previous work.

The basic stratigraphic, sedimentologic and structural framework of Ghadames Basin have been well demonstrated through various studies Massa and collomb, 1960, dealing with the basic stratigraphic definitions in Libya; Klitzsch, 1971, studied the structural development of parts of north Africa since Cambrian times and in 1981, studied the Lower Paleozoic rocks of Libya, Egypt and Sudan; BEICIP, 1973, dealing with evaluation and geological study of the western part of Libya in Ghadames basin, Massa, 1980, Ballini and Massa 1980, they studied the stratigraphic contribution to the Palaeozoic of the southern basins of Libya, and Santa Maria, 1991; Elfigih, 1991; and Cridland, 1991, demonstrated the main studies dealing with geological exploration in Ghadames basin. Some of these studies have dealt with facies change, reservoir quality variation of some prolific horizons and investigated the possible hydrocarbon potentiality of the Ghadames Basin (Santa Maria; 1991, Echikh, 1996; Elfigih, 2000; Don Hallett, 2000; and Sikandaer, 2000).

In this study, an attempt should be taken to identify the possible facies distribution of the Lower Acacus Formation in concession NC100 (Fig. 2), along with the definition of the most effective reservoir sandstones and their quality variations through-out this concession.

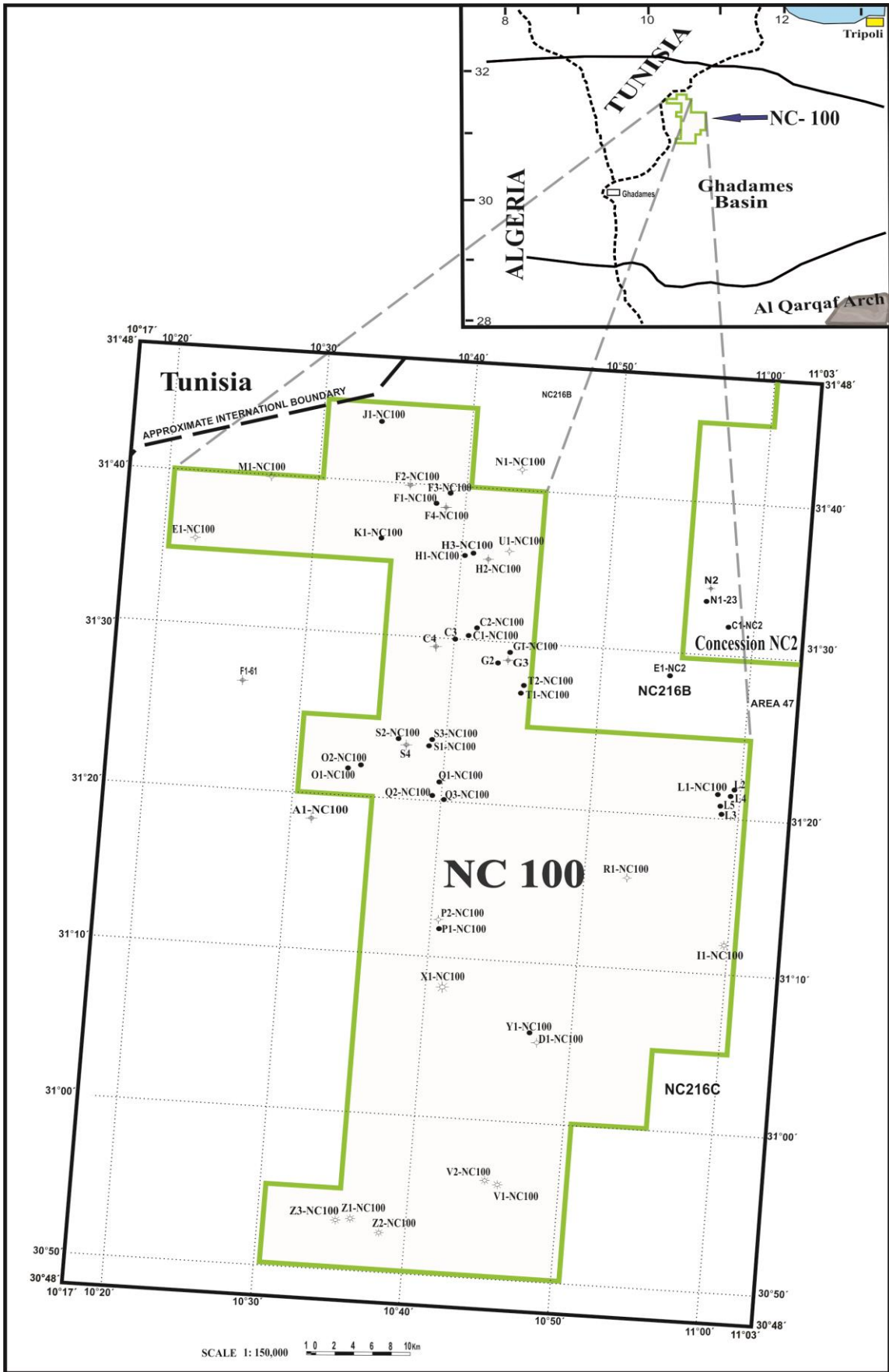


Figure 2. Location map of the study area (concession NC100), showing drilled wells in Concession NC100, (Ghadames) Basin NW Libya, (AGOCO, 2008).

## **1.1 Research Problems.**

The exploration and development of a reservoir requires reasonable understanding of its occurrence, facies types and morphology. Sandstone occurs in different sedimentary environments, which is a part of the earth's surface that is physically, chemically and biologically distinct from adjacent terrains (Selley, 1985). The variation in sedimentary facies may be attributed to differences in energy levels, flow velocity and climate, resulting in differences in morphologies and qualities of sandstone reservoir.

The Upper Silurian, Lower Acacus Formation is largely fluvial-deltaic system deposited between the Lower Silurian marine shale of Tanezzuft Formation and Upper Silurian transgressive marine shales of Middle Acacus Formation (BEICIP, 1973; Santa Maria, 1991; Elfigih, 1991, 2000).

In hydrocarbon terms, the Lower Acacus Formation contains the stratigraphically highest, relatively thin to moderately thick sand units represent the main reservoirs intercalated with shales that interplays an important role as seal and caps in Ghadames Basin. The reservoirs in this position are commonly oil charged but productivity is strongly controlled by depositional facies with generally low production rates and recovery factors, (Skindear, 2000).

Petrographic and petrophysical studies of some selected sandstone units of Lower Acacus Formation have revealed some diagenetic impacts on reservoir quality and distribution of these sandstone units throughout the Ghadames Basin (Elfigih, 2000).

In this study, some scientific problems will be discussed regarding:

- Facies identification and thorough understanding of environmental and reservoir facies relationship of the Lower Acacus Formation in Concession NC100.
- Predicting facies changes in an established stratigraphic framework of Lower Acacus Formation in concession NC100.
- The influence of some possible diagenetic processes on reservoir sandstone quality and heterogeneity.

## **1.2 Objectives.**

The general purpose of this research is to establish a facies-stratigraphic framework through which the paleogeography of the study area could be addressed.

The specific objectives of this study are:

- To identify the possible lithofacies distribution of the Lower Acacus Formation characterized by different depositional environments throughout the concession NC100, and an attempt to be made to compare and contrast facies types their extension and continuity relative to the previously studied nearby NC2 concession.
- To define the most effective sandstone reservoirs of Lower Acacus Formation and to evaluate their quality variations throughout the concession NC100.

## **1.3 Scope of the study.**

The concept of facies is particularly suited for study of reservoir quality, (Zalat, 1991; Cosentino, 2001; Katherine A. Pollard, 2013; Henares, 2014). Once wireline-logs have been integrated with core data and in some case could possibly supported by available seismic data, the environmental facies sequences could be easily established between correlated wells.

In every preformed reservoir study (Donald G. Mccubbin, 1973; Remi Eschard and Brigitte Doliges 1992; Freiberg, 2003; Trond Lien & Ole J, 2006) it is essential to deal with facies. In fact geological intervals or sequences always imply the generation of some facies which can be defined on cores, through description of lithological, petrophysical and depositional features of the rock unit.

A further step that is often preformed in describing any sedimentological unit is to represent that unit by means of their lithologies and then defined as lithofacies. These basic lithofacies would provide a simple lithological facies distribution and minimize geological complexity through log-lithofacies maps or lithofacies modeling.

The integration of the available wireline-logs and cores data from wells within concession NC100 can provide and demonstrate the fundamental depositional facies of Lower Acacus Formation and reduces their stratigraphic complexity.

However, lithofacies complexities may arrised locally in some wells at some intervals, that is may attributed to some diagenetic influences which may effect the recovered sandstone quality, hence, will effect reservoir potentiality.

## 2. REGIONAL GEOLOGY OF GHADAMES BASIN.

### 2.1 Tectonic and structures.

The Ghadames Basin is a large intracratonic sag basin of Paleozoic to Mesozoic age that formed over the suture of the ancient microplates (West East African Cratons) that joined during the Pan-African Orogeny, which is located in the central western part of Libya. The Nafusa uplift and Gargaf Arch flank the basin to the north and to the south respectively, where as eastern boundary is not well defined and can be represented by Tripoli-Assoda Arch which being overlapped by the western margin of the younger Sirt Basin. The western limit is represented by the partial northern extension of Tihemboka uplift, and Dahar-El-Biod uplift as the basin stretches in Algeria to the west and the basin widened into a broad depocenter extending into Tunisia and Algeria west of the Tihemboka Uplift, (Fig. 3), (Don Hallett, 2004).

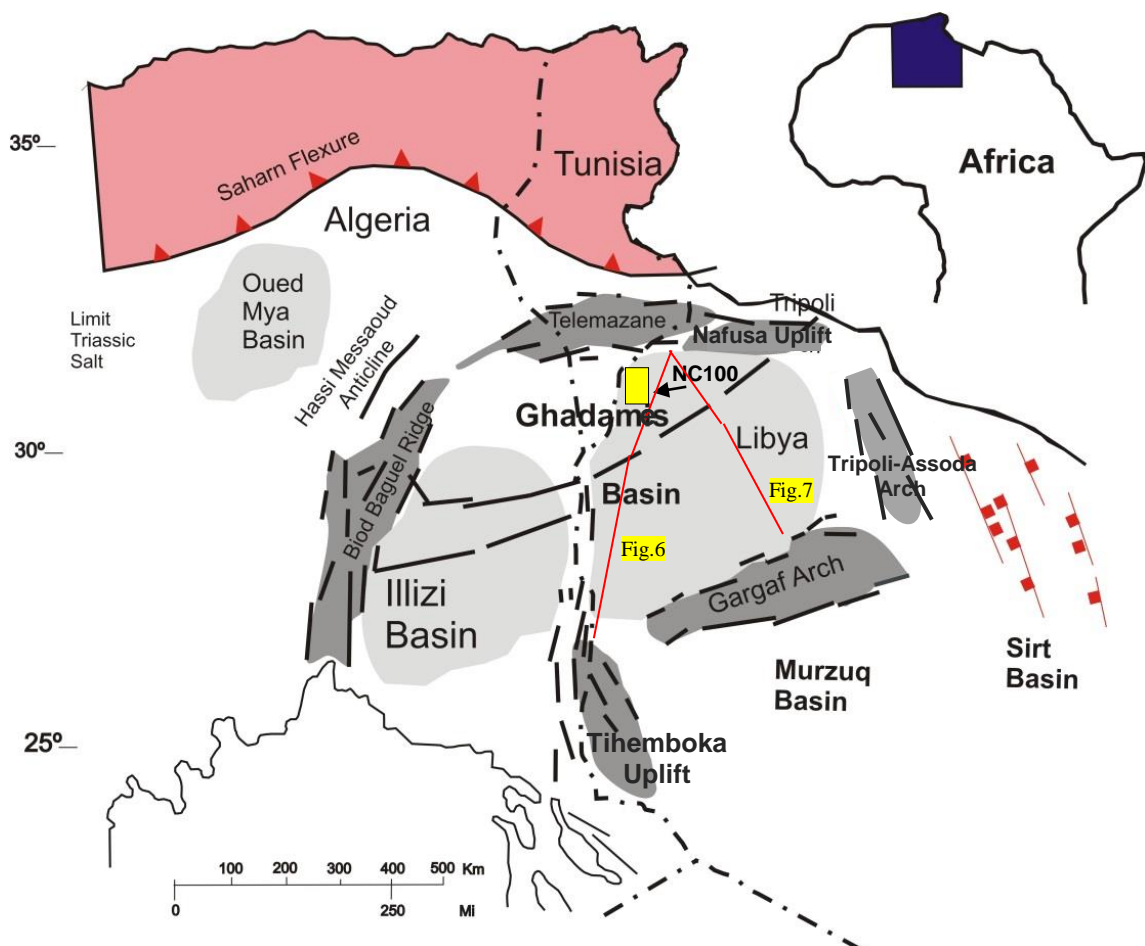


Figure 3. Main structural elements of Ghadames basin and location of concession NC100, (modified after Acheche et al., 2001).

The evolution history of Ghadames basin occurred in three phases: (1) initiation through reactivation of Pan-African fault systems of a subsiding Palaeozoic basin; (2) uplift and erosion of much of the basin during the Hercynian phase; (3) a northwest tilting and superimposition of a Mesozoic extensional basin (Echikh, 1998). As consequence, there is a wide variety of structural styles in the basin, different fault patterns and relief changes that may shaped the whole of the basin (Klitzsch, 1970).

### **Pan African phase.**

The Pan-African lineaments that widely affect the basement have played a major role throughout the basin's history (Elruemi, 2000). Basement in much of this area is formed by Pharusian accreted terranes, but further south, and particularly in the Illizi Basin of Algeria, it is represented by rocks of the Pan-African remobilized belt (Klitzsch, 1971), (Don Hallett, 2002). The early Palaeozoic history of the basin was controlled by the northwest -southeast Pan-African tectonic trend (Fig. 4). The basin narrows southwards, confined between the Tripoli-Tibisti and Tihemboka Uplifts, into the Murzuq Basin. (Klitzsch, 1971).

The final pulses of Pan-African tectonism continued into the Ordovician. During Llandeilian times, uplift and erosion occurred on the Tihemboka Arch and the Ahara Uplift in Algeria, and during the Caradocian, folding, faulting, uplift and erosion occurred which removed much of the early and middle Ordovician section on the Dahar Uplift in Tunisia, (Echikh, 1998).

### **Taconian phase.**

Early Ordovician time was characterized by a tectonic instability (Attar, 1987) indicated by the absence of the Cambrian over the main uplifts, e.g. the Ahara Uplift and the Tihemboka Arch. Peak activity of Taconic phase occurred during Llandovrian time, when there was substantial activity, particularly on the southern rim of the Ghadames Basin. These unconformably overlie older Ordovician strata. An erosional phase is also noted in southern Tunisia (Chandoul 1992). The Taconian unconformity marks the transition to the Early Silurian sequences.

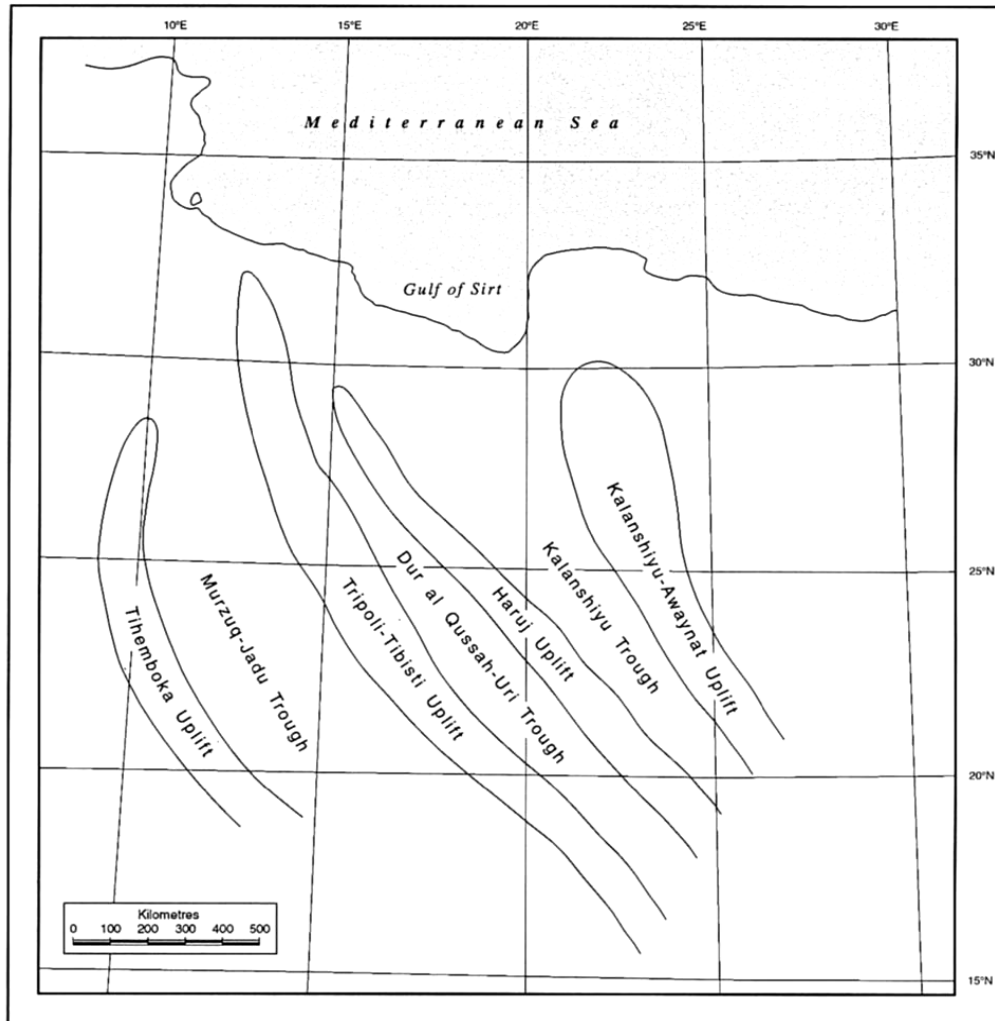


**Figure 4. Post Pan-African (Caledonian NW-SE) structural trends in Libya. (Klitzsch, 1971).**

### **Caledonian phase.**

A significant Caledonian tectonic event was initiated during the Late Silurian to Early Devonian as a result of the collision between West Africa and North America. This caused the uplifting and erosion of the southwestern and southern flank of the Ghadames Basin, where the Lower Devonian Tadrart is seen to directly overlay the Upper Silurian basal Acacus, (Echikh 1992). In this stage NW-SE tectonic trend (Fig. 4) still persisting as it shows structural alignment imprinted on the younger sedimentary covers (Klitzsch, 1971).

### **Hercynian phase.**

The major period of deformation and erosion during the Late Carboniferous and Permian time of the Hercynian orogeny. During this period the Nafusa uplift emerged, reversing the regional dip and deeply eroding the Paleozoic's, and formed the north side of the basin. There was also renewed uplift, along with erosion, of the Gargaf arch.



Uplift of the Gargaf Arch to the north converted the Ghadames Basin into an interior sag basin and provided a new source of clastic sediments from the north as the previous deposits in the area were eroded. Precambrian and/or Lower Paleozoic faults were rejuvenated during this time (Elfigih, 2000).

The Hercynian orogeny reached its peak during the Late Carboniferous and major new tectonic elements were formed oriented NE-SW (Fig. 5), including the Gargaf Arch and Nafusa Uplift in Libya, the Dahar Arch in Tunisia and the Talemzane and El Biod Arches in Algeria. The entire area was uplifted and subjected to intense erosion during the Permian which left the basin surrounded by highs which, in the case of the Nafusa, Tihemboka and Gargaf Arches, were eroded to their Cambro-Ordovician roots (Fig. 6). A Subcrop pattern of progressively younger rocks can be traced into the centre of the basin where a complete section up to Late Carboniferous is preserved (Klitzsch, 1971).

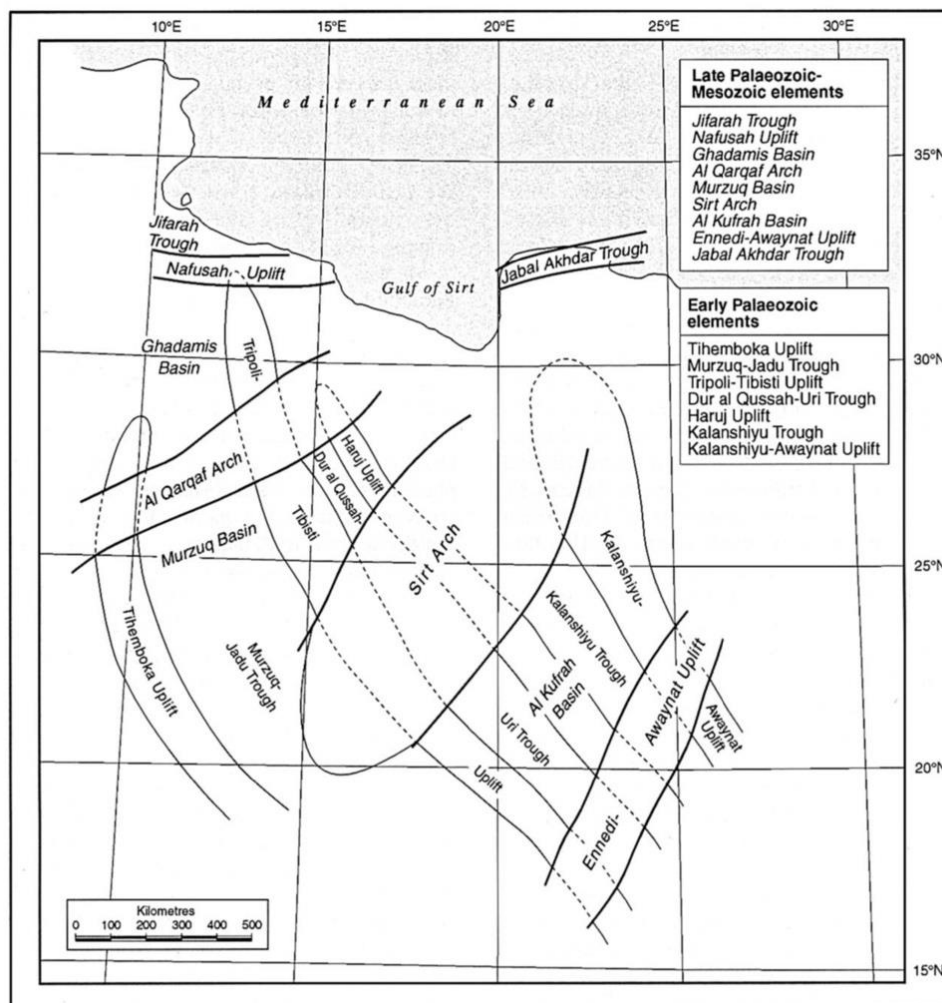
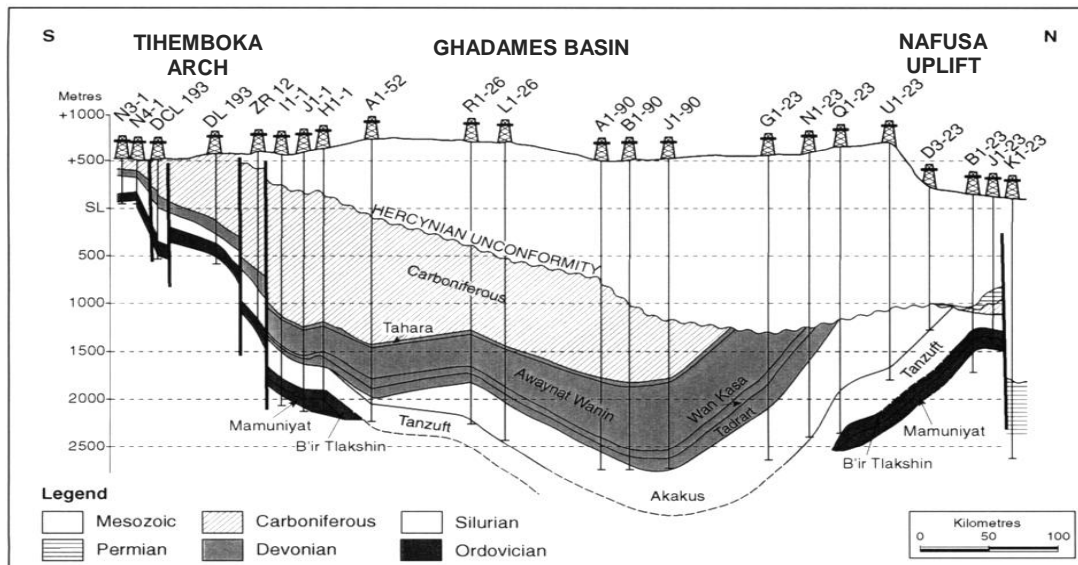


Figure 5. Hercynian Structural Trends, in Libya, (Klitzsch, 1971).



**Figure 6. N-S Structural Cross-Section illustrates configuration of the Palaeozoic succession in Ghadames Basin, and the effect of the Hercynian unconformity, (Don Hallte, 2000). (see Fig. 3 to locate line of N-S cross section).**

### Post Hercynian phase.

During the Mesozoic an important northward tilting took place throughout the basin resulting in the generation of a significant space for a thick Mesozoic section to be deposited. That was in accordance with the passive margin that developed throughout North Africa. (Echikh, 1998). Thick successions of Mesozoic continental deposits, including Triassic sandstones and evaporates, were deposited in the post-Hercynian sag basin, in which the depocenter was located much further north than that during the Palaeozoic (Don Hallte, 2000) (Fig. 7).

### Austrian phase.

At the end of the Baramian, the tectonic movements tied to the Austrian phase occurred (Skindear, 2000), these were pronounced over the El Biod Arch and its eastern flank, with east-west compression producing high-amplitude structures along north-south trending reverse faults. Jurassic transgressive sequences are followed by an Early Cretaceous regression which was terminated by deformation during the Aptian time related to detachment of the Apulian plate from the north African margins and the establishment of the Mesogean axis of sea floor spreading in the southern Tethys which produced wrenching along line of Sabratah-Cyrenica fault. Wrenching of Aptian age has been reported from Illizi Basin and Tihemboka uplift area (Don Hallte, 2000).

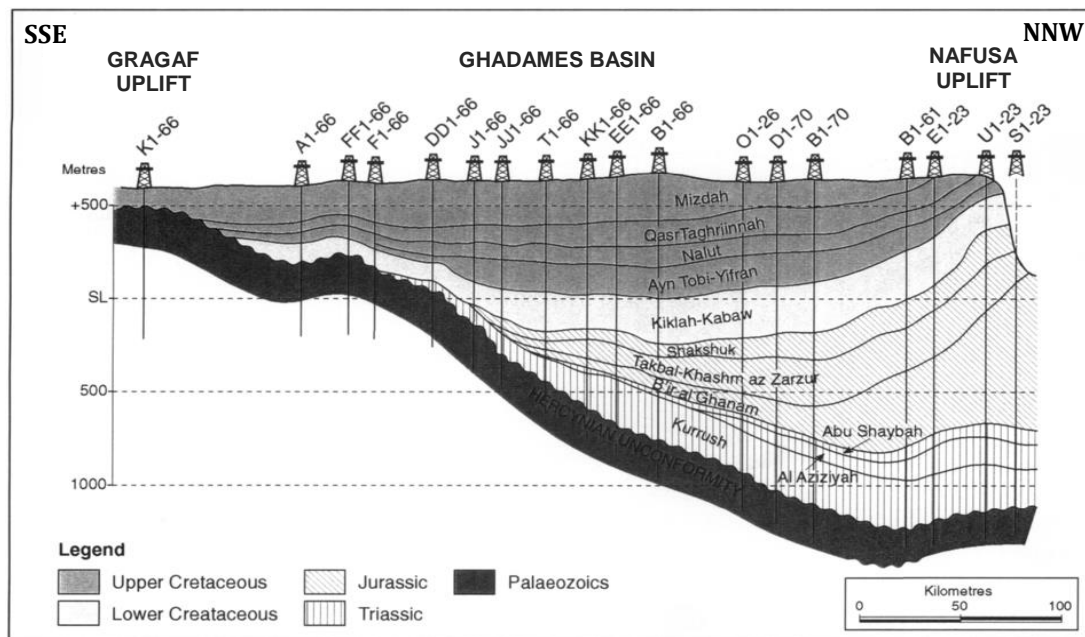


**Figure 7. NNW-SSE Structural Section, Ghadames Basin, NW Libya. (Don Hallte, 2000). (see Fig. 3 to locate line of NNW-SSE cross section).**

### **Alpine phase.**

The Alpine Orogeny (Late Cretaceous) marked the last major geodynamic event to affect Ghadames Basin. It had great impact on the details of the final structural architecture of the basin and led to a change in tectonic conditions. Its erosional intensity was greatest over the uplift margins to the south (Gargaf and Thihemboka Arches) and to the north (Nafusa uplift). Other extensional events affected the area related to the continuing rifting of Tethys and the opening of the Atlantic. This led to the development of a series of en echelon (closely- spaced parallel) normal faults and tilted blocks, with associated volcanism, in the northwestern part of the Ghadames Basin and southern Tunisia (Don Hallte, 2000).

## 2.2 Stratigraphy.

The Ghadames Basin is a large intracratonic basin located on the NW part of Libya (Fig. 3) and contains up to 12,000ft of Palaeozoic-Mesozoic sections. The Paleozoic and Mesozoic sections are separated from each other by a major regional Hercynian unconformity of Late Carboniferous (Fig. 8). However the most preserved thicker sequence in the basin is represented by Paleozoic sediments, which have been modified at some levels by unconformity surfaces associated with periods of emergent that related to eustatic changes across the basin, (El-Rweimi, 1991), (Underdown and Jonathan, 2008). These unconformities are:

- HERCYNIAN Unconformity. (*Late Carboniferous*).
- ACADIAN Unconformity. (*Late Devonian Early Carboniferous*).
- CALEDONIAN Unconformity. (*Late Silurian Early Devonian Unconformity*).
- TACONIAN Unconformity. (*Late Ordovician Unconformity*).
- PANAFRICAN Unconformity. (*Early Cambrian Unconformity*).

Massa and Moreau-Benoit (1976, 1985); Moreau-Benoit (1979, 1980, 1988) and Massa, (1988) established the broad stratigraphical framework for the Ghadames Basin. In Libya, the Palaeozoic sections were studied by BEICIP, TOTAL, AGIP and AGOCO Company. The Paleozoic stratigraphic succession of the Ghadames Basin is summarized in (Fig. 8).

This stratigraphic section (Fig. 8) is characterized by sediments composed of sandstones and shales of continental, deltaic, shallow marine, and glacio-marine origin in the lower part (Cambrian-Silurian) representing most the southern wells in Ghadames Basin, whereas fluvio-deltaic shallow marine and lagoonal sediments are characterizing the upper part of the section (Devonian-Carboniferous) representing most of the northern wells in Ghadames Basin (E. Edward, Tawadros, 2001).

This study deals with the stratigraphy of the Lower Acacus Formation of Late Silurian age in NW of Ghadames Basin.

ERA	PERIOD	EPOCH	AGE	FORMATIONS	Thickness (m)	CHARACTERISTICS	Depositional Cycles and Origin	
MESOZOIC	CRETACEOUS	LATE	CAMPANIAN	ALPINE				
			SANTONIAN	MIZDA	450	DOLO-DOLO LST. massive	Marine-Restrict Lagoonal	
			TURONIAN	GASPTIGRINA	500	CHIKY LST. w/calc. CLAYS at places		
		CENOMANIAN	GARIAN	500	LST. DOLO LST.			
		EARLY	ALBIAN	SIDI-ASSID	700	GYP. w/grn SH at the top. LST. DOLO LST. OOL LST at the base.	Regr. (Fluvio-Cont)	
			APTIAN	CHICLA	600	SST: yellowish wht., med-c grained, congl. at places w/some reddish clay.		
	JURASSIC	LATE	PORTLANDIAN	AUSTRIAN	500	SST. SLTST. and CLAY, alternations	Evap.-Lagoonal	
		MIDDLE	KIMMERIDGIAN	SHAKSHUK	600	LST. DOLO. Clay occ. w/SST alternations.		
		EARLY	CALTOVIAN	LES ABREGHS	900	GYPs: crm-yellow, fibrous-blocky (at top) w/yellow-grn clay and limy beds. ANH. is dominant at the base.		
	TRIASSIC	LATE	TOARCIAN	BIR-ELGHANEM	1100	ANH: wht., milky, occ. glassy, amorphous, w/dolomitic lst bands.		
			NORIEN	BUSHEBA	500	SST: yellowish brn., med-c grained, w/red clay		
		MIDDLE	LADINIAN	AZIZA	750	LST: wht., crm wht, calcu-calka., massive, w/ sh alternations	Trans. (Shallow Marin)	
			ANISIAN	RAS HAMIA	950	SST: greyish wht., med-c grained, mica, occ. w/ sh streaks.		
	EARLY	SCYTHIAN	OULED CHEBBI	320	SST: wht, fine-med, occ. c-grained, massive, kaol. crm.	Regr. (Fluvio-Labu)		
			BIR ALJAJA	60	SH: dark green, occ. grey, fss-subfss, non calc.			
	PALAEOZOIC	CARBONIFEROUS	LATE	STEPHANIAN	HERCYNIAN	600	CLYST: red-brown, soft, sticky, slightly calcareous, occ. w/ ANH layers. SH: red-brown, soft, calc., non-fossil, w/ Some SST beds: white, fine, calc., dolomitic in parts.	Regr. (Lagoonal)
				WESTPHALIAN	DEMBABA	900	LST: white-light brown, silty, fossil (biocalcarente), w/ dense SH; grey-green, fissile, occ. silty, w/ some ANH. interb.	Transgressive SH/LST
				NAMURIAN	ASSEDJEFAR	500	SH: grey, thin SLTST interlamination, calcareous, w/ fine SST, macro/micro fossils.	
EARLY			WISEAN	MIRAR	1200	SST/SH: cyclic alternations; SST: white, fine, micro-cross bed. SH: dark grey, mic., fss, silty, Pelec., Brach., wood frag.	Reg./Trans. (Delt/Proclit)	
			TOURNAISIAN					
DEVONIAN			LATE	FAMENNIAN	TAHARA	200	SST/SH: coarsening upward seq., SST cross bed., skolith., wood frag.	Reg. (Deltaic)
		FRANSIAN		ACADIAN	300	SH: grey, fss., mic., w/ minor SST. fine grained, cross-bedded.	Transgressive Shallow Marine SH/LST	
		GIVETIAN		AQUINET OUEININE	200	LST: white-light grey, occ. fossil. at the top of the unite, w/alter. biot. silty-SH, and SST. at the base.		
		MIDDLE	COLUMNIAN		400	SH: grey-dark grey, fissile at the base, overlain by SST: fine-medium grained, coarsening upward sequences at the top	Regressive SS (Deltaic)	
			EMISIAN	OUAN KASA	600	SH: v. silty, biot., sandy at the top, LST: white-grey, silty, brach. at the base.	Trans. Shallow Marine	
		EARLY	SIEGENIAN	TADRART	600	SST: fine-conglom., kaolinitic, occ. sil./ferr. cement, cross-bedded, w/ wood fragments, Cruziana.	Regressive SS (Fluvial)	
SILURIAN		LATE	LUDLOVIAN	CALEDONIAN	700	SST: white-light grey, occ. brown, v. fine-fine grained, moderately-sorted, kaolinitic, occ. w/ferr. SST at the top, interb. W/SH.	Regressive SS (Fluvial)	
			WENLOCKIAN	ACACUS	500	SH: grey-green, firm, subfissile-fissile, flaky, micaceous, w/ thin Lenticular SLST. lenses, bioturbated.	Transgressive S (Shallow marin)	
		EARLY	LLANDOVERYAN	TANEZZUFT	1500	SH: grey-green, fissile, silty, micaceous, w/ graptolites, Radioactive at the base, interlaminated w/ SST, white-light Grey, micaceous.	Transgressive S (Shallow marin)	
ORDOVICIAN		LATE	ASHGILLIAN	MEMOUNIAT	700	SST: white-tan, fine-coarse, cross-bedded, kaolinitic, Tigillites, Skolithus. SH: green, micaceous, calcareous, occ. w/limestone inter-beds.	Transgressive SH/L. Regr. Iran. SST	
			CARADOCIAN	MELEZ CHOGRANE	700	SH: green, micaceous, chloritic, interbeds w/ SST, fine-coarse, occ. pebbi-bould, usually stratified filling paleovalleys w/ ferr. oolites at the base, Trilobites and Brachiopods.	Shallow marin periglacial SH/SST	
		EARLY	LLANDEILIAN	HAOUAZ	300	SST: white, fine-medium grained, occ. argillaceous, arkosic; SLST: bioturbated, Tigillites, Skolithus, Trilobites.	Regressive Marginal marin (SST, SLST.)	
			LLANVIRNIAN					
	ARENIDIAN SKIDDAVIAN							
TREMADOCIAN	ACHEBYAT	150	SST: white, medium-coarse grained, w/ Tigillites, Brachiopods.					
CAMBRIAN	LATE	HASSAONA	650	SST: medium-v.coarse grained at the base, kaolinitic at the top, occasionally cross-bedded, fluvial in origin, non-fossiliferous.	Regressive (Continental (SST.)			
	MIDDLE							
	EARLY					MOURIZIDIE (INFRA-CAMBRIAN)	500	SST: red, conglomeritic, cross-bedded, with tillites.
PRE-CAMBRIAN	ALGONKIAN			BASEMENT		Metamorphic and igneous rocks: slate, phyllite, gneisses, schists and granites associated.		

Figure 8. Generalized Stratigraphic type section of Ghadames Basin, NW Libya, (compiled from: Elfigh, 1991, 2000; and NOC, 1995).

## **SILURIAN PERIOD.**

The North African area subsided considerably during Silurian times, developing as a northerly dipping passive ramp margin with dominant structural axes oriented at a high angle to the plate margin (Craig; Rizzi. 2006). The Silurian strata are preserved in gentle sag basins in North Africa, the similar stratigraphy implies deposition on a uniform shelf which underwent subsequent warping, leaving the strata preserved within the basins and eroded from the intervening arches, (Selley, 1997).

The Early Silurian included a major postglacial transegressive episode flooded the North African shelf, that peaked during the Wenlockian, with deposition of thick, laterally continuous marine mudstones Tanezzuft Formation. Subsequent regression of the Silurian sea resulted in the deposition of the overlying Upper Silurian marine sandstones and mudstones of the Acacus Formation (Klitzsch, 1981).

In NW Libya, the total thickness of the Tanezzuft shales increases northwestwards in the distal Ghadames Basin reflecting the northwestward progradation of a sandy deltaic system during middle Llandovery to Ludlovian time (Craig; Rizzi. 2006), which may be probably one continuous transgressive-regressive cycle progradational northward (Buroillet & Manderscheid, 1967; Le Heirisse, 2002; Bonnefous, 1963). These sediments are truncated toward the southeast of the basin against the Caledonian unconformity (Hammuda, 1980; Buroillet & Manderscheid, 1967; Le Heirisse, 2002).

The Silurian progressively disappears from Tunisia in the west to the Gargaf Arch in the east, by either erosion or non-deposition.

### **The Lower Acacus Formation.** (Late Silurian, Wenlockian – Ludlovian Age).

The Acacus sedimentation package has been subdivided into three mappable formations; Lower, Middle and Upper formations (Massa, 1988), each one of these formations has specific geometrical and sedimentological characteristics by which accounted for a particular stratigraphic and environmental meanings. It is worth mentioning that Acacus Formation or Acacus sandstones (Lexicon Libya 1973), have been divided by BEICIP group (1973) into unformed division of A, B, and C parts equivalent to (Lower, Middle, and Upper parts of Acacus Formation). Later according to Klitzsch (1981), and all published literatures of Ghadames Basin, the Acacus Formation was described as Lower Acacus Formation, Middle Acacus Formation, and Upper Acacus Formation. Which considered to be formal name identifying different mappable parts of Acacus Formation. In this research, the Lower Acacus Formation is used to define the studied section.

These formations are well represented in the northern parts of the Ghadames basin (Bracaccia, 1991). The Lower Acacus Formation in the Libyan part of Ghadames Basin (Hamada Basin) is of Wenlockian age and characterized by progradational deltaic system commenced from the SE towards the NW (Massa and Jaeger, 1971).

Due to a high sediment supply, progradation of deltaic Lower Acacus Formation into the shaly shelfal sea was encountered to the north, where the sea-level rise had slowed enough to induce a change from retrogradation to cliniform progradation fashion (Berry and Boucot, 1967, 1973; Massa and Jaeger, 1971; Bellini and Massa, 1980).

Accordingly, the Lower Acacus Formation can be defined by progradational depositional systems trending SE-NW (Fig. 9) represented by fluvial channels to coastal deltaic and marginal marine sandstone and shale to eventually basinal shales.

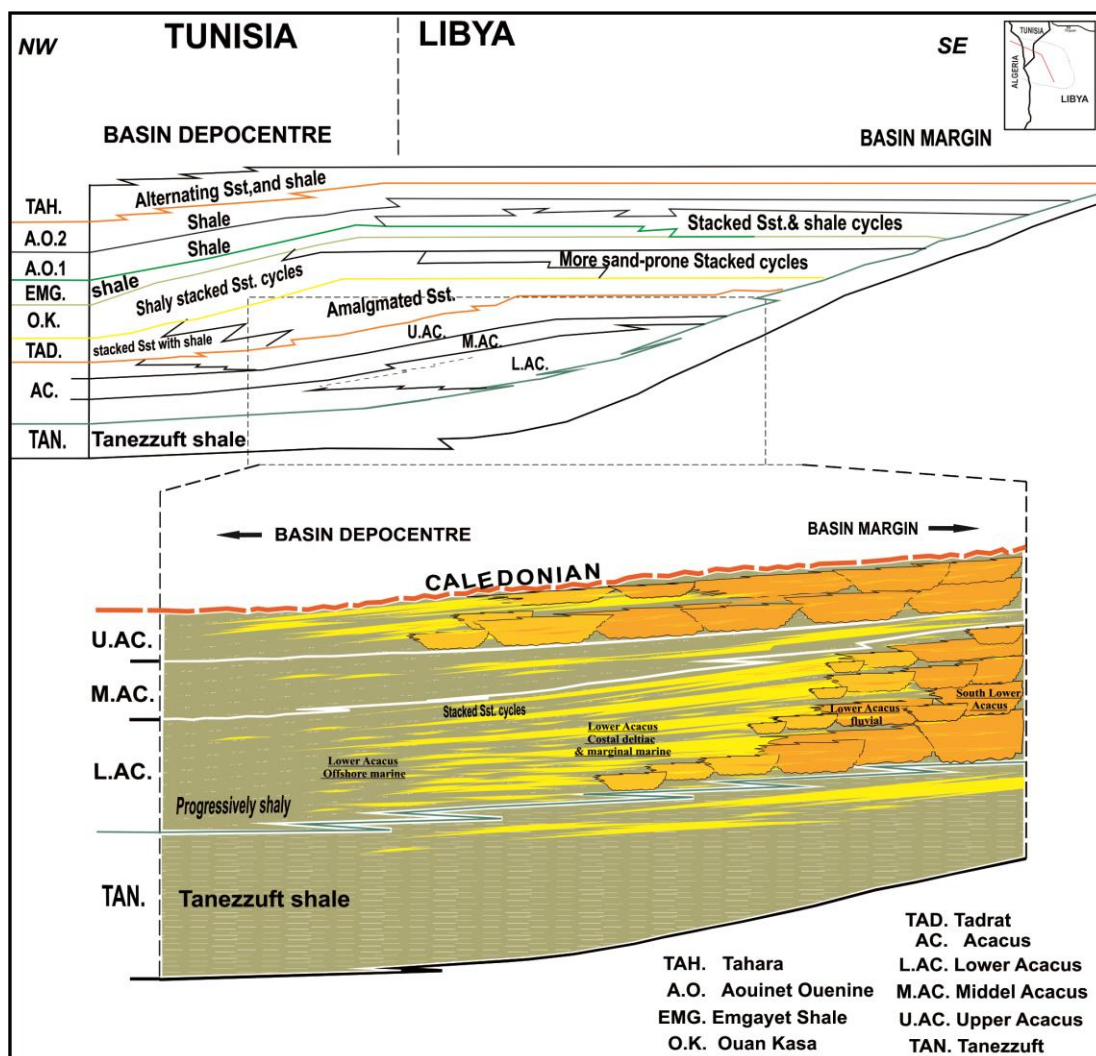
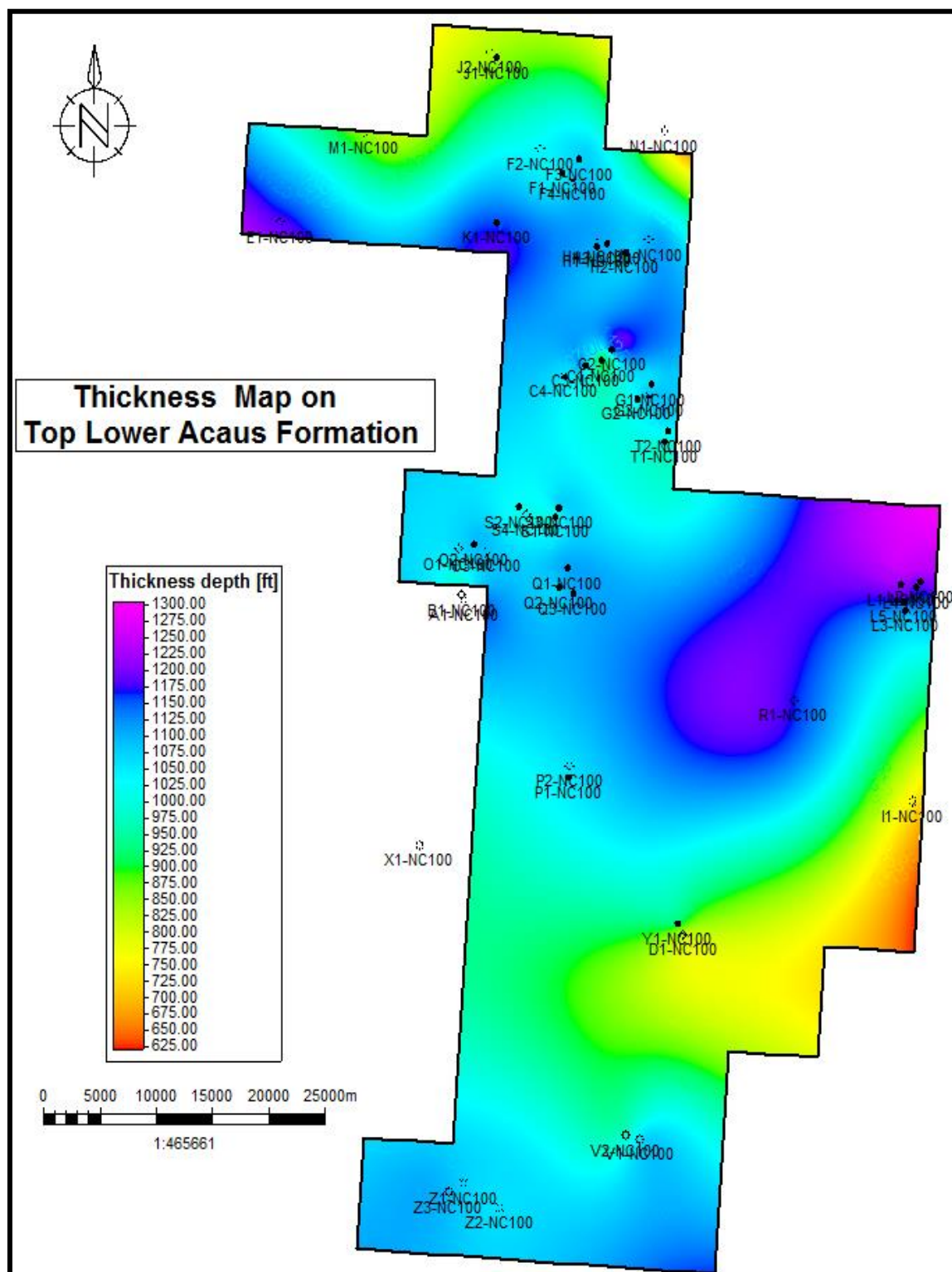


Figure 9. Sketch showing the progradation and variation in sand/shale of the Silurian and Devonian sequences in SE-NW trend, (Note: Acacus package includes Lower Acacus, Middle Acacus, Upper Acacus Formations where L.AC. represents progradational fluvio-deltaic sequences, M.AC. represents transgressive shaley unit and U.AC. represents fluvial dominated coastal plain deposits, (modified after Elrumie, 2000).

Total thickness of Lower Acacus Formation in the study area concession NC100 is ranging from 625 ft to 1300 ft (Fig. 10), this variation in thickness may reveal some post-Silurian reactivation (tilting / uplift) of the depositional basin.



**Figure 10. Total thickness map of the Lower Acacus Formation, Concession NC100, Ghadames Basin, NW Libya.**



Sandstone percentage map, (Fig. 11) of Lower Acacus Formation reveals that sand contents at its maximum of about 80% south of Ghadames Basin ( north of Gargaf Arch, and decreases generally to the north to record about 40% around the study area concession NC100 where it shaling-out farther NW as the basin gets its maximum depth (Echikh, 1998).

Locally NE-SW trended structures encountered at the middle of the basin revealing positive area during deposition of Lower Acacus Formation. Hence, it records the minimum sand percentage (30%) as the Lower Acacus Formation is partially eroded.

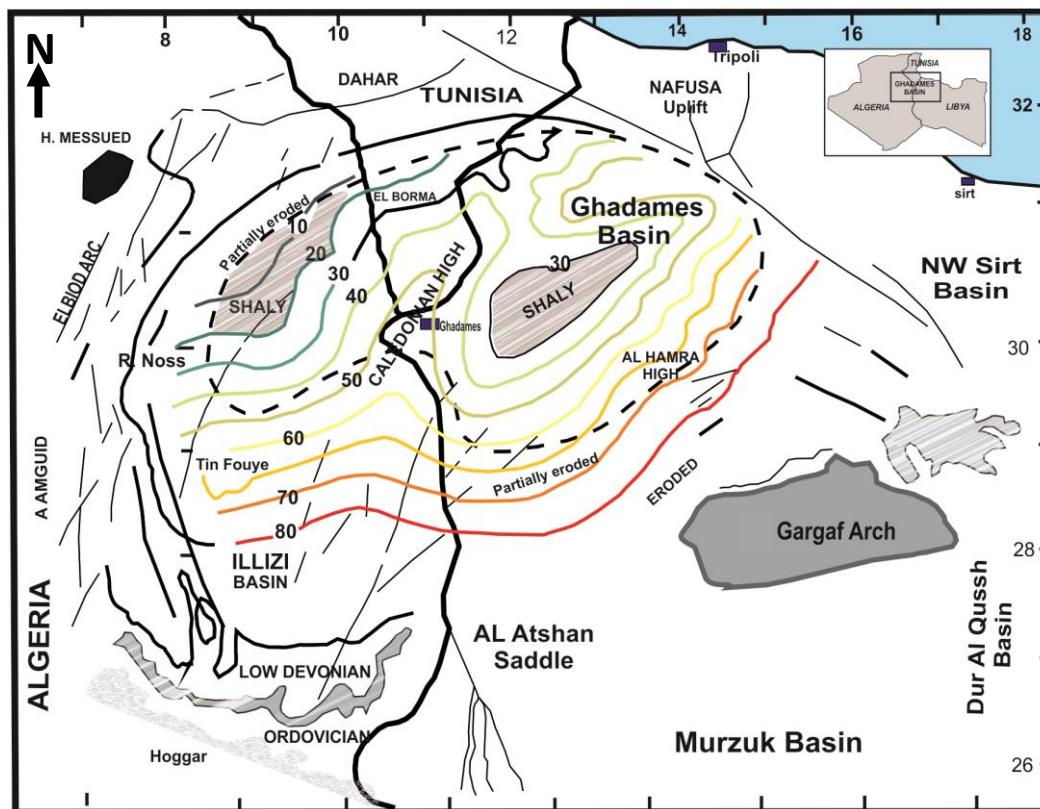


**Figure 11. Sand content (percentage) of Lower Acacus Formation. (Note the presence of a Hercynian high in the central part of the basin, with an associated SW-NE trending sand-rich belt.). (modified after Echikh, 1998).**

The Stratigraphic framework of the Lower Acacus Formation in some concessions of the Ghadames Basin have been studied through published and unpublished reports by several authors including: (BEICIP, 1973; Elfigih, 1991, 2000; Cridland, 1991; Santa Maria, 1991; Dilekoz and Daniels, 1998; Shahlool, 1998).

According to Elfigih (1991; 2000) the Stratigraphic framework of the Lower Acacus Formation, reveals the individual sandstone units begin with marine shales representing a transgressive phase and terminate with a regressive deltaic sandstone/siltstone phase (progradational units). This latter phase is overlain by less persistent, thin, reworked

marine sands representing the destruction phase. Thus, each of the sandstone units make up major progradational sequences bounded by local or regional time stratigraphic markers. These prograded sediments were contributed their sedimentation by major river systems which occur to the south and flowed northward.

(Elfigih, 1991) subdivided the Lower Acacus Formation into 14 coarsening-upward coastal deltaic units (A1 - A14), which are laterally equivalent to 7 fining upward fluvial units (Af 1–Af 7). Facies represented in these rocks include: fluvial sandstones, proximal delta front sandstones/siltstones, distal delta front bioturbated silty-sandstones, and prodeltaic silt/shales and reworked marine sandstones.

Aurdini (2003) divided the Lower Acacus Formation into four basic facies associations (with the relative depositional processes) that are cyclically repeated in the vertical stacking pattern. These sedimentological facies and their vertical stacking pattern, induced both by unidirectional currents tidal and wave action, suggest a depositional setting under relative sea-level oscillations.

(Shahlool, 1998). Divided the Lower Acacus Formation into numerous transgression and regressive rhythms, which are represented in electric logs by coarsening upward sequences.

Similarly the stratigraphic framework of the Lower Acacus Formation in concession NC100 can be divided into (11) coarsening-upward coastal deltaic sandstone units (A1-A11), which are laterally equivalent to fining upward fluvial sandstones (Lf1-Lf11) dominating the southern part of the concession NC100, (Enclosure A-A', B-B').

Lithofacies types of Lower Acacus Formation have been identified and described by cores and eclectic-logs to illustrate some cyclic sequences bounded mainly by stratigraphic markers, will be described in detailed in the following chapters.

### 3. MATERILAS AND METHODS

This study is mainly based on well data relevant to Concession NC100 (Fig. 12) in which 49 wells (Table 1) were available at the time this study was undertaken and penetrated the Lower Acacus Formation, and deeper units. Wireline logs; GR log and SP log “if available” were digitized for formation tops (Table 2) and used as a facies tool for identifying sandstone body types.

For all studied Lower Acacus sandstones units of Gamma-Ray cutoff (65API) was applied and digitized for each well to define potential reservoir thickness and to asses for map construction.

A total of 215ft of cores from five wells (Table 3) described by using core description sheet (Fig. 13) using a vertical scale of (1cm : 4ft). The principal attributes used to interpret various facies and their environments. are shown on the description sheet (Fig. 13).

Following the detailed core description, well-to-well correlations were conducted to generate some regional cross sections [A-A', B-B'], to establish facies stratigraphic framework. These cross sections have been generated using coral draw and petrel software. Thin sections cut from selected sandstone units of Lower Acacus Formation were prepared impregnated by blue epoxy to define porosity. These thin sections were described using modal petrographic description sheet (Fig. 14) where 200 grains point counting per thin section was conducted to more accurately characterize depositional and diagenetic textures and pore types of representative facies. Sandston thin-sections plotted and classified using QFR classification of sandstone (Folk, 1980).

A number of (25) core-plugs were studied for porosity and permeability using AGOCO-core lab for petrophysical analysis. Additional data were obtained from DST reports, well files and internal company reports.

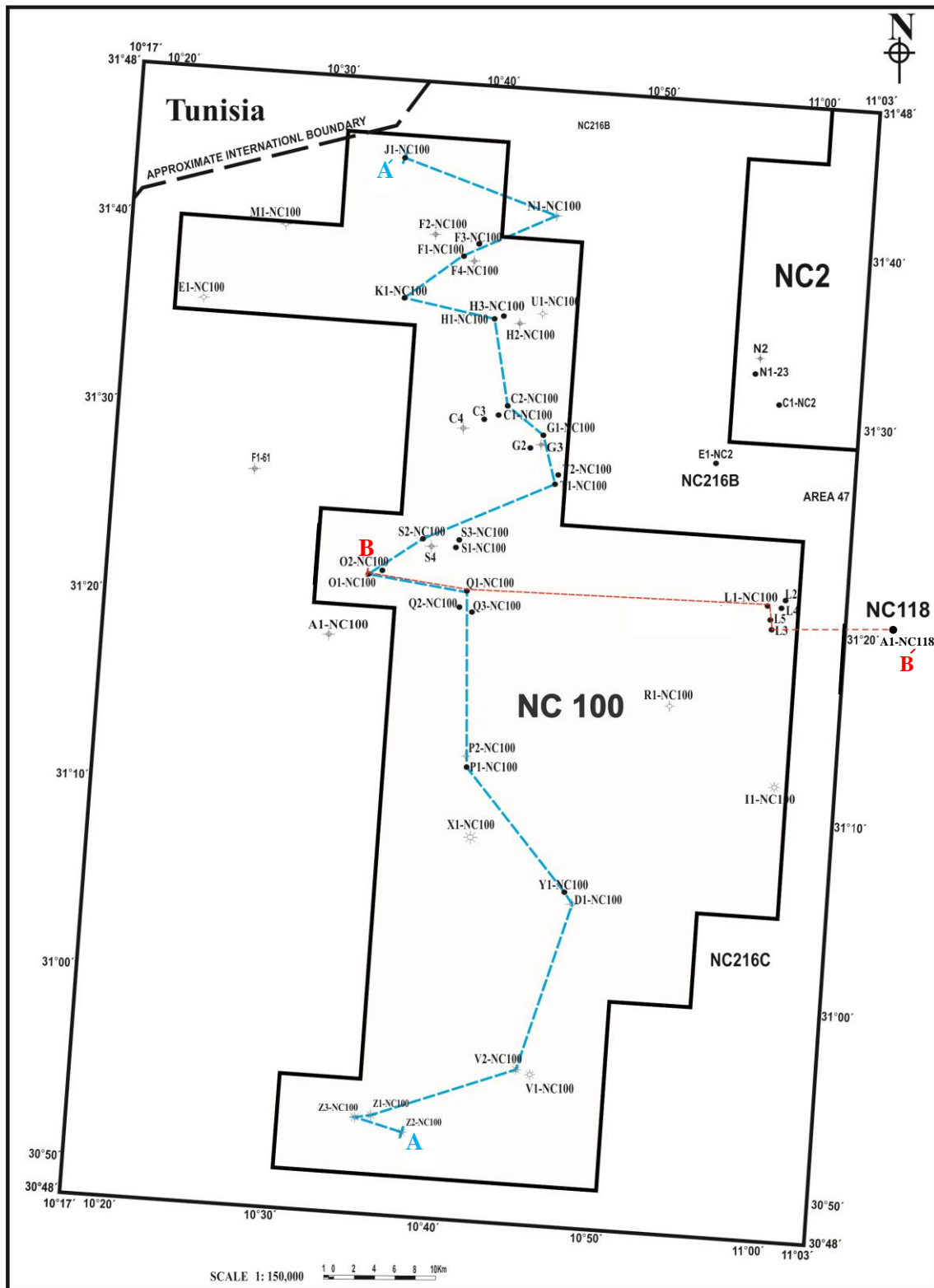


Figure 12. Base map of Concession NC100, showing wells distribution, and lines of stratigraphic cross-section (A-A', B-B') used in this study. Ghadames Basin NW Libya. (AGOCO, 2008).

**Table 1. List of drilled wells and their status in the study area concession NC100 ,Ghadames Basin. (based on location map, Fig. 12 & company internal reports, 2008).**

Well Name	Well Status	Well Name	Well Status
J1-NC100	●	L5-NC100	●
F1-NC100	●	P1-NC100	●
F3-NC100	●	Y1-NC100	●
K1-NC100	●	X1-NC100	☀
H1-NC100	●	V1-NC100	☀
H3-NC100	●	V2-NC100	☀
C1-NC100	●	Z1-NC100	☀
C2-NC100	●	Z2-NC100	☀
C3-NC100	●	Z3-NC100	☀
G1-NC100	●	I1-NC100	☀
G2-NC100	●	F2-NC100	○
T1-NC100	●	F4-NC100	○
T2-NC100	●	H2-NC100	○
S1-NC100	●	C4-NC100	○
S2-NC100	●	G3-NC100	○
S3-NC100	●	S4-NC100	○
Q1-NC100	●	A1-NC100	○
Q2-NC100	●	N1-NC100	⊖
Q3-NC100	●	M1-NC100	⊖
O1-NC100	●	E1-NC100	⊖
O2-NC100	●	U1-NC100	⊖
L1-NC100	●	R1-NC100	⊖
L2-NC100	●	P2-NC100	⊖
L3-NC100	●	D1-NC100	⊖
L4-NC100	●		
<p>● Oil well    ☀ Gas well    ○ Suspended oil well    ⊖ Dry Hole</p>			

**Table 2. Digitized well-log formation tops (drilling depth, and subsurface depth) of the Tanezzuft, Lower Acacus and Middle Acacus Formations as picked from studied wells in concession NC100, Ghadames Basin, NW Libya.**

Well Name	Surface	Coordinates		KB	Drilled depth (DD)	Subsurface depth (S.S.D)
		X	Y			
A1-NC100	Middle Acacus	292940.45	609756.51	1739.63	9842.48	-8102.85
A1-NC100	Lower Acacus	292940.45	609756.51	1739.63	10249.04	-8509.41
A1-NC100	L. Acacus MFS 3	292940.45	609756.51	1739.63	10351.13	-8611.5
A1-NC100	L. Acacus MFS 2	292940.45	609756.51	1739.63	10670.67	-8920.56
A1-NC100	L. Acacus MFS 1	292940.45	609756.51	1739.63	11033.88	-9294.25
A1-NC100	Tanezzuft Shale	292940.45	609756.51	1739.63	11420.06	-9680.43
C1-NC100	Middle Acacus	305202.2	629570	1654	8831.67	-7177.67
C1-NC100	Lower Acacus	305202.2	629570	1654	9259.68	-7605.68
C1-NC100	L. Acacus MFS 3	305202.2	629570	1654	9338.25	-7684.25
C1-NC100	L. Acacus MFS 2	305202.2	629570	1654	9606.77	-7952.77
C1-NC100	L. Acacus MFS 1	305202.2	629570	1654	9981.61	-8327.61
C1-NC100	Tanezzuft Shale	305202.2	629570	1654	10171.96	-8517.96
C2-NC100	Middle Acacus	306098.8	630474.2	1706	8820.23	-7114.23
C2-NC100	Lower Acacus	306098.8	630474.2	1706	9241.44	-7535.44
C2-NC100	L. Acacus MFS 3	306098.8	630474.2	1706	9325.9	-7619.9
C2-NC100	L. Acacus MFS 2	306098.8	630474.2	1706	9786	-8080
C2-NC100	L. Acacus MFS 1	306098.8	630474.2	1706	10166.56	-8460.56
C2-NC100	Tanezzuft Shale	306098.8	630474.2	1706	10373.75	-8667.75
C3-NC100	Middle Acacus	303792	629157.8	1663	8889.82	-7226.82
C3-NC100	Lower Acacus	303792	629157.8	1663	9300.75	-7637.75
C3-NC100	L. Acacus MFS 3	303792	629157.8	1663	9381.83	-7718.83
C3-NC100	L. Acacus MFS 2	303792	629157.8	1663	9819.8	-8156.8
C3-NC100	L. Acacus MFS 1	303792	629157.8	1663	10179.88	-8516.88
C3-NC100	Tanezzuft Shale	303792	629157.8	1663	10368.97	-8705.97
C4-NC100	Middle Acacus	301829.6	628280.2	1620	8847.17	-7227.17
C4-NC100	Lower Acacus	301829.6	628280.2	1620	9255.33	-7635.33
C4-NC100	L. Acacus MFS 3	301829.6	628280.2	1620	9341.63	-7721.63
C4-NC100	L. Acacus MFS 2	301829.6	628280.2	1620	9781.11	-8161.11
C4-NC100	L. Acacus MFS 1	301829.6	628280.2	1620	10120.94	-8500.94
C4-NC100	Tanezzuft Shale	301829.6	628280.2	1620	10312.57	-8692.57
D1-NC100	Middle Acacus	312398.3	582035.9	1715.72	10250.57	-8535.23
D1-NC100	Lower Acacus	312398.3	582035.9	1715.72	10250.57	-8535.23
D1-NC100	L. Acacus MFS 3	312398.3	582035.9	1715.72	10350.56	-8635.28
D1-NC100	L. Acacus MFS 2	312398.3	582035.9	1715.72	10578.87	-8863.56
D1-NC100	L. Acacus MFS 1	312398.3	582035.9	1715.72	10969.36	-9245.73
D1-NC100	Tanezzuft Shale	312398.3	582035.9	1715.72	11558.16	-9842.44
E1-NC100	Middle Acacus	276644	641045.4	1505.25	7972.37	-6664.66
E1-NC100	Lower Acacus	276644	641045.4	1505.25	7972.37	-6664.66
E1-NC100	L. Acacus MFS 3	276644	641045.4	1505.25	8056.4	-6748.69
E1-NC100	L. Acacus MFS 2	276644	641045.4	1505.25	8056.4	-6748.69

E1-NC100	L. Acacus MFS 1	276644	641045.4	1505.25	8213.9	-6906.19
E1-NC100	Tanezzuft Shale	276644	641045.4	1505.25	9835.76	-8330.51
F1-NC100	Middle Acacus	301700.69	645075.97	1688	8160.55	-6472.55
F1-NC100	Lower Acacus	301700.69	645075.97	1688	8584.05	-6896.05
F1-NC100	L. Acacus MFS 3	301700.69	645075.97	1688	8720.87	-7158.23
F1-NC100	L. Acacus MFS 2	301700.69	645075.97	1688	9123.11	-7435.11
F1-NC100	L. Acacus MFS 1	301700.69	645075.97	1688	9480.61	-7792.61
F1-NC100	Tanezzuft Shale	301700.69	645075.97	1688	9632.81	-7944.81
F2-NC100	Middle Acacus	316500.0	107000.0	1652	8141.25	-6453.55
F2-NC100	Lower Acacus	316500.0	107000.0	1652	8553.05	-6875.05
F2-NC100	L. Acacus MFS 3	316500.0	107000.0	1652	8699.87	-7137.23
F2-NC100	L. Acacus MFS 2	316500.0	107000.0	1652	9102.11	-7414.11
F2-NC100	L. Acacus MFS 1	316500.0	107000.0	1652	9459.61	-7771.61
F2-NC100	Tanezzuft Shale	316500.0	107000.0	1652	9611.81	-7923.81
F3-NC100	Middle Acacus	303181.91	646227.61	1592	8065.97	-6473.97
F3-NC100	Lower Acacus	303181.91	646227.61	1592	8503.42	-6911.42
F3-NC100	L. Acacus MFS 3	303181.91	646227.61	1592	8720.87	-7158.23
F3-NC100	L. Acacus MFS 2	303181.91	646227.61	1592	9051.16	-7459.16
F3-NC100	L. Acacus MFS 1	303181.91	646227.61	1592	9399.87	-7807.87
F3-NC100	Tanezzuft Shale	303181.91	646227.61	1592	9573.13	-7981.13
F4-NC100	Middle Acacus	302658.1	644614.2	1626	8119.69	-6493.69
F4-NC100	Lower Acacus	302658.1	644614.2	1626	8565.16	-6939.16
F4-NC100	L. Acacus MFS 3	302658.1	644614.2	1626	8720.87	-7158.23
F4-NC100	L. Acacus MFS 2	302658.1	644614.2	1626	9118.23	-7492.23
F4-NC100	L. Acacus MFS 1	302658.1	644614.2	1626	9363.7	-7737.7
F4-NC100	Tanezzuft Shale	302658.1	644614.2	1626	9636.73	-8010.73
G1-NC100	Middle Acacus	309606.7	627599.9	1736	8928.84	-7192.84
G1-NC100	Lower Acacus	309606.7	627599.9	1736	9327.58	-7591.58
G1-NC100	L. Acacus MFS 3	309606.7	627599.9	1736	9417.14	-7681.14
G1-NC100	L. Acacus MFS 2	309606.7	627599.9	1736	9838.1	-8102.1
G1-NC100	L. Acacus MFS 1	309606.7	627599.9	1736	10188.73	-8452.73
G1-NC100	Tanezzuft Shale	309606.7	627599.9	1736	10397.09	-8661.09
G2-NC100	Middle Acacus	308367.21	626401.57	1688	8912.71	-7224.71
G2-NC100	Lower Acacus	308367.21	626401.57	1688	9323.95	-7635.95
G2-NC100	L. Acacus MFS 3	308367.21	626401.57	1688	9412.98	-7724.98
G2-NC100	L. Acacus MFS 2	308367.21	626401.57	1688	9807.17	-8119.17
G2-NC100	L. Acacus MFS 1	308367.21	626401.57	1688	10147.9	-8459.9
G2-NC100	Tanezzuft Shale	308367.21	626401.57	1688	10364	-8676
G3-NC100	Middle Acacus	309387.5	626686.3	1727	8967.56	-7240.56
G3-NC100	Lower Acacus	309387.5	626686.3	1727	9363.88	-7636.88
G3-NC100	L. Acacus MFS 3	309387.5	626686.3	1727	9445.56	-7718.56
G3-NC100	L. Acacus MFS 2	309387.5	626686.3	1727	9882.36	-8155.36
G3-NC100	L. Acacus MFS 1	309387.5	626686.3	1727	10222	-8495
G3-NC100	Tanezzuft Shale	309387.5	626686.3	1727	10441.39	-8714.39
H1-NC100	Middle Acacus	304764.2	638983.2	1683.27	8412.08	-6728.81

H1-NC100	Lower Acacus	304764.2	638983.2	1683.27	8847.26	-7163.99
H1-NC100	L. Acacus MFS 3	304764.2	638983.2	1683.27	8915.76	-7372.19
H1-NC100	L. Acacus MFS 2	304764.2	638983.2	1683.27	9383.38	-7700.11
H1-NC100	L. Acacus MFS 1	304764.2	638983.2	1683.27	9778.86	-8095.59
H1-NC100	Tanezzuft Shale	304764.2	638983.2	1683.27	9951.43	-8268.16
H2-NC100	Middle Acacus	307276.2	638514.6	1730.41	8530.42	-6800.01
H2-NC100	Lower Acacus	307276.2	638514.6	1730.41	8973.15	-7242.74
H2-NC100	L. Acacus MFS 3	307276.2	638514.6	1730.41	8915.76	-7372.19
H2-NC100	L. Acacus MFS 2	307276.2	638514.6	1730.41	9513.95	-7783.54
H2-NC100	L. Acacus MFS 1	307276.2	638514.6	1730.41	9816.62	-8086.21
H2-NC100	Tanezzuft Shale	307276.2	638514.6	1730.41	10016.59	-8286.18
H3-NC100	Middle Acacus	305658.8	639242.4	1711	8449.15	-6738.15
H3-NC100	Lower Acacus	305658.8	639242.4	1711	8891.86	-7180.86
H3-NC100	L. Acacus MFS 3	305658.8	639242.4	1711	8915.76	-7372.19
H3-NC100	L. Acacus MFS 2	305658.8	639242.4	1711	9420.54	-7709.54
H3-NC100	L. Acacus MFS 1	305658.8	639242.4	1711	9824.71	-8113.71
H3-NC100	Tanezzuft Shale	305658.8	639242.4	1711	9994.94	-8283.94
I1-NC100	Middle Acacus	314500.0	107333.3	1787	9600.56	-7813.56
I1-NC100	Lower Acacus	314500.0	107333.3	1787	10496.0	8709
I1-NC100	L. Acacus MFS 3	314500.0	107333.3	1787	9676	-7889
I1-NC100	L. Acacus MFS 2	314500.0	107333.3	1787	9971.2	-8184.2
I1-NC100	L. Acacus MFS 1	314500.0	107333.3	1787	10282.8	-8495.8
I1-NC100	Tanezzuft Shale	314500.0	107333.3	1787	10496.0	-8709
J1-NC100	Middle Acacus	295874.7	654668.2	1787.47	7547.48	-6148.48
J1-NC100	Lower Acacus	295874.7	654668.2	1787.47	7948.18	-6549.18
J1-NC100	L. Acacus MFS 3	295874.7	654668.2	1787.47	8057.89	-6317.65
J1-NC100	L. Acacus MFS 2	295874.7	654668.2	1787.47	8473.24	-7074.24
J1-NC100	L. Acacus MFS 1	295874.7	654668.2	1787.47	8730.86	-7245.87
J1-NC100	Tanezzuft Shale	295874.7	654668.2	1787.47	8763.95	-7364.95
K1-NC100	Middle Acacus	295868.8	640973	1579	8424.52	-6845.52
K1-NC100	Lower Acacus	295868.8	640973	1579	8835.6	-7256.6
K1-NC100	L. Acacus MFS 3	295868.8	640973	1579	8948.67	-7431.58
K1-NC100	L. Acacus MFS 2	295868.8	640973	1579	9388.67	-7809.67
K1-NC100	L. Acacus MFS 1	295868.8	640973	1579	9842.35	-8263.35
K1-NC100	Tanezzuft Shale	295868.8	640973	1579	9989.34	-8410.34
I1-NC100	Middle Acacus	331747.9	611004.82	1746	8864.99	-7118.99
I1-NC100	Lower Acacus	331747.9	611004.82	1746	9225.17	-7479.17
I1-NC100	L. Acacus MFS 3	331747.9	611004.82	1746	9333.47	-7587.47
L1-NC100	L. Acacus MFS 2	331747.9	611004.82	1746	9678.97	-7965.98
L1-NC100	L. Acacus MFS 1	331747.9	611004.82	1746	10011.56	-8265.56
L1-NC100	Tanezzuft Shale	331747.9	611004.82	1746	10443.68	-8697.68
L2-NC100	Middle Acacus	333477.82	611250.59	1719.36	8860.54	-7141.18
L2-NC100	Lower Acacus	333477.82	611250.59	1719.36	9224.49	-7505.13
L2-NC100	L. Acacus MFS 3	333477.82	611250.59	1719.36	9345.33	-7625.97
L2-NC100	L. Acacus MFS 2	333477.82	611250.59	1719.36	9698.57	-7989.78



L2-NC100	L. Acacus MFS 1	333477.82	611250.59	1719.36	9996.79	-8277.43
L2-NC100	Tanezzuft Shale	333477.82	611250.59	1719.36	10435.46	-8716.1
L3-NC100	Middle Acacus	332138.04	608848.25	1789.37	8943.95	-7154.58
L3-NC100	Lower Acacus	332138.04	608848.25	1789.37	9296.6	-7507.23
L3-NC100	L. Acacus MFS 3	332138.04	608848.25	1789.37	9415.88	-7626.51
L3-NC100	L. Acacus MFS 2	332138.04	608848.25	1789.37	9578.97	-7866.45
L3-NC100	L. Acacus MFS 1	332138.04	608848.25	1789.37	10059.48	-8270.11
L3-NC100	Tanezzuft Shale	332138.04	608848.25	1789.37	10418.26	-8628.89
L4-NC100	Middle Acacus	333105.77	610797.27	1727	8858.4	-7131.4
L4-NC100	Lower Acacus	333105.77	610797.27	1727	9214.82	-7487.82
L4-NC100	L. Acacus MFS 3	333105.77	610797.27	1727	9329.44	-7602.44
L4-NC100	L. Acacus MFS 2	333105.77	610797.27	1727	9778.97	-8865.98
L4-NC100	L. Acacus MFS 1	333105.77	610797.27	1727	9991.89	-8264.89
L4-NC100	Tanezzuft Shale	333105.77	610797.27	1727	10401.04	-8674.04
L5-NC100	Middle Acacus	332013.1	609639.18	1773	8941.07	-7168.07
L5-NC100	Lower Acacus	332013.1	609639.18	1773	9307.02	-7534.02
L5-NC100	L. Acacus MFS 3	332013.1	609639.18	1773	9420.1	-7647.1
L5-NC100	L. Acacus MFS 2	332013.1	609639.18	1773	9678.97	-7965.98
L5-NC100	L. Acacus MFS 1	332013.1	609639.18	1773	10088.76	-8315.76
L5-NC100	Tanezzuft Shale	332013.1	609639.18	1773	10479.94	-8706.94
M1-NC100	Middle Acacus	284148.4	648403.3	1307.71	7972.37	-6664.66
M1-NC100	Lower Acacus	284148.4	648403.3	1307.71	8357.32	-7049.61
M1-NC100	L. Acacus MFS 3	284148.4	648403.3	1307.71	8656.4	-6448.69
M1-NC100	L. Acacus MFS 2	284148.4	648403.3	1307.71	8910.4	-7602.69
M1-NC100	L. Acacus MFS 1	284148.4	648403.3	1307.71	8913.9	-7906.19
M1-NC100	Tanezzuft Shale	284148.4	648403.3	1307.71	9206.38	-7898.67
N1-NC100	Middle Acacus	310776.5	648568.6	1606.2	7705.25	-6099.05
N1-NC100	Lower Acacus	310776.5	648568.6	1606.2	8190.07	-6583.87
N1-NC100	L. Acacus MFS 3	310776.5	648568.6	1606.2	8350.65	-6289.06
N1-NC100	L. Acacus MFS 2	310776.5	648568.6	1606.2	8725.05	-7118.85
N1-NC100	L. Acacus MFS 1	310776.5	648568.6	1606.2	8862.50	-7256.3
N1-NC100	Tanezzuft Shale	310776.5	648568.6	1606.2	8880.67	-7274.47
O1-NC100	Middle Acacus	292517.3	613978.15	1743	9770.53	-8027.53
O1-NC100	Lower Acacus	292517.3	613978.15	1743	10169.43	-8426.43
O1-NC100	L. Acacus MFS 3	292517.3	613978.15	1743	10282.5	-8539.5
O1-NC100	L. Acacus MFS 2	292517.3	613978.15	1743	10658.11	-8915.11
O1-NC100	L. Acacus MFS 1	292517.3	613978.15	1743	10959.1	-9216.1
O1-NC100	Tanezzuft Shale	292517.3	613978.15	1743	11236.91	-9493.91
O2-NC100	Middle Acacus	293874.65	614352.6	1720	9735.36	-8015.36
O2-NC100	Lower Acacus	293874.65	614352.6	1720	10128.39	-8408.39
O2-NC100	L. Acacus MFS 3	293874.65	614352.6	1720	10282.5	-8539.5
O2-NC100	L. Acacus MFS 2	293874.65	614352.6	1720	10623.43	-8903.43
O2-NC100	L. Acacus MFS 1	293874.65	614352.6	1720	10923.16	-9203.16
O2-NC100	Tanezzuft Shale	293874.65	614352.6	1720	11215.51	-9495.51
P1-NC100	Middle Acacus	302288.99	595066.41	1689	10057.89	-8713.98

P1-NC100	Lower Acacus	302288.99	595066.41	1689	10449.79	-8760.79
P1-NC100	L. Acacus MFS 3	302288.99	595066.41	1689	10623.75	-9875.75
P1-NC100	L. Acacus MFS 2	302288.99	595066.41	1689	10934.09	-9245.09
P1-NC100	L. Acacus MFS 1	302288.99	595066.41	1689	11219.96	-9530.96
P1-NC100	Tanezzuft Shale	302288.99	595066.41	1689	11503.77	-9814.77
P2-NC100	Middle Acacus	302288.99	595066.41	1689	10578.60	-8889.6
P2-NC100	Lower Acacus	302288.99	595066.41	1689	11499.68	-9810.68
P2-NC100	L. Acacus MFS 3	302288.99	595066.41	1689	10705.92	-9016.92
P2-NC100	L. Acacus MFS 2	302288.99	595066.41	1689	10922.4	-9233.4
P2-NC100	L. Acacus MFS 1	302288.99	595066.41	1689	11316.07	-9627.07
P2-NC100	Tanezzuft Shale	302288.99	595066.41	1689	11499.68	-9810.68
Q1-NC100	Middle Acacus	302168.11	612392.81	1585.47	9487.98	-7902.51
Q1-NC100	Lower Acacus	302168.11	612392.81	1585.47	9841.28	-8255.81
Q1-NC100	L. Acacus MFS 3	302168.11	612392.81	1585.47	9949.58	-8364.11
Q1-NC100	L. Acacus MFS 2	302168.11	612392.81	1585.47	10364.28	-8799.28
Q1-NC100	L. Acacus MFS 1	302168.11	612392.81	1585.47	10604.16	-9018.69
Q1-NC100	Tanezzuft Shale	302168.11	612392.81	1585.47	10948.44	-9362.97
Q2-NC100	Middle Acacus	301445.72	610783.6	1565	9541.58	-7976.58
Q2-NC100	Lower Acacus	301445.72	610783.6	1565	9887.34	-8322.34
Q2-NC100	L. Acacus MFS 3	301445.72	610783.6	1565	9949.58	-8364.11
Q2-NC100	L. Acacus MFS 2	301445.72	610783.6	1565	10364.28	-8799.28
Q2-NC100	L. Acacus MFS 1	301445.72	610783.6	1565	10639.34	-9074.34
Q2-NC100	Tanezzuft Shale	301445.72	610783.6	1565	10894.17	-9329.17
Q3-NC100	Middle Acacus	302676.87	610274.57	1585	9567.43	-7982.43
Q3-NC100	Lower Acacus	302676.87	610274.57	1585	9920.73	-8335.73
Q3-NC100	L. Acacus MFS 3	302676.87	610274.57	1585	10027.48	-8442.48
Q3-NC100	L. Acacus MFS 2	302676.87	610274.57	1585	10364.28	-8799.28
Q3-NC100	L. Acacus MFS 1	302676.87	610274.57	1585	10694.59	-9109.59
Q3-NC100	Tanezzuft Shale	302676.87	610274.57	1585	11024.27	-9439.27
R1-NC100	Middle Acacus	322239.8	601430.1	1645	9578.90	-7917.54
R1-NC100	Lower Acacus	322239.8	601430.1	1645	9631.14	-7986.14
R1-NC100	L. Acacus MFS 3	322239.8	601430.1	1645	9777.57	-8132.57
R1-NC100	L. Acacus MFS 2	322239.8	601430.1	1645	10212.7	-8616.98
R1-NC100	L. Acacus MFS 1	322239.8	601430.1	1645	10456.68	-8811.68
R1-NC100	Tanezzuft Shale	322239.8	601430.1	1645	10799.35	-9154.35
S1-NC100	Middle Acacus	301084.7	616627.3	1659	9470.12	-7811.12
S1-NC100	Lower Acacus	301084.7	616627.3	1659	9870.36	-8211.36
S1-NC100	L. Acacus MFS 3	301084.7	616627.3	1659	9919.12	-8345.66
S1-NC100	L. Acacus MFS 2	301084.7	616627.3	1659	10367.13	-8708.13
S1-NC100	L. Acacus MFS 1	301084.7	616627.3	1659	10661.21	-9002.21
S1-NC100	Tanezzuft Shale	301084.7	616627.3	1659	10894.05	-9235.05
S2-NC100	Middle Acacus	297854.3	617465.26	1573.46	9416.79	-7843.33
S2-NC100	Lower Acacus	297854.3	617465.26	1573.46	9797.76	-8224.3
S2-NC100	L. Acacus MFS 3	297854.3	617465.26	1573.46	9919.12	-8345.66
S2-NC100	L. Acacus MFS 2	297854.3	617465.26	1573.46	10288.71	-8715.25

S2-NC100	L. Acacus MFS 1	297854.3	617465.26	1573.46	10588.27	-9014.81
S2-NC100	Tanezzuft Shale	297854.3	617465.26	1573.46	10824.91	-9251.45
S3-NC100	Middle Acacus	301408.5	617361.6	1648.5	9494.92	-7846.42
S3-NC100	Lower Acacus	301408.5	617361.6	1648.5	9905.59	-8257.09
S3-NC100	L. Acacus MFS 3	301408.5	617361.6	1648.5	9929.16	-8295.66
S3-NC100	L. Acacus MFS 2	301408.5	617361.6	1648.5	10402.02	-8753.52
S3-NC100	L. Acacus MFS 1	301408.5	617361.6	1648.5	10714.07	-9065.57
S3-NC100	Tanezzuft Shale	301408.5	617361.6	1648.5	10968.21	-9319.71
S4-NC100	Middle Acacus	296754.3	618125.26	1688.46	9905.6	-8217.14
S4-NC100	Lower Acacus	296754.3	618125.26	1688.46	10869.92	-9181.46
S4-NC100	L. Acacus MFS 3	296754.3	61812.26	1688.46	10086	-8397.54
S4-NC100	L. Acacus MFS 2	296754.3	618125.26	1688.46	10364.8	-8676.34
S4-NC100	L. Acacus MFS 1	296754.3	618125.26	1688.46	10584.56	-9181.46
S4-NC100	Tanezzuft Shale	296754.3	618125.26	1688.46	10869.92	-9181.46
T1-NC100	Middle Acacus	310785.2	622843.6	1726	8991.82	-7265.82
T1-NC100	Lower Acacus	310785.2	622843.6	1726	9385.85	-7659.85
T1-NC100	L. Acacus MFS 3	310785.2	622843.6	1726	9534.87	-7989.93
T1-NC100	L. Acacus MFS 2	310785.2	622843.6	1726	9859.5	-8133.5
T1-NC100	L. Acacus MFS 1	310785.2	622843.6	1726	10185.54	-8459.54
T1-NC100	Tanezzuft Shale	310785.2	622843.6	1726	10391.35	-8665.35
T2-NC100	Middle Acacus	311091.8	623740.9	1742	8988.08	-7246.08
T2-NC100	Lower Acacus	311091.8	623740.9	1742	9382.16	-7640.16
T2-NC100	L. Acacus MFS 3	311091.8	623740.9	1742	9497.5	-7755.5
T2-NC100	L. Acacus MFS 2	311091.8	623740.9	1742	9867.92	-8125.92
T2-NC100	L. Acacus MFS 1	311091.8	623740.9	1742	10209.79	-8467.79
T2-NC100	Tanezzuft Shale	311091.8	623740.9	1742	10420.7	-8678.7
U1-NC100	Middle Acacus	309360.56	639595.25	1748.03	8419.76	-6419.76
U1-NC100	Lower Acacus	309360.56	639595.25	1748.03	8878.96	-6878.96
U1-NC100	L. Acacus MFS 3	309360.56	639595.25	1748.03	8675.98	-7356.87
U1-NC100	L. Acacus MFS 2	309360.56	639595.25	1748.03	9164.32	-7164.32
U1-NC100	L. Acacus MFS 1	309360.56	639595.25	1748.03	9496.4	-7896.4
U1-NC104	Tanezzuft Shale	309360.56	639595.25	1748.03	3639.92	-3639.92
V1-NC100	Middle Acacus	308533	565098.6	1705.54	10200.8	-10200.8
V1-NC100	Lower Acacus	308533	565098.6	1705.54	10463.2	-10463.2
V1-NC100	L. Acacus MFS 3	308533	565098.6	1705.54	10660.12	-8953.98
V1-NC100	L. Acacus MFS 2	308533	565098.6	1705.54	10889.6	-10889.6
V1-NC100	L. Acacus MFS 1	308533	565098.6	1705.54	11201.2	-11201.2
V1-NC100	Tanezzuft Shale	308533	565098.6	1705.54	11516.08	-11516.08
V2-NC100	Middle Acacus	307325.3	565455	1708.17	10292.64	-10292.64
V2-NC100	Lower Acacus	307325.3	565455	1708.17	10555.04	-10555.04
V2-NC100	L. Acacus MFS 3	307325.3	565455	1708.17	10660.12	-8953.98
V2-NC100	L. Acacus MFS 2	307325.3	565455	1708.17	10879.76	-10879.76
V2-NC100	L. Acacus MFS 1	307325.3	565455	1708.17	11266.8	-11266.8
V2-NC100	Tanezzuft Shale	307325.3	565455	1708.17	11621.04	-11621.04
X1-NC100	Middle Acacus	289027.8	589471.7	1531.43	9948.24	-9948.24

X1-NC100	Lower Acacus	289027.8	589471.7	1531.43	10315.6	-10315.6
X1-NC100	L. Acacus MFS 3	289027.8	589471.7	1531.43	10487.12	-9134.98
X1-NC100	L. Acacus MFS 2	289027.8	589471.7	1531.43	10561.6	-10561.6
X1-NC100	L. Acacus MFS 1	289027.8	589471.7	1531.43	10906	-10906
X1-NC100	Tanezzuft Shale	289027.8	589471.7	1531.43	11237.28	-11237.28
Y1-NC100	Middle Acacus	311937.7	582954.1	1676.02	9833.44	-9833.44
Y1-NC100	Lower Acacus	311937.7	582954.1	1676.02	10141.76	-10141.76
Y1-NC100	L. Acacus MFS 3	311937.7	582954.1	1676.02	10270.87	-8573.92
Y1-NC100	L. Acacus MFS 2	311937.7	582954.1	1676.02	10414.34	-10414
Y1-NC100	L. Acacus MFS 1	311937.7	582954.1	1676.02	10945.36	-10945.36
Y1-NC100	Tanezzuft Shale	311937.7	582954.1	1676.02	11060.16	-11060.16
Z1-NC100	Middle Acacus	292926.9	561470.1	1726.48	10630.48	-10630.48
Z1-NC100	Lower Acacus	292926.9	561470.1	1726.48	10896.1	-10896.1
Z1-NC100	L. Acacus MFS 3	292926.9	561470.1	1726.48	10988.8	9224.87-
Z1-NC100	L. Acacus MFS 2	292926.9	561470.1	1726.48	11201.2	-11201.2
Z1-NC100	L. Acacus MFS 1	292926.9	561470.1	1726.48	11562	-11562
Z1-NC100	Tanezzuft Shale	292926.9	561470.1	1726.48	11972	-11972
Z2-NC100	Middle Acacus	296134	559449.3	1798.62	10699.36	-10699.36
Z2-NC100	Lower Acacus	296134	559449.3	1798.62	10961.7	-10961.7
Z2-NC100	L. Acacus MFS 3	296134	559449.3	1798.62	11012.98	-9257.98
Z2-NC100	L. Acacus MFS 2	296134	559449.3	1798.62	11276.64	-11276.64
Z2-NC100	L. Acacus MFS 1	296134	559449.3	1798.62	11758.8	-11758.8
Z2-NC100	Tanezzuft Shale	296134	559449.3	1798.62	12021.2	-12021.2
Z3-NC100	Middle Acacus	291612.7	560752.7	1670.7	10814.16	-9645.32
Z3-NC100	Lower Acacus	291612.7	560752.7	1670.7	10883.04	-9712.44
Z3-NC100	L. Acacus MFS 3	291612.7	560752.7	1670.7	11017.94	-9347.88
Z3-NC100	L. Acacus MFS 2	291612.7	560752.7	1670.7	11201.2	-9531.50
Z3-NC100	L. Acacus MFS 1	291612.7	560752.7	1670.7	11578.4	-9908.4
Z3-NC100	Tanezzuft Shale	291612.7	560752.7	1670.7	11975.28	-10304.58

**Table 3. Core intervals (depths) in the Lower Acacus Formation, Concession NC100, Ghadames Basin, NW Libya. (Note, the highlighted boxes are examined cores).**

<b>CORE INTERVAL OF LOWER ACACUS FM. NC100.</b>									
<b>Well</b>	<b>Total No. cores</b>	<b>No. core L.A.F</b>	<b>Core No:1 (ft)</b>	<b>Core No:2 (ft)</b>	<b>Core No:3 (ft)</b>	<b>Core No:4 (ft)</b>	<b>Core No:5 (ft)</b>	<b>Core No:6 (ft)</b>	<b>Core No:7 (ft)</b>
<b>C2</b>	<b>8</b>	<b>6</b>	9259.4 - 9316.8	<b>9403.7 - 9462.8</b>	9531.6 - 9577.6	9659.6 - 9715.3	9747 - 9797.3	9908.8 - 9967.9	
<b>D1</b>	<b>3</b>	<b>1</b>	10815 - 10873						
<b>F1</b>	<b>3</b>	<b>3</b>	9161 - 9187	9220 - 9275.8	9275.8 - 9334.8				
<b>G1</b>	<b>2</b>	<b>2</b>	9610.4 - 9649.7	9954.8 - 9971.2					
<b>H1</b>	<b>3</b>	<b>3</b>	9387.3 - 9446.4	9476 - 9531.6	9531.6 - 9590.7				
<b>I1</b>	No cores								
<b>J1</b>	<b>2</b>	<b>1</b>	9026 - 9075	8623 - 8682.1					
<b>K1</b>	<b>1</b>	<b>1</b>	2646.4 - 9705.5						
<b>L1</b>	<b>1</b>	<b>1</b>	10063 - 10122						
<b>L3</b>	<b>6</b>	<b>6</b>	9111.8 - 9145.9	<b>9311.9 - 9325</b>	<b>9325 - 9338.1</b>	9748.1- 9797	9936.4- 9961.3	10105.6 -10139.4	
<b>N1</b>	No cores								
<b>O1</b>	No cores								
<b>P1</b>	<b>2</b>	<b>2</b>	11325 - 11355	11355 - 11384.8					
<b>Q1</b>	<b>4</b>	<b>4</b>	<b>10465.5 -10496</b>	<b>10533.3- 10558</b>	<b>10558.3- 10604</b>	<b>10665.2- 10640.3</b>			
<b>R1</b>	No cores								
<b>S2</b>	<b>8</b>	<b>7</b>	10276- 10335.2	10436.9- 10476	10505.8- 10528.8	10528.8- 10579.6	10620.6- 10653.4	10653.4- 10702.6	10705.9- 10745.2
<b>T1</b>	<b>3</b>	<b>3</b>	10171- 10190.9	10213- 10234.9	10234.9- 10259				
<b>V2</b>	<b>2</b>	<b>2</b>	11371.7 - 11427.5	11591.5 - 11535					
<b>Y1</b>	<b>4</b>	<b>4</b>	10856.8 -10888	10888- 10930.6	11273- 11284.8	11320.9- 11378			
<b>Z1</b>	<b>3</b>	<b>3</b>	<b>11680- 11706.3 ft</b>						
<b>Z2</b>	<b>3</b>	<b>3</b>	10833- 10883	11650- 11709.6	11709- 11758.8	11932.6- 11955.6	11955.6- 11998	11998- 12024	
<b>Z3</b>	<b>5</b>	<b>5</b>	11575- 11634	11634- 11683.2	<b>11709.6- 11748.9</b>	11883.4- 11912.9	11912.9- 11935		

**Note:** Core recovery (%) of core No.: 2 in well C2-NC100 = 50%

- Core recovery (%) of core No.: 2 in well L3-NC100 = 45%

- Core recovery (%) of core No.: 3 in well L3-NC100 = 45%

- Core recovery (%) of core No.: 1 in well Q1-NC100 = 55%

- Core recovery (%) of core No.: 3 in well Q1-NC100 = 70%

- Core recovery (%) of core No.: 1 in well Z1-NC100 = 16%

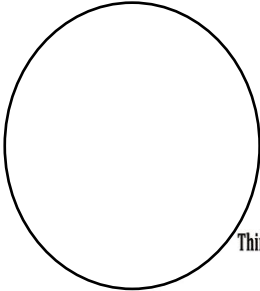
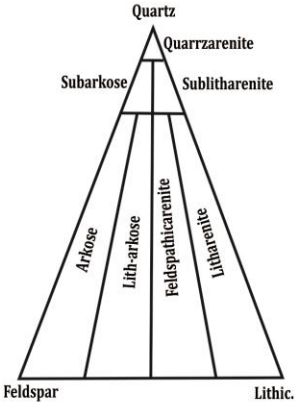
- Core recovery (%) of core No.: 3 in well Z3-NC100 = 35%

## CORE DESCRIPTION

**Well:** \_\_\_\_\_ **Formation:** \_\_\_\_\_  
**Area:** \_\_\_\_\_ **Core No. #:** \_\_\_\_\_ **interval: (ft)** \_\_\_\_\_

TYPE LOG CORED INTERVAL <small>GR (API)</small>	DEPTH (ft)	SEDIMENTARY STRUCTURE	GRAIN SIZE								DESCRIPTION	OIL STAIN POROSITY				LITHOFACIES
			SH	SLT	VF	F	M	C	VC	CON		H	M	L	P	
	4 } ft 0															

**Figure 13. Core description sheet used for describing core samples.**

Modal Analysis of some selected samples of : ..... Formation			Well : Sample depth :
<b>Sandstone unit:</b>			
<p>Sample number</p> <p>Mean grain size</p> <p>Sorting</p> <p>Rounding</p> <p>Architectures (total)</p> <p>Volume percent</p> <p>FrameWork</p> <p>Matrix</p> <p>Cement</p> <p>Porosity</p> <p>Framework (total %)</p> <p>Quartz</p> <p>Feldspar</p> <p>Rock fragments</p> <p>Pyroxene</p> <p>Amphibole</p> <p>Biotite</p> <p>Opaque</p> <p>Allochemes</p> <p>Interframework (total%)</p> <p>Volume percent</p> <p>Clay coat</p> <p>Clay rim</p> <p>Clay proefill</p> <p>Calcite porefill</p> <p>Zeolite Porefill</p> <p>Hematite cement</p> <p>Celadonite</p> <p>Calcite replacment</p> <p>Chlorozition</p>	 <p style="text-align: right; margin-right: 10px;">Thin-section view</p>	 <p style="text-align: center; margin-top: 5px;">Classification of SST. (Folk, 1980).</p>	
<p>Mean grain size:</p> <p>PC : pebble conglomerate</p> <p>GC : granular conglomerate</p> <p>CS : coarse sanstone</p> <p>MS : medium sandstone</p> <p>FS : fine sandstone</p>	<p>Sorting:</p> <p>M : moderate</p> <p>P : poor</p> <p>VP : very poor</p>	<p>Rounding:</p> <p>SR : subrounded</p> <p>SA : subangular</p> <p>A : angular</p>	<p>Quality:</p> <p>Ab : abundant more 10</p> <p>C : common 1-10</p> <p>R : rare less 0.1</p>
<p>Data must be obtained from point counting thin-sections</p>			

**Figure 14. Petrographic description sheet used for model analysis of thin sections in the study area, concession NC100.**

## **4. LITHOFACIES TYPES OF LOWER ACACUS FORMATION.**

Lithofacies types and vertical profile models of reservoir rocks have been studied by many researches including (N. Eyles CH- Eyles & Mail, 1983; Deutch, 1998; Klingbeil et al. 1999; Hoang Van Tha et al., 2015; Cant and Walker, 1976; Y. Zee Ma et al., 2016).

Lithofacies is comprehensive performance for sedimentary environments on the lithological characters of sediments including color, rock texture, and sedimentary structures, based on these features, lithofacies can reflect paleoflow conditions and the different ways of sediment transportation.

By viewing and describing the cores of five wells and analyzing the data by integrated well-logs (GR/SP), the Lower Acacus Formation can be divided into numbers of lithofacies types could be defined by combination and integrated study of cores description and wireline-logs characteristics as following:

### **4.1 Core descriptions.**

One of the most essential steps in facies analysis of clastic reservoirs interpretation of available cores. According to Archer et al, (1986), a core can be defined as a sample of rock from a well section generally obtained by drilling into the formation with a hollow section drill pipe or bit, was observed and described based on descriptive parameters, which include rock color, grain size trend, texture (sorting, and roundness), ichnofossils, lithology, primary and secondary sedimentary structures. An important result of core description is the subdivision of cores into lithofacies.

A total of (215ft) of cores were recovered from the Lower Acacus Formation in five penetrated wells in different intervals (Table 4), and (Fig. 15). Examination and description of these cores identified five lithofacies including:

- (1) -Bioturbated marine silty shale lithofacies.
- (2) -Reworked marine sandstone lithofacies.
- (3) -Distal delta front silty sandstone lithofacies.
- (4) -Proximal delta front-coastal sandstone lithofacies.
- (5) -Fluvial channel sandstone lithofacies.



**Table 4. Shows the available cores cut in the Lower Acacus Formation in some drilled wells of concession NC100, Ghadames Basin.**

<b>Well Name</b>	<b>Core Number</b>	<b>Lithofacies No.</b>	<b>Core Interval (ft)</b>	<b>Core Description (Fig. No.)</b>	<b>Core photo (Fig. No.)</b>
<b>C2-NC100</b>	<b>Core # 2</b>	<b>1 &amp; 2</b>	<b>9403 - 9463</b>	<b>16</b>	<b>17</b>
<b>Q1-NC100</b>	<b>Core # 1</b>	<b>1, 2, 3 &amp; 4</b>	<b>10465.4 - 10496</b>	<b>19</b>	<b>20</b>
<b>Q1-NC100</b>	<b>Core # 3</b>	<b>1, 2, 3 &amp; 4</b>	<b>10558 - 10604.2</b>	<b>22</b>	<b>23</b>
<b>L3-NC100</b>	<b>Core # 2, 3</b>	<b>1, 2, &amp; 4</b>	<b>9312 - 9338.8</b>	<b>31</b>	<b>32</b>
<b>Z1-NC100</b>	<b>Core # 1</b>	<b>5</b>	<b>11680 - 11706</b>	<b>25</b>	<b>26</b>
<b>Z3-NC100</b>	<b>Core # 3</b>	<b>5</b>	<b>11709.5 - 11749</b>	<b>28</b>	<b>29</b>

The description of these lithofacies can be summarized as following:

**(1) – Bioturbated marine silty shales lithofacies.**

This sediments consists mainly of thick sequences of greenish grey to dark grey silty shale occasionally micaceous (Figs. 16 and 17), with rippled lenticular silty sandstone lenses (Fig. 18a), bioturbated at base and gradually increasing above in grain size. This lithofacies is regionally extensive across the study area characterized log high GR- reading of serrated to featureless GR. Motive as in well C2-NC100 Core#2, @ 9425 – 9462ft (Fig. 16). The bioturbation and the lenticular laminae resembling ripple laminae suggest deposition from episodic low energy currents basin of moderate-depth setting.

**(2) – Reworked marine sandstone lithofacies.**

These sediments are composed of very fine to fine-grained sandstone, light greenish grey, with wavy, intercalated sand lenses and shales streaks (Fig. 17 and 18b), ranging in thickness from 1.7-18.5ft, characterized by either fining or coarsening upward, spiky GR-log motif as in well C2-NC100 @ 9413-9421ft, well K1-NC100 @ 9120-9131ft, well N1-NC100 @ 8410-8420ft. These sandstones are of lense shaped usually enclosed between marine shales and much common in the north and northwestern part of study area which may suggest its marine origin. This lithofacies can also be seen in cores of other wells (Figs. 16, 23 and 25).

# RECOVERED CORE INTERVALS

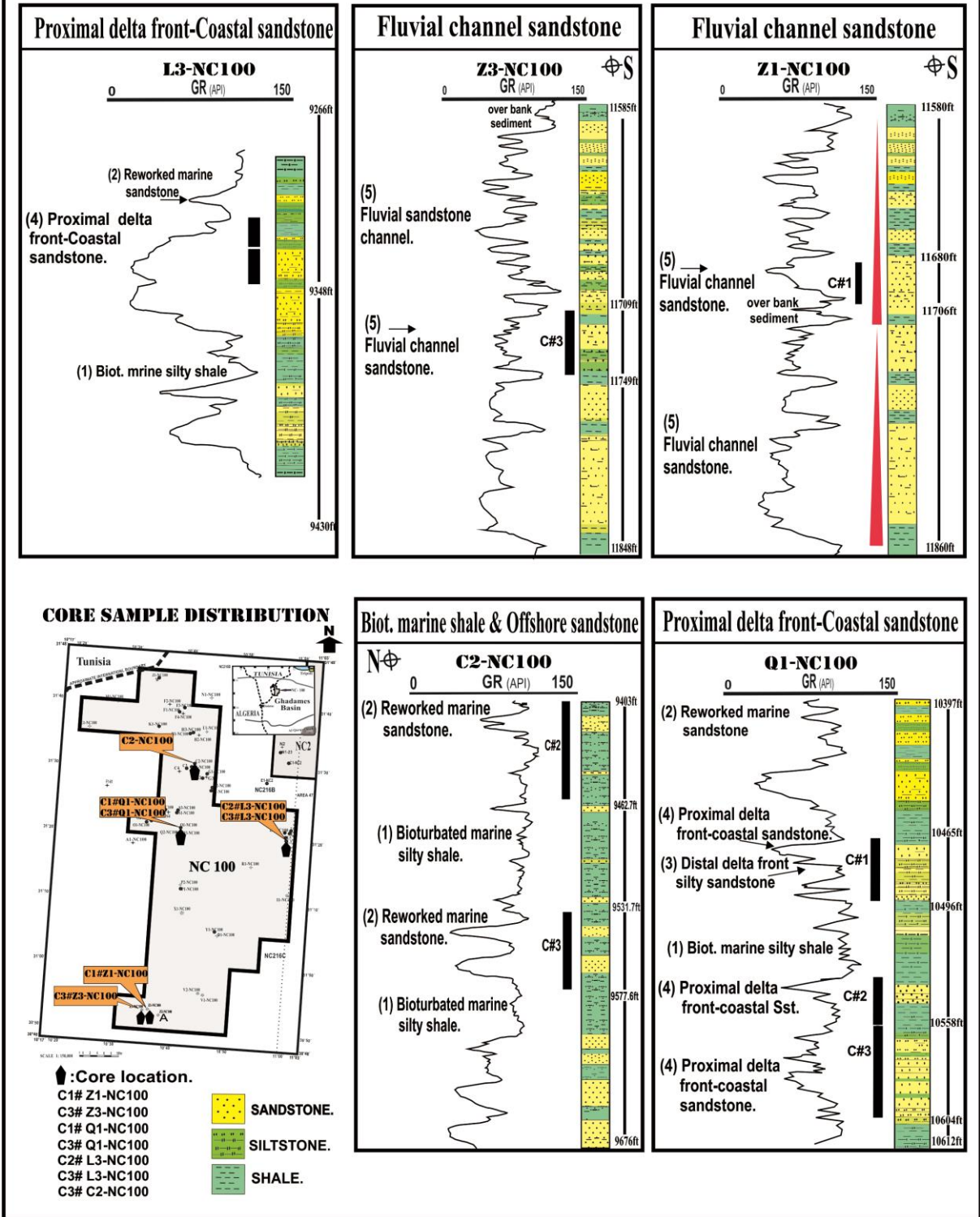


Figure 15. Showing wells location, cored intervals, and GR-log motifs of the identified lithofacies of Lower Acacus Formation, Concession NC100, Ghadames Basin NW Libya.

- Lithofacies (1) - Bioturbation marine silty shale.
- Lithofacies (2) - Reworked marine sandstone.
- Lithofacies (3) - Distal delta front silty sandstone.
- Lithofacies (4) - Proximal delta front-coastal sandstone.
- Lithofacies (5) - Fluvial channel sandstone.

## LITHOLOGICAL DESCRIPTION CORE

Well: C2-NC100    Formation: Lower Acacus Formation    Core#: 2    interval: 9403' - 9463'  
 Area: Concession NC100, Ghadames Basin, NW Libya

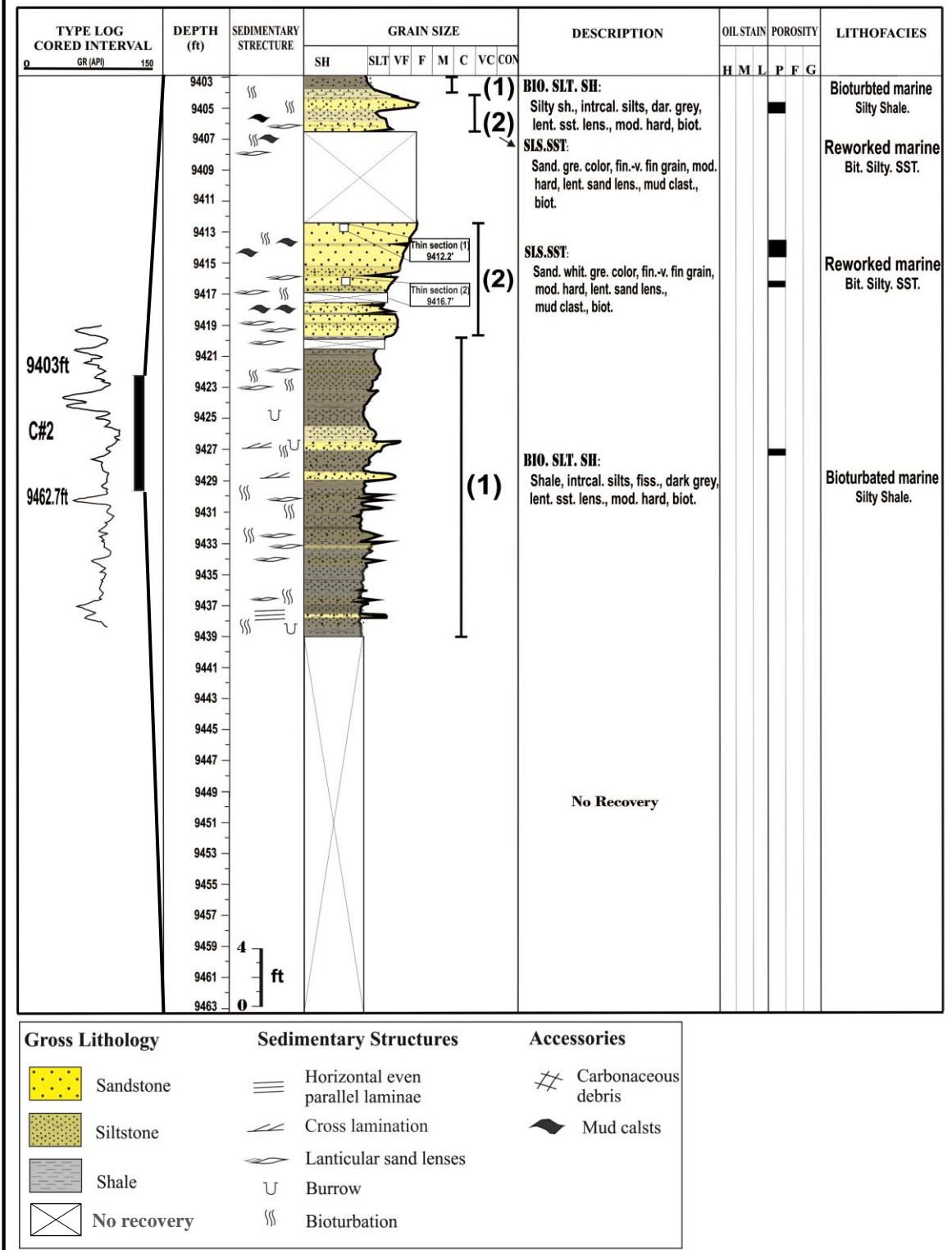


Figure 16. Graphic log of core samples cut in the bioturbation marine silty shale and reworked marine sandstone lithofacies of Lower Acacus Formation in well C2-NC100, core # (2), concession NC100, Ghadames Basin, NW Libya.

Well: C2-NC100 Formation: Lower Acacus Formation Core#: 2 interval: 9403' - 9462.8'  
 Area: Concession NC100, Ghadames Basin, NW Libya

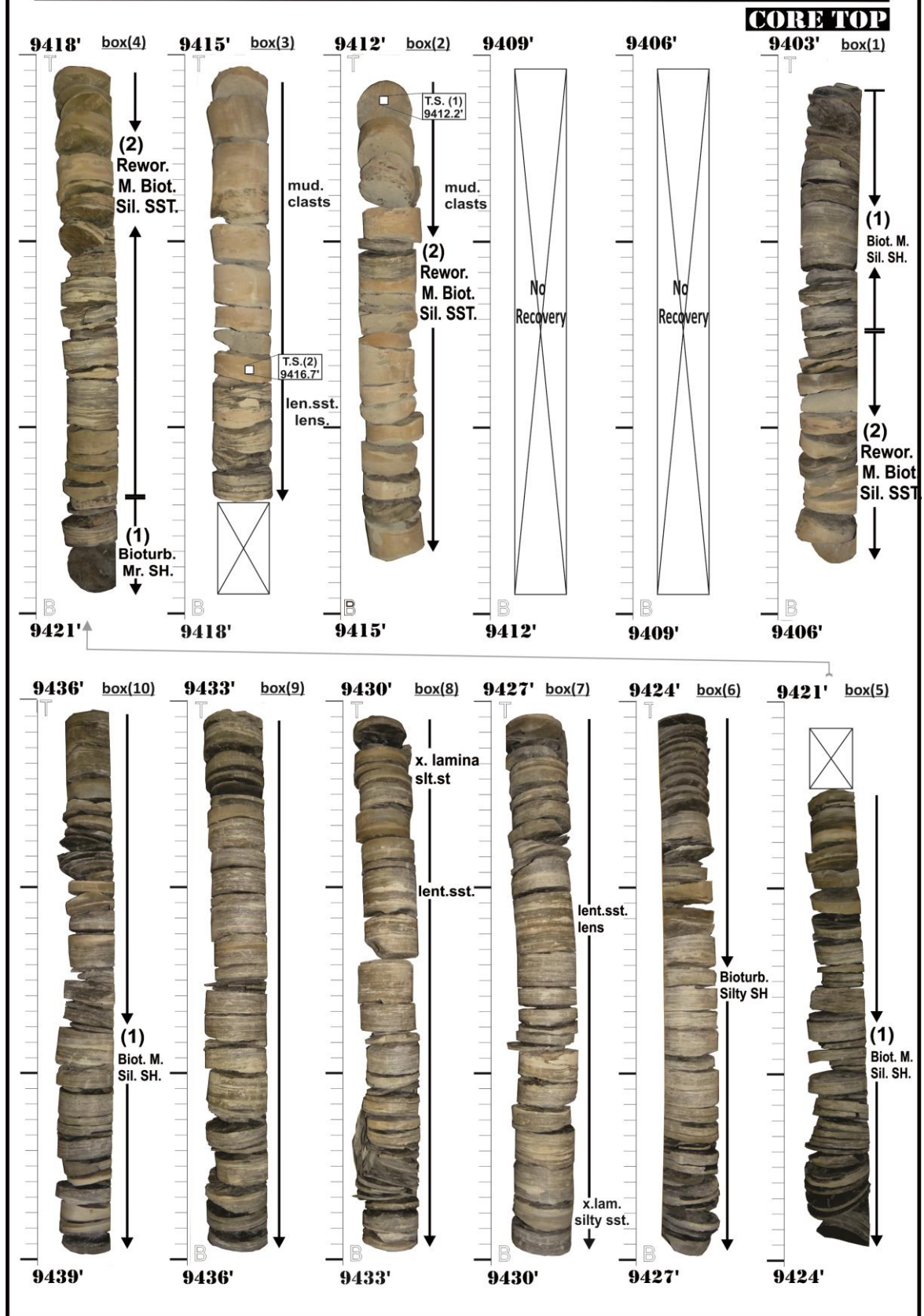
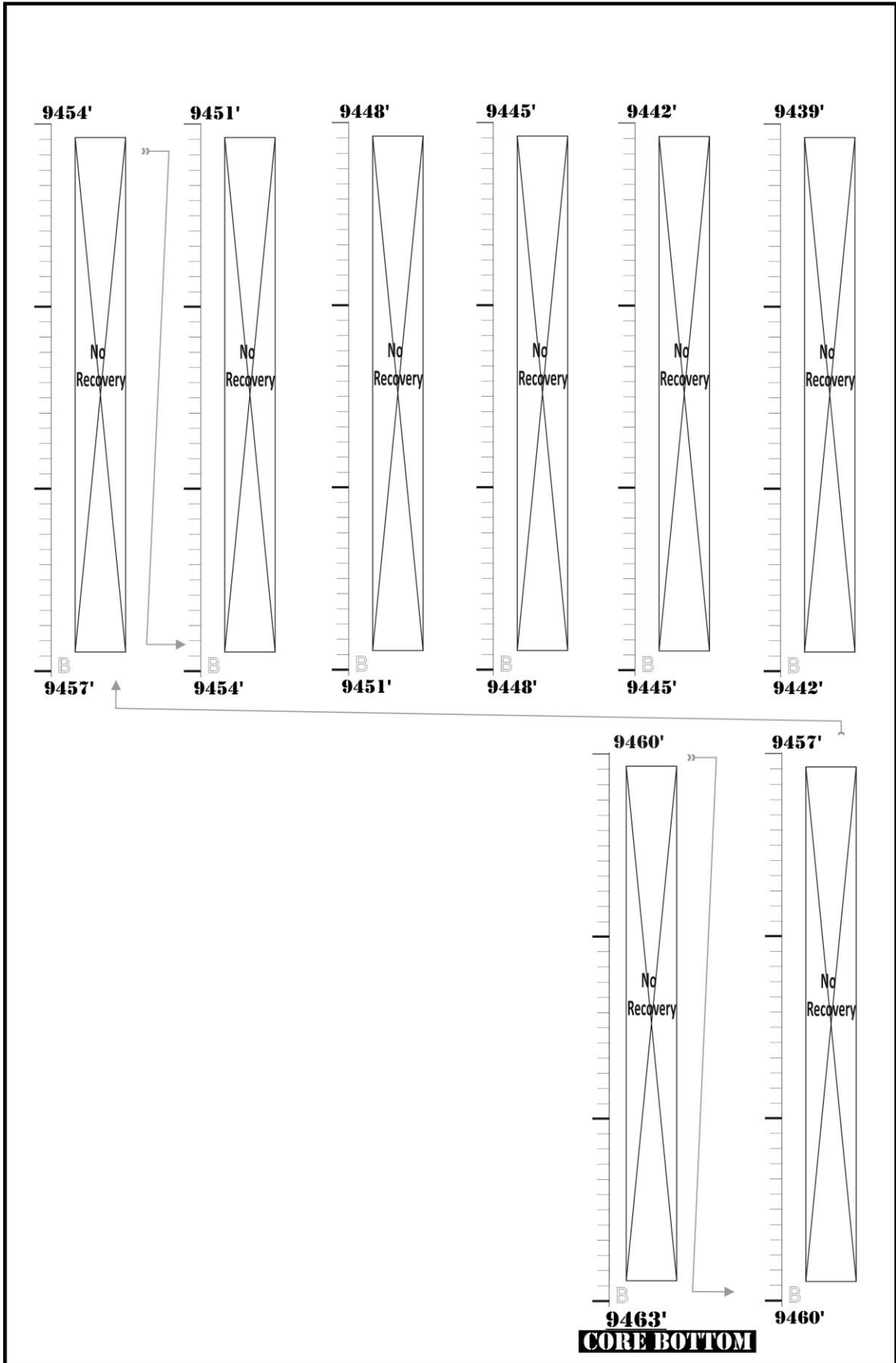


Figure 17. Cores samples (core # 2), cut in Lower Acacus Formation, well C2-NC100, concession NC100, Ghadames Basin, NW Libya.

Cont.... (Figure 17).



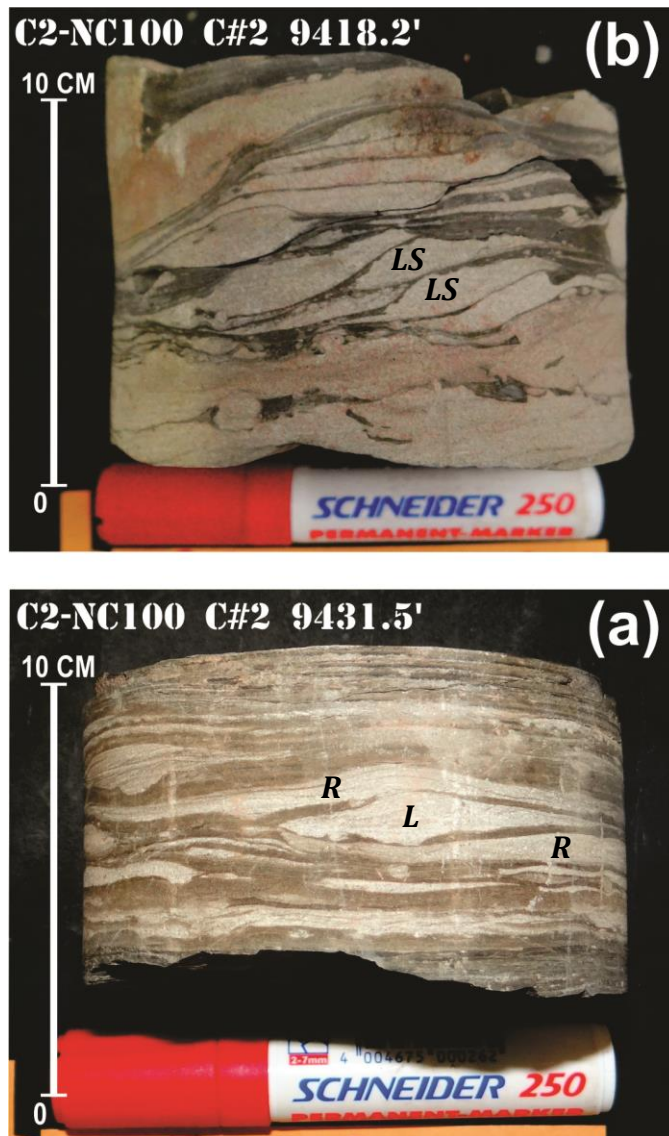


Figure 18. Core samples showing: (a) - Bioturbated marine silty shale lithofacies @9431.5', with intercalated rippled {R} and lenticular {L} silty sandstone lenses. (b)- Reworked marine sandstone lithofacies @9418.2', with wavy to cross lenticular sand lenses {LS} and enclosed shale laminae, well C2-NC100, Lower Acacus Formation, core (2), concession NC100, Ghadames Basin.

### **(3) - Distal delta front silty sandstone lithofacies.**

This lithofacies consists of very silty sandstone with a thickness of (2.5-7ft) occasionally alternating silty sandstone with shale and of vertical burrows (Fig 21a), showing deformed lenticular sand lenses as in well Q1-NC100 (Fig. 21b), may be due to subsidence of sands into soft mud. It's characterized by gradational contact with the underlying bioturbated silty shale and the overlying proximal delta front and coastal sandstone (Figs. 20-23). This lithofacies may be characterized by parallel to cross laminations at the base to bioturbation at the middle to more shaly at top at some intervals (Fig 24a) as it reveals general decrease in energy upward.

### **(4) - Proximal delta front-coastal sandstone lithofacies.**

This lithofacies consists of very fine to fine grained, occasionally medium grained at places, moderately sorted, sub angular to rounded, showing upward decrease in clay contents, calcareous in parts, with thickness ranging from 14-35ft where gradual decrease in thickness is noticeable northward as in well T1-NC100, and G1-NC100, with common parallel laminations (Fig. 21), with some rip-up clasts (Fig. 21c, in well Q1-NC100 @ 10469.5ft), occasionally with finally parallel lamination (Fig. 24b) and of heavily bioturbation (Fig. 24c). This lithofacies is most prominent in the middle and northeastern part of the concession NC100, in the vicinity of well Q1-NC100 (Figs. 22, 23), well O1-NC100, S2-NC100, and L1-NC100.

This lithofacies may be regarded as coastal sandstone as in well L3-NC100 (Figs. 25 and 26), which could be described as partially bioturbated sandstone alternating with some silty laminae at places, where silt to sand gradation can be seen at some places (Figs. 27a, and 27b). This lithofacies was also recovered from examined cores in other wells (Figs, 22-27).





Well: Q1-NC100 Formation: Lower Acacus Formation Core#: 1 interval: 10465.4' - 10495'  
 Area: Concession NC100, Ghadames Basin, NW Libya

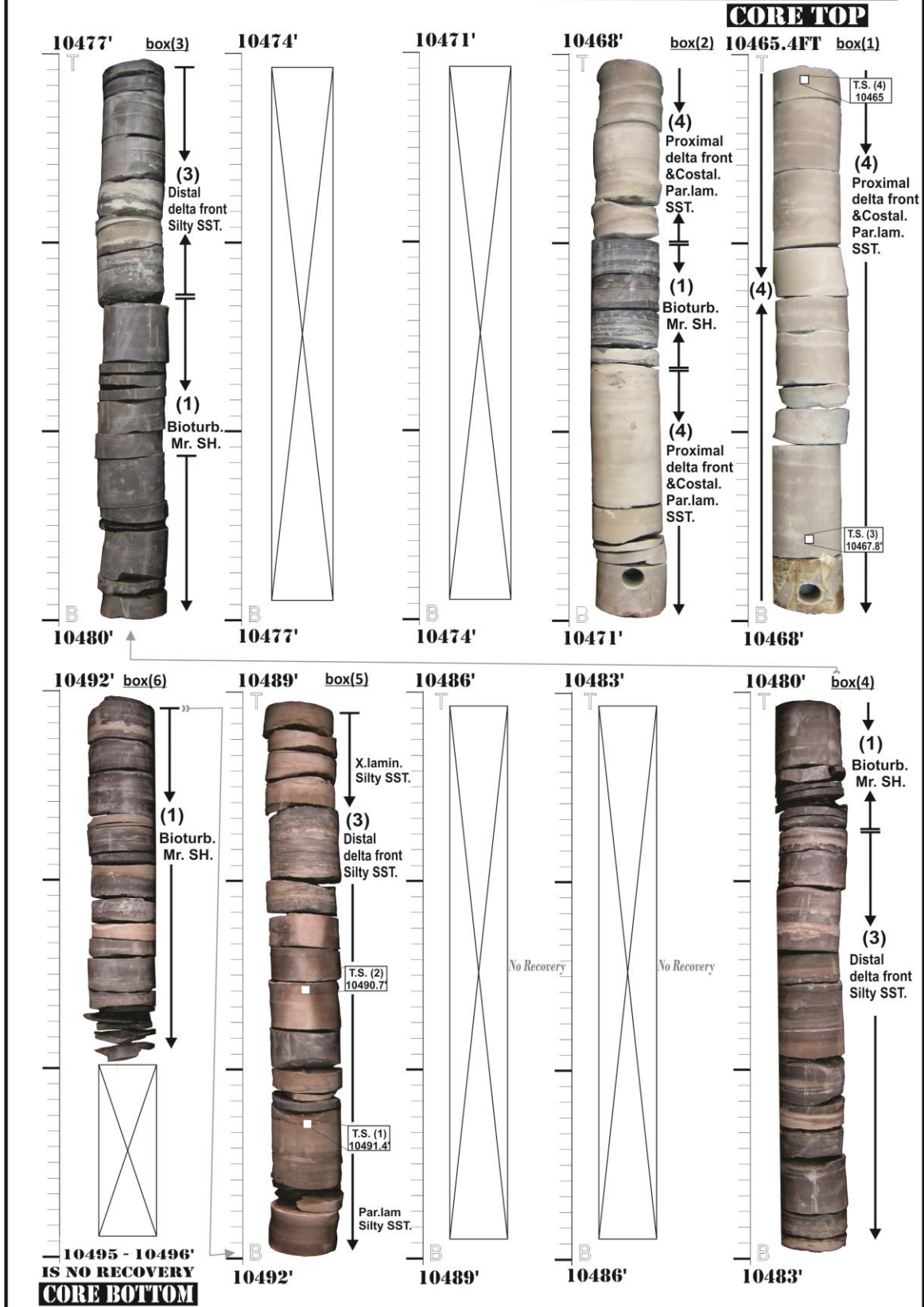


Figure 20. Core samples, (core # 1), cut in Lower Acacus Formation, well Q1-NC100, concession NC100, Ghadames Basin, NW Libya.

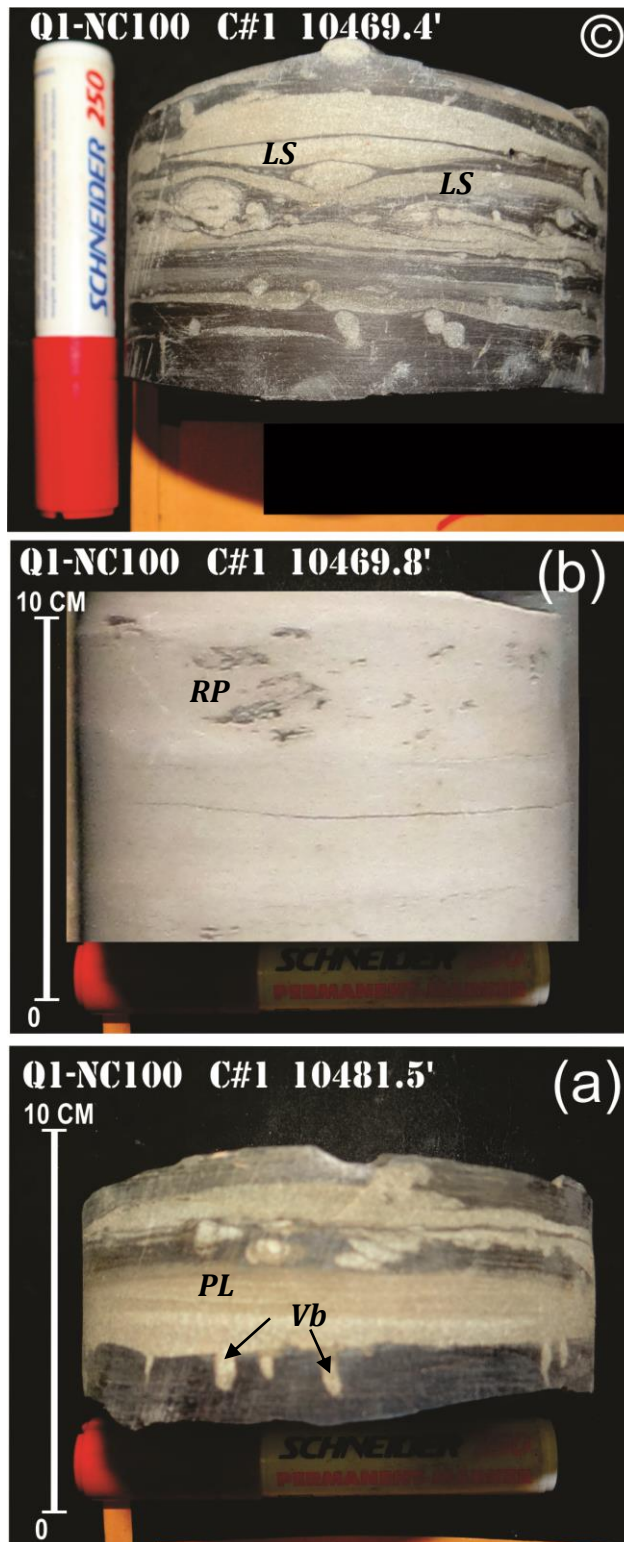


Figure 21. Core samples showing: (a)-Alternating siltstone and shale, occasionally with parallel lamination{*PL*}, and vertical burrows (skalithos) (*Vb*) @10481.5'. (b)- Proximal delta front lithofacies @ 10469.8', clean fine sand, finely lamination, with some rip-up clasts {*RP*}. (c)- Distal delta front silty sandstone lithofacies @10469.4', showing deformed lenticular sand lenses (may be due to subsidence of sands into soft mud) so that the process of liquefaction was associated with deformation bioturbation.



Well: Q1-NC100 Formation: Lower Acacus Formation Core#: 3 interval: 10555' - 10604.2'  
 Area: Concession NC100, Ghadames Basin, NW Libya

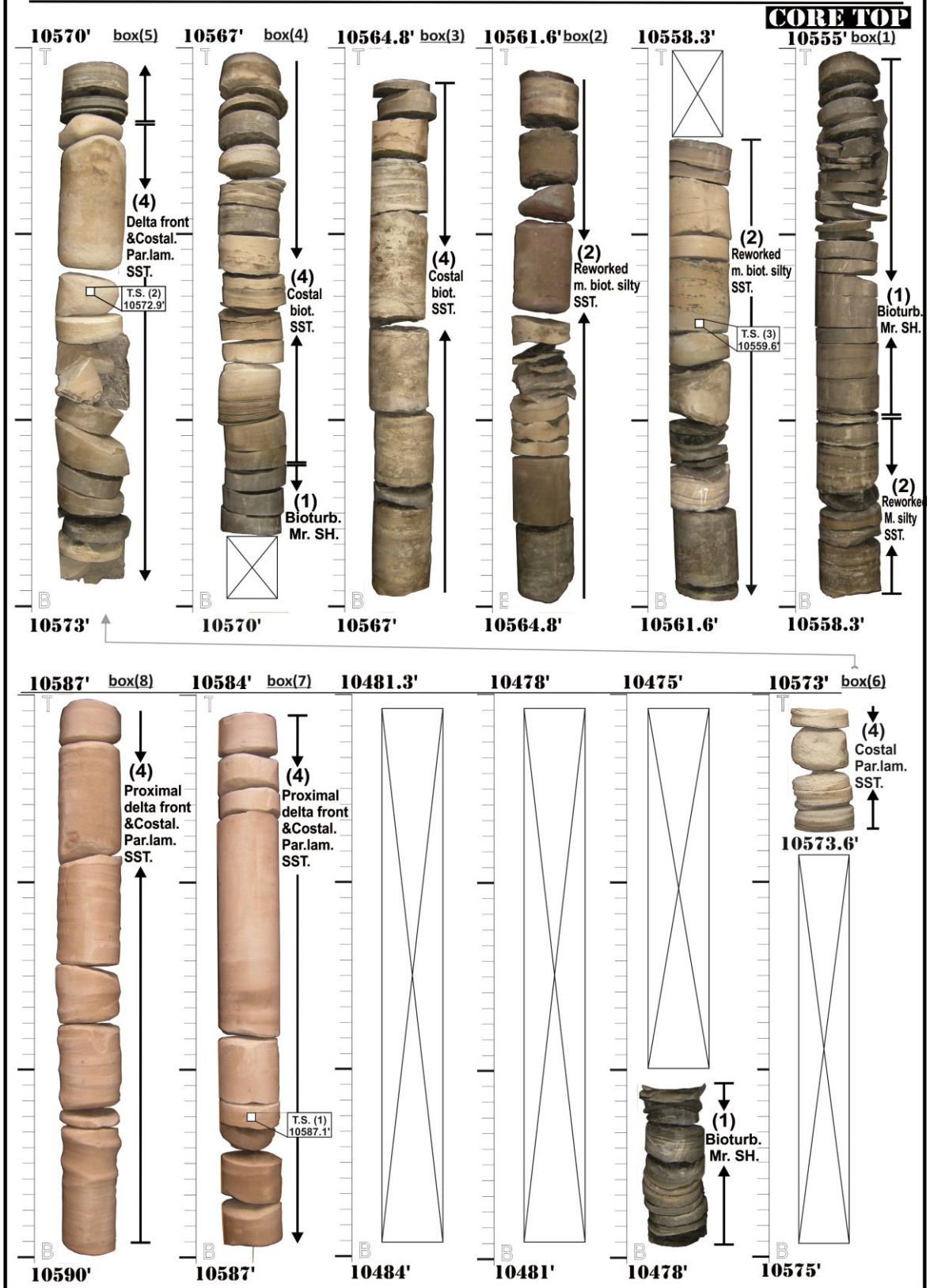
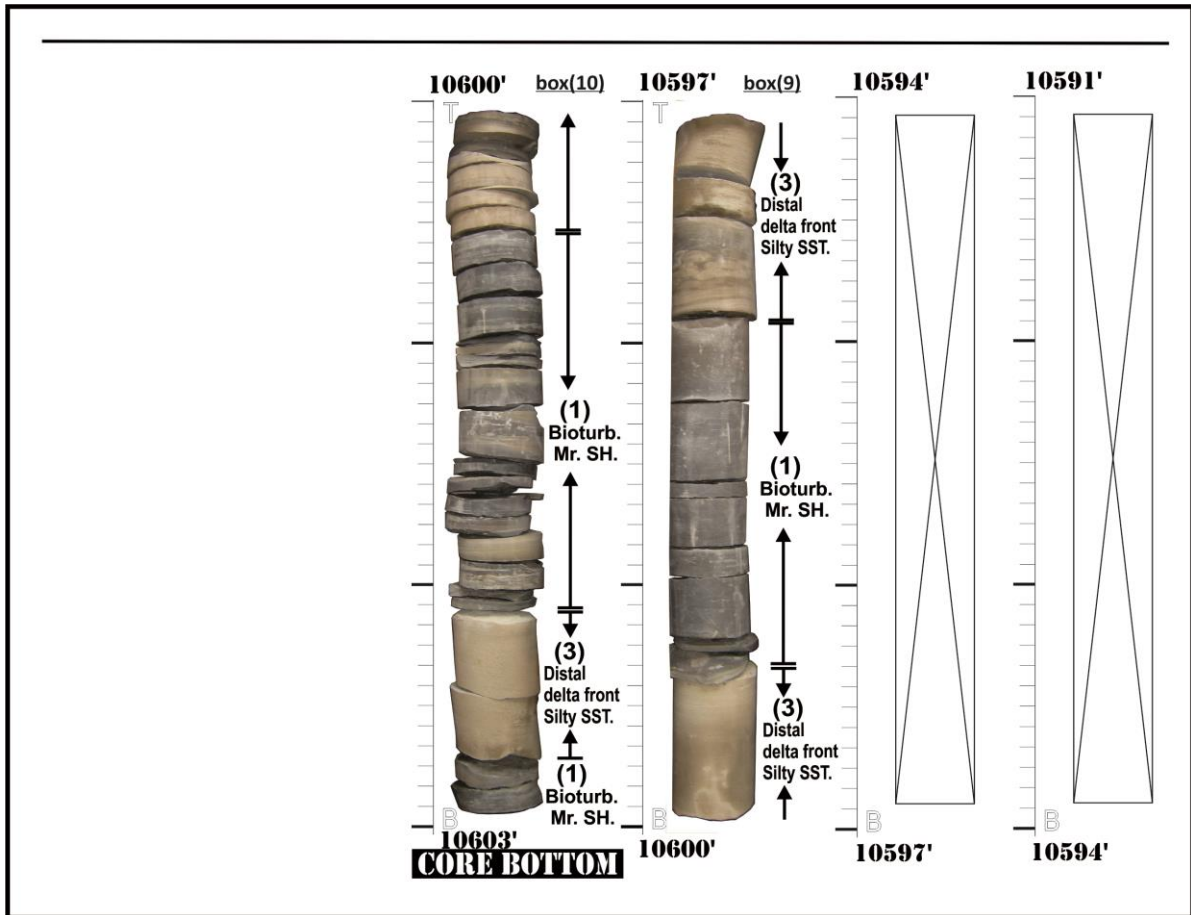


Figure 23. Core samples, (core #3), cut in Lower Acacus Formation, well Q1-NC100, concession NC100, Ghadames Basin, NW Libya.

Cont.....(Figure 23).



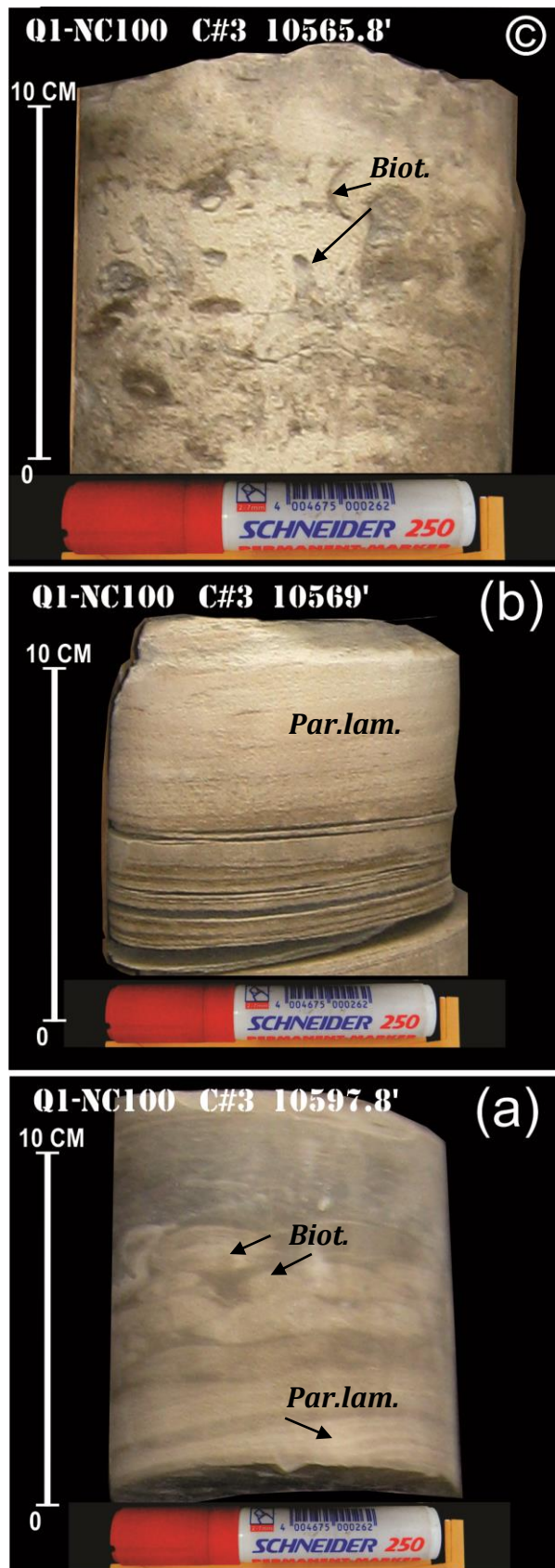
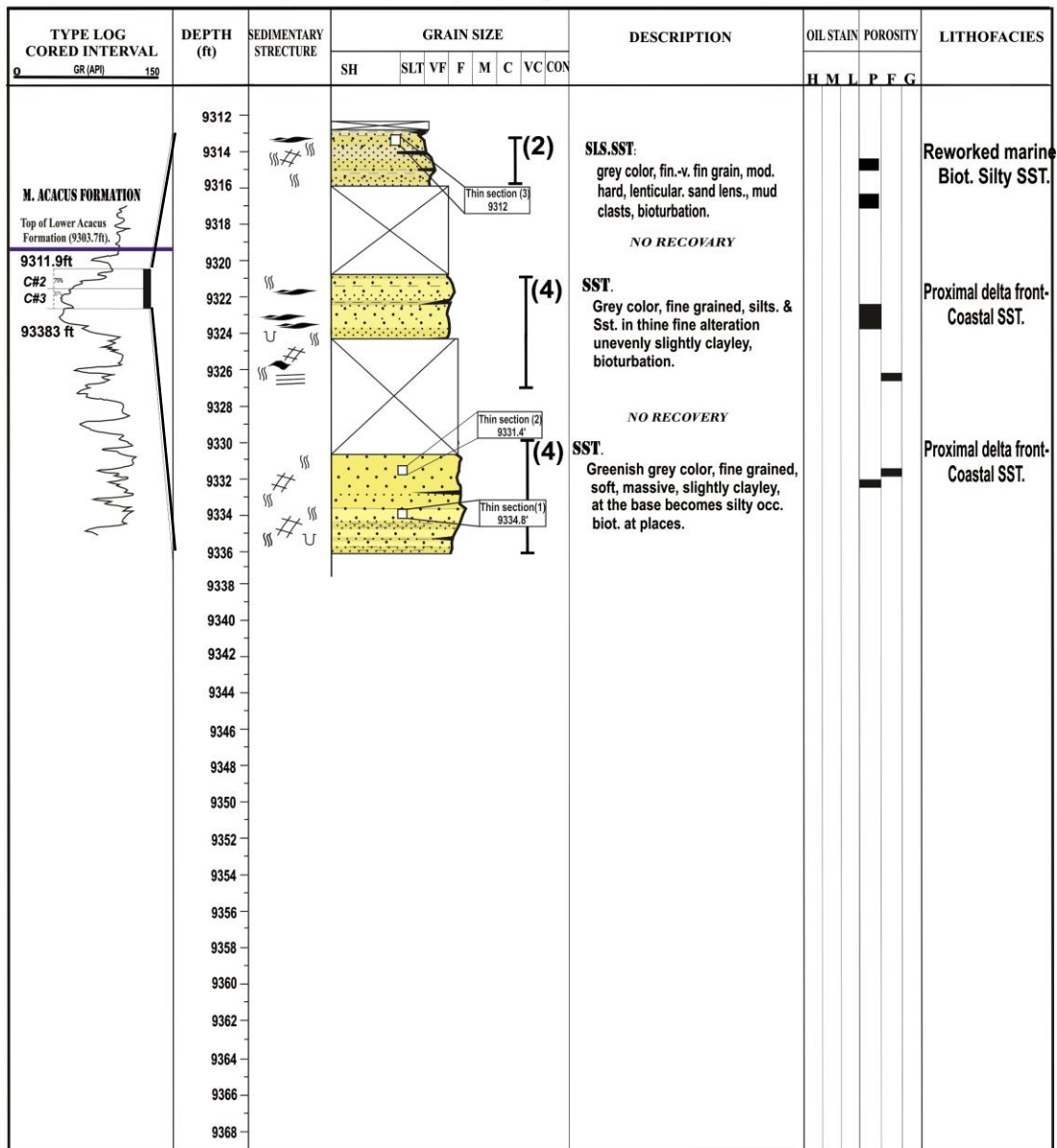


Figure 24. Core samples showing: (a)-Distal delta front silty sandstone lithofacies @10597.8', showing parallel to cross lamination {*X.Lam.*} at the base, bioturbation {*Biot.*} at the middle, shaly at the top. (b)-Coastal sandstone lithofacies @10569', with finely parallel laminations {*Par.Lam.*}. (c)-Coastal silty sandstone lithofacies @10565.8', heavily bioturbated {*Biot.*}.

### LITHOLOGICAL DESCRIPTION CORE

Well: L3-NC100    Formation: Lower Acacus Formation    Core#: 2, 3    Interval: 9312' - 9336'  
 Area: Concession NC100, Ghadames Basin, NW Libya



Gross Lithology	Sedimentary Structures	Accessories
Sandstone	Horizontal even parallel laminae	Carbonaceous debris
Siltstone	Cross lamination	Mud clasts
Shale	Lenticular sand lenses	
No recovery	Burrow	
	Bioturbation	

**Figure 25. Graphic log of core samples cut in the proximal delta front-coastal sandstone and reworked marine sandstone lithofacies of Lower Acacus Formation in well L3-NC100, core # (2 and 3), concession NC100, Ghadames Basin.**

Well: L3-NC100    Formation: Lower Acacus Formation    Core#: 2,3    Interval: 9312' - 9336'  
 Area: Concession NC100, Ghadames Basin, NW Libya

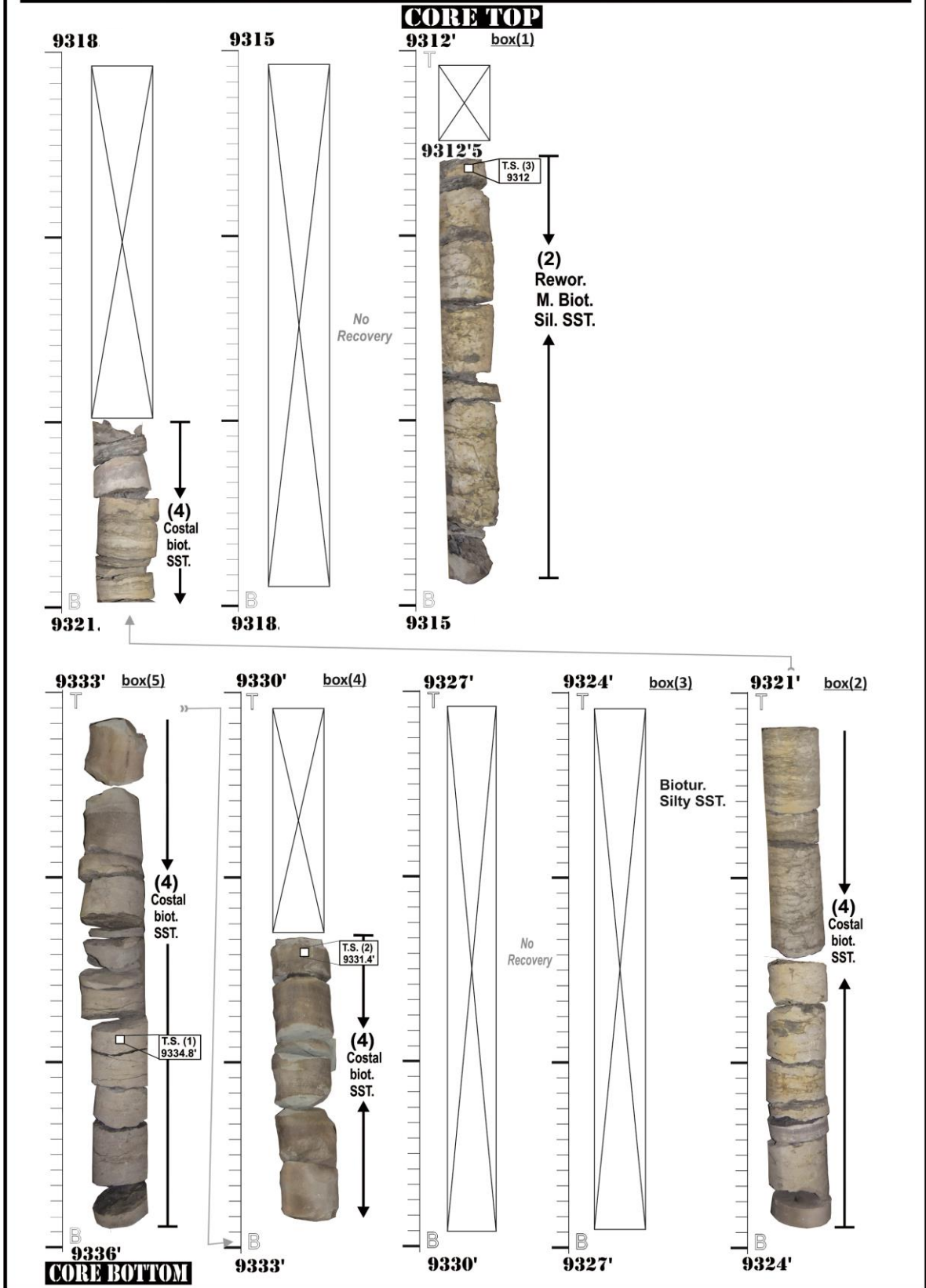


Figure 26. Core samples, (core # 2), cut in Lower Acacus Formation, well L3-NC100, concession NC100, Ghadames Basin, NW Libya.



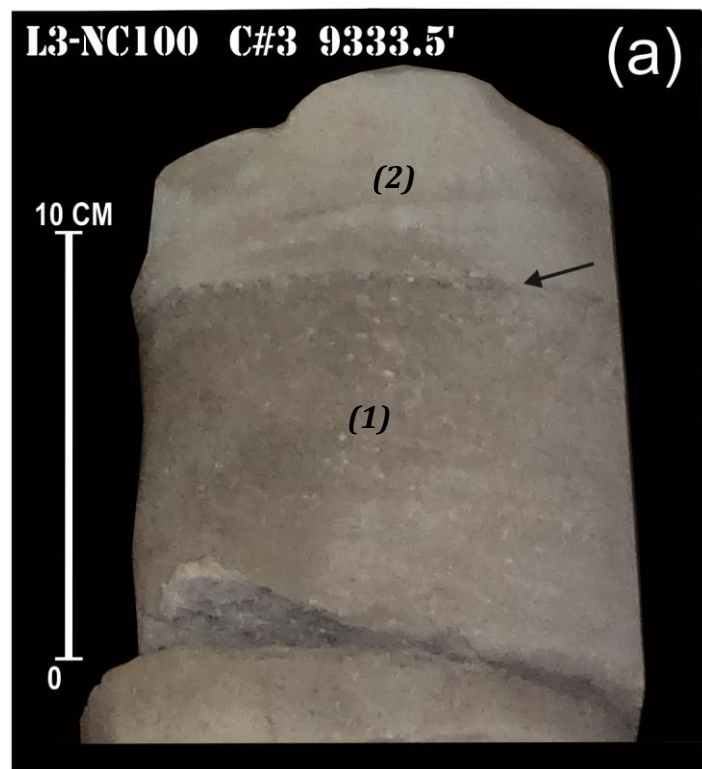
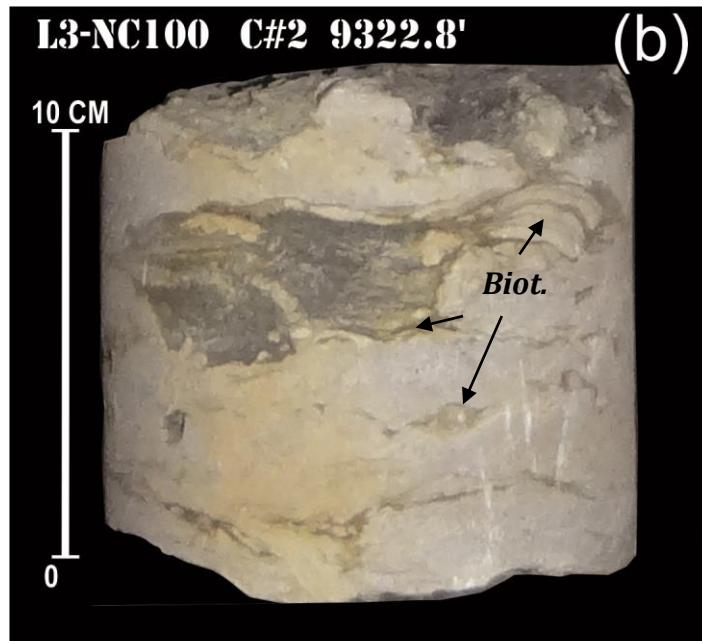


Figure 27. Core samples showing: (a)- proximal delta front and coastal sandstone lithofacies @9333.5', showing gradational boundary (arrow) between silty sandstone at the base {1} and fine grained sandstone at the top {2} which imply an upward high energy regime. (b)- proximal delta front and coastal sandstone lithofacies @9322.8', with intensive bioturbation {*Biot.*}, well L3-NC100, Lower Acacus Formation, core# (2).

## **5 - Fluvial channel sandstone lithofacies.**

This lithofacies is occurred locally within incised fluvial channels of some wells (Z1-NC100, Z3-NC100, Figs. 28, 31) based on core samples and log interpretation. Generally it is corresponded of cream to white, light gray sandstones with increasing clay contents to the top. It is composed of medium grained sandstone with coarse mud clasts at places (Fig. 30a, in well Z1-NC100, @ 11700.8ft), grades upward to finally laminated medium grained silty sandstone (Fig. 30b, in well Z1-NC100 @ 11699ft), occasionally with carbonaceous materials (Fig. 30c, in well Z1-NC100 @ 11688.6ft), to more parallel laminated fine grained sandstone and clayey sandstone at top in (Fig. 30d, in well Z1-NC100 @ 11686.5ft),

From two recorded occurrences in core (C#1 in well Z1-NC100 and C#3 in well Z3-NC100), this lithofacies is approximately 10 – 20ft thick. The components of sandstone, siltstone, and mud clasts of this lithofacies is interpreted as fluvial channel fill, forming from high energy currents flow and bed load deposition. Absence of marine fossils support non-marine (fresh water) deposits.



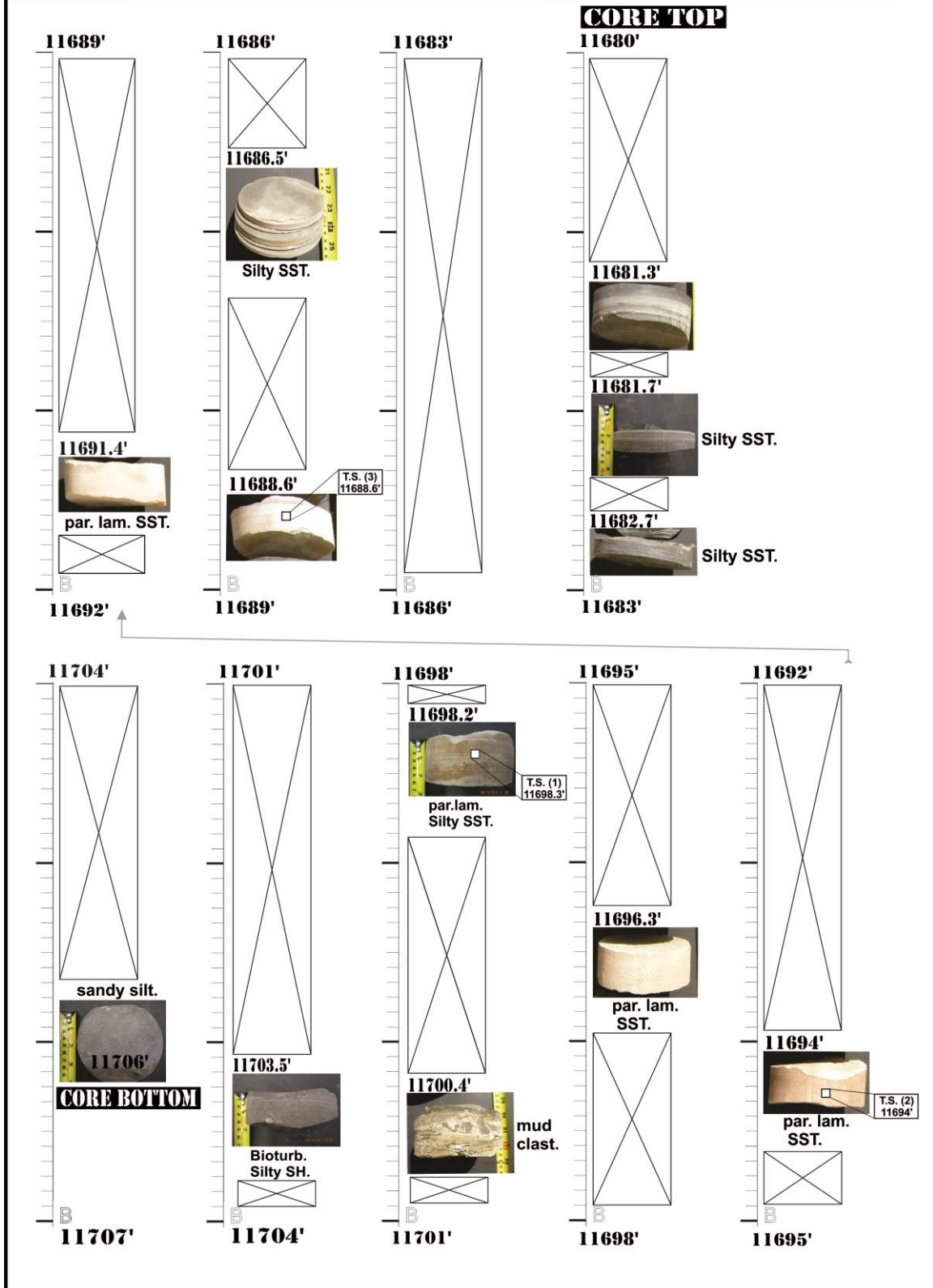


Figure 29. Partially recovered Core samples (core#1), from the fluvial channel sandstone lithofacies of the Lower Acacus Formation in well Z1-NC100, concession NC100, Ghadames Basin NW Libya.

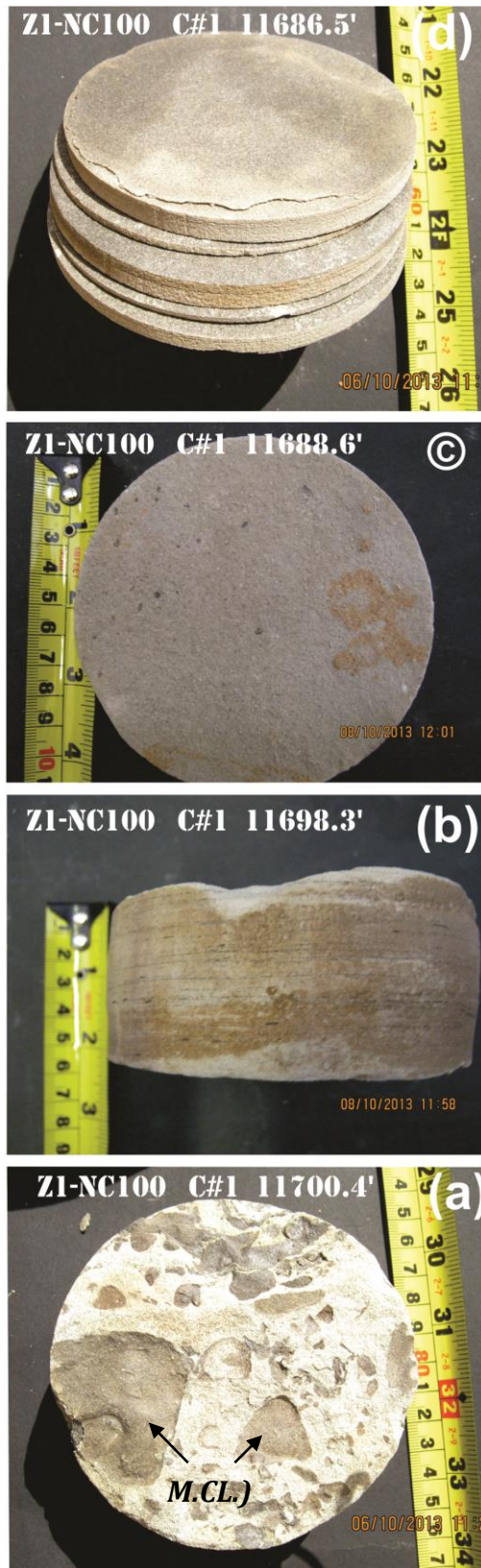
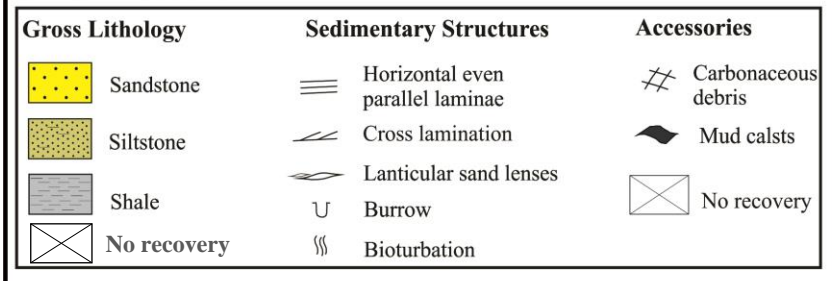
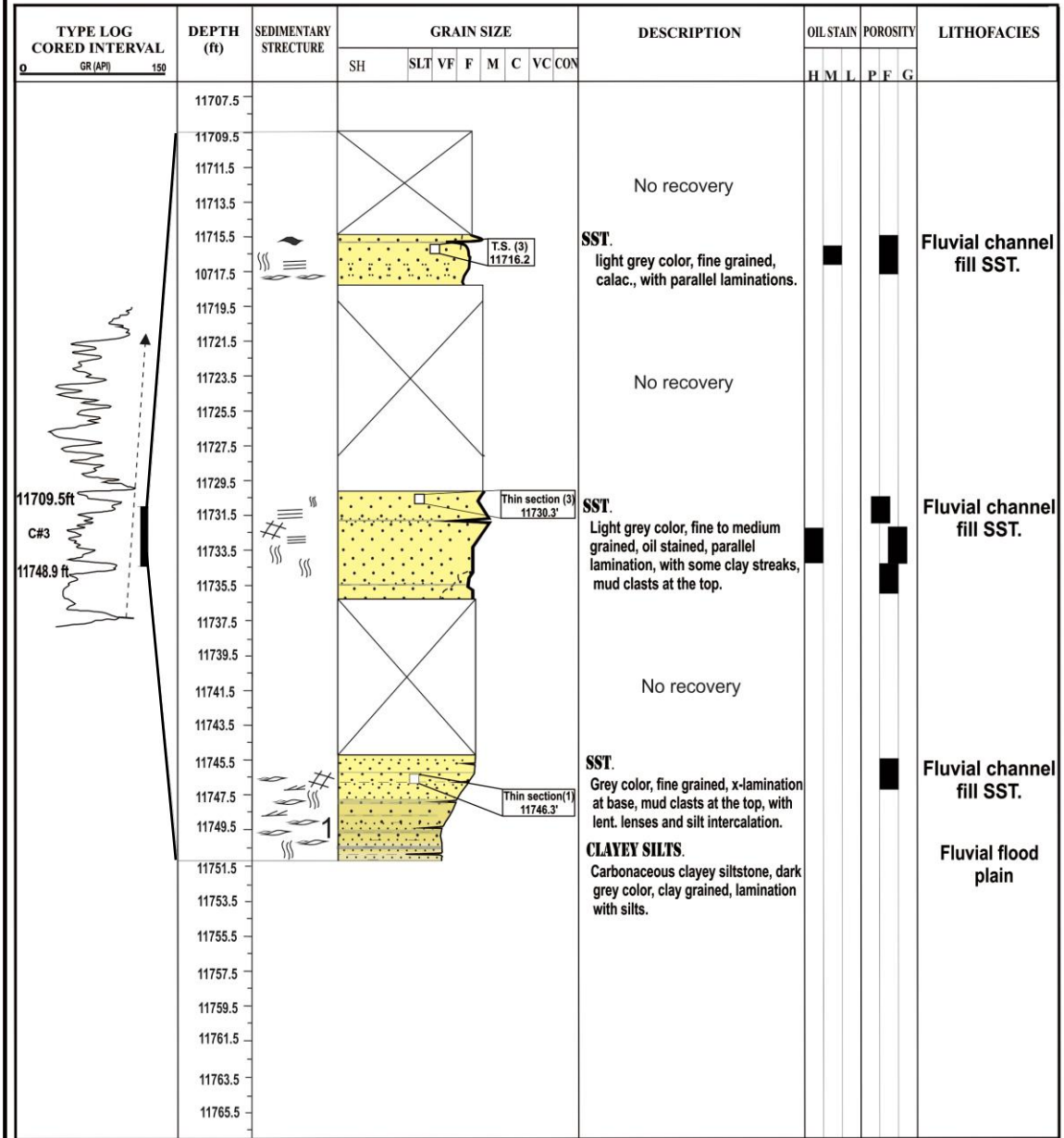


Figure 30. Core samples of fluvial channel sandstone lithofacies showing (a) - Medium grained sandstone with coarse carbonaceous mud clasts {*M. CL.*} @11700.4', (b)-Finely lamination medium grained silty sandstone @11698.3', (c)-Carbonaceous silty sandstone @11688.6', (d)-Parallel lamination fine grained sandstone. In well Z1-NC100 @11686.5', Lower Acacus Formation, core (1), concession NC100, Ghadames Basin.

## LITHOLOGICAL DESCRIPTION CORE

Well: Z3-NC100    Formation: Lower Acacus Formation    Core#: 3    interval: 11709' - 11751'  
 Area: Concession NC100, Ghadames Basin, NW Libya



**Figure 31. Graphic log of core samples (core#3), cut in the fluvial channel sandstone lithofacies of Lower Acacus Formation in well Z3-NC100, concession NC100, Ghadames Basin, NW Libya.**

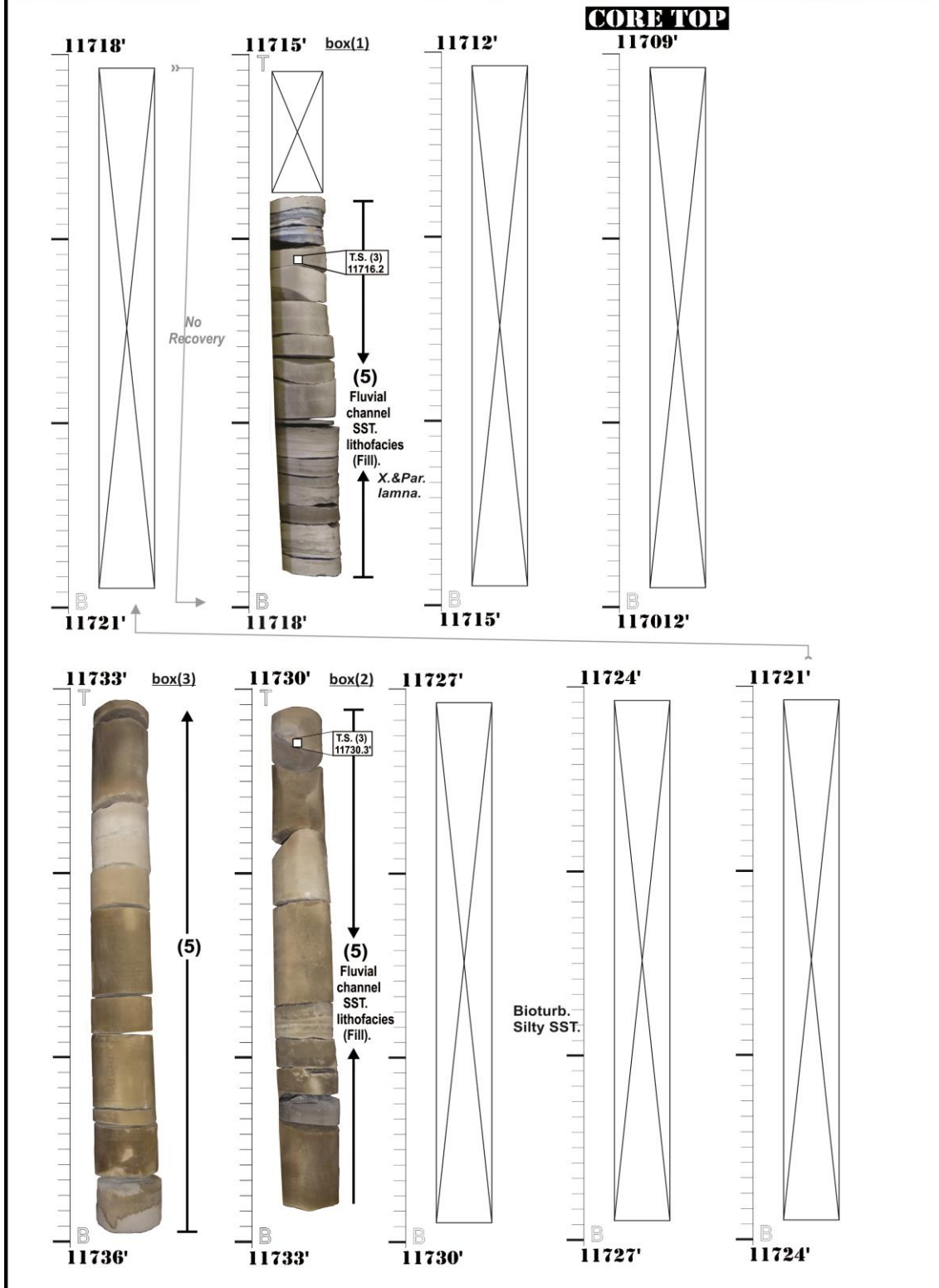
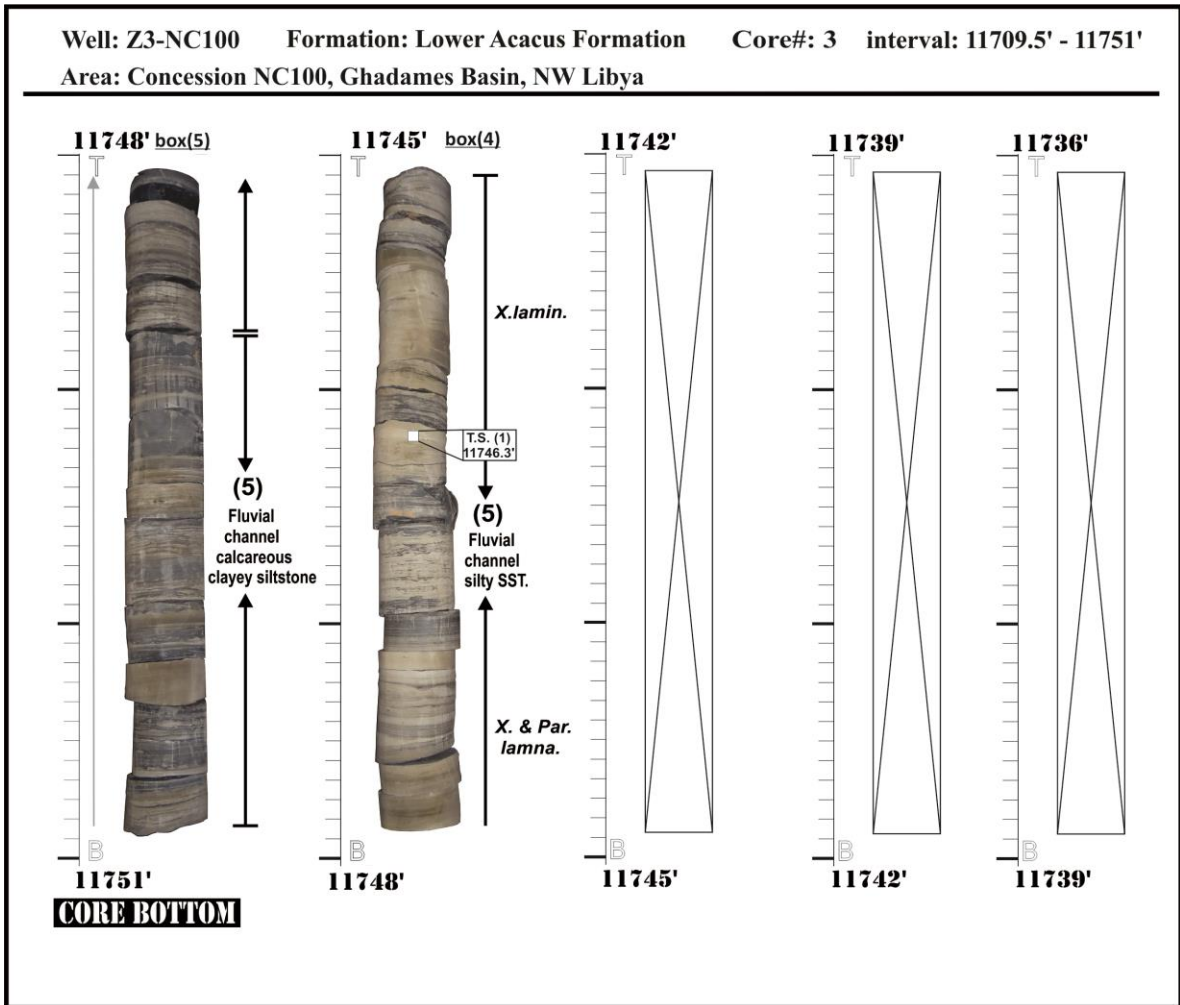


Figure 32. Core samples (core#3), cut in Lower Acacus Formation, well Z3-NC100, concession NC100, Ghadames Basin, NW Libya.

Cont.... (Figure 32).





## **4.2 Wireline-log characterization.**

Wireline-log which were run routinely on most of drilled wells in Concession NC100 was investigated as facies tools for identifying sandstone types of the Lower Acacus Formation.

The principle observations on GR and/or SP curves are:

- Trend of the curve inclined to right or left or blocky of uniform clay contents.
- The nature of the basal contact of the studied sandstone unit.

The various observed GR-log characteristics of the various sandstone unit of Lower Acacus in concession NC100 as examined in cores can be grouped in four (4) categories (Fig. 33).

### **1<sup>st</sup> Category (Bell shape GR-log motif):**

Comparison with core descriptions, the GR curve sloping to the left (Bell shape) correspond with the fluvial channel sequences. The sands are characterized by a sharp base and fining-upward sequence. The GR- curves is generally smooth in the lower part and becomes more serrated toward the top, due to an increase in shale laminae (Fig 33a, in well L3-NC100).

### **2<sup>rd</sup> Category (Funnel shape GR-log motif):**

In this case, GR- curve is showing a slope to the right (funnel shape), is found to correspond with proximal deltaic to coastal deposits. These sediments are characterized by gradational shaly/silty base corresponds with distal delta front lithofacies and an overall increase in grain size and decrease in mud contents upward. These features can be seen as reflected by the shape and slope of GR-curve (Fig. 33b, in well Q1-NC100).

### **3<sup>rd</sup> Category (Spiky shape GR-log motif):**

Few sands show a GR-curve of spiky shape that has a sharp base and sharp top revealing a thin sand characterized by coarsening base and fining top corresponds to reworked marine sandstones usually found offshore in the front of each deltaic lobe (Fig. 33b, in wells Q1-NC100).

### **4<sup>th</sup> Category (Thinly serrated to smooth “featureless” GR-log motif):**

GR- curve is showing high reading of thinly serrated to smooth (featureless) surface, usually show sharp contacts with lower and upper units corresponds to marine shale lithofacies as in (Fig. 33b, in wells Q1-NC100).

## GR-well log characterization.

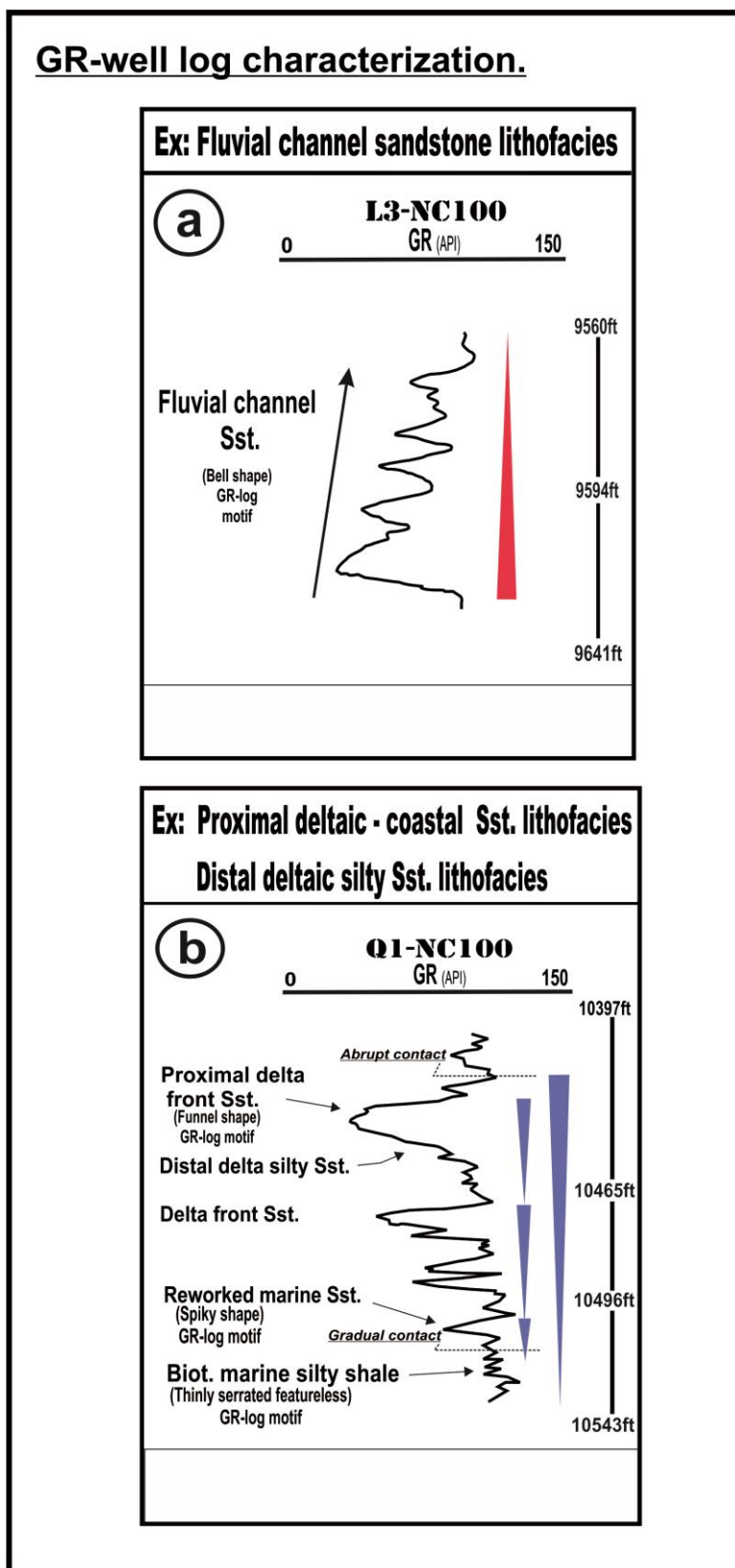


Figure 33. GR-log motifs for the identified lithofacies in some studied wells drilled in the Lower Acacus Formation, concession NC100, Ghadames Basin, NW Libya.

## **5. TRENDS OF DEPOSITIONAL SYSTEM OF THE LOWER ACACUS FORMATION IN CONCESSION NC100.**

### **5.1 Cross section construction.**

The Lower Acacus Formation is characterized by depositional cyclic sequences bounded by regional transegressive markers (TS and MFS) as shown in the stratigraphic profile of the type well L3-NC100 (Fig. 34).

The Paleogeography of the NC100 Concession can be revealed by constructing a suit of stratigraphy cross sections (Figs. 35, 36, Encl. 1, and 2). In which lateral relationships between sandstone unit or facies packages identified in cores have been examined.

Several sandstone bodies or sequences can be shown by their lithology types, grain sizes, depositional structures and their trace of GR logs. The Stratigraphic datum used in the correlation of these Stratigraphic cross sections is the base of Middle Acacus shale overlying the Lower Acacus Formation, as this horizon marks a rapid and widespread transgression event and it is believed to represent a relatively flat time-line paleosurface.

By using a combination of GR log signatures and examined lithologies, the Lower Acacus Formation in the NC100 Concession can be subdivided into five depositional sandstone lithofacies.

In north-south cross section (Fig. 35, Encl. 1) the identified vertical sequences of each correlated well are represented by marine shale at the bottom and terminate with either fining or coarsening sandstones of regressive phase. Therefore, each vertical sequence is bounded by regional time-stratigraphic markers (TS: Transegressive surface, and MFS1-MFS3: Maximum flooding surfaces) as shown in the type well L3-NC100 (Fig. 34).

Laterally, the stratigraphic framework established between correlated wells illustrates in general, the fluvial channel sandstone lithofacies (Lf2, Lf5, Lf6, Lf7, Lf8, Lf9, and L11), in wells (Z1-NC100, Z2-NC100, Z3-NC100, V1-NV100, and V2-NC100) to the southeast of concession NC100 passes northwesterly into proximal delta front sandstone and distal delta front silty sandstone lithofacies in wells (A5, A6, A7, A8, A9, and A11), (D1-NC100, P1-NC100, Y1-NC100, Q1-NC100, O2-NC100, S2-NC100, and T1-NC100), which grades eventually into an offshore marine silty shale lithofacies in wells (F1-NC100, N1-NC100, and J1-NC100). Some thin reworked marine sandstones can be seen in front of prograded deltaic packages and enclosed between marine silty shales, represented by reworked marine sandstone lithofacies.

A similar progressive change of lithofacies can be seen on east-west cross section (Fig. 36, Encl. 2). A fluvial channel sandstone to the east (Lf2, Lf5, Lf6, Lf7, and Lf8 in wells A-NC118, L3-NC100, and L1-NC100) grades westward into proximal deltaic sandstone (A2, A5, A6, and A7) in wells Q1-NC100, and O1-NC100), to distal deltaic silty sandstone northerly and in the northwestern areas in wells (G1-NC100, C2-NC100, H1-NC100, and K1-NC100), to eventually bioturbated marine silty shale in wells (F1-NC100, N1-NC100, J1-NC100, M1-NC100 and E1-NC100).

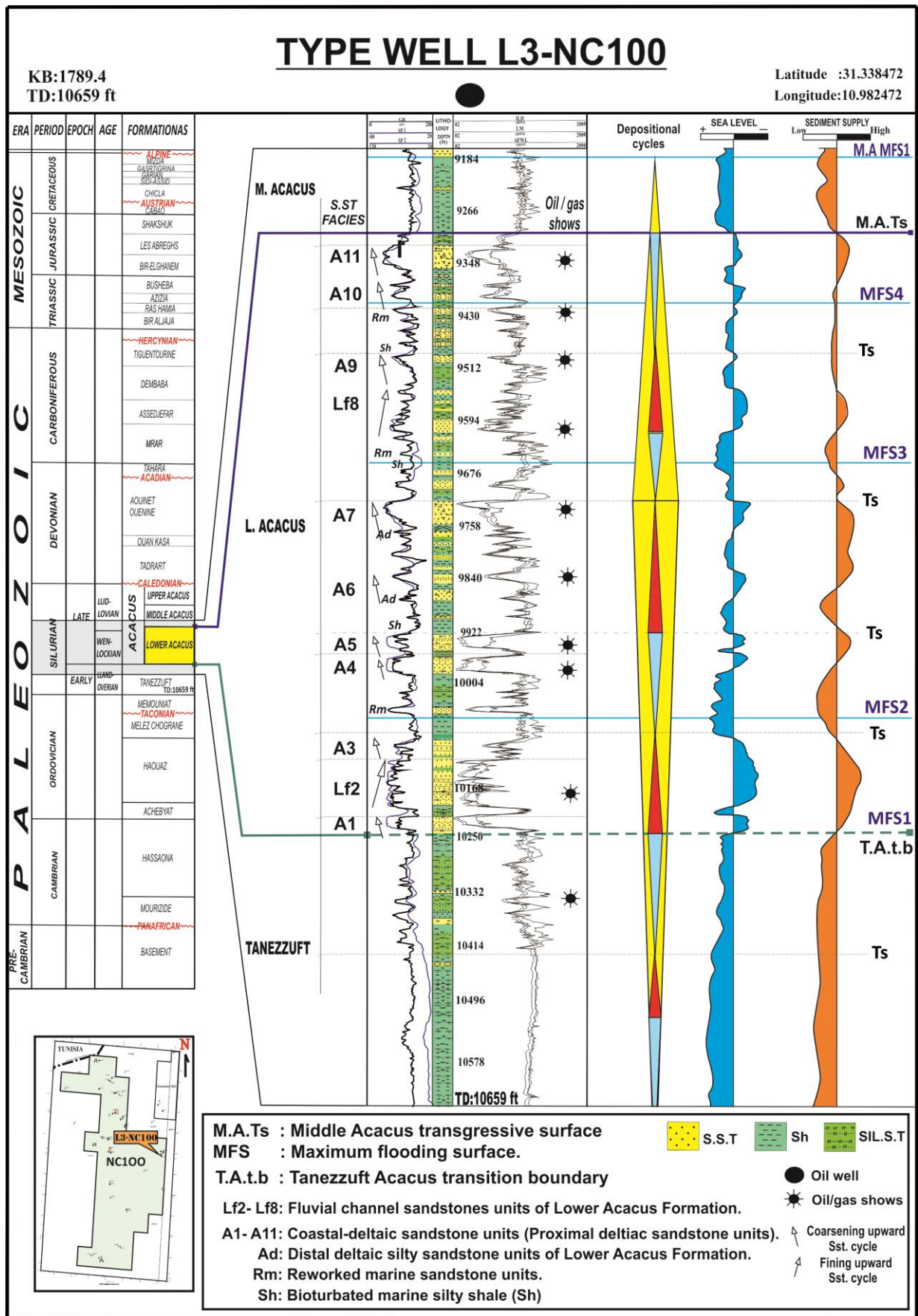


**Figure 34. L3-NC100 type well, showing signature of well log (GR, SP, R), depositional cycles (Sequences), and regional time stratigraphic markers (TS, and Mfs), Concession NC100, Ghadames basin, NW Libya.**

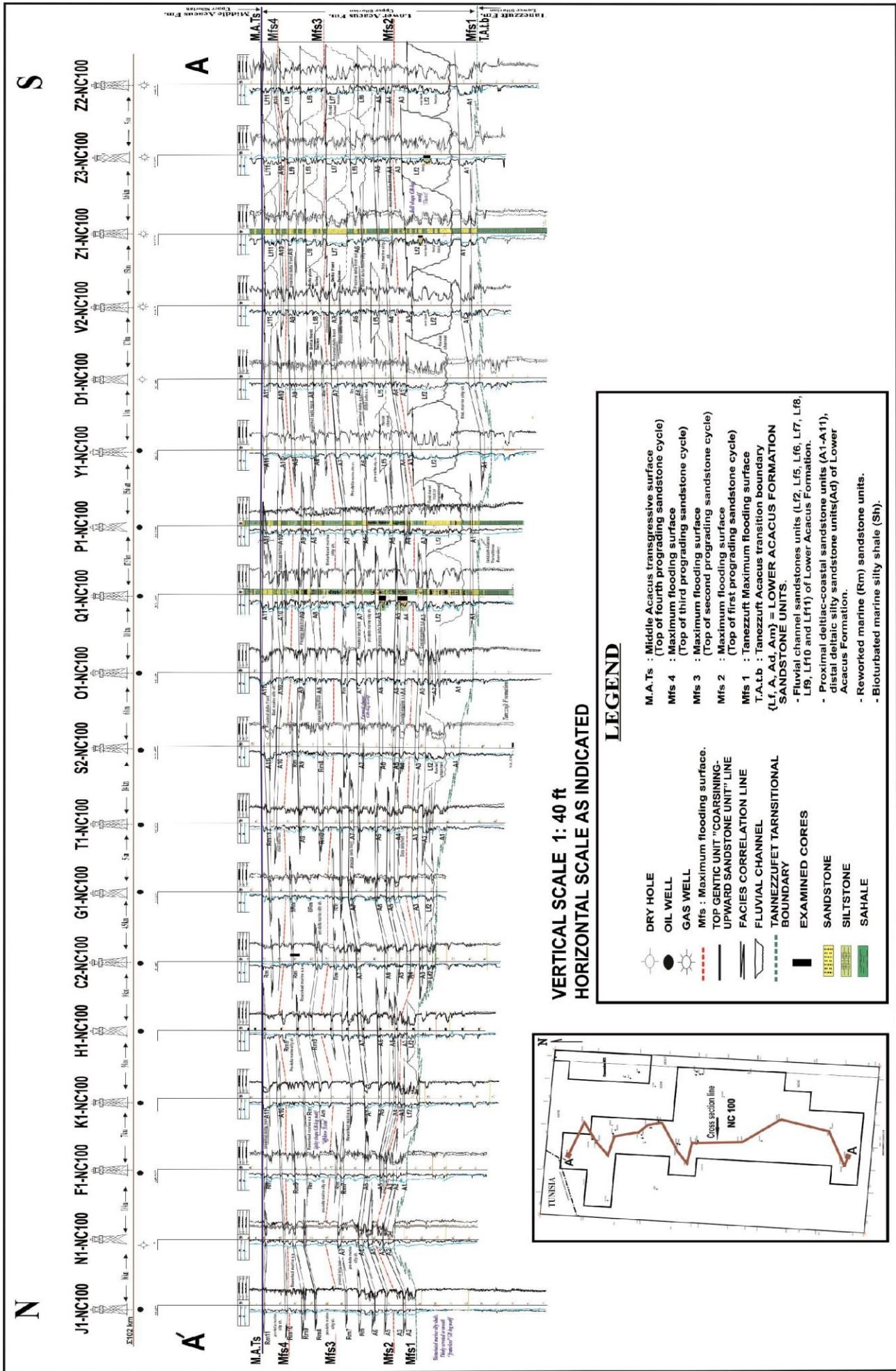


Figure 35. South-North (A-A') stratigraphic cross section of Lower Acacus Formation, concession NC100, NW of Ghadames Basin, NW Libya. (See Enclosure. 1 for more details).

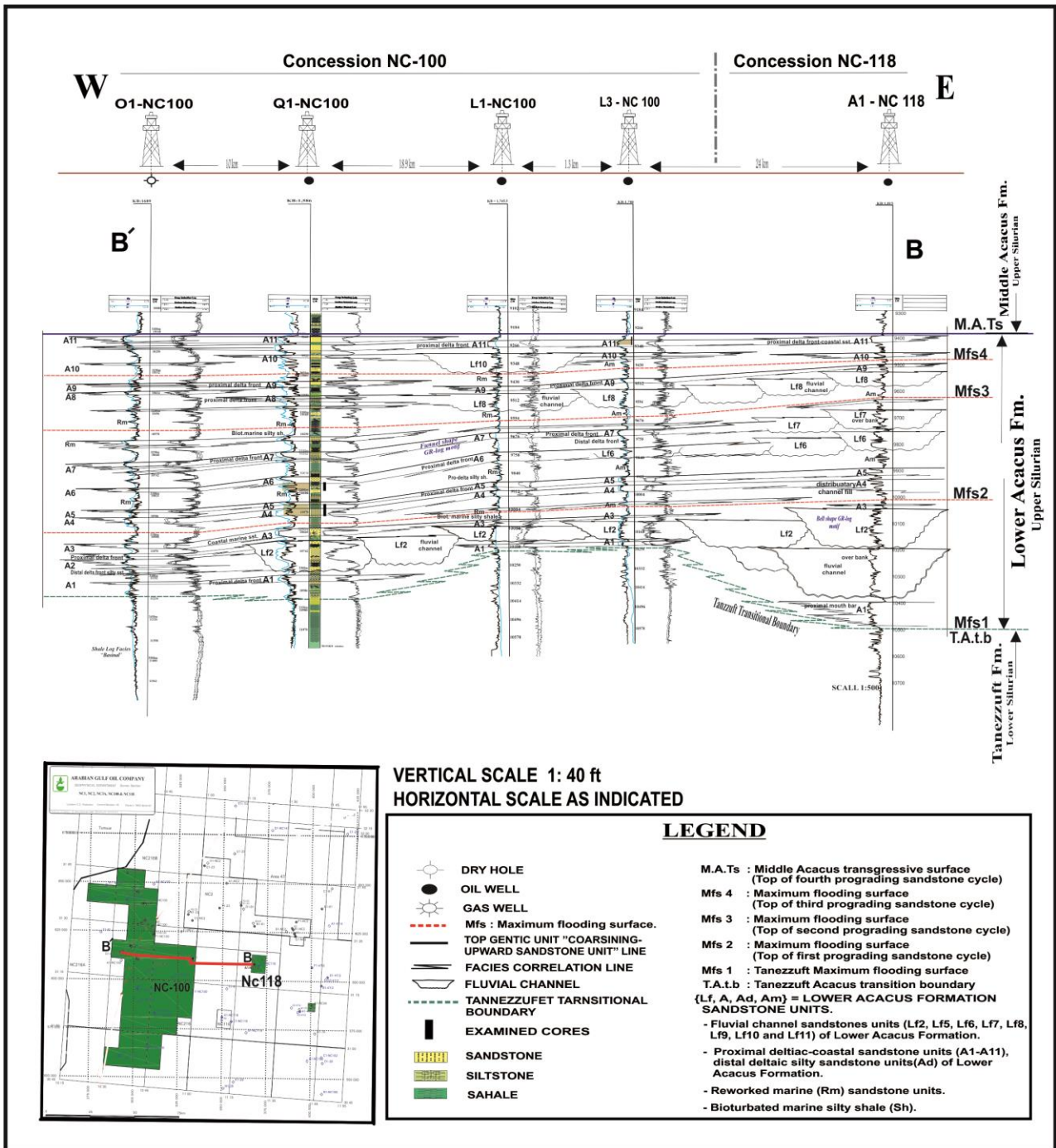


Figure 36. East - West (B-B') stratigraphic cross section of Lower Acacus Formation, crossing concession NC-100 and neighbor area (A1-NC118 area), Ghadames Basin, NW Libya. (See Enclosure. 2 for more details).

## 5.2 Geological maps.

Subsurface geological maps made of data compilations from drilled wells in the study area concession NC100, for structure and stratigraphic purposes (Tables 2 and 5).

There are three constructed types of maps:

- 1- Structural maps that show the depth of a specific mappable horizon.
- 2- Isopach maps that show changes of thickness of an interested unit.
- 3- Lithofacies maps, that show the distribution of lithological composition of a unit based on log-curve shapes to infer their possible environmental transition. These maps are as following:

### 1- Structural maps.

In Ghadames Basin, the structure is classic paleo-high formed during folded basement and later during post-Caledonian and Hercynian erosional events.

By using well-log formation tops (Table 2) for 49 exploratory wells in concession NC100, structural maps have been constructed on top of some selected formations to revealing basin configuration through time, these structural maps include:

#### a) - Time structural contour maps on top of Memouniat Formation:

The top of Memouniat Formation is traced at 1855ms in the northern part of concession NC100 and increased to 2495ms in the southern part (Fig. 37), as it reveals southwesterly dip direction due to mainly post Hercynian uplift and basin tilting.

#### b) - Structural contour map on top of Tanezzuft Formation:

The Memouniat Formation is overlain unconformably by Tanezzuft Formation. The top of Tanezzuft Formation can be picked up from well-logs over the study area.(Table 2). The Tanezzuft Formation is mainly composed of dark greyish to black color, graptolitic shales with intercalation of siltstone and very fine- grained sandstones, often forming rhythmic alterations. Depth structural contour map on top of Tanezzuft Formation (Fig. 38) indicates the depth of this formation ranges between 7200ft in the north and increases to more than 10500ft in the south of the study area, and increases gradually as well from east to west of the concession NC100.

#### c) - Structural contour map on top of Lower Acacus Formation:

Lower Acacus Formation is the main target in concession NC100 represented by regressive surface and it is overlain principally by Middle Acacus transegressive shale which defined



as transegressive surface (TS) and conformably overlies Tanezzuft Formation which represented by maximum flooding surface (MFS) (Fig. 34).

The Lower Acacus Formation is characterized by fine-medium grained sandstones occasionally interbeds with some silty shales and silty sandstones of fluvial- deltaic origin. The depth structure contour map on top of Lower Acacus Formation (Fig. 39) has been generated and is picked at (-6500ft) in the northern part of the study area and increases to (-9300ft) in southern part.

The three previous constructed structural contour maps (Figs 37, 38 and 39) are showing the same tendency of today's structural configuration which revealing post – Hercynian tilting and reshaping of the depositional basin which reflected partially on the study area (concession NC100).

**Table 5. Thickness variation of Lower Acacus Formation (Total and unit thickness) in studied wells of concession NC100, Ghadames Basin, NW Libya.**

Well \ Thickness	Lower Acacus Formation Thickness (ft)					
	Total	Lf2	A6	A7	A9	A11
<b>C2-NC100</b>	1076.54	76.53	47.73	48.87	19.23	26.23
<b>D1-NC100</b>	818.70	207.57	56.87	58.76	28.86	55.45
<b>F1-NC100</b>	1055.83	48.75	42.20	40.22	25.76	23.88
<b>G1-NC100</b>	1075.52	78.66	45.75	53.45	24.85	31.32
<b>H1-NC100</b>	1106.74	73.74	44.76	47.87	28.89	25.78
<b>I1-NC100</b>	782.52	192.7	66.23	92.87	70.43	72.27
<b>J1-NC100</b>	857.57	47.78	35.87	17.85	12.86	22.55
<b>K1-NC100</b>	1157.58	74.85	36.75	45.67	26.23	25.75
<b>L1-NC100</b>	1211.73	198.75	66.88	77.24	68.64	59.87
<b>L3-NC100</b>	1145.60	187.94	67.30	95.73	59.87	56.24
<b>N1-NC100</b>	787.57	64.73	45.29	48.65	22.75	30.97
<b>O1-NC100</b>	1087.73	112.35	51.23	53.67	38.86	43.20
<b>P1-NC100</b>	1053.86	126.62	50.89	43.76	47.85	62.56
<b>Q1-NC100</b>	1107.27	134.73	52.36	54.77	42.35	52.22
<b>R1-NC100</b>	1174.54	163.40	59.20	70.22	47.54	56.34
<b>S2-NC100</b>	1028.74	122.78	51.47	53.43	42.76	46.27
<b>T1-NC100</b>	1007.56	77.78	50.75	57.23	36.85	32.88
<b>V2-NC100</b>	1011.67	248.75	69.34	58.78	147.74	76.24
<b>Y1-NC100</b>	880.73	204.73	54.22	57.86	36.76	53.76
<b>Z1-NC100</b>	1114.76	232.20	75.87	98.67	54.86	73.45
<b>Z2-NC100</b>	1121.64	238.95	82.65	113.55	60.88	79.22
<b>Z3-NC100</b>	1107.55	237.88	80.75	97.45	50.53	76.23

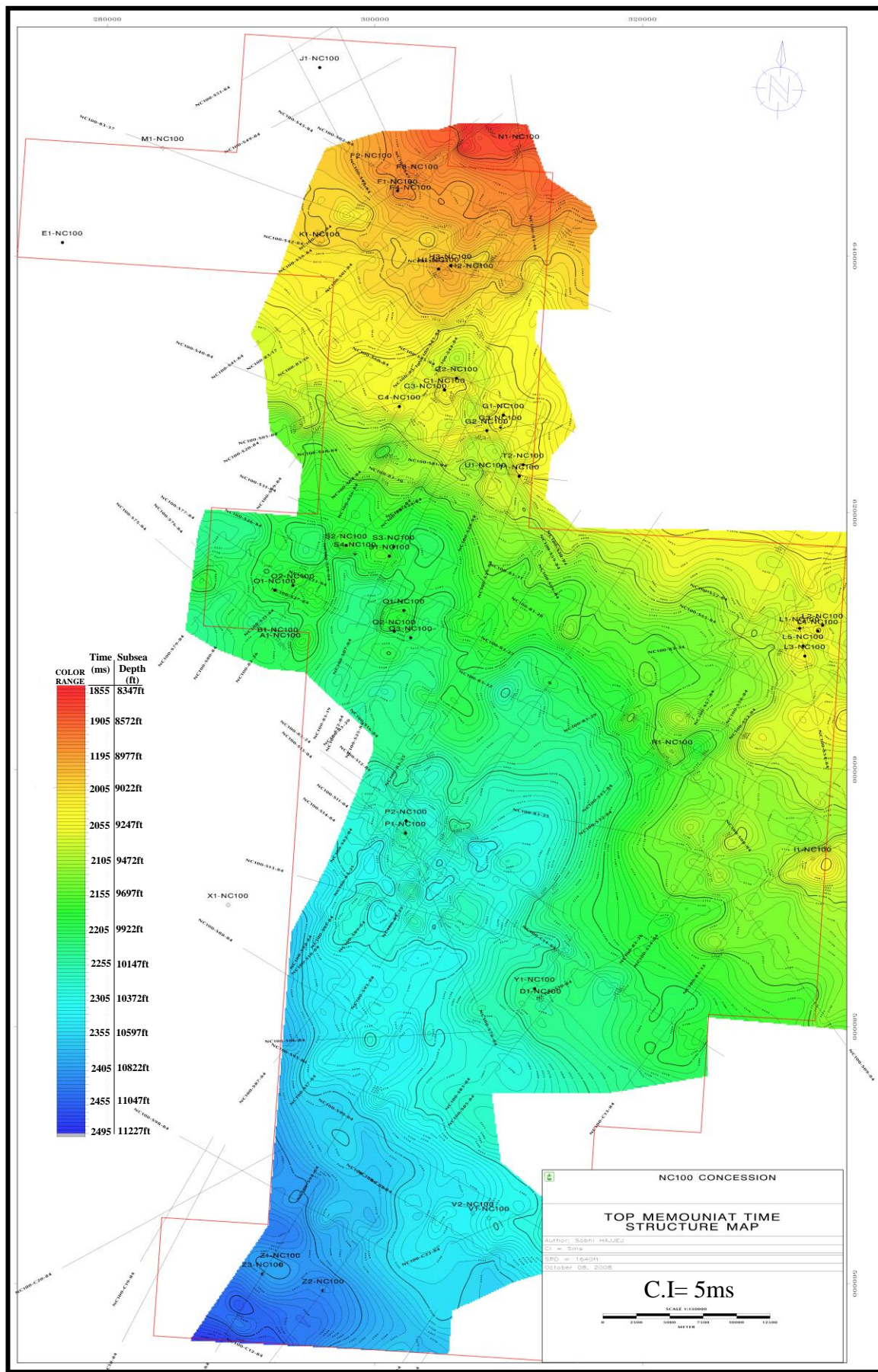


Figure 37. Time structural map on top of the Memouniat Formation, Concession NC100, Ghadames Basin, NW Libya, modified after AGECO (2008).

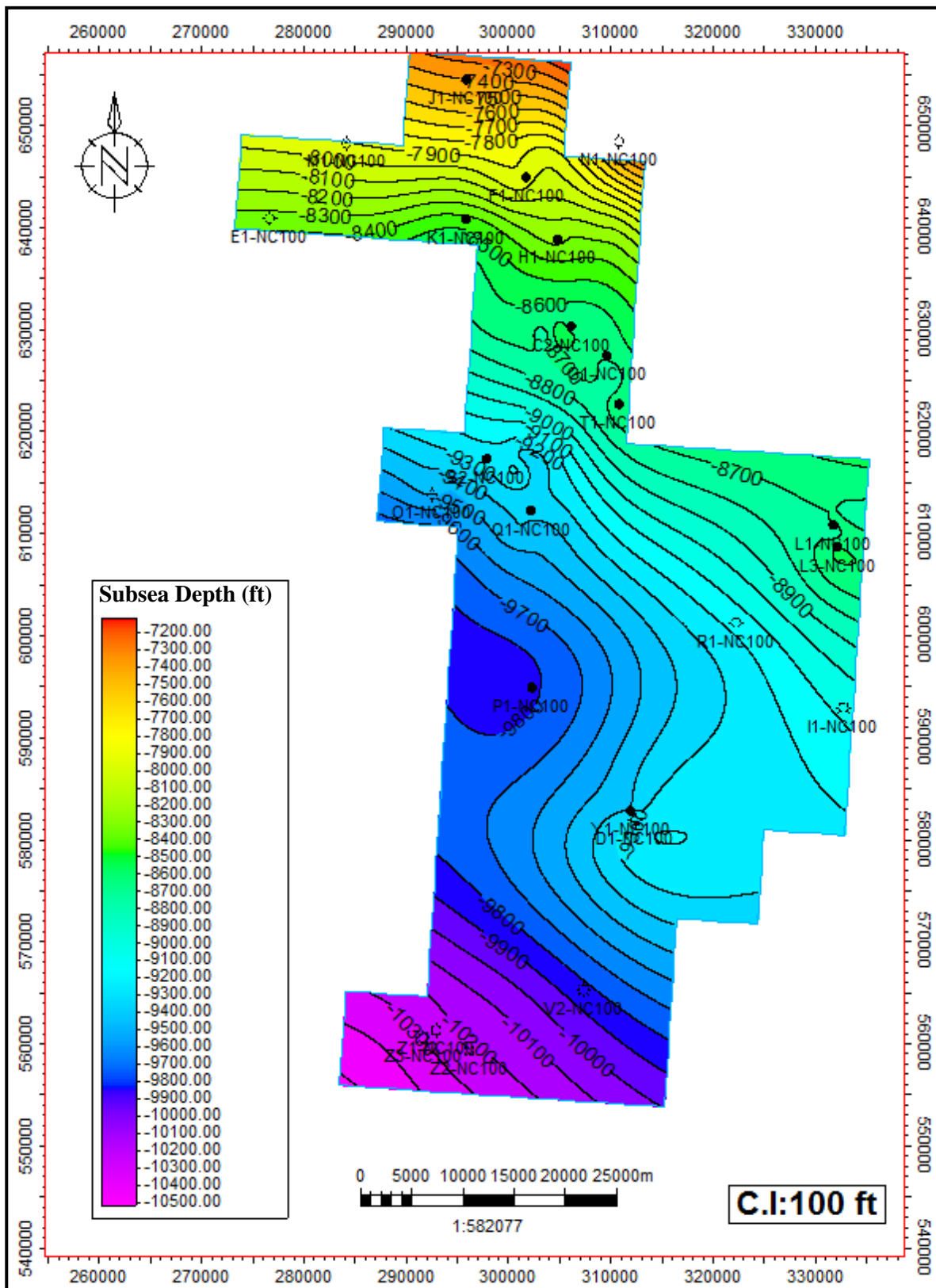


Figure 38. Structural contour map on top of the Tanezzuft Formation, Concession NC100, Ghadames Basin, NW Libya.

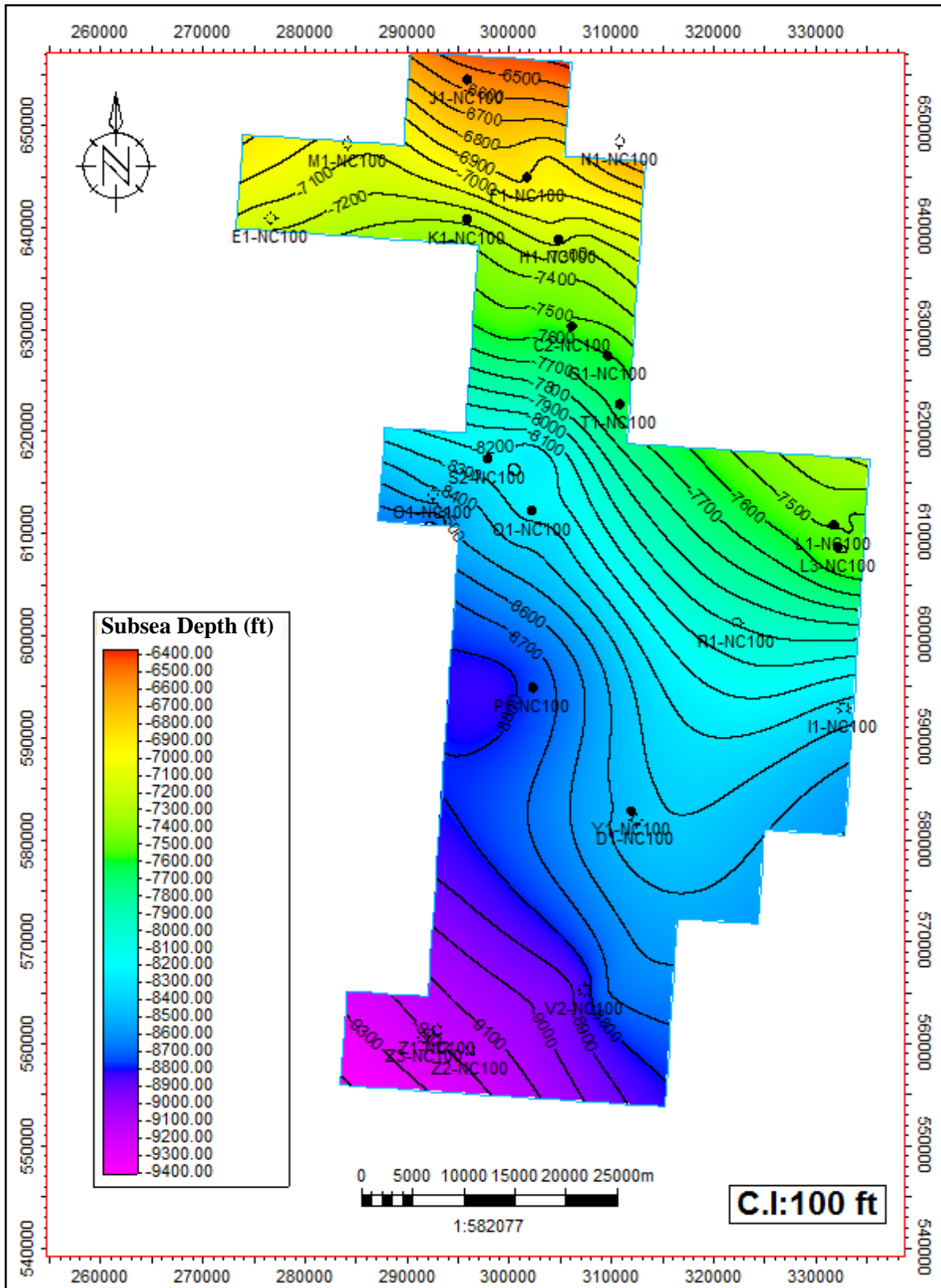


Figure 39. Structural contour map on top of the Lower Acacus Formation, Concession NC100, Ghadames Basin, NW Libya.

## **2 - Isopach maps.**

### **a)- Total isopach map of Lower Acacus Formation:**

The structural configuration on top of Lower Acacus Formation (Fig. 39) is mostly influencing the thickness distribution of Lower Acacus Formation (Fig. 40).

In (Fig. 40) the Lower Acacus Formation decreased in thickness to about 800 ft in the northern part of concession NC100 around wells (N1-NC100, J1-NC100, and M1-NC100). However, gradual increase in thickness southwest was recorded in wells (F1-NC100, H1-NC100 and C2-NC100).

A remarkable thickening of Lower Acacus Formation have been recognized in the middle part of concession NC100 between wells L1-NC100, L2-NC100, L3-NC100 and R1-NC100, which coincides with paleo-topographic low (Fig. 39). Further southward at the vicinity of wells F1-NC100, Y1-NC100 and D1-NC100 a decrease in thickness of about 625ft – 825ft was recorded as this area revealing paleo-high rising from possible erosional surface. To the far south of concession NC100 in the vicinity of wells Y1-NC100, Z1-NC100, Z2-NC100 and Z3-NC100, again a graded increase in thickness took place as sedimentation filled paleo-troughs at these locations.

### **b)- Isopach map of unit Lf2:**

The isopach map of unit Lf2 (Fig. 41) shows a minimum thickness of about 60ft in wells F1-NC100, J1-NC100, and N1-NC100 to the north and maximum thickness of about 250ft around wells V2-NC100, and Z2-NC100 to the south, while a thickness ranging from 110ft to 130ft is mostly around wells O1-NC100, Q1-NC100, S2-NC100, and P1-NC100 characterizing the middle area of concession NC100 resembling a linear feature signified the presence of channels which characterized by fining upward sequence of bell-shape GR-motif, distributed all-area the concession to represent the source of sediment dispersal and progradation from south to north direction.

### **c)- Isopach map of unit A6:**

This unit is represented one of the proximal delta - coastal sandstone lithofacies has a minimum thickness of 30ft around wells E1-NC100, J1-NC100 and M1-NC100 and a maximum thickness of about 75ft in well V2-NC100, Z2-NC1-00, Z2-NC100 and Z3-NC100 to the south also in the vicinity of wells L1-NC100, L3-NC100 and I1-NC100 to the east (Fig. 42).

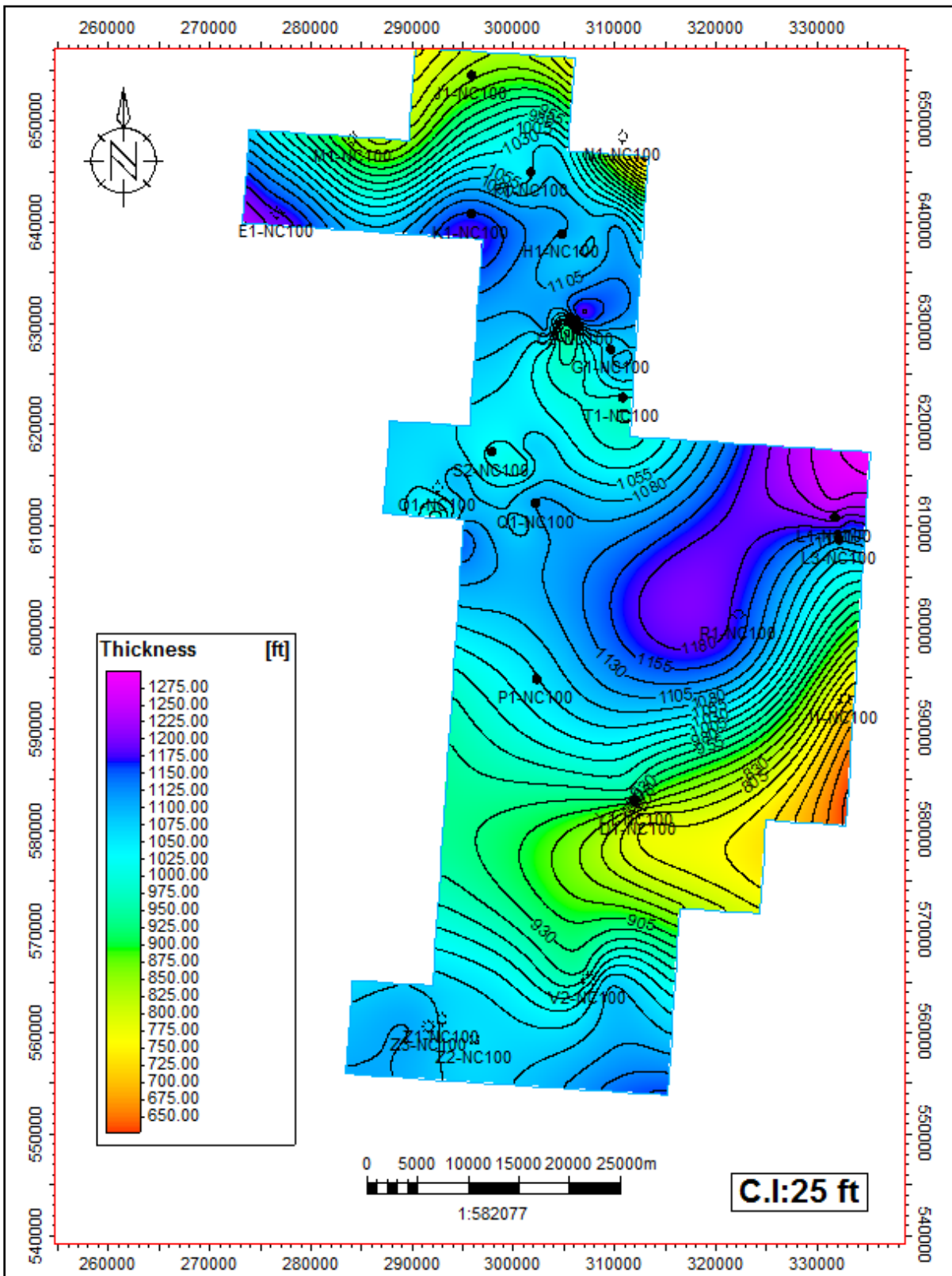


Figure 40. Total isopach map of the Lower Acacus Formation, Concession NC100, Ghadames Basin, NW Libya.

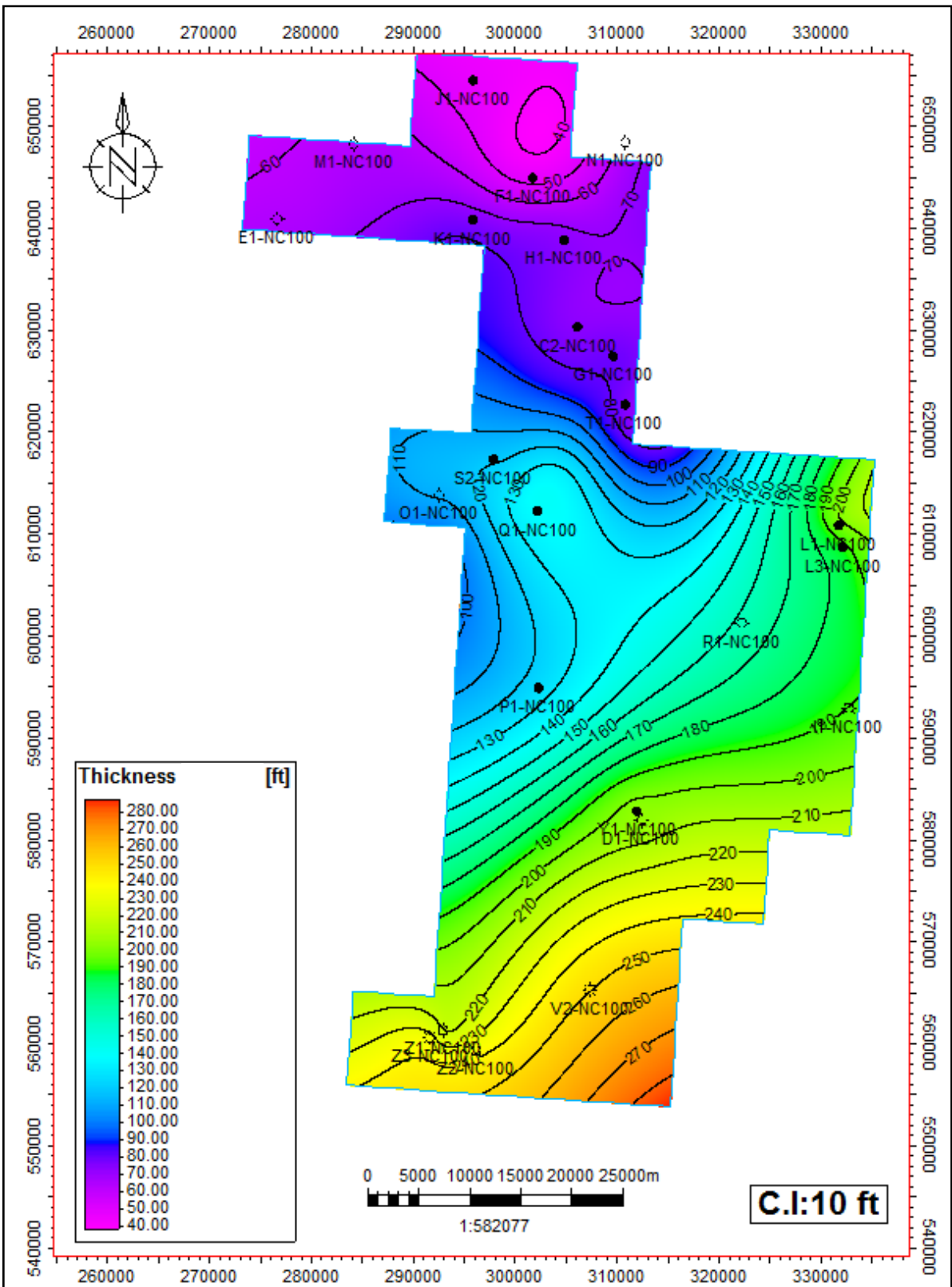


Figure 41. Isopach map of unit Lf2 of the Lower Acacus Formation, Concession NC100, Ghadames Basin, NW Libya.

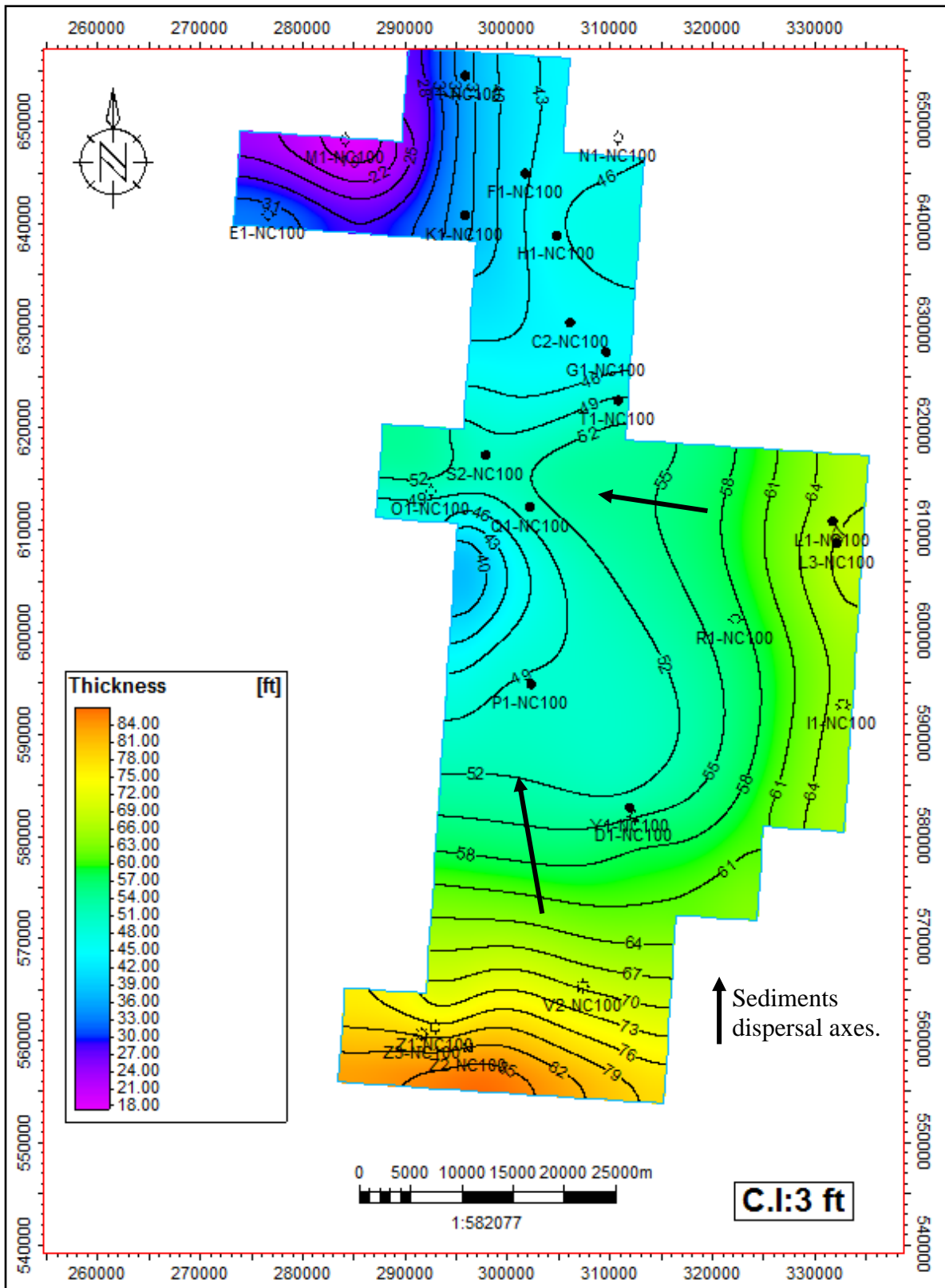


Figure 42. Isopach map of unit A6 of the Lower Acacus Formation, Concession NC100, Ghadames Basin, NW Libya.



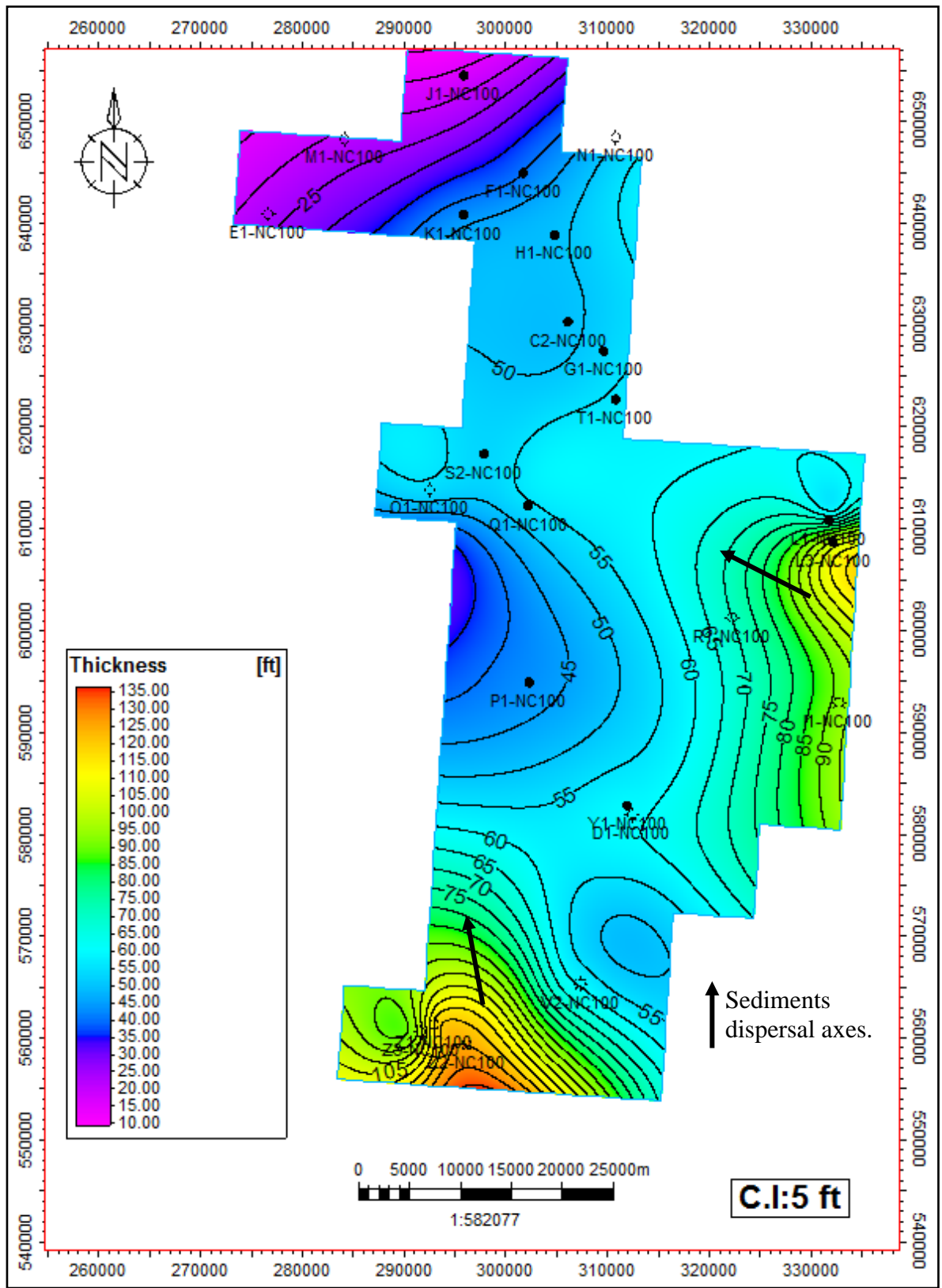


Figure 43. Isopach map of unit A7 of the Lower Acacus Formation, Concession NC100, Ghadames Basin, NW Libya.

From south to north the isopach contours of this (A6) unit (Fig. 42) shows some wavy contour patterns that may be related to progradation event represented by sedimentary dispersal axes that bend progressively westward and northward suggesting multi-channel components affected the sediments dispersal, where sediments decreased in thickness to about 45-50ft in wells P1-NC100, Q1-NC100, G1-NC100, C2-NC100, H1-NC100 and F1-NC100. Hence these wells are characterized by funnel shaped GR-log motif of proximal delta-coastal sandstone lithofacies.

Reduction in thickness of this unit (A6) is very pronounced in the far northern-end of concession NC100 in the vicinity of well N1-NC100 which believed to represent marginal-offshore marine lithofacies of spiky shaped GR-log motif.

**d)- Isopach map of unit A7:**

The isopach map of unit A7 (Fig. 43) shows some retreat of coastline which marked by 65ft contour closer to wells L1-NC100, L3-NC100 to the east and to well V3-NC100 to the south. The maximum thickness of this unit is 130ft around wells Z1-NC100, Z2-NC100, and Z3-NC100 to the south and of about 115ft in the vicinity of wells L1-NC100 and L3-NC100 to the east. It changing thickness northward from 65ft to 35ft crossing wells D1-NC100, Y1-NC100, P1-NC100, R1-NC100 to wells Q1-NC100, S2-NC100, T1-NC100, G1-NC100, C2-NC100, H1-NC100, K1-NC100 and F1-NC100.

More reduction in thickness reached 10-20ft was encountered at the most northern end of the concession NC100 in wells M1-NC100 and J1-NC100, where they represent the marginal-offshore site of reworked marine sandstone and bioturbated marine silty shale lithofacies.

**e)- Isopach map of unit A9:**

Figure 44 shows more pronounced stepping-back southerly and westerly coastline, where the maximum thickness of this unit was recorded at 190ft in the most southern edge of the concession east of well V2-NC100, whereas, local high area was minimized the thickness of this unit to about 30ft at the wells D1-NC100 and Y1-NC100 (Fig. 44).

The marginal-offshore limit of this unit was recorded beyond the wells G1-NC100, and C2-NC100 where reworked marine sandstone and bioturbated marine silty shale lithofacies took place.

**f)- Isopach map of unit A11:**

On the level of this unit A11 (Fig. 45), a highly coastline retreat still pronounced with more wavy contour patterns to the south with maximum thickness of 85ft and to the west of maximum thickness of 75ft. The wavy behavior of contour lines is still persisting northward in the vicinity of wells Q1-NC100, S2-NC100 and O1-NC100 defining the maximum extension of the proximal delta-coastal sandstone lithofacies at the level of unit A11 (Encl. 1). Again the marginal limit of this unit was encountered south of wells G1-NC100 and C2-NC100.

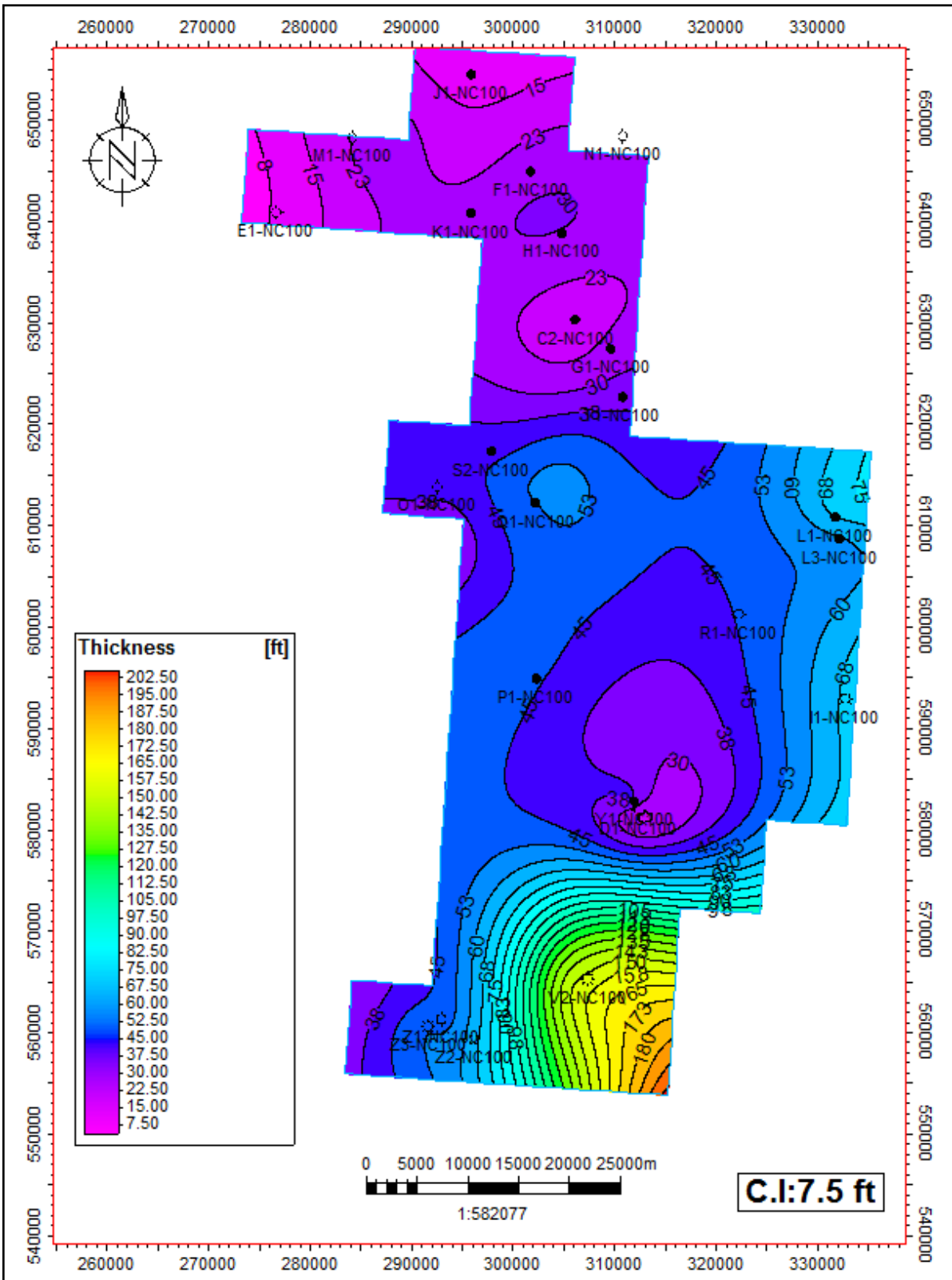


Figure 44. Isopach map of unit A9 of the Lower Acacus Formation, Concession NC100, Ghadames Basin, NW Libya.

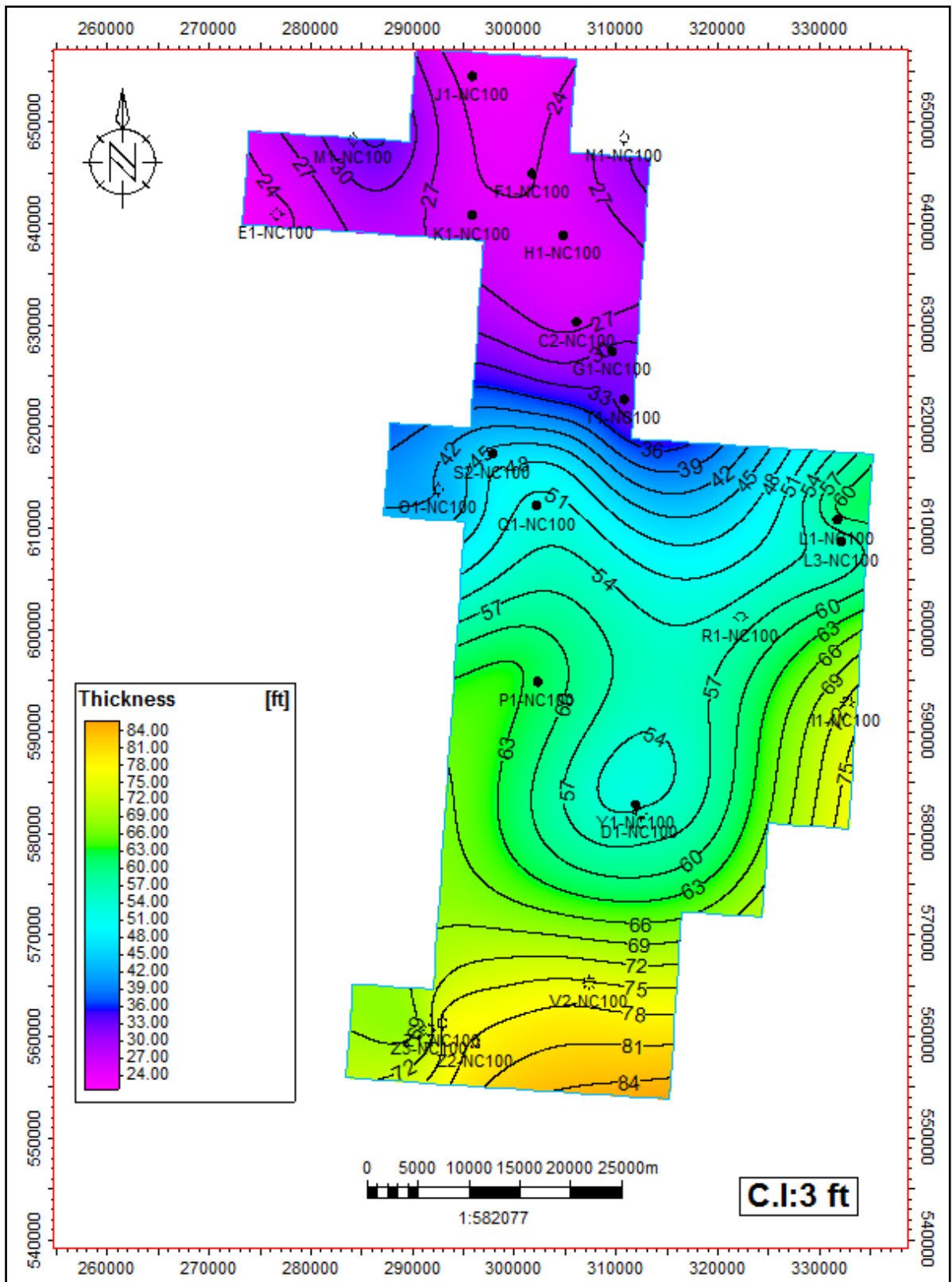


Figure 45. Isopach map of unit A11 of the Lower Acacus Formation, Concession NC100, Ghadames Basin, NW Libya.

### **3- Lithofacies maps.**

Lithofacies maps (Figs. 46 – 50) on a scale of 1:625,000 have been made for some selected studied sandstone units (Lf2, A6, A7, A9, and A11) which are characterized by having good affective thickness, stratigraphic continuity, and better reservoir quality and of hydrocarbon bearing (Enclosure 1). Lithofacies maps (Figs. 46 – 50) are considered a composite map of all available stratigraphic log-data, which assembled in vertical sections for each studied wells (Enclosure 1). Therefore, the constructed lithofacies maps (Figs. 46 – 50) for each stratigraphic unit effectively depict the main trend of the prograding fluvial-channel systems and ultimately the direction from which the clastics were derived from.

Series of lower sea levels occurring during Upper Silurian are strongly affected sedimentation of Lower Acacus Formation. From (Fig. 46) and during deposition of unit Lf2 and its equivalent, fluvial-channel incisions at the south-southeastern part of concession NC100 are recognized during sea level drop and channels prograded northward to shift the coastal deltaic edge (the shelf-slop break or beach) northward in the vicinity of wells F1-NC100, N1-NC100 and westward in the vicinity of wells A1-NC100, and O1-NC100.

During relatively highstands, valleys were stepped-back, back filled and broad costal-deltaic sedimentation covered the area during deposition of A6 unit in the vicinity of wells L1-NC100, D1-NC100 (Fig. 47). Hence, coastal-deltaic sedimentations of Lower Acacus Formation covered the most middle and northern part of concession NC100. At the most northwestern part of concession NC100 conducted as distal deltaic to marine lithofacies were recorded or recovered in the vicinity of J1-NC100, M1-NC100, and E1-NC100.

Similar scenario was also persisting during deposition of unit A7 (Fig. 48), but with a little retreat of coastline behind the well L3-NC100 in which unit A7 was encountered to be of deltaic origin.

Stepped-back and forth coastline around wells V2-NC100, Z1-NC100, and Z2-NC100, Z3-NC100 to the south on the level of units A9, and A11 (Figs. 49, and 50), where the coastal-deltaic zone was reduced during highstands sea level and of southward spread of the offshore-marine margin to cover most of the northern part of concession NC100 and recorded its lithofacies (distal deltaic marginal silts & shale) between well G1-NC100 and well T1-NC100 and extended between A1-NC100, D1-NC100, and V2-NC100 to the south (Fig. 49) and between well T1-NC100 and well S2-NC100 (Fig. 50).

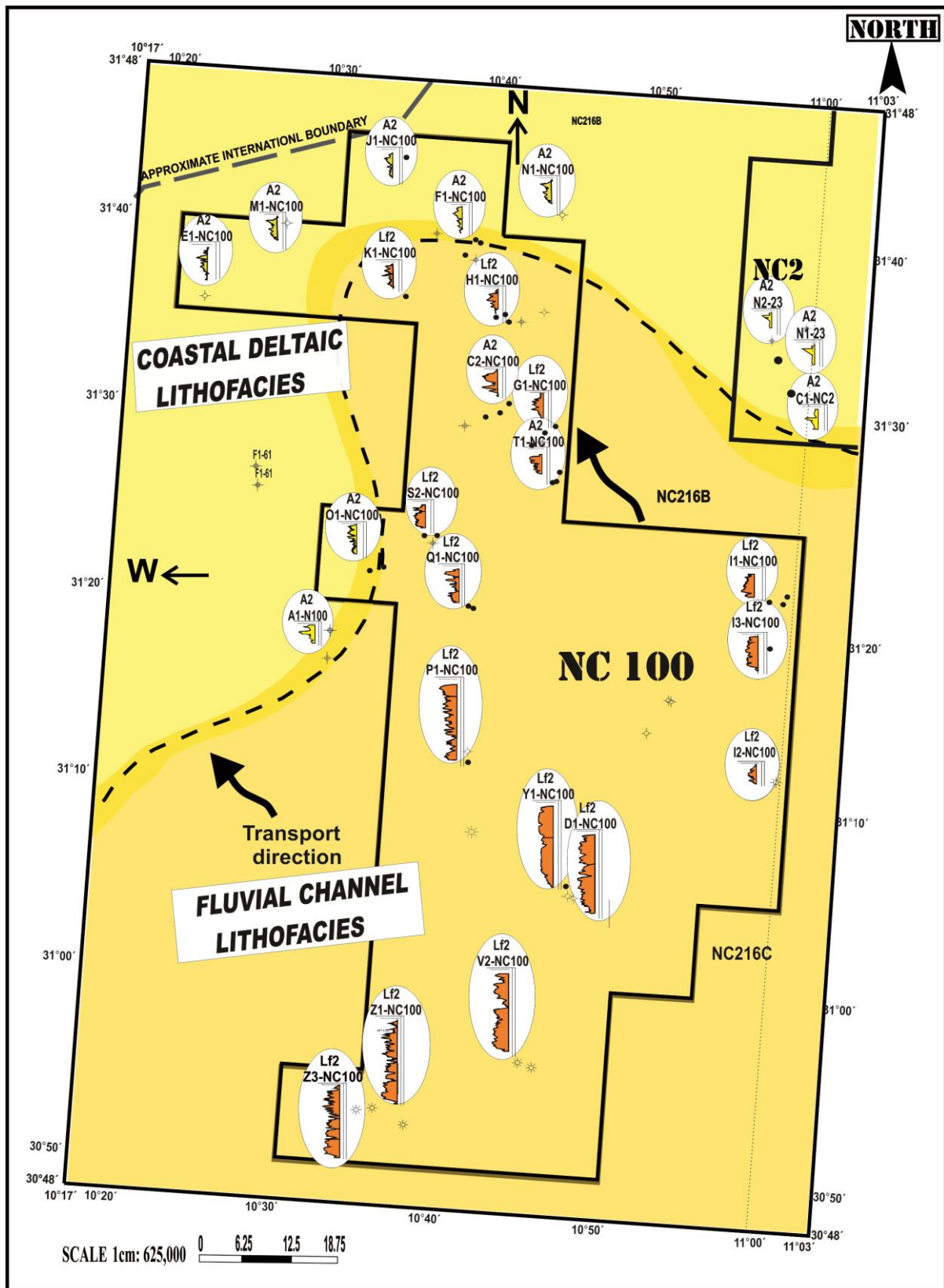


Figure 46. Lithofacies map of Lf2 sandstone unit and its equivalent of the Lower Acacus Formation, Concession NC100, Ghadames Basin, NW Libya.

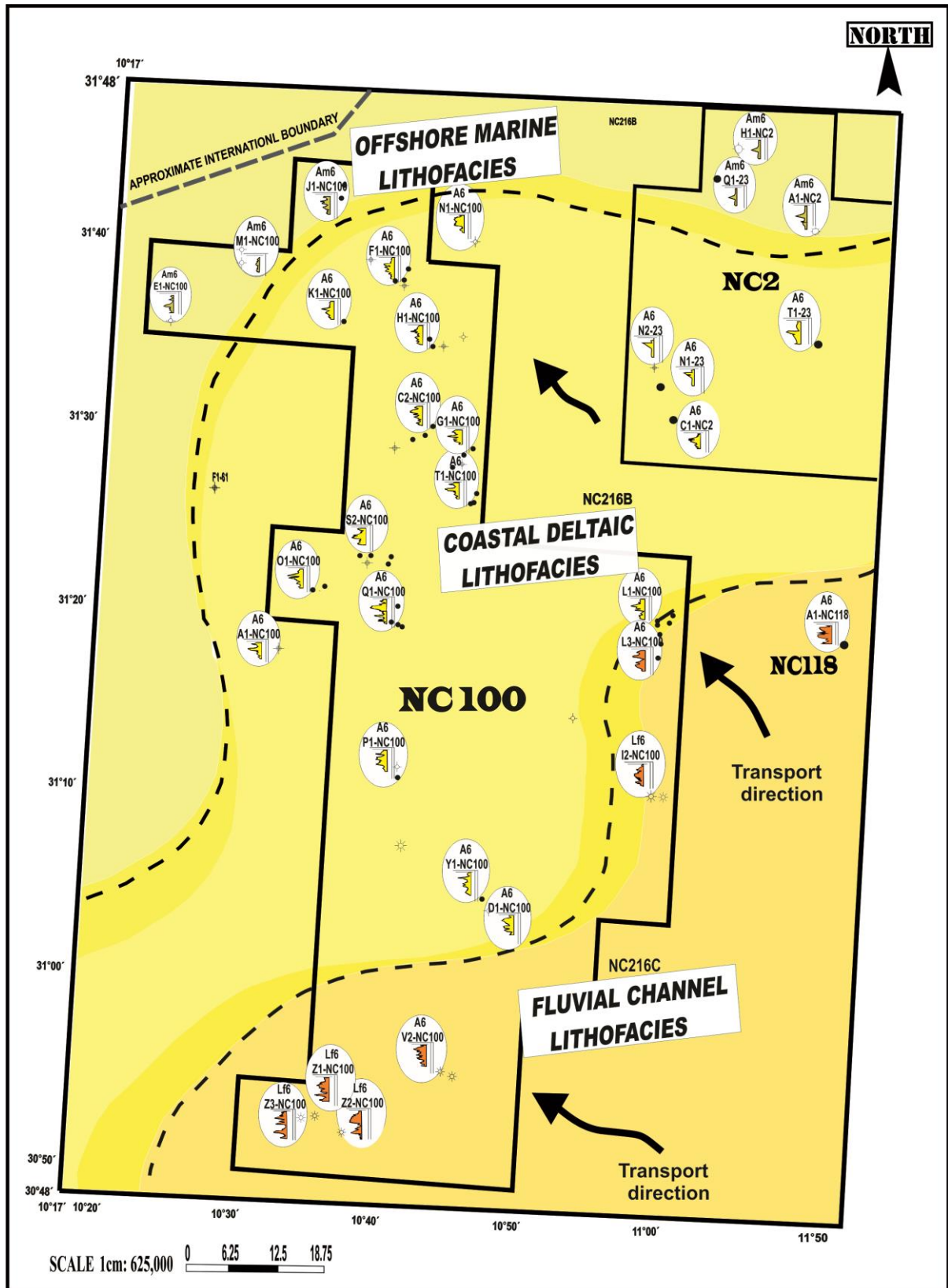


Figure 47. Lithofacies map of A6 sandstone unit and its equivalent of the Lower Acacus Formation, Concession NC100, Ghadames Basin, NW Libya.



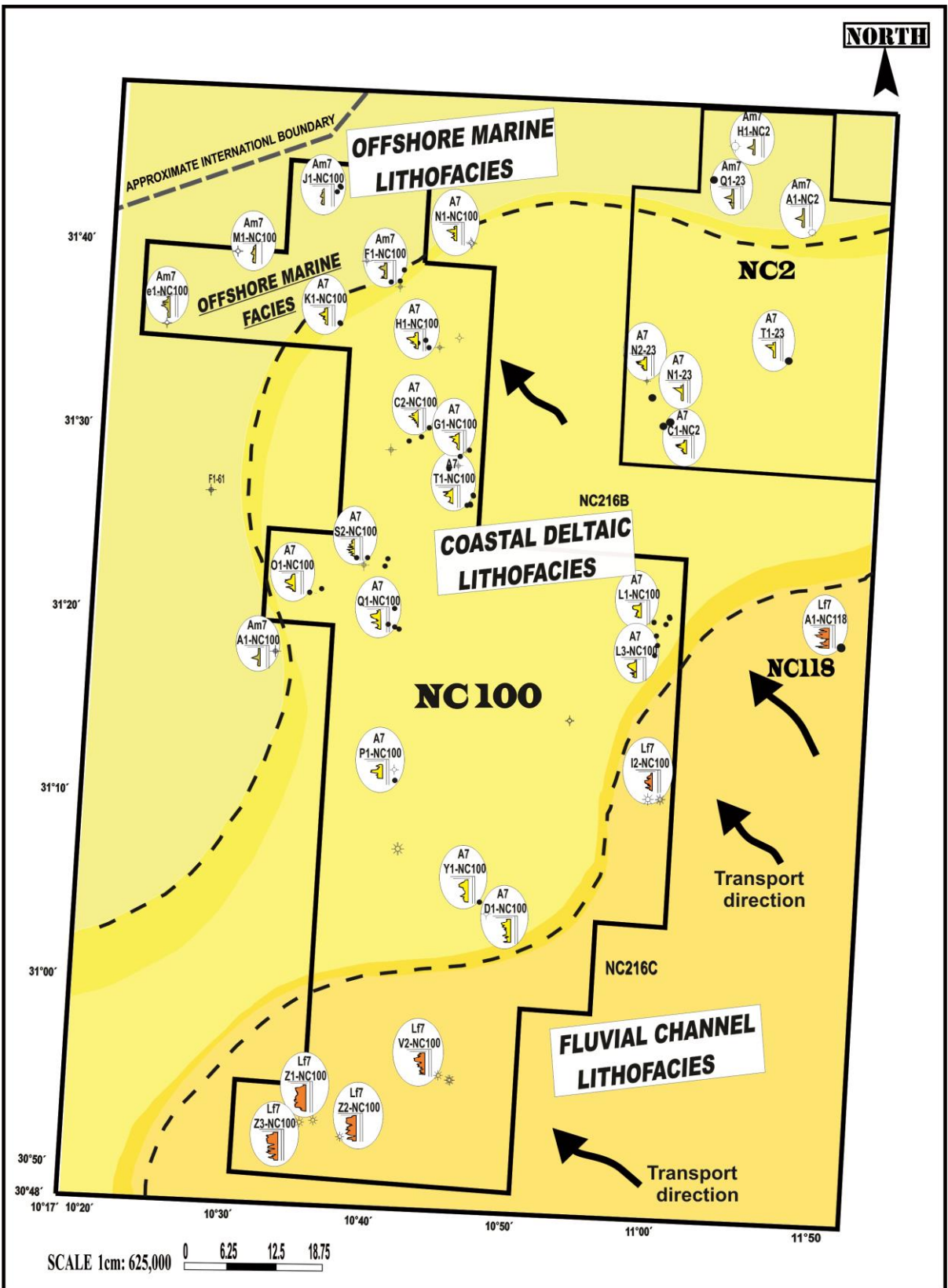


Figure 48. Lithofacies map of A7 sandstone unit and its equivalent of the Lower Acacus Formation, Concession NC100, Ghadames Basin, NW Libya.

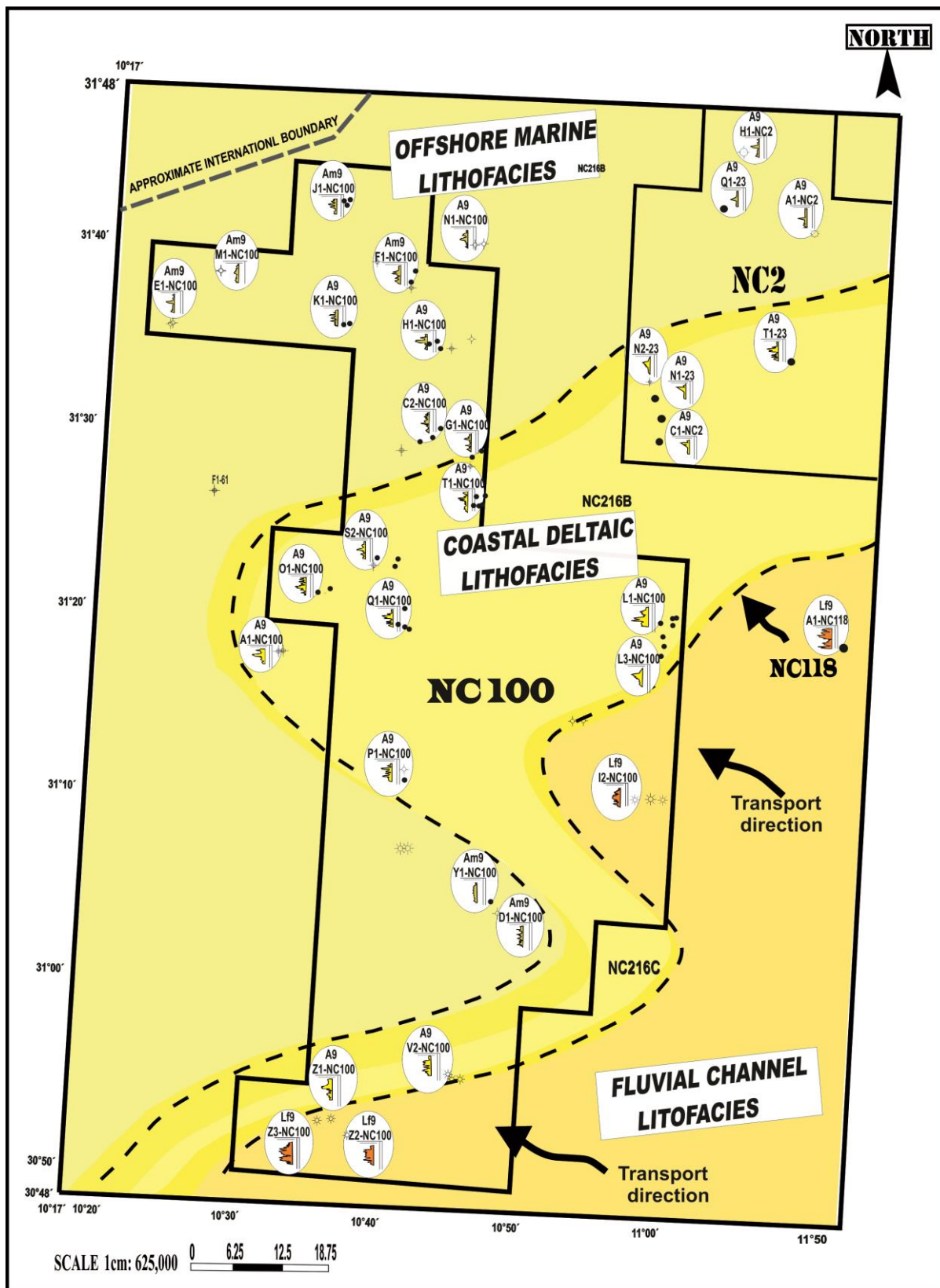


Figure 49. Lithofacies map of A9 sandstone unit and its equivalent of the Lower Acacus Formation, Concession NC100, Ghadames Basin, NW Libya.

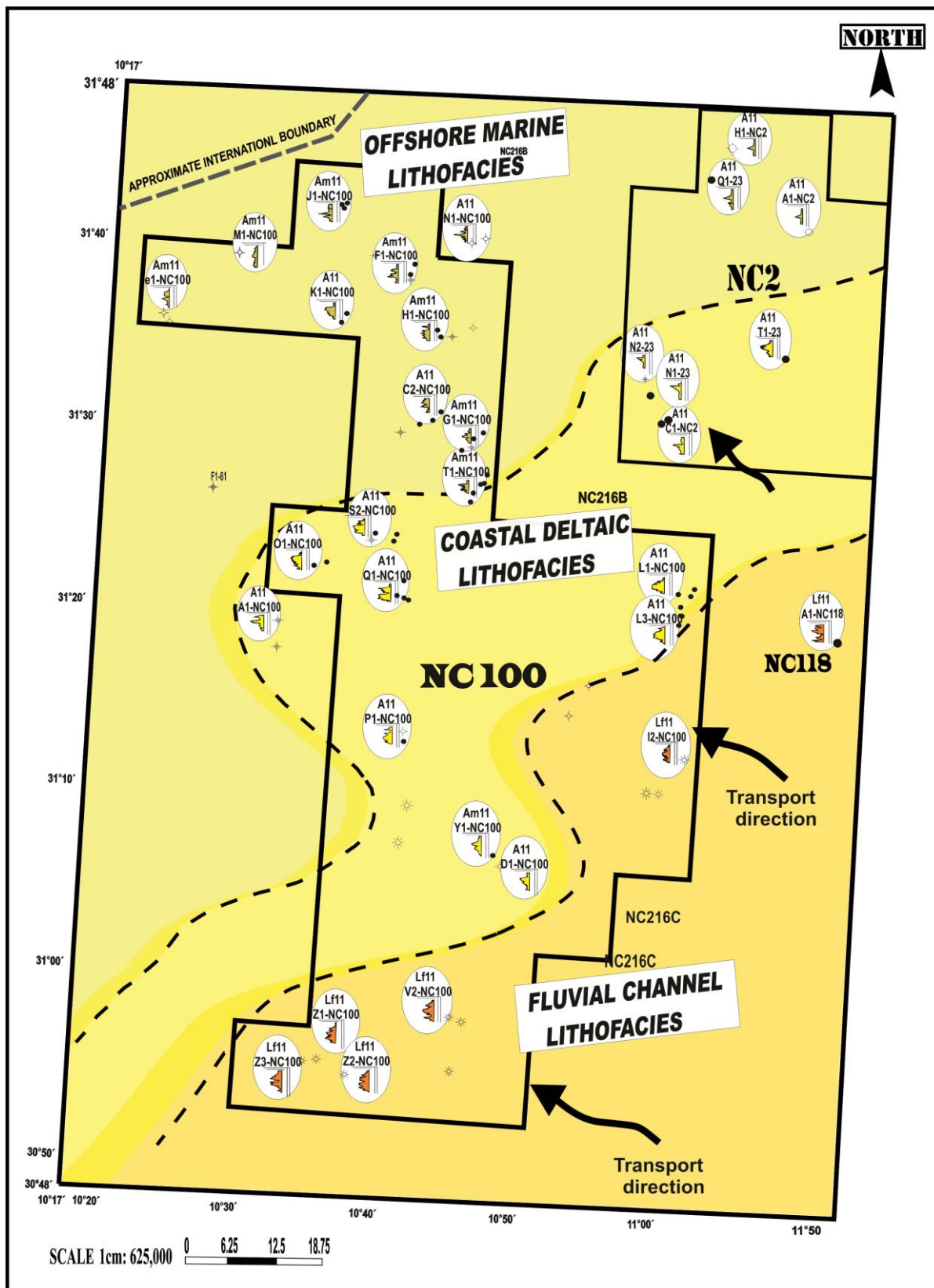


Figure 50. Lithofacies map of A11 sandstone unit and its equivalent of the Lower Acacus Formation, Concession NC100, Ghadames Basin, NW Libya.

## 6. PETROGRAPHY.

Petrographic study conducted on (18) thin sections obtained from different sandstones of Lower Acacus Formation by counting (200) points per thin section aiming to define rock texture and quantity detrital composition, cement types and matrix generated diagenetic constituents and pore types (Table 6), using Gazzi; Dickinson modal method employed by Dickinson, (1970) and Zuffa, (1980 & 1985).

**Table 6. Average mineral framework composition, cement types, and thin section porosity, in percent, for the various sandstone units of the Lower Acacus Formation, concession NC100, Ghadames Basin, NW Libya. (Based on modal point counts (200 points) and modal estimates of thin section).**

Lower Acacus Sandstone Units	Sandstone Lithofacies	Well Name Core # No	Sample Depth (ft)	Framework Composition (%)					QFL Normalization Calculations			Grain Size (mm)	Authigenic Cement Types (%)			T.S. $\phi$ (%)
				Q	F	L	M & O	Cly Mtx	Q	F	L		Sil	C	D	
Lf2 Lf2 Lf2  Lf2 Lf2 Lf2	Fluv. Sst.	Z1-NC100 C#1	11688.6	91	4	2	2	1	94	4	2	0.42	8	6	1	5
	Fluv. Sst.		11694.3	89	5	4	1	1	90	6	4	0.36	7	4	1	10
	Fluv. Sst.		11698.3	88	5	3	2	1	92	5	3	0.33	7	5	1	10
	Fluv. Sst.	Z3-NC100 C#3	11716.2	88	5	3	2	2	92	5	3	0.34	8	5	1	10
	Fluv. Sst.		11730.3	85	6	5	1	3	88	7	5	0.40	7	6	2	9
	Fluv. Sst.		11746.3	81	6	7	2	3	85	6	9	0.30	7	5	2	3
A6 A6  Rm A4 A4  A11	Prx. delt. frt.	Q1-NC100 C#1	10465.4	89	2	5	1	3	93	2	5	0.27	2	10	3	18
	Prx. delt. frt.		10467.8	88	2	5	2	3	92	2	5	0.25	3	12	4	14
	Rew. mar.	Q1-NC100 C#3	10559.5	83	3	6	2	6	90	3	7	0.18	2	8	2	7
	Prx. delt. frt.		10571.4	86	2	6	2	4	89	2	9	0.32	2	10	4	16
	Prx. delt. frt.		10587.3	87	2	7	2	2	90	3	7	0.30	3	9	3	19
	Prx. delt. frt.	L3-NC100 C#2,3	9312	80	4	6	5	4	89	4	7	0.18	2	6	4	8
Prx. delt. frt.	9331.4		85	4	6	2	4	89	5	6	0.21	4	8	6	13	
Prx. delt. frt.	9334.8		83	3	9	2	3	87	3	10	0.19	3	7	7	8	
Ad Ad	Dis. delt. frt.	Q1-NC100 C#1	10491.4	68	7	9	4	12	80	9	11	0.13	1	6	2	1
	Dis. delt. frt.		10490.7	75	5	8	3	9	85	6	9	0.08	2	8	4	2
Rm Rm	Rew. mar.	C2-NC100 C#2	9412.2	84	3	6	2	5	90	3	7	0.16	2	11	4	10
	Rew. mar.		9416.7	82	4	6	2	6	89	4	7	0.15	3	1	5	8

Lf2: Lower Acacus Fluvial sandstone unit; A4, A6, and A11: Lower Acacus deltaic sandstone units, Ad: Lower Acacus distal deltaic silty sandstone unit; Rm: Lower Acacus reworked marine sandstone unit.

Prx.: proximal delta front-costal sandstone lithofacies; Dis. delt. frt.: distal delta front silty sandstone lithofacies; Fluv. Sst.: Fluvial channel sandstone lithofacies, Rew.mar. : Reworked marine sandstone lithofacies.

Q : Quartz.

F : Feldspar.

L : Lithic Fragments.

Cly Mtx : Clay matrix.

M & O : Mica and other labile grains.

Sil : Silica cement; C: Calcite cement; D: Dolomite cement.

T.S. $\phi$  : Thin section porosity.

### **A) – Rock texture.**

The examined sandstones are very fine to medium grained, subangular-subrounded (Figs. 51a & b), showing some clastics orientation and deformation structures may be seen at places (Fig. 52). They are poorly to well sorted with localized fractures filled by clay matrix. (Figs. 53a, & b). Presence of quartz overgrowths and compaction of some mud clasts may modify the roundness in some samples.

### **B) – Detrital composition.**

The main composition of the studied samples is sublitharenities with quartzarenite and rarely litharenites (Fig. 54). The studied lithofacies show some substantial differences in average composition; **Q90, F6, L4** for the fluvial sandstone lithofacies, **Q90, F4, L6** for the proximal deltaic and coastal sandstone lithofacies, **Q83, F7, L10** for the distal deltaic sandstone lithofacies, and **Q89, F4, L7** for the reworked marine sandstone lithofacies.

These compositional differences may be seen with the distal deltaic sandstone lithofacies (Ad), and reworked marine sandstone (Rm) lithofacies which have tendency for higher percentages of feldspar, lithices, and clay contents (Fig.55) and hence they characterized by less thin section porosity. However fluvial channel sandstone lithofacies (Lf) and proximal deltaic and coastal sandstone lithofacies (A6, A4 and A11) are characterized by having high percentage of quartz and feldspar and of less percentage of lithic and clay contents (Fig 55). Moreover, they are characterized by silicate and carbonate cements on their leaching they enhanced secondary porosity.

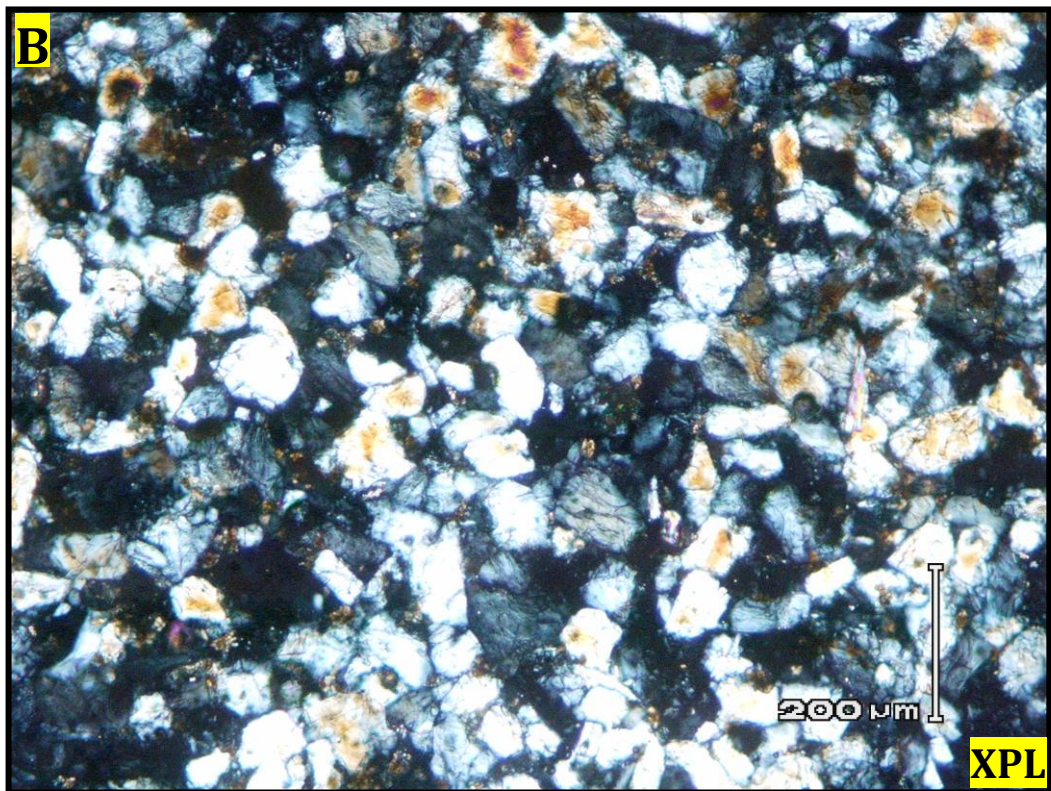
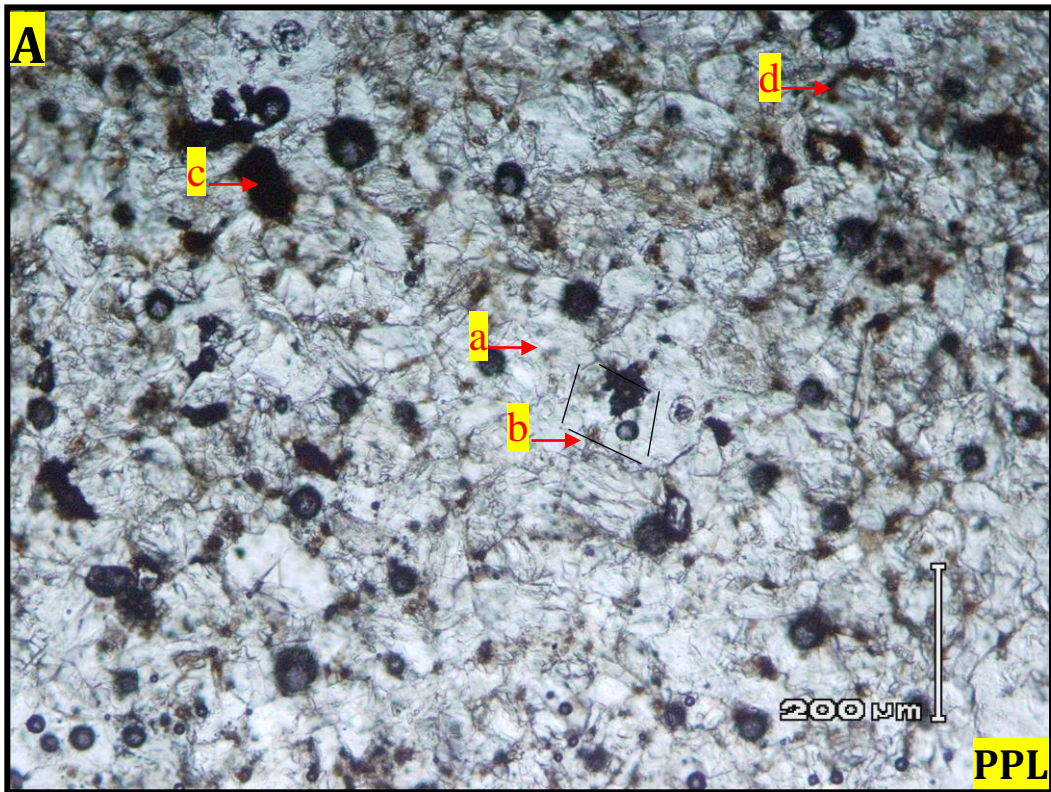


Figure 51a, b. Thin section photomicrograph of sublitharenite, fine-medium grained, sub angular to sub rounded, in fluvial channel lithofacies of Lower Acacus Formation, showing (a) Monocrystalline quartz, (b) Feldspar, (c) Clay clast, (d) Clay matrix, core # 3 @ 11716.2ft, well Z1-NC100.

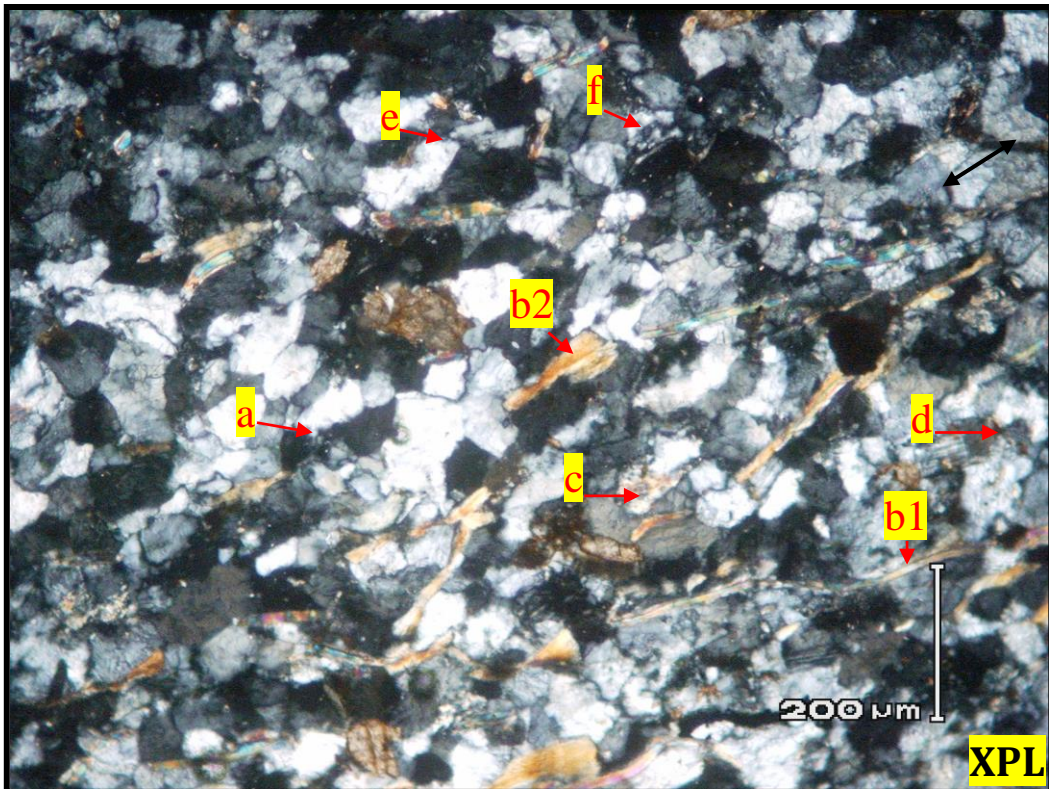


Figure 52. Thin section photomicrograph of Quartzarenite, in fluvial channel sandstone lithofacies, fine-medium, poorly sorted, showing (a) Monocrystalline quartz, (b1) Mica (muscovite) show deformation between quartz grains, (b2) Mica biotite flakes pale with yellow birefringence, (c) Clay clasts, (d) Feldspar, (e) Quartz overgrowth, (f) Polycrystalline quartz. Note: grain supported texture of highly compacted grains, poor porosity, core # 1 @ 11688.6ft, well Z1-NC-100.

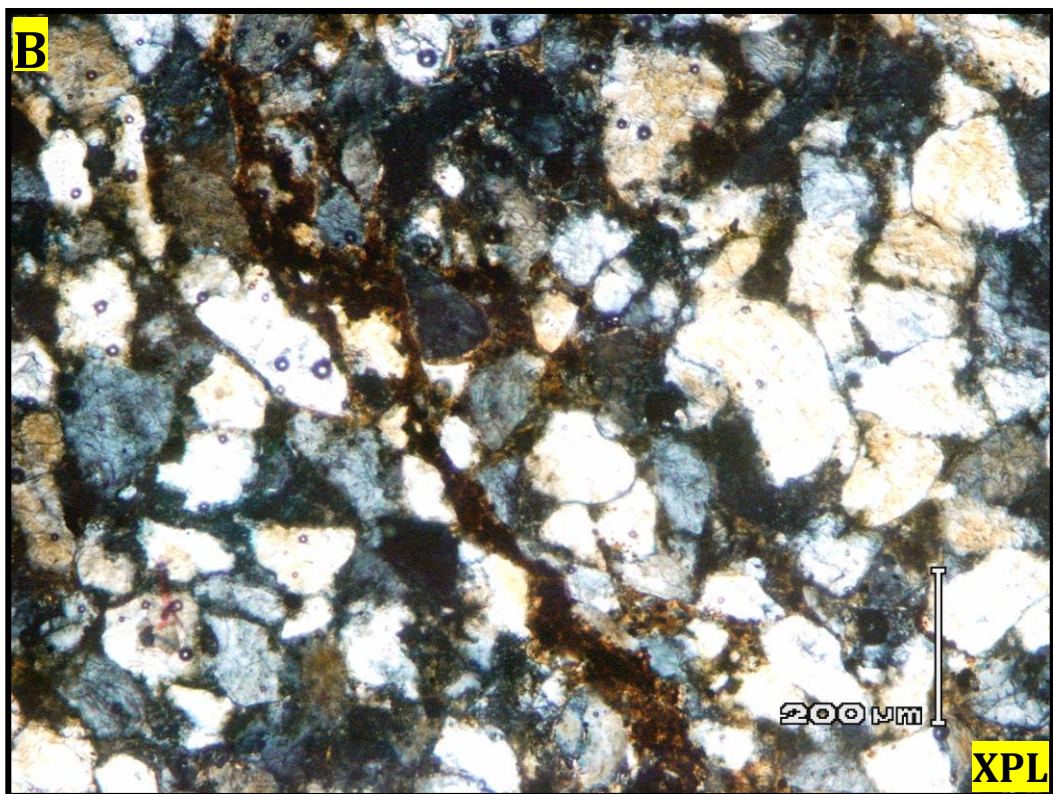
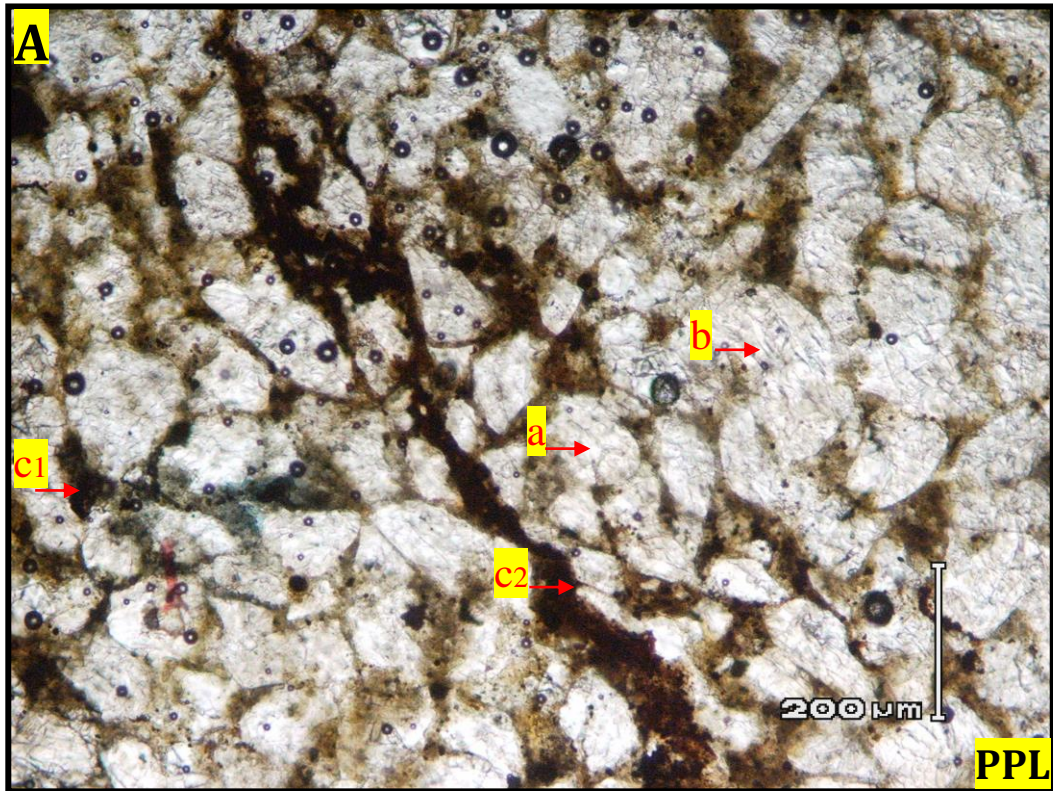
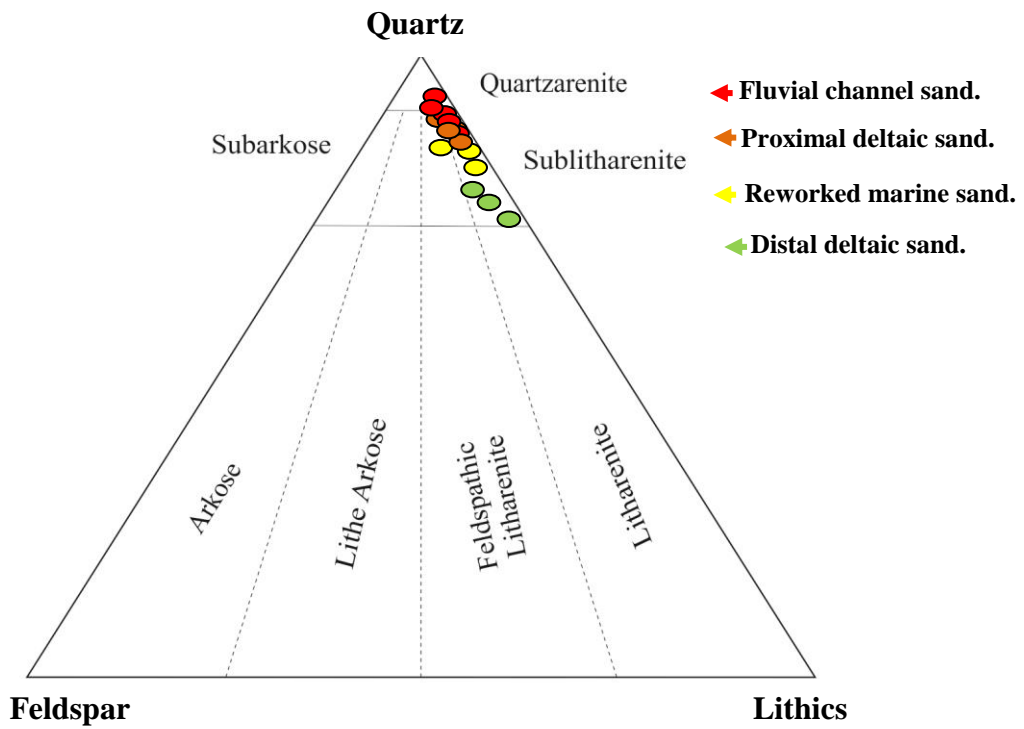


Figure 53a, b. Thin section photomicrograph of sublitharenite in proximal delta front-costal sandstone lithofacies of Lower Acacus Formation showing (a) Monocrystalline quartz, (b) Feldspar, (c1) Clay filling pores, (c2) Clay filling localizing fractures, poor porosity, in (XPL). Note the birefringence colors of clay mineral (possible illite) show in crossed nicols are yellowish dark brown, core # 3 @ 9312ft, well L3-NC-100.





**Figure 54. Detrital plot of various sandstone lithofacies in the Lower Acacus Formation, Concession NC100, Ghadames Basin, NW Libya. At least two sample for each lithofacies. [QFL classification of sandstone, after Folk, 1980].**

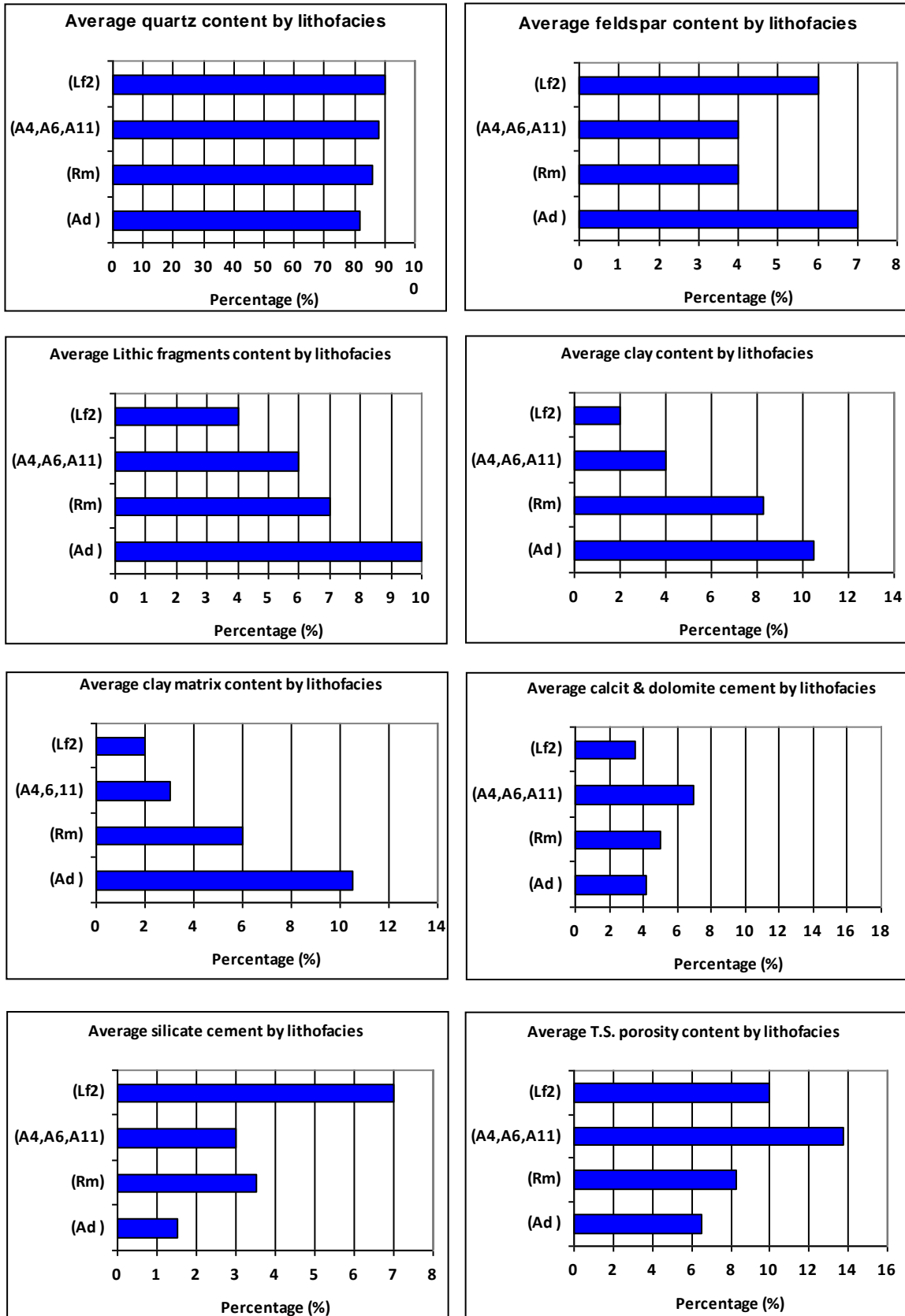


Figure 55. Summary histogram for each constituent identified in the sandstone lithofacies of Lower Acacus Formation.

## **Quartz.**

Quartz grains are dominantly monocrystalline (Fig. 56a and b) (average: 87%; maximum 94% in fluvial sandstone lithofacies, and minimum 80% in the distal deltaic lithofacies).

Most of quartz grains are ranging from 0.14mm to 0.21mm in diameter for the reworked marine sandstone lithofacies (Rm), from 0.07mm to 0.13mm for the distal deltaic siltstone/sandstone lithofacies (Ad), from 0.14mm to 0.35mm for the proximal deltaic and coastal sandstone lithofacies (A4 and A6), and from 0.18mm to 0.40mm for the fluvial channel sandstone lithofacies (Lf), Quartz grains are equant to irregular form, with straight to undulose extinction, occasionally with rounded quartz overgrowth (Figs. 56a and b), and individual grain may exhibit some fractures.

Polycrystalline grains are less common average 3 %, maximum of 5% in fluvial channel sandstone lithofacies (Fig. 52) and minimum of 1% in distal delta front sandstone lithofacies. They are characterized by composite quartz grains, with undulose to wavy extinction.

## **Feldspar.**

Feldspars are volumetrically a minor constituent of the detrital grains, being an average of (5%) (Table 6), range from (2-9%) of total framework constituents. Feldspar grains mostly exhibit lath-like forms occasionally patchy, with polysynthetic twinning show cleavage patterns (Figs. 51a,b, 53a,b and 56a,b). Feldspars commonly increased in the fluvial channel sandstone lithofacies due to proximity to source area, also increased in distal deltaic silty sandstone lithofacies which may suggest shelf break (shelf slope) area preventing decomposition of feldspar.

## **Rock fragments (Lithics).**

Rock fragments or Lithics represent the other dominant detrital constituents. They range from (2% -11%), with (averaging 6.5%) of the detrital grain population and demonstrate an overall increase in percentages from the southern fluvial channel lithofacies northward towards the distal deltaic facies. Lithics are sedimentary rock fragments represented by clay or shale clasts of 2-4mm in diameter, are occasionally light brown to dark brown and filling pores between the rigid quartz grains (Figs. 52 and 53a, b). In addition, polycrystalline quartz grains are comprising about 1-5% of total lithics, it is characterized by composite quartz, stretched with wavy extinction. Other lithic fragments such as fine sandstone or siltstone are rare, but show a small percentage

throughout the studied samples (approximately one grain per thin section which was not statistically significant enough to be recorded in every 200-point count).

**Accessory minerals.**

Other accessory minerals represent (1%-2%) of the total detrital composition and comprise an (average of 1.5%). The apparent accessory minerals include, mica muscovite and biotite flakes with designative birefringence, and garnet with inclusions (Figs 52 and 57a, b).

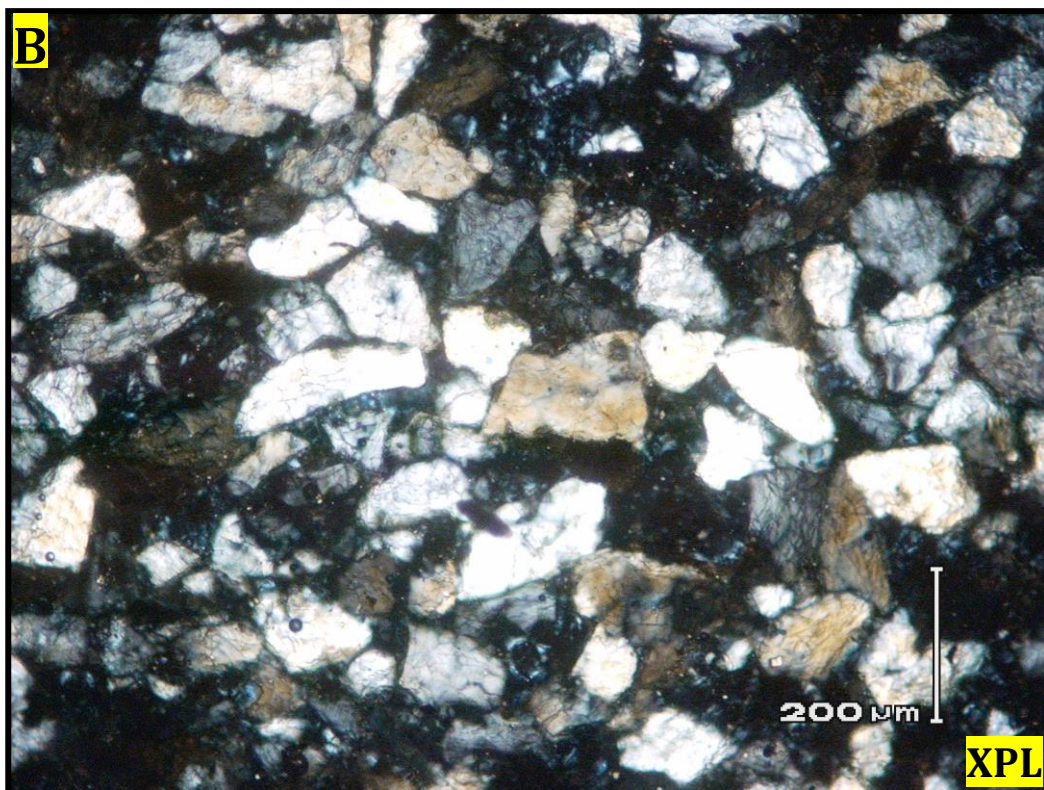
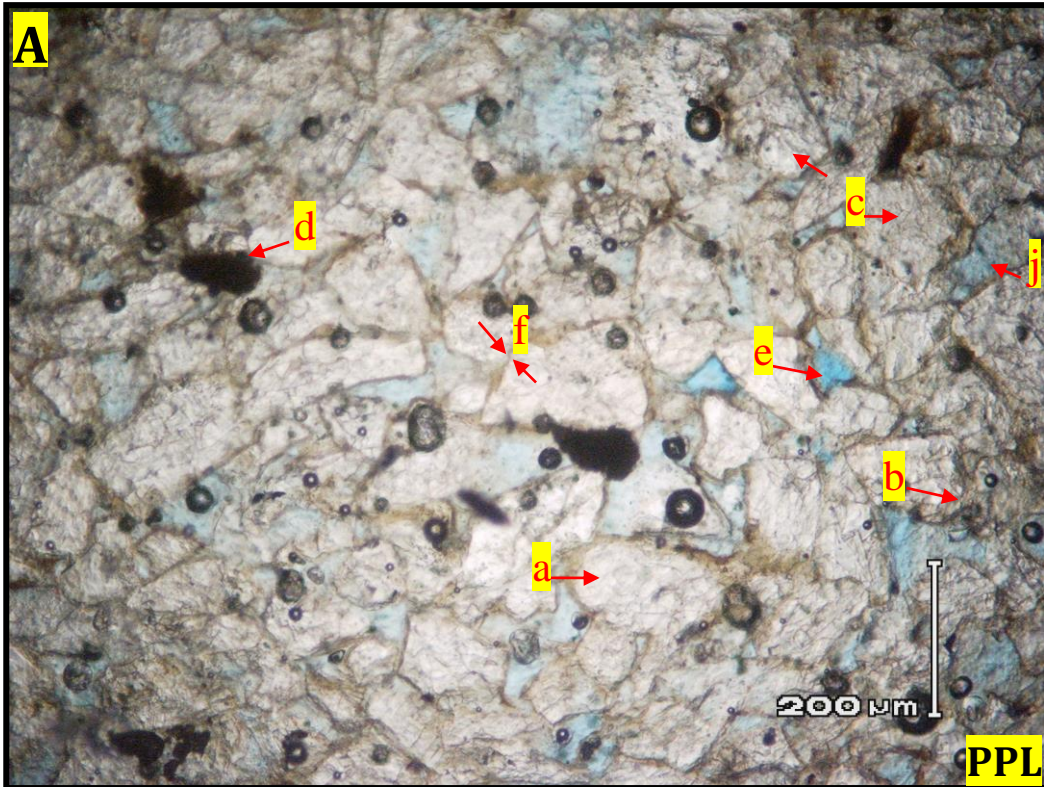


Figure 56a,b. Thin section photomicrograph of sublitharenite in fluvial sandstone lithofacies of Lower Acacus Formation, showing, (a) Equant monocrystalline quartz grains, (b) Quartz overgrowth, (c) Feldspar grains, (d) Partially pore-filling clay clasts, (e) Primary porosity (blue) between uncorroded quartz grains, (f) Pressure solution (arrows). Note: secondary porosity at (j) due to partial leaching of feldspar grain, core#1, @ 11694.3ft well Z1-NC100.

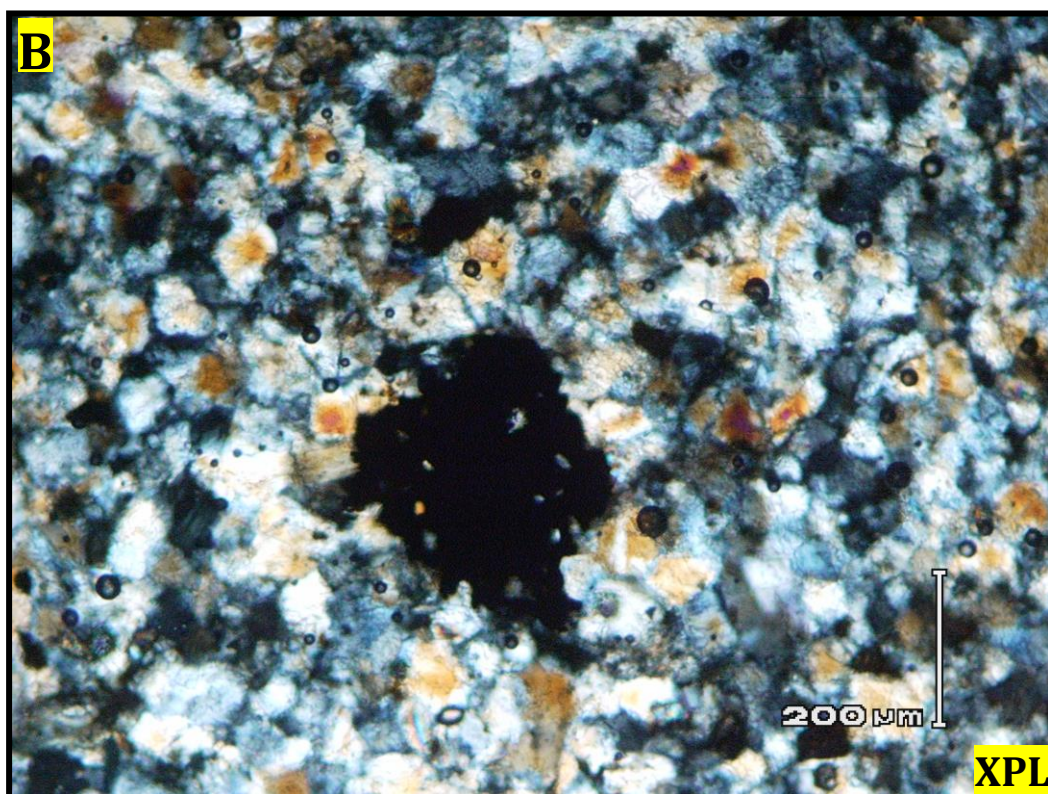
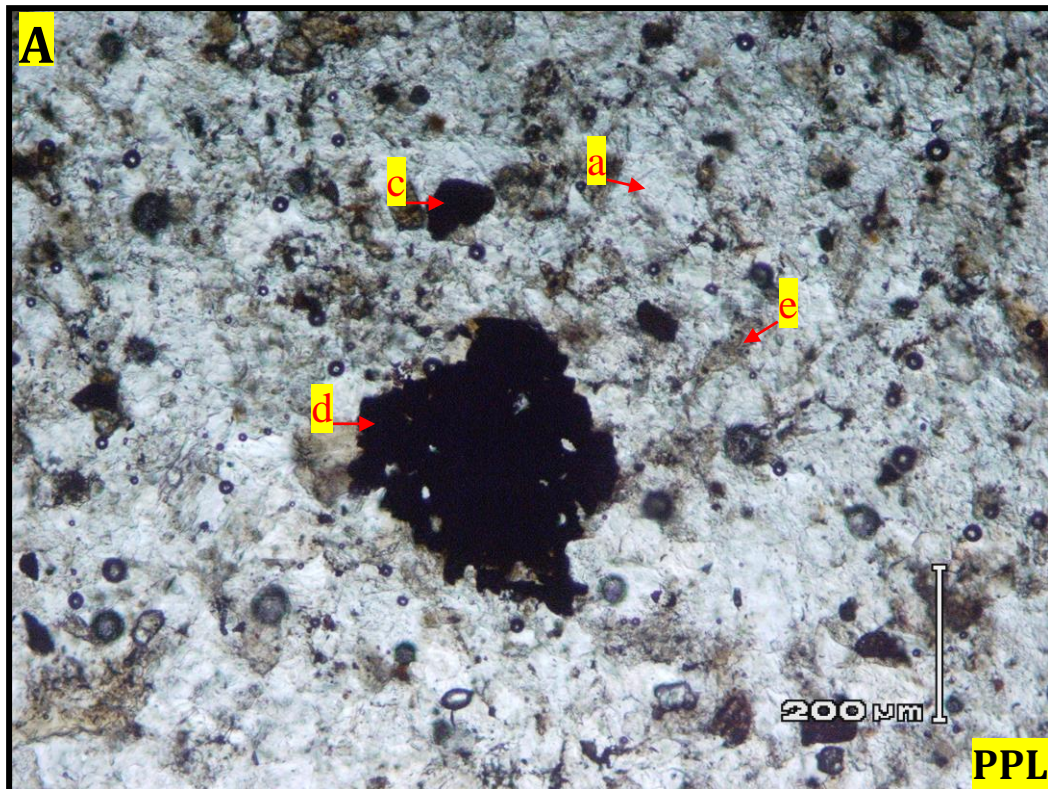


Figure 57a, b. Thin section photomicrograph in fluvial channel sandstone lithofacies of Lower Acacus Formation, showing, (a) Monocrystalline quartz grains, (b) Feldspar grains, (c) Clay clast with rhombic shape may be sideritic, (d) Garnet with inclusions. Note, the grain-to-grain contact and the excessive silicate cement through pressure solution, (e) Thin clay matrix rims quartz grains at some places, core #3, @ 11746.3ft, well Z3-NC100,.

### C) - Cement types and matrix.

Three different types of cements are present in the examined Lower Acacus sandstone: silica, calcite, and dolomite (Table 6).

#### 1) - Silica cement:

Silica is the dominant cement in the fluvial channel sandstone lithofacies, accounting for up to 8% of some samples (Table 6). In general, and on cross-polar the quartz grains appear white through some grey to black shade, where silica cement is presented as quartz overgrowth on detrital grains (Figs. 52 and 56) and as pressure solution between grain contacts during some rock compaction (Fig. 58).

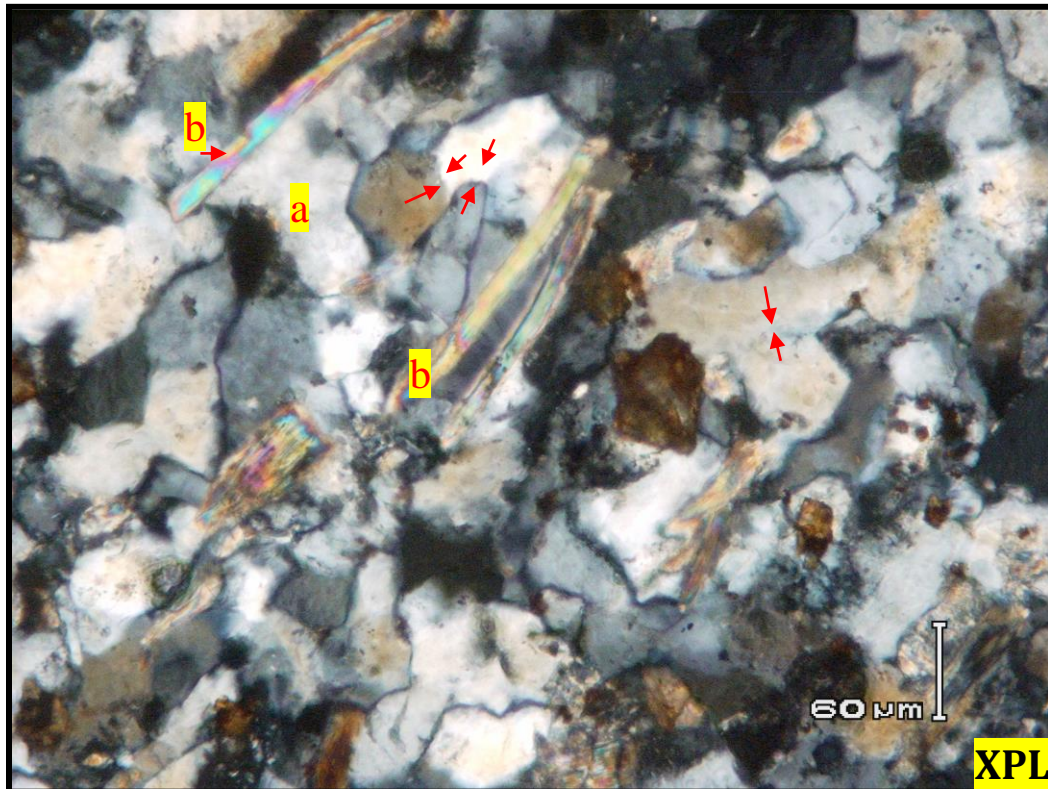


Figure 58. Thin section photomicrograph of quartzarenite, in fluvial channel sandstone lithofacies showing, (a) Compacted detrital quartz grains and the arrows show an interpreting grain contact through which pressure solution may take place. Note: Muscovite (b) is communally deformed by compaction, causing it to wrap around quartz grains, core #1, @ 11688.6ft, well Z1-NC100, concession NC100.

**(2) - Calcite cement:**

Calcite is the dominant cement in the proximal delta front-coastal sandstone lithofacies, accounting for up to 9% of some samples (Table 6). Calcite cement is present as poikilotopic fabric which appear to compose by small pearly speckled grains showing high order yellow to golden birefringence (Fig. 59a and b), occasionally calcite cement occurs as patches filling primary porosity especially in the compacted grain-supported fluvial channel sandstone lithofacies indicating that early compaction preceded calcite cementation (Fig. 60).

**(3) - Dolomite cement:**

Dolomite cement is rarely present and partially account for only 1% of some samples (Table 6) in the fluvial channel sandstone lithofacies (Fig. 61), and as replasive and partially pore-filling in proximal delta front-coastal lithofacies (Figs. 59 and 62) and account for up to 7% (Table 6). Dolomite cement in these samples appears to be weathered, pear-grey crystals with extreme birefringence and of high order greyish-white interference colors, and show rhombohedral cleavages and occasionally with iron oxide stain.



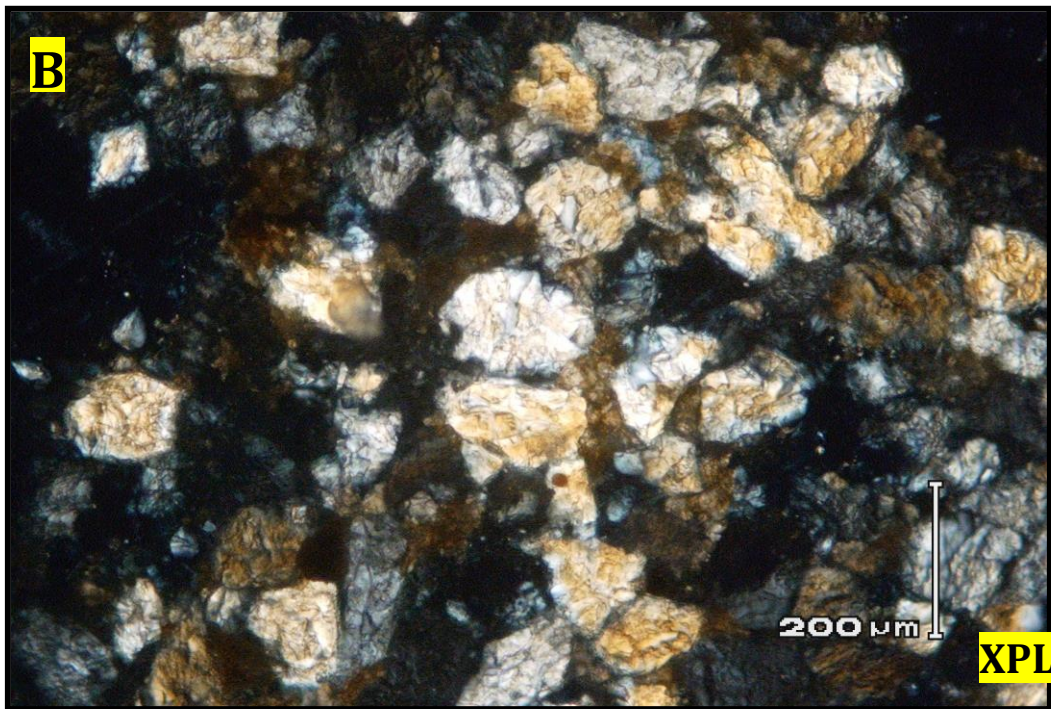
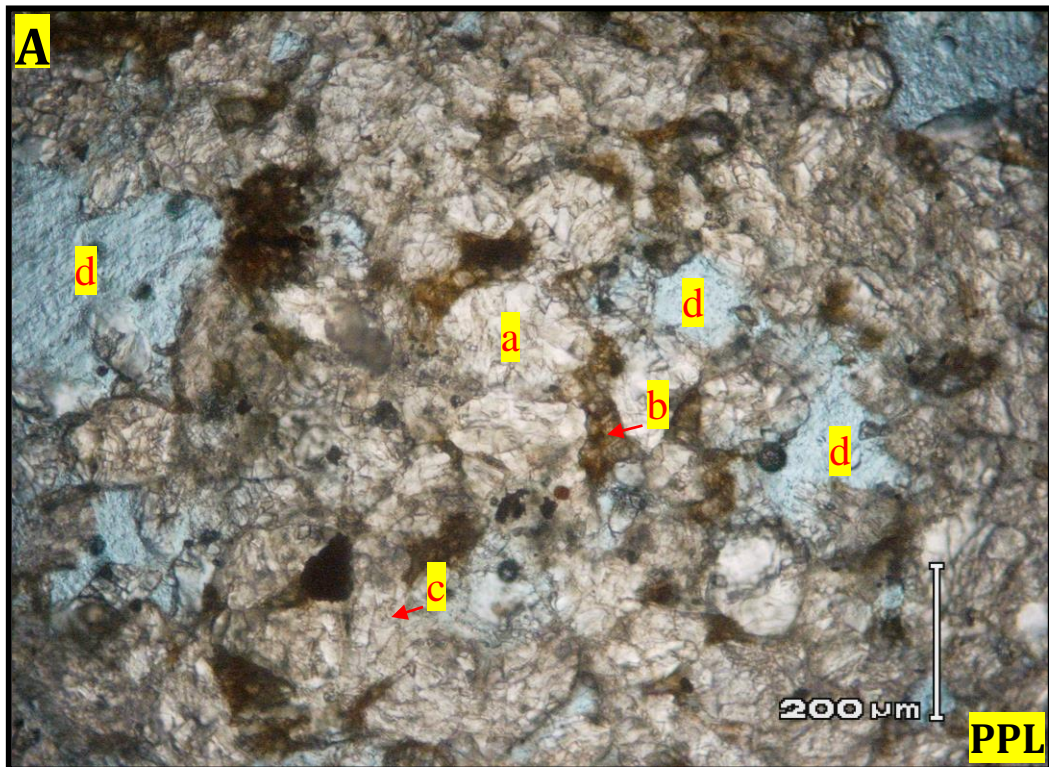


Figure 59a. Thin section photomicrograph delta front-coastal sandstone lithofacies (A4) showing: (a) Quartz grain framework , (b) Partially cemented by poikilotopic calcite , (c) Partial replacive dolomite cement, (d) Secondary pores (large blue areas) formed partially by dissolution of labile grains (feldspar), core #3, @ 10587.3ft, well Q1-NC100, concession NC100.

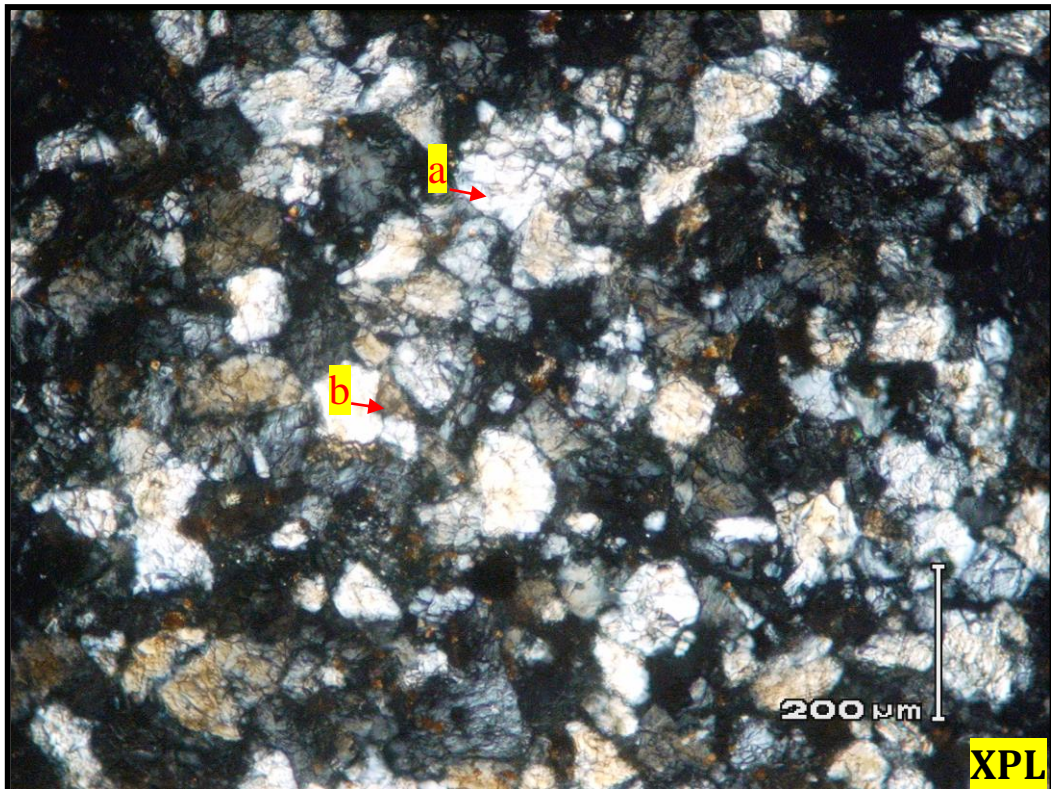


Figure 60. Thin section photomicrograph in fluvial channel sandstone lithofacies of Lower Acacus Formation, showing, (a) Quartz grains supported texture, (b) Partial calcite cement filling primary porosity, core #3, @ 11730.3ft well Z3-NC100.

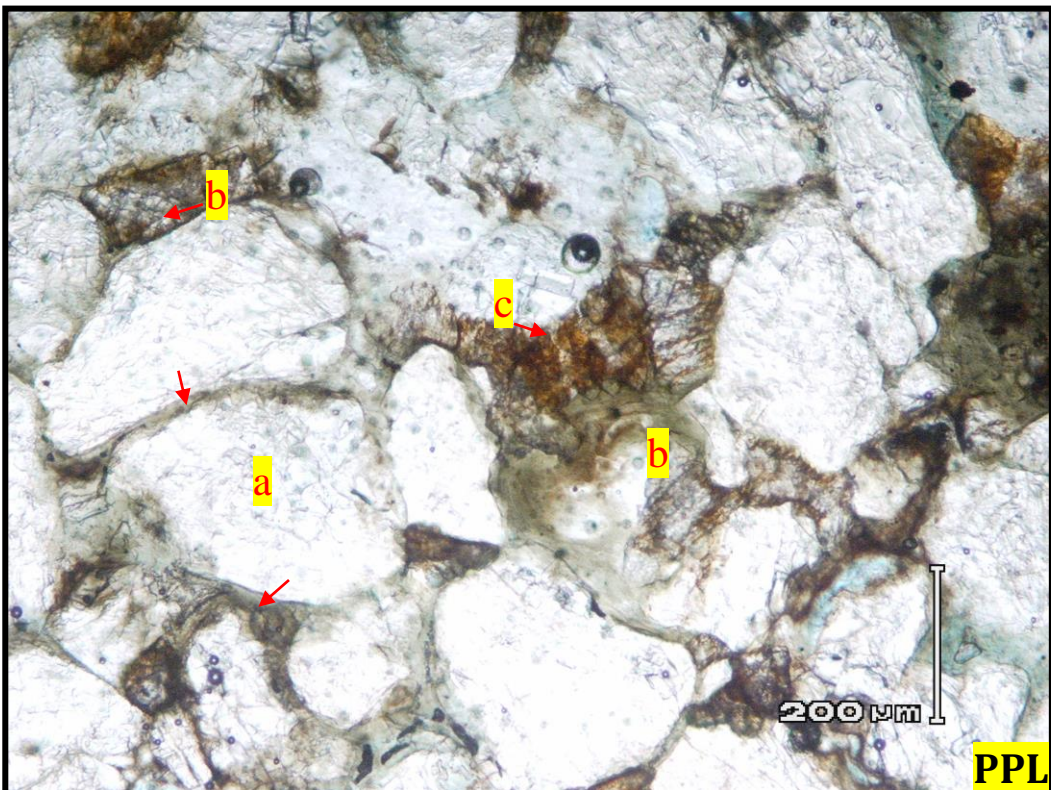


Figure 61. Thin section photomicrograph in fluvial channel sandstone lithofacies of Lower Acacus Formation, showing, (a) Equant monocrystalline Quartz grains with thin clay rim (arrows), (b) Partially cemented dolomite which appeared to be stained partially by iron oxides (c). Note, development of secondary porosity (blue) along ragged edges of quartz grains, core #3, @ 11716.2ft, well Z3-NC100, concession NC100.

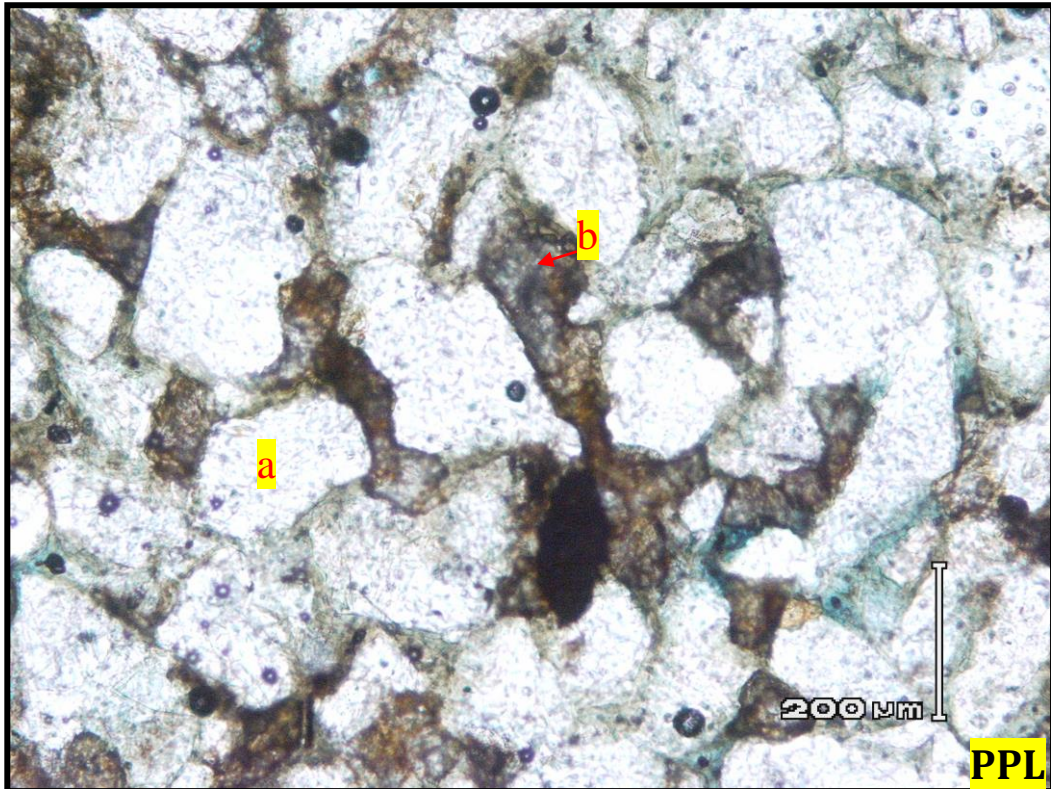


Figure 62. Thin section photomicrograph of delta front-coastal sandstone lithofacies showing: (a) Monocrystalline quartz, (b) Partially dolomite cement filling pores with primary & secondary leaching porosity (blue) may be developed at places, core #2, @ 9334.8ft, Well L3-NC100, concession NC100.

### Clay matrix.

Clay is present as matrix. It marks up as 12% of distal delta front silty sandstone lithofacies (Ad) and about 6% of reworked marine sandstone lithofacies (Am), but of less dominant in the fluvial channel sandstone lithofacies (Lf) and proximal delta front and coastal sandstone lithofacies (A4, A6 and A11) as it is account up to 3% and 4% respectively (Table 6).

It is possible that most of the clay in the studied rock units is authigenic and formed during the alteration of feldspars and some lithics. Most of the apparently authigenic clay in these samples occurs as pore-filling (Fig. 63), fracture fillings (Figs 53a, b), pore lining and rimming quartz grains (Figs. 64 and 65). This clay matrix is characterized by speckled yellowish- brown birefringence of illite (Figs. 53a, b) or in some cases appears to be as clay clasts of illite origin which have been squeezed around the adjacent grains by compaction (Fig. 66). Occasionally it characterized by having small rhombic shaped crystals of possible siderite found to be partially associated with fluvial channel sandstone lithofacies (Fig. 57a) and reworked marine sandstone lithofacies (Fig. 67).

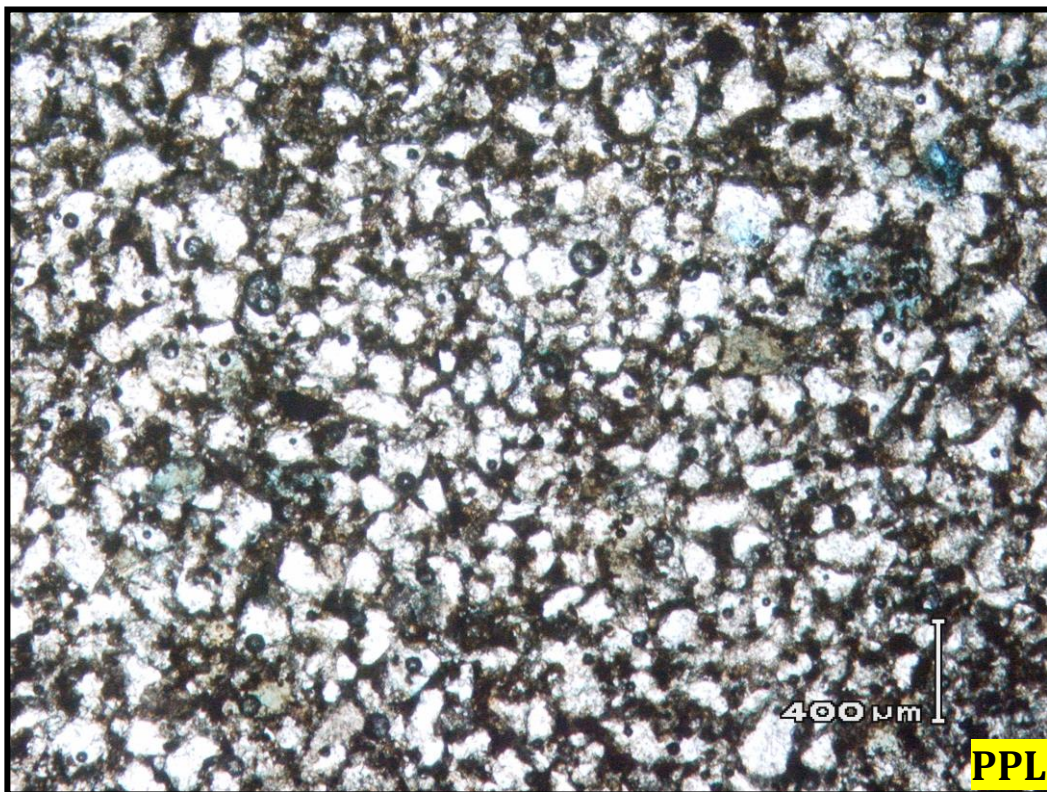


Figure 63. Thin section photomicrograph distal delta silty sandstone lithofacies showing: totally pore-filling clay matrix (dark spots). Note, partial remaining secondary porosity (blue), core #1, @ 10490.7ft, well Q1-NC100.

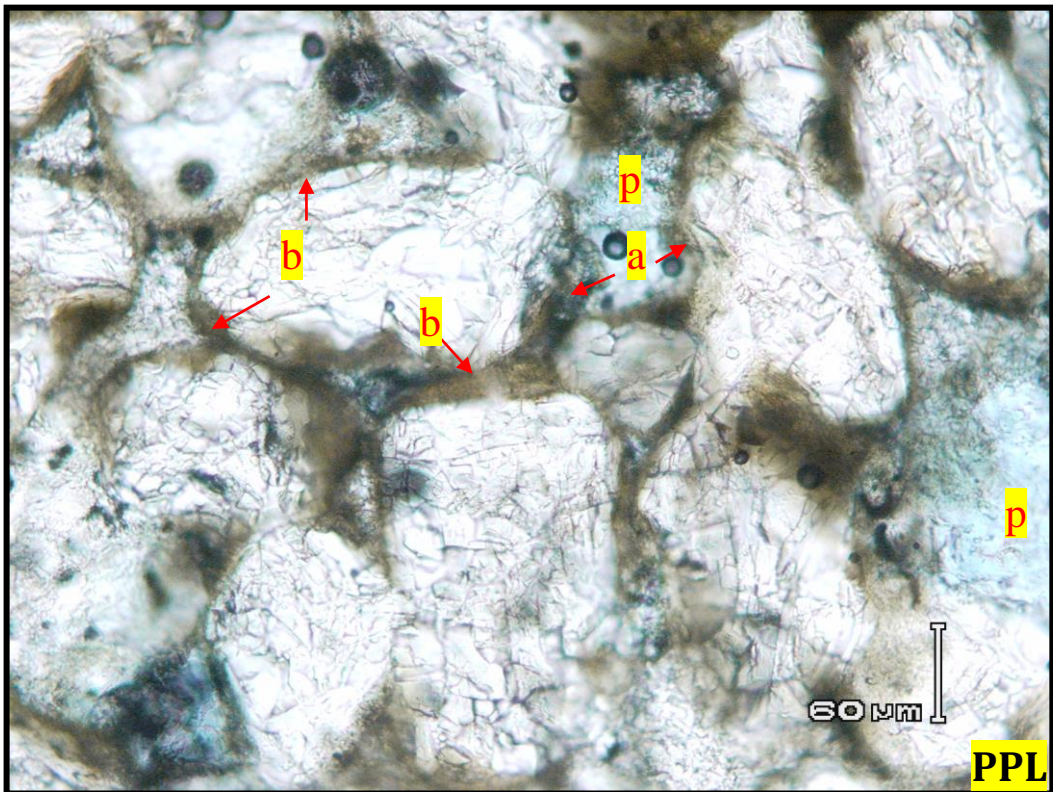


Figure 64. Thin section photomicrograph of proximal delta front-coastal sandstone lithofacies showing: (a) Clay matrix lining pores, (b) Clay matrix rimming quartz grains. Note, development of secondary porosity (blue) as a result of total leaching of cements and labile grains, core #1, @ 10465.4ft, well Q1-NC100.

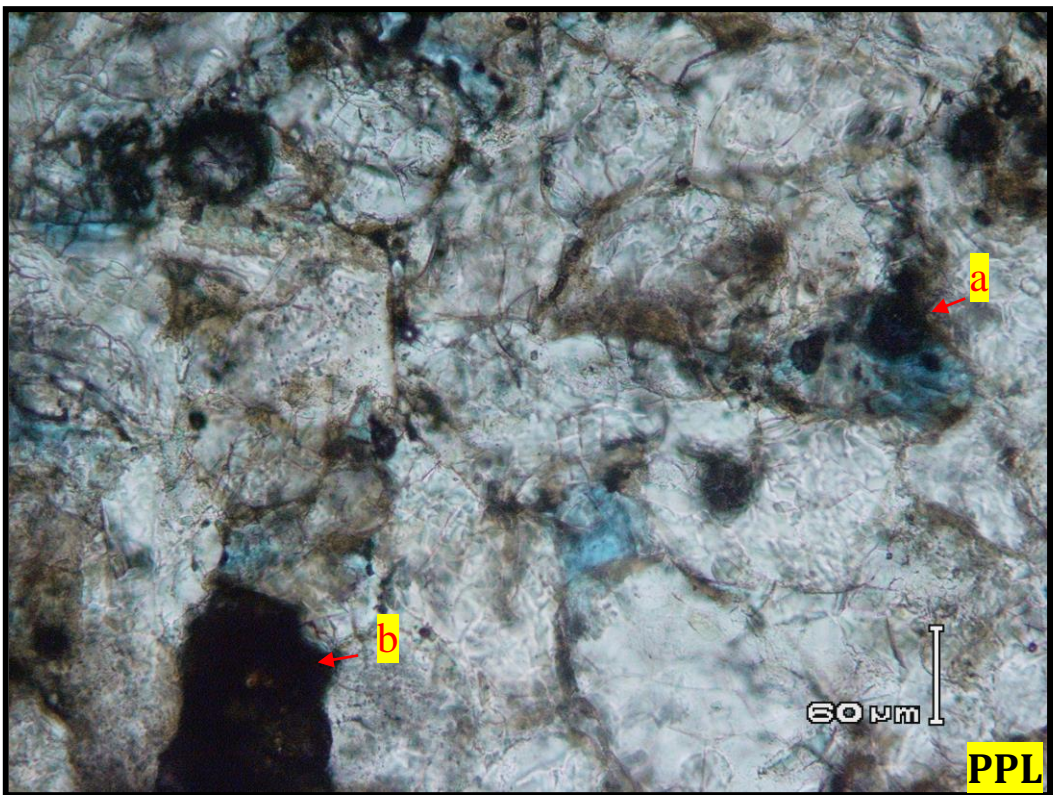


Figure 65. Thin section photomicrograph of reworked marine sandstone lithofacies showing: Clay matrix rimming quartz grains cement and partially filling secondary porosity at (a) and (b), core #2, @ 9412.2ft, well C2-NC100.

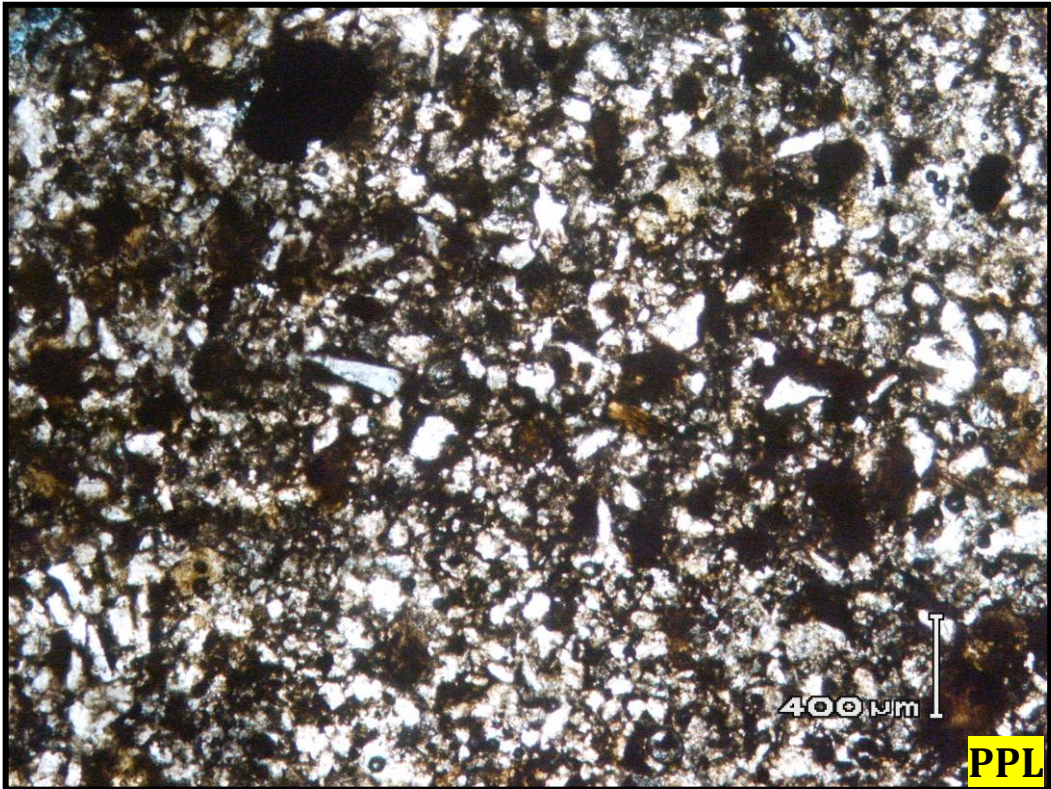


Figure 66. Thin section photomicrograph of distal delta front silty sandstone lithofacies showing: Clay clasts of illite (dark brown) which have been squeezed around the adjacent grains by compaction, core#1, @ 10491.4ft, well Q1-NC100, concession NC100.

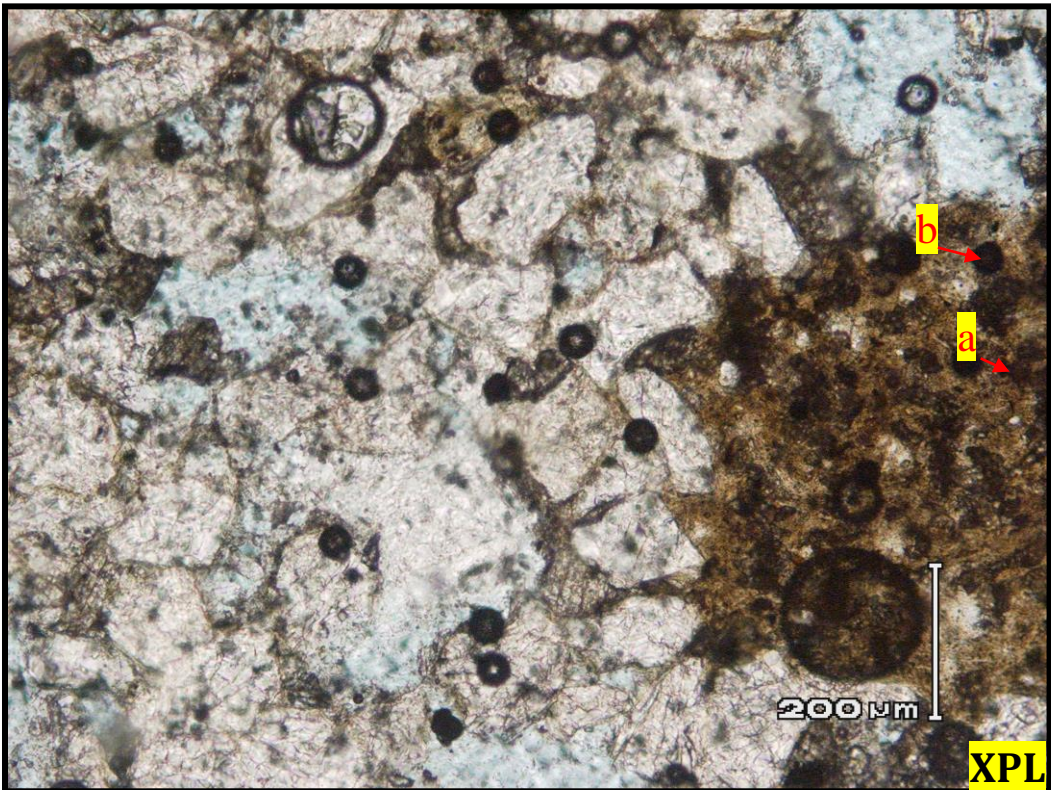


Figure 67. Thin section photomicrograph of reworked marine sandstone lithofacies showing: Pore-filling clay matrix (a), contains possible opaque rhombic siderite crystals (b). Note, partial dissolution dolomite cement and secondary porosity (blue), core #3, @ 10559.5ft, well Q1-NC100, concession NC100.

## **D) – Diagenetic constitutes.**

Petrographic observations have revealed that the studied sandstone units of different lithofacies have undergone several changes during their history from the coastal plain to beach deltaic margin to more shelf slope and basinal areas.

Post depositional processes caused a significant modification of depositional (primary) porosity. The major porosity reducing factors are mechanical compaction, cementation by quartz, carbonates, and clay minerals. The different intergranular volumes of the carbonates (calcite, dolomite) cements in the studied sandstones (Table 6), indicated that the cementation is pre- compactional as well as post compactional.

Shallow water fluvial lithofacies is characterized by early compactional phase through which silica cement represented by pressure solution and of some quartz overgrowths took place (Figs. 51a, b, 56a, b and 58). Hence at this stage the silica enrichment in solution due to dissolution of feldspar grains allowed the precipitation of quartz overgrowths.

Partial clay rim quartz grains, clay clasts, and organic matters between quartz grains (Figs. 53a, b) possibly associated with channel sandstones at low temperature (50°C - 70°C) in the presence of acidic fluids, give rise to partial dissolution of carbonate cements and feldspar grains (Figs. 56a, b). At this stage some siderite crystals may be formed (Figs. 57a, b) this occurrence may be appear in some other lithofacies (Fig. 67).

By changing depth (1.5-2.5 km) and temperature (70°-120° C) mechanical compaction affected the clay clasts, mica and other rock fragments. Poikilotopic regular texture calcite cement in proximal deltaic sandstone (Figs. 59a, b), postdated quartz overgrowth, some dolomite (may be Fe-riched) cement evolved at this stage (Figs. 59a, b and 62). Organic acids through decomposition may be occurred, where calcite/ dolomite cements and other remaining feldspar grains were partially or totally dissolved producing secondary porosity (Figs. 59a, b and 64).

At maximum burial depth (more than 2.5km) alteration of lithic fragments and dissolution of more silicate grains generating very fine clay minerals and matrix rimming and clogging pore-spaces resulting loss of porosity with increasing compaction (Fig. 63). Thus, detrital compaction has a considerable influence on porosity generation or reduction: quartz grains with quartz overgrowths (in fluvial sandstone lithofacies) were important for the maintenance of porosity partially because they sustained the framework and limiting mechanical compaction. Also sandstones with feldspar and intergranular calcite cement (in

proximal delta front lithofacies) showed generation of secondary porosity by dissolution of these constituents.

On the other hand, sandstones with more contents of lithic fragments (distal delta sandstone lithofacies) displayed high porosity reduction by mechanical compaction and pore-filling clay matrix (Fig. 66).

### E) – Pore types.

The petrographic study also reveals that the visible primary porosity is fairly good with mostly well preserved intergranular pores ranging from 5% to 13% (Table 6), and characterized the studied samples of fluvial channel sandstone lithofacies which has not significantly affected by compaction (Figs. 56a and 56b), whereas this primary porosity has been slightly damaged by cementation in samples of proximal deltaic-coastal sandstone lithofacies (Fig. 62).

On the other hand the enhanced visible porosity forming secondary pores account for 8% to 19% (Table 6) and mainly associated with samples of proximal deltaic-coastal sandstone lithofacies, due to partial or total dissolution of cements (Figs. 59a, 59b and 64) or some labile grains producing moldic and oversized pores.

Few secondary porosity was ranging from 5% to 10% (Table 6) found at places in the clay matrix rich reworked marine sandstone lithofacies and distal delta silty sandstone lithofacies (Figs. 63, 65 and 67).

Figure 68 shows the diagenetic events active on the deposition of Lower Acacus Formation in the study area (concession NC100).

	Fluvial channel sandstone lithofacies	Proximal delta-coastal sandstone lithofacies	Distal delta front silty sandstone lithofacies
Sediments deposition	(50°-70°) ( < 1.5 Km) <u>Early compaction</u> <u>Early siliceous cementation</u> <u>Dissolution feldspar</u> <u>Calcite dissolution</u>	(70°-120°) (1.5 - 2.5 Km) <u>Mechanical compaction</u> <u>Calcite cementation</u> <u>Dolomite cementation</u> <u>Dissolution carbonate cements.</u> <u>Secondary porosity Ø</u>	(> 120°) ( > 2.5 Km) <u>Siliceous grain dissolution</u> <u>Clay matrix development (Illite)</u> <u>Porosity reduction</u>

**Figure 68. Paragenetic sequences showing diagenetic events in the studied Lower Acacus sandstone in concession NC100.**



## **7. RESERVOIR CHARACTERIZATION.**

Reservoir characterization integrates all available data to define distribution of physical parameters and flow properties of a petroleum reservoir (Benzagouta, 2012, and Odah et al., 2012).

In this chapter the goal is to accurately study the relationship between porosity ( $\emptyset$ ) and permeability (K) of the interested selected reservoir unit of Lower Acacus Formation.

This involves sedimentological study to define reservoir lithology, reservoir distribution, boundaries and possible diagenetic modifications of the reservoir heterogeneities and its quality variations between studied wells. Moreover, reservoir quality assessment was based on the recognized reservoir lithofacies which is defined in terms of the main attributes affecting reservoir quality including primary lithologic description, textures, diagenetic processes, pore types, and permeability.

Based on previous investigations and number of papers have been dedicated to reservoir characterization both for sandstone and carbonate rocks including: Asquith and Krygowski, 2004; Slatt, 2013; Weber, 1986.

Data analysis techniques involved in reservoir characterization of Lower Acacus Formation in concession NC100 can be addressed as following:

### **1- Diagenetic impact on reservoir properties.**

Different diagenetic alterations have been described petrographically from the studied Lower Acacus Formation including compaction, quartz overgrowths, carbonate cements and authigenic clay minerals and matrix. These diagenetic alterations have great impact on modifying reservoir properties across the study area “concession NC100”, when rocks underwent shallow to deep burial conditions.

Compaction comprised the mechanical rearrangement of grains throughout the sandstones, where the detrital quartz grains mainly have point contacts to suture contacts (Fig. 58), as well as the chemical compaction along sandstone to sandstone where intergranular pressure solution in clean sandstones has been observed (Fig. 56). Differences in the degree of mechanical compaction are probably related to maximum burial depth and variations in the depositional texture and some resistance of sand to mechanical compaction.

Pore reduction by mechanical compaction is one of the main controls of the petrophysical properties of Lower Acacus sandstones. Hence, compaction is diagenetic process negatively influencing the reservoir properties of Lower Acacus Formation in concession NC100.

The importance of mechanical compaction in reducing porosity and causing rock lithification is stressed by Jones and Leddra (1989), Fisher et al. (1999) and Wong and Band (1999).

Compositional variations of sandstone cements have been detected petrographically, with authigenic quartz prevailing in the marginal and shallow part of the study area, while carbonate cements and clay matrix prevailing in the relatively deep part. Quartz cementation that formed during the early diagenetic stage and decreases with depth is the main factor influencing the reservoir properties of rocks mainly in fluvial channel sandstone lithofacies areas. Quartz is the main cement mineral occurring in the form of authigenic overgrowths on detrital quartz grains of fluvial channel sandstone lithofacies (Fig. 52), but is highly variable on a local scale and even within individual well or unit.

Quartz cement contents show negative correlation with porosity and with carbonate cements and clay contents (Table 6 and Fig. 55).

At nearly intermediate depth (1.5-2.5 km) the carbonate cements of Lower Acacus sandstone is varying in mineralogy from common calcite to less common iron-rich dolomite (Figs. 59 and 62) associated with the proximal delta front-coastal sandstone lithofacies, characterizing by pore-filling carbonate cements (calcite/dolomite) reduced porosity whereas partial or total dissolution of these carbonate cements resulted in secondary porosity (Figs. 62 and 64). At greater depth of burial (>2.5 km), increasing compaction, alteration of lithic fragments and more dissolution of silicate grains, may generating clay minerals and matrix filling and clogging pore spaces (Fig. 63) resulted in porosity reduction that associated with distal delta front silty sandstone lithofacies and occasionally rimming grains and lining pore-spaces as observed in the proximal delta front-coastal sandstone lithofacies in wells Q1-NC100 and C2-NC100 (Figs. 64 and 65). At this great burial (>2.5km), there is a clear negative correlation between porosity and clay matrix (Table 6), where mechanical compaction is probably the most important process down to this depth and porosity changes therefore depends on framework grains stability which is a function of clay matrix ratio to stable framework grains.

## 2- Reservoir quality variation.

A typical reservoir for hydrocarbons is characterized by a geological formation consisting of sandstone or carbonate rock having good effective porosity and permeability (Eni, 2005). Effective porosity (open-space) is the connected porosity that is available for free fluids; it excludes non-effective, non-connected porosity including those spaces occupied by clay bound water (Schön, 1996). According to Djebbar and Donaldson (2013), the ranges of good effective porosity and permeability for hydrocarbon reservoirs are 15-20% and 50-250md respectively. As a general rule the formation permeability must exceed 100md for a specific reservoir to provide sufficient fluid conduit (Van der Meer, 1993). According to Khanin (1965, 1969) classification of hydrocarbon reservoir quality (Table 7), the porosities should be greater than 14% for average - high reservoir quality, while those have porosity below 10% and permeability below 100md are considered reduced-low reservoir quality. Practically, a homogenous 50m (164ft) thick reservoir with a permeability > 500md and porosity > 18% is estimated as a “high quality” reservoir, while heterogeneous 15m (49ft) thick reservoir with permeability > 10md and porosity < 15% is considered as a “low-quality” reservoir for hydrocarbons.

**Table 7. Classification of hydrocarbon reservoir according to permeability and porosity (modified after Khanin, 1965, 1969).**

<b>Group</b>	<b>Class</b>	<b>Reservoir quality</b>	<b>Permeability K (md)</b>	<b>Porosity <math>\phi</math> (%)</b>
<b>1</b>	<b>i</b>	<b>Very high</b>	<b><math>\geq 1000</math></b>	<b><math>\geq 20</math></b>
	<b>ii</b>	<b>High</b>	<b>500-1000</b>	<b>18 - 20</b>
	<b>iii</b>	<b>Average</b>	<b>100-500</b>	<b>15 - 17</b>
<b>2</b>	<b>iv</b>	<b>Reduced</b>	<b>10-100</b>	<b>9 - 14</b>
	<b>v</b>	<b>Low</b>	<b>1-10</b>	<b>2 - 8</b>
	<b>vi</b>	<b>Very low</b>	<b><math>\leq 1</math></b>	<b><math>\leq 2</math></b>

### Porosity – permeability relationship of Lower Acacus reservoir sandstones.

Attempts are often made at finding a relationship between permeability (K) and porosity ( $\emptyset$ ) in sandstone samples by making a plot of the available data.

In this case, by using data in (Table 8) core plug total porosity ( $\emptyset_c$  in %) was plotted versus the permeability (in md) for the studied lithofacies of Lower Acacus Formation (Fig. 69).

(Figure 69) shows that the plotted samples are relatively heterogeneous, since sample points deviate and can be extremely tenuous due to large scatter in the data between lithofacies. This heterogeneity was probably caused by changing in reservoir properties between different lithofacies which effected porosity ( $\emptyset_c$ ) and permeability (K) readings such as bioturbation, microfractures, cementation, and matrix filling-pore spaces.

Figure 69 shows no relationship or no distinct K- $\emptyset_c$  trend where rock samples of all lithofacies with different properties are lumped together.

**Table 8. Thin section macro porosity ( $\emptyset_{TS}$ ) estimation and routine core plug total porosity ( $\emptyset_c$ ) and permeability (k) measurement for some selected units of Lower Acacus Formation, concession NC100, Ghadames Basin, NW Libya.**

Lower Acacus Sandstone unit	Sample No.	Well	Core No.	Depth (ft)	Vertical Permeability K (md)	Thin section Macro Porosity ( $\emptyset_{TS}$ %)	Core Plug Total Porosity ( $\emptyset_c$ %)
Lf2	3	Z1-NC100	1	11688.6	1.000	5	6.48
Lf2	2	Z1-NC100	1	11694.3	2.338	10	10
Lf2	1	Z1-NC100	1	11698.3	2.409	10	11
Lf2	3	Z3-NC100	3	11716.2	2.599	10	11.30
Lf2	2	Z3-NC100	3	11730.3	1.305	9	10
Lf2	1	Z3-NC100	3	11746.3	0.180	3	3.71
A6	4	Q1-NC100	1	10465.4	20.80	18	23.23
A6	3	Q1-NC100	1	10467.8	18.72	14	17.53
A4	2	Q1-NC100	3	10571.4	63.8	16	20.44
A4	1	Q1-NC100	3	10587.3	388.4	19	24.57
A11	3	L3-NC100	C2, C3	9312	33.95	8	17.26
A11	2	L3-NC100	C2, C3	9331.4	76.46	13	24
A11	1	L3-NC100	C2, C3	9334.8	27.88	8	12
Ad	2	Q1-NC100	1	10490.7	0.03	2	3
Ad	1	Q1-NC100	1	10491.4	0.024	1	1
Am	3	Q1-NC100	3	10559.5	0.40	7	8.01
Am	1	C2-NC100	2	9412.2	17.81	10	17.6
Am	2	C2-NC100	2	9416.7	6.375	8	20

In this study, it is possible to isolate or separate core plug porosities and their permeability equivalent of the same lithofacies type that have similar rock properties and try to plot their permeability (K)-core plug porosity ( $\phi_c$ ) readings, where K-  $\phi_c$  trend relationships can be more readily observed (Fig. 70).

From Figure 70 a linear relationship and correlation has been found to exist between permeability (K)- core plug-porosity ( $\phi_c$ ) readings of the same lithofacies type. Moreover, for this analyzed data (Fig. 70) and for each lithofacies type a statistical value can be used to define possible productive intervals via detecting porosity/permeability cutoff readings.

So that, a minimum cutoff core plug porosity of 6% corresponds to a permeability of about 0.1md in the fluvial channel sandstone lithofacies, a minimum cutoff core plug porosity of about 13% corresponds to a permeability of about 28md in proximal delta front-coastal sandstone lithofacies, while a minimum cutoff core plug porosity of about 8% corresponds to a permeability of about 0.02md in the distal delta front silty sandstone lithofacies, and a minimum cutoff core plug porosity of about 8% corresponds to a permeability of 0.4md characterized the reworked marine sandstone lithofacies.

In general, and based on porosity/permeability cutoff, the fluvial channel sandstone lithofacies is characterized by quartz cement and compaction through pressure solution of grains are the principle causes of porosity/permeability reduction. The porosity-permeability plots (Fig. 70) indicate a positive and progressive uniform of permeability increase as porosity is enhanced which characterized the proximal delta front-coastal sandstone lithofacies, which suggests this sandstone underwent some diagenetic history and late processes during which leaching of carbonate cements and other silicate grains (feldspars) may took place producing secondary porosity and hence improving reservoir quality of this lithofacies.

With respect to the distal delta front silty sandstone lithofacies and reworked marine lithofacies they are characterized by low cutoff core plug porosity and equivalent corresponding permeability of 8% / 0.02md and 8% / 0.4md respectively indicating progressive decrease in permeability (K) due to relatively carbonate cement, increasing clay content, pore-filling matrix and decreasing grain size which are all possible contributes to the decreasing K- $\phi_c$  trend and reducing reservoir quality of these two lithofacies.

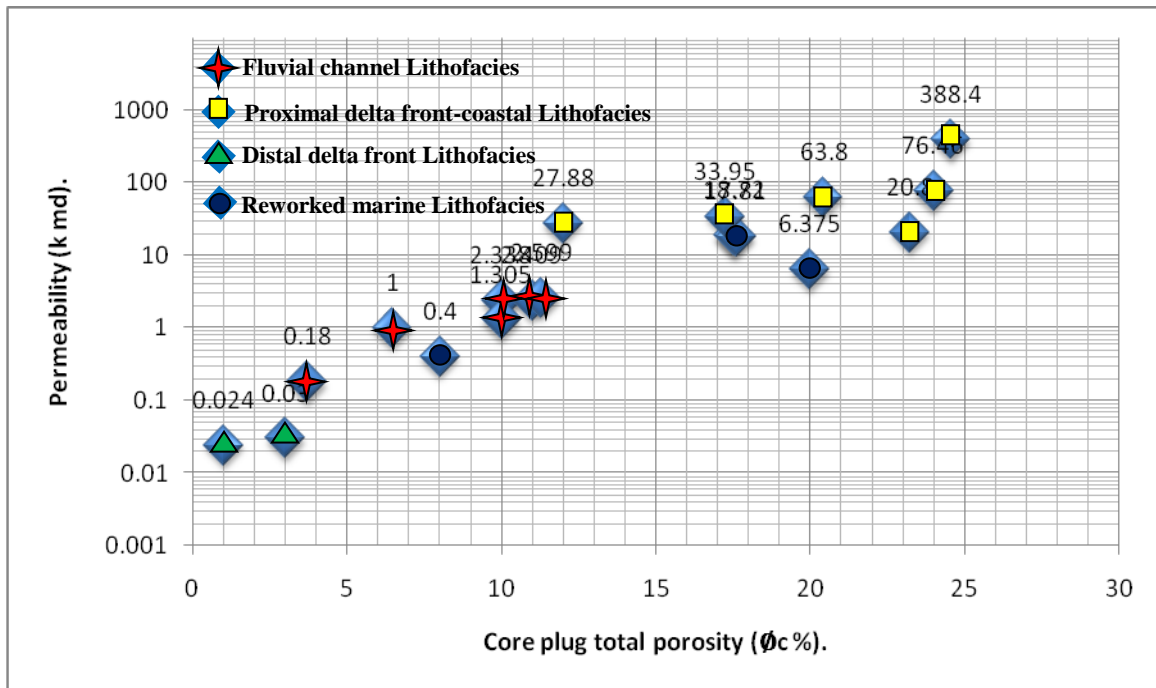
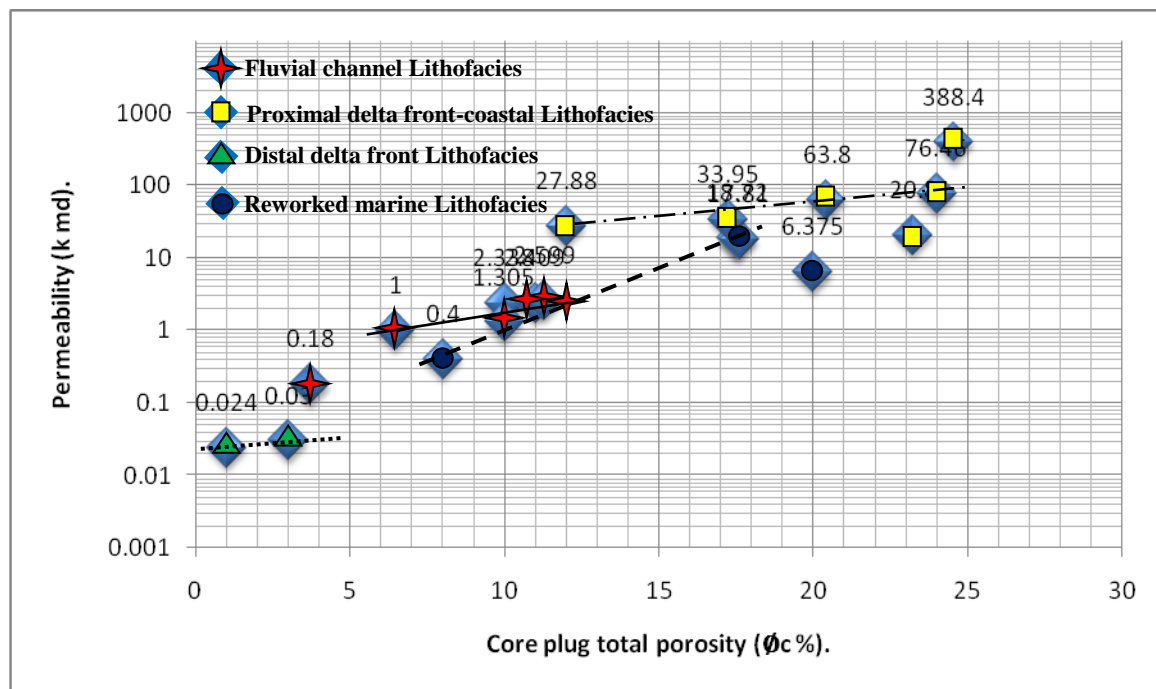


Figure 69. Core plug porosity ( $\phi_c$ ) versus permeability (k) data of all studied lithofacies of Lower Acacus Formation, concession NC100, Ghadames Basin, NW Libya. Note: Large scatter of data between different lithofacies.



- linear trend is linking points of fluvial channel lithofacies
- · - · - linear trend is linking points of proximal delta front-coastal lithofacies
- linear trend is linking points of distal delta front lithofacies
- - - - - linear trend is linking points of reworked marine lithofacies

Figure 70. Core plug total porosity ( $\phi_c$ ) versus permeability (k) data of all studied lithofacies of Lower Acacus Formation, showing linear relationship between points of the same lithofacies type, concession NC100, Ghadames Basin, NW Libya.

By using (Table 8) for thin section macro porosity ( $\phi_{T.S}$ ) was plotted versus the permeability (k) for all the studied lithofacies (Fig. 71) in which a good linear positive relationship has been established between various lithofacies, where some lithofacies points for thin section porosity ( $\phi_{T.S}$ )-permeability (K) were located either on top of the trend line suggest samples of relatively low thin section porosity ( $\phi_{T.S}$ ) (5-13%) but of relatively high permeability (K) (1-76md) probably due to mainly some microfractures and/or some bioturbation which inducing good connectivity, or, below the trend line which is characterized by low thin section porosity (5-8%) and of low permeability (0.02-0.03 md) due to increasing clay matrix contents and decreasing grain size as these readings of thin section porosity ( $\phi_{T.S}$ )-permeability (K) are associated with distal delta front silty sandstone lithofacies. With respect to the below point of proximal delta front-coastal sandstone lithofacies having good thin section porosity (18%) and of relatively low to reduced permeability (20.8  $\approx$  21md) due to mainly some partial pore-filling matrix, carbonate cementation and excessive compaction.

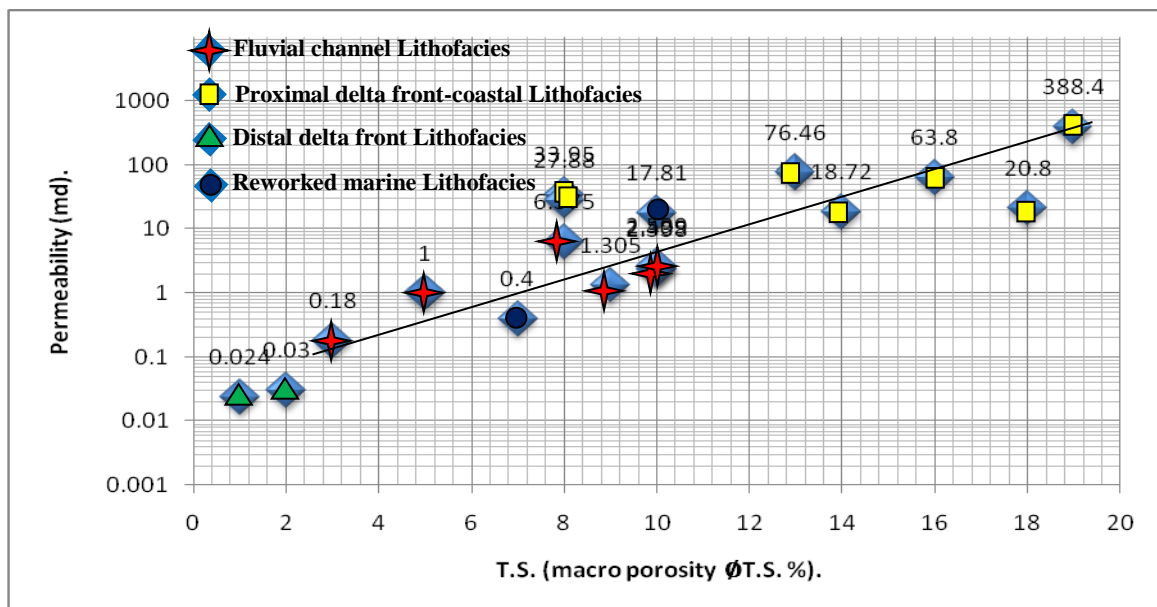


**Figure 71. Thin section macro porosity ( $\phi_{T.S}$ ) versus permeability (k) data of all studied lithofacies of Lower Acacus Formation, Concession NC100, Ghadames Basin, NW Libya.**

Cross plot of core plug total porosity ( $\phi_c$ ) versus thin section macro porosity ( $\phi_{T.S}$ ) (Fig. 72) reveals that a good correlation of a linear relationship is existed between various lithofacies points with some scattered points below trend line which may suggest relatively high core plug porosity which could be account for micro-porosity associated with clay matrix in these data points. Hence, this micro-porosity should be included in the effective core plug porosity (total porosity) measurements.

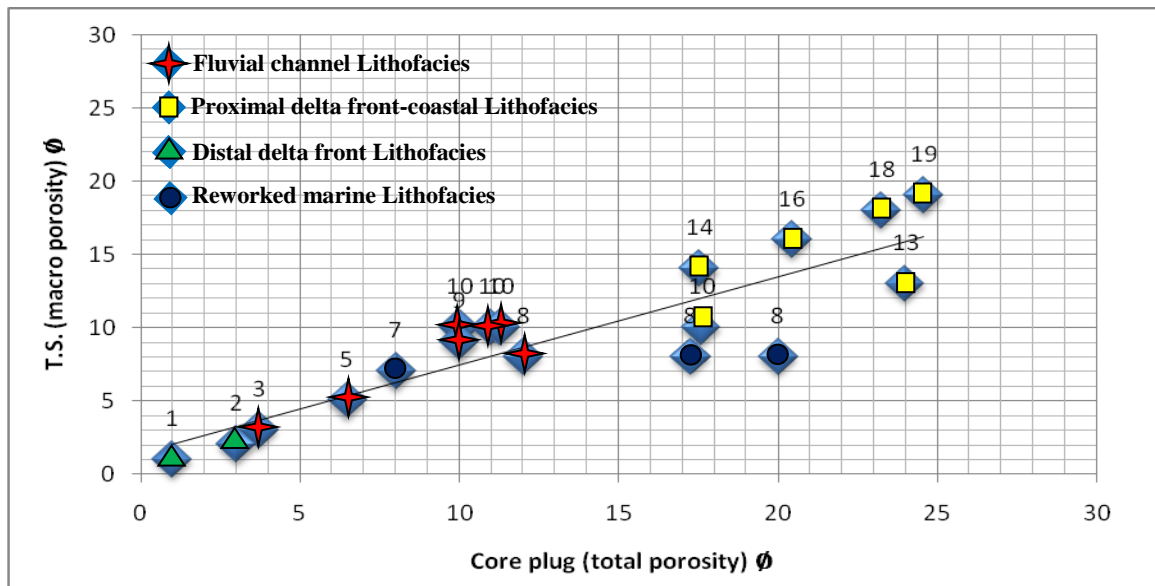


**Figure 72. Core plug total porosity ( $\phi_c$  %) versus thin section macro porosity ( $\phi_{T.S}$  %) data of all studied lithofacies samples of Lower Acacus Formation, Concession NC100, Ghadames Basin, NW Libya.**

### 3- Assessment of the reservoir quality of Lower Acacus Formation.

According to the classification of (Khanin, 1965, 1969) based on permeability and porosity of hydrocarbon reservoirs (Table. 7), the studied thin section along with the analysis of core plug samples of some selected sandstone units in the Lower Acacus Formation (Table 8) the fluvial channel sandstone units (Lf2) in wells Z1-NC100, and Z3-NC100 with porosity range from 3% to 11% and of average porosity 7% (Fig.73) and permeability range from 0.18 md to 2.59 md with average permeability 2 md (Fig. 73) are mainly of low reservoir quality, as they are characterized by extensive silica cement presented either as quartz overgrowth on detrital grains or as pressure solution between grains during some compaction, which in turn reduces the affective porosity of these reservoir units.



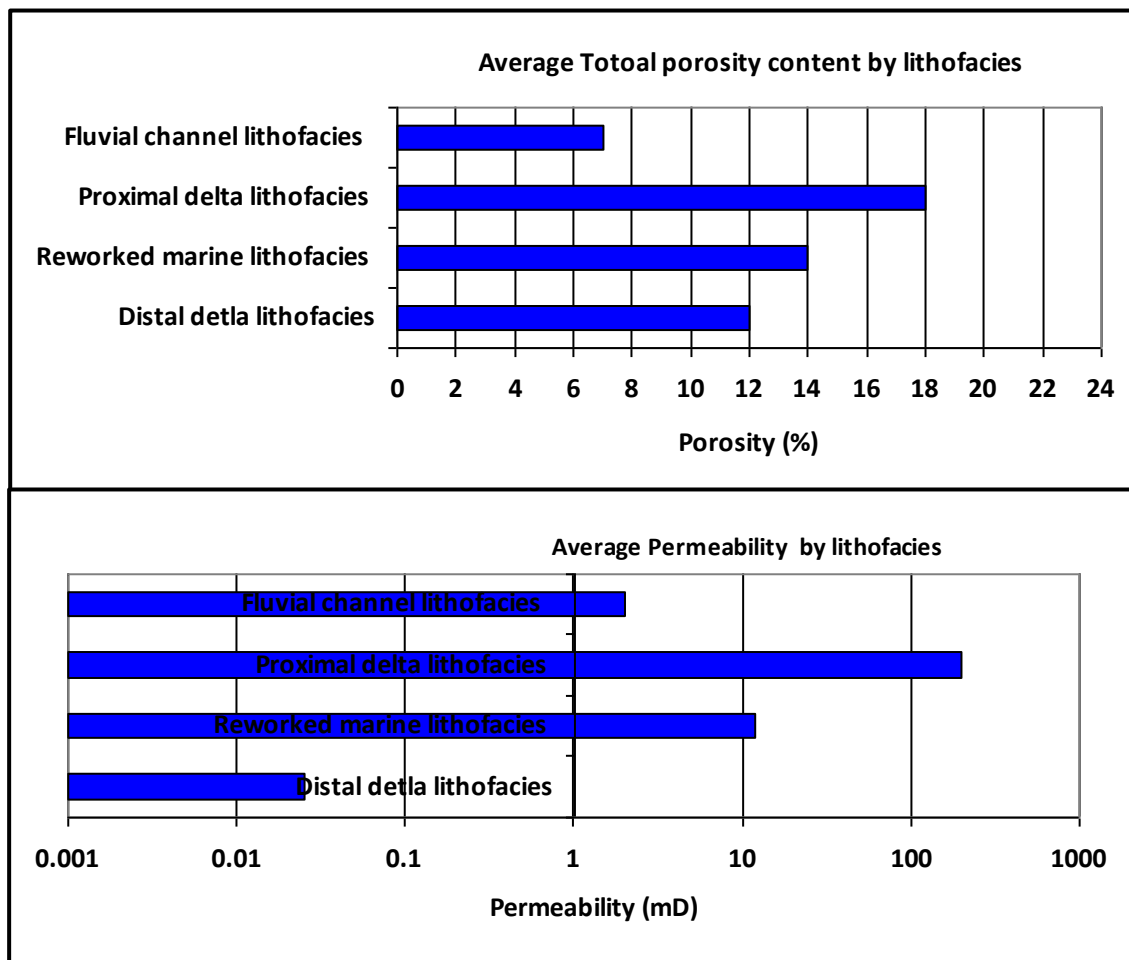


**Figure 73. Summary histogram of average total porosity and permeability readings from all lithofacies of Lower Acacus Formation, Concession NC100. (Based on readings from table 8)**

Proximal delta front-coastal sandstone units (A4, A6, A11) in wells Q1-NC100, and L3-NC100 with porosity range from 12 % to 24 % and average porosity 18% (Fig. 73) and permeability range from 18.72 md to 388.4 md with average permeability 204 md (Fig. 73) are mainly of average reservoir quality, as they are characterized by extensive dissolution of calcite and other unstable labile grains, resulted in high dissolutional secondary porosity. Distal delta front silty sandstone units (Ad) in well Q1-NC100, with porosity range from 8.3% to 16.85% and average porosity 12% (Fig. 73) and permeability range from 0.024 md to 0.031 md with average permeability 0.025 md are mainly of very low reservoir quality, as they characterized by extensive clay-matrix filling pore spaces and reducing porosity. Reworked marine sandstone units (Rm) in wells C2-NC100, and Q1-NC100 with porosity range from 8% to 20% and average porosity 14% (Fig. 73) and permeability range from 0.40 md to 23.9 md and average permeability 12 md are mainly reduced reservoir quality, as they are characterized by partial clay-filling pore spaces and calcite cement.

Therefore, the good reservoir quality of examined sandstone units (A4, A6 and A11) of proximal delta front-coastal origin was assessed as “average” (average porosity 18% and permeability 204md) for hydrocarbons accommodation in these reservoirs.

The reservoir quality of the sandstone unite (Ad) of distal delta-front origin was assessed to be estimated as “very low” (average porosity 2% and permeability 0.025md) for hydrocarbon accommodation and was the lowest in the studied sandstone units in the concession NC100.

However, reservoir quality of fluvial channel sandstone unit (Lf2) was assessed as “low” (average porosity 7% and permeability 2md) for hydrocarbons accommodation.

The obtained assessed results indicate some possible physical and diagenetic processes associated with lithofacies types and reservoir sandstones and could effect hydrocarbon accommodation in the studied onshore, transitional and offshore structures.

### **Reservoir quality variations and lithofacies distribution:**

Composite lithofacies log map (Fig. 74) was constructed from overlapping stacked mapped slices (Figs. 46 – 50) of Lower Acacus sandstone units across the concession NC100 to give the sense of the lithofacies patterns which are readily related to depositional, diagenetic and reservoir quality variations trends. In this figure 74, discrete zones of log character were mapped out to define wells located in the southern part of the study area of fining upward GR-log profiles which related to fluvial channel sandstone lithofacies of low reservoir quality, whereas upward coarsening GR-log profiles are related to proximal delta-coastal sandstone lithofacies of average reservoir quality which mostly characterizing wells located in the center of the study area concession NC100, and serrated to spiky to featureless GR-log motif are related to reworked marine sandstones to distal delta silty sandstones to marine shale lithofacies of reduced reservoir quality characterizing wells located in the most northern part of the concession NC100.

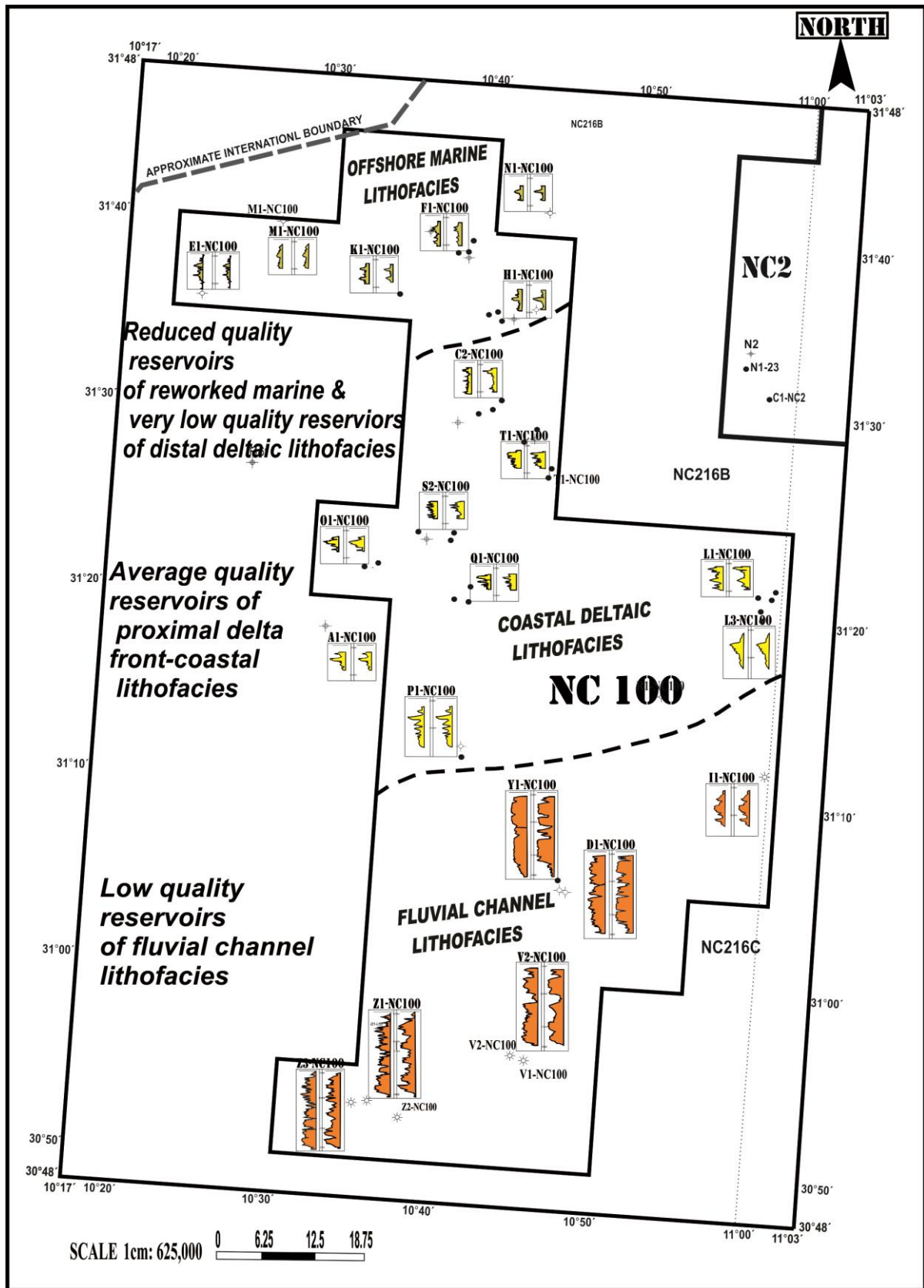


Figure 74. Composite lithofacies log map, showing discrete zones and distribution of GR-log patterns tied in to a lithofacies scheme of some selected sandstone units of Lower Acacus Formation, concession NC100, Ghadames Basin, NW Libya.

## **8. EXPLORATION STRATEGY FOR LOWER ACACUS FORMATION IN CONCESSION NC100.**

Upper Silurian Lower Acacus sandstones are oil and gas productive throughout a large area in concession NC100 of Ghadames Basin, NW Libya. The Lower Acacus sandstones were derived from the south/southeast direction during regressive event took place by fluvial prograded system toward the north/northwest direction interrupted by periods of marine transgressions.

The trap within the sandstone reservoirs of Lower Acacus Formation in concession NC100 was reported by (Beicip, 1972, 1973; Echikh, 1998; Elfigih, 2000; Howlett, 2000 and Hallett, 2004) to be mainly structural types as revealed by the structural contour map (Fig. 75) which is defining various lead locations and hydrocarbon pools structures. However, this study shows that stratigraphic influences and the availability of the good quality lithofacies are playing a role to completely define the trapping mechanism on the Lower Acacus sandstone reservoirs in concession NC100. This may be achieved by overlapping the composite lithofacies map (Fig. 74) on the leads-hydrocarbon pools map (Fig. 75) which may result to a superimposed map (Fig. 76) in which structural leads and pool structures located in concession center area in the vicinity of wells Q1-NC100, O1-NC100, S2-NC100, T1-NC100, C2-NC100, L1-NC100 and P1-NC100 are characterized by proximal delta front-coastal lithofacies of good reservoir quality (average porosity 21% and permeability 90md and of an effective sandstone thickness of 20 to 65ft) and hence they are characterized by widespread occurrence of oil and the lack of gas and free water zones. In contrast, structural leads and pools located in southeastern parts of the concession NC100 in the vicinity of wells Z1-NC100, Z2-NC100, Z3-NC100, V1-NC100, V2-NC100, I1-NC100 and X1NC100 are characterized by tight/quartz rich fluvial channel sandstone lithofacies of low reservoir quality (average porosity 9% and permeability 2md and of a sandstone thickness of 30 to 85ft) in which reservoir sandstones if found, it could produce only gas. Other minor structural leads and pools located in the most north – northwestern part of the concession NC100 are mostly characterized by reworked marine sandstone to distal delta front silty sandstone lithofacies of reduced to very low reservoir quality (average porosity 14% and average permeability 4.012md and of thin sandstone thickness of 8 to 15ft), having the least hydrocarbons occurrence.

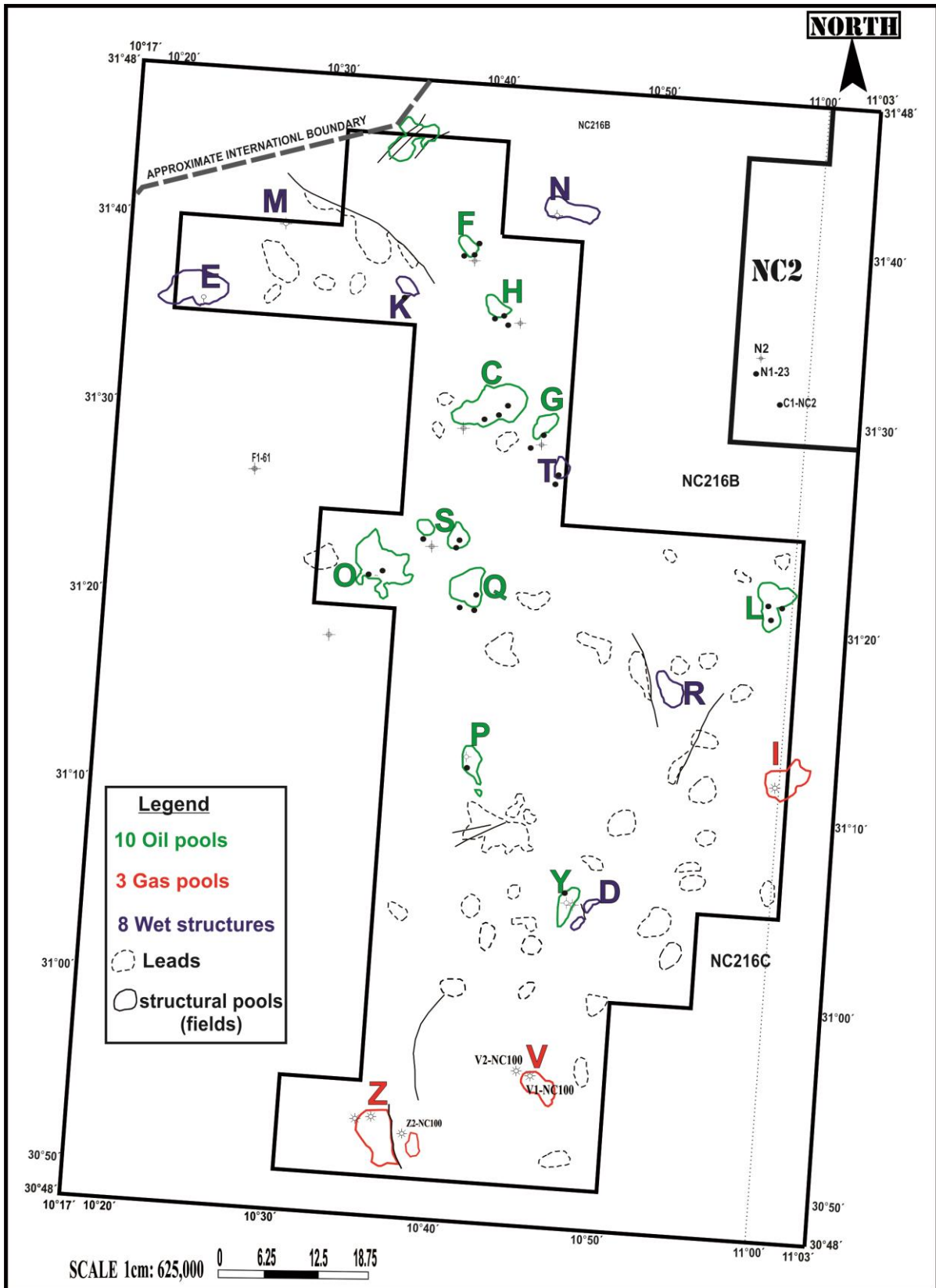


Figure 75. Undrilled structures and drilled structural pools on the level of Lower Acacus Formation concession NC100, Ghadames Basin, NW Libya, (AGOCO, 2008).

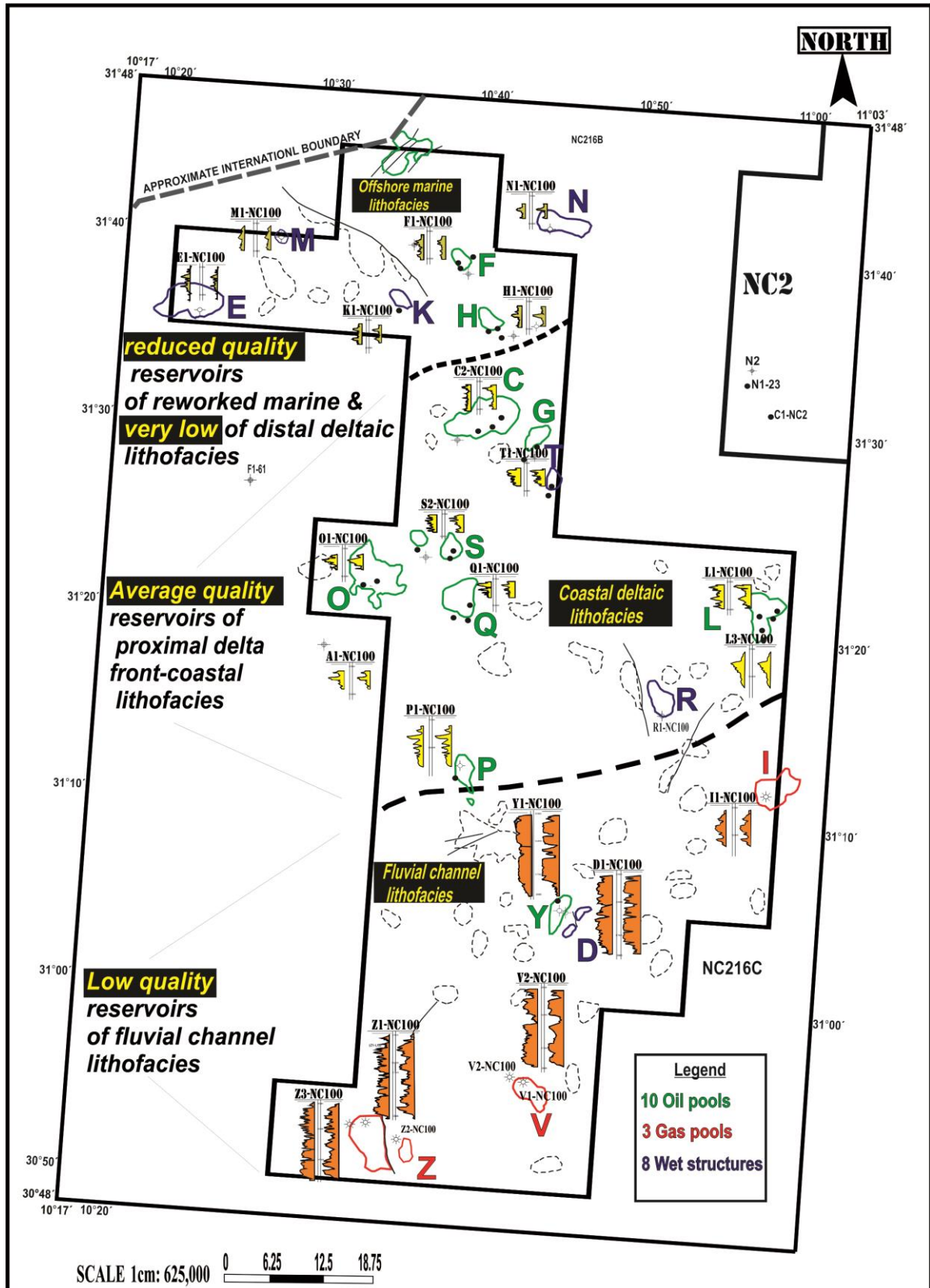


Figure 76. A superimposed map achieved by overlapping the composite lithofacies map (Fig. 74) on the leads-hydrocarbon pools map (Fig. 75), and showing discrete zones of lithofacies characterized by variations in reservoir quality which could be used for future exploration of concession NC100, Ghadames Basin, NW Libya.

The exploration results from the drilling of some structures on the level of Lower Acacus Formation have indicated variable fluid recoveries from different structural pools located within the concession NC100 (Fig. 75).

In figure 75, I, V and Z structural pools located in south and southeastern of concession NC100 have produced only gas with low chance of producing oil.

E, K and N, structural pools located in the northern part of concession NC100 are of low chance of producing any hydrocarbons, so that have discouraged exploration and development.

The best of highest oil recovery area is located in the middle of concession NC100 which characterizing structural pools C, G, L, Q, O and S. Future exploration activities should be concentrated and give priority to drill new wells located in this area.

On the basis of these observations the following steps can establish better understanding and definition of the future exploration strategy in concession NC100 including:

- 1- Constructing total isopach map for Lower Acacus Formation to delineate local and regional depositional strike and dip of the concession NC100.
- 2- Construct sandstone isopach maps for each defined unit in the Lower Acacus Formation, using interval of 65-70 API deflections of the GR-log to outline gross sandstone thickness trends.
- 3- Construct many cross-sections through target areas or prospect location along depositional strike and dip.
- 4- On the basis of selected stratigraphic datum, divide each cross section into intervals or slices based on lateral facies changes, using GR-log signature of each sandstone and its equivalent to define depositional environments (fluvial channel, proximal or distal deltaic, marine offshore edge, ..etc) and note the thickness of each edge mappable sandstone.
- 5- Construct lithofacies log maps for all mapped slices or units.
- 6- Carefully compare lithofacies log maps in (point 5) with that of sandstone isopach maps in (point 2) and detect the trends of facies changes and their distribution throughout the concession area.
- 7- Construct a composite lithofacies map after superimposing the lithofacies maps for each studied sandstone unit.
- 8- Carefully prepare a structural leads map or structural prospect map on the level of Lower Acacus Formation or nearest horizon and overlap it on the composite lithofacies map (in point 7), to produce a preferable drilling location map to be used to define priority areas for exploring the possible matching multi sandstone units at that location.

The previously mentioned steps (1-8) are effectively related exploration to depositional environments based on sandstone units distribution, their lithofacies patterns and GR-log signatures. As such, it effectively integrates all geological exploration components for the Lower Acacus sandstone reservoirs in concession NC100.



## 9. CONCLUSIONS.

Integrated dataset of core examination, well logs and regional strato/structural map construction are all together used to identify the lithofacies distribution, reservoir quality variations of the sandstones of the Lower Acacus Formation in concession NC100, Ghadames Basin, NW Libya. The Lower Acacus Formation in the study area (concession NC100), is divided into five lithofacies types including; 1) Bioturbated marine silty shale lithofacies, 2) Reworked marine sandstone lithofacies, 3) Distal delta front silty sandstone lithofacies, 4) Proximal delta front – coastal sandstone lithofacies and 5) Fluvial channel sandstone lithofacies. Mostly GR is used as common log motif to interpret sedimentary lithofacies of the examined sandstones and shales of Lower Acacus Formation in concession NC100. Four major categories of GR-log motif were identified, which are: 1) 1<sup>st</sup> category represented by bell shape GR-log motif corresponds with the fluvial channel lithofacies, 2) 2<sup>nd</sup> category of funnel shape GR-log motif corresponds with the gradational sequence of the shaly siltstone of distal delta front at the base to proximal delta front-coastal lithofacies at the top, 3) 3<sup>rd</sup> category of spiky shale GR-log motif corresponds to reworked marine sandstone lithofacies and 4) 4<sup>th</sup> category of thinly serrated to smooth "featureless" GR-log motif corresponds to bioturbated marine shale lithofacies.. These datasets were complemented by petrographic analyses of 18 thin sections obtained from selected sandstone units in the Lower Acacus Formation and revealed the composition of these sandstones which mainly of sublitharenites with quartzarenites and rarely litharenites. Diagenetic processes were also observed to include compaction of framework grains, silica cement by pressure solution and precipitation of quartz overgrowths, feldspar grains dissolution, calcite/dolomite cementation, partial and total dissolution of labile grains and calcite/dolomite cements which contributed to the development of some secondary porosity which occasionally at some places is filled partially or totally by clay matrix. Reservoir quality of the identified lithofacies was investigated using core plug total porosity ( $\emptyset_c$ ) and permeability (k) for their selected sandstone units. In this investigation, negative relationship was established between core plug total porosity ( $\emptyset_c$ ) and permeability (k) of the different type of lithofacies which admit their heterogeneous. Other positive relationships between thin section macro porosity ( $\emptyset_{T.S}$ ) and permeability (k), and between core plug total porosity ( $\emptyset_c$ ) versus thin section macro porosity ( $\emptyset_{T.S}$ ) has been established between points of same lithofacies types which having similar rock properties.

Integrated thoughts of the various geological exploration components characterizing the Lower Acacus Formation in concession NC100 help to generate some basic steps (1-8) as they effectively related exploration to depositional environments based on sandstone units distribution, their lithofacies patterns and their reservoir characterization and quality variation. As such, these steps are hardly recommended to be used for the establishment of better understanding of the future exploration strategy in concession NC100.

## REFERENCES

- Acheche. M. H., M' Rabet. A., Gharini, H., Ouahchi, A. and Montgomery. S.L., 2001, Ghadames Basin, southern Tunisia: a reappraisal of Triassic reservoirs and future prospectivity. *Bull. AmerSsoc. Pet. Geol.*, vol. 85, p.765-780.
- Arabian Gulf Company (AGOCO), 2008, Location map of the study area concession NC100, Ghadames Basin, NW Libya .TDL, AGOCO, Benghazi, Scale 1 : 150,000.
- Archer, D., S. Emerson, and C. Reimers. 1986. Dissolution of calcite in deep-sea sediments: pH and  $\theta$ , microelectrode results. *Geochim. Cosmochim. Acta* 53: p. 2831-2845.
- Arduini M., M. Barassi, F. Golfetto, A. Ortenzi, G. Serafini, E. Tebaldi, E. Trincianti, and C. Visentin 2003, Silurian-Devonian sedimentary geology of the Libyan Ghadames Basin: example of an integrated approach to the Acacus Formation study, 210p.
- Asquith, G.B. and Krygowski, D. (2004), *Basic Well Log Analysis. Methods in Exploration* No.16 Tulsa, O.K.: American Association of Petroleum Geologists.
- Attar, A. 1987, Evolution structural Illizi basin. Internal Exploration Report 2575, Sonatrach, Algiers, p.12-65.
- BEICIP, 1973, Evaluation and geological study of the western part of Libya (Ghadames Basin), Final report, N. O. C., Libya, 197p.
- Bellini, E. and Massa, D., 1978, A stratigraphic contribution to the Palaeozoic of the southern basins of Libya. In: *Symposium on the Geology of Libya, Second Edition, Vol. 1* (eds. M.J. Salem and M.T. Busrewil), Tripoli Libya, p.3-56.
- Benzagouta M.S. , 2012, Reservoir characterization: Evaluation for the channel deposits – Upper part using scanning electron microscope (SEM) and mercury injection (MICP): Case of tight reservoirs (North Sea). *Journal of King Saud University – Engineering – Sciences* (2015) 27, p.57 -62.
- Berry, W. B. N. and Boucot, A. J., (1973), Pelecypod-graptolite association in the Old World Silurian *Geol. Soc. Amer. Spec. Paper*, p.83- 143.
- Bonnefous, J., 1963, Syntheses stratigraphic sur le Gothlandien des sondages du SudTunisien. *Rev.*
- Bracaccia, V., Carcano., and Drera. K. 1991, Sedimentology of the Silurian –Devonian Series in the southeastern part of the Ghadames Basin. *Third symposium on the geology of Libya, vol. 5* (eds. M.J. Salem and M. N. Belaib), Elsevier, Amsterdam, p.1727-1744.

- Burollet, P.F. and Manderscheid, G. 1967, The Devonian in Libya and Tunisia. Int. Symp. Devonian System, Calgary, vol. 1. p.285-302.
- Cant, D. J., and Walker, R. G., 1976, Development of a braided-fluvial facies model for the Devonian Battery Point sandstone, Quebec: Can. J. Earth Sci., v. 13, p. 102-119.
- Chandouhl., 1992, Pal Cartographies du Paliozoiquedans le sud de la Tunisie et son implication sur le potentielp Ctrolikr de la region. 3Pnzes Journals de l' Exploration Pktrolidreen Tunisia, ETAP, Tunisia.
- Cosentino L., 2001, Integrated Reservoir Studies, Editions Techno, Paris, 2001, Institute Francis of Petrol Publications.336p.
- Craig, J. L., Rizzi, C., et al. 2008, Structural styles and prospectivity in the Precambrian and Palaeozoic hydrocarbon systems of North Africa. In: Salem, M.J., Oun, K.M. & Essed, A.S. (eds) The Geology of East Libya, vol. 4. Gutenberg Press, Tarxien, Malta, p.51–122.
- Cridland, R., 1991, Seismic stratigraphic evaluation of NC2 concession, Ghadames Basin, internal report, AGOCO, Benghazi, Libya, 78p.
- Deutsch C.V. and Journel A.G., 1998, GSLIB: Geostatistical Software Library and User's Guide, Second Edition, Oxford University Press, 369p.
- Dickinson, W, R., 1970, Interpreting detrital modes of greywacke and arkose : Jour. Sed. Petrology, V. 40, P. 695-707.
- Dilekoz, E, and Daniles, H, (1998), Lithology & Petrography of A1-NC1. Internal report, Exploration Division, AGOCO Benghazi, Libya, 3p.
- Djebbar Tiab, Erle C. Donaldson, 2013, Petrophysics: Theory and Practice of Measuring Reservoir Rock and Fluid Transport Properties, 319p.
- Don Hallett, 2002, Petroleum Geology of Libya. 1<sup>st</sup> edition 2002, 2<sup>nd</sup> edition impression 2004, Amsterdam, 503p.
- Donald G. Mccubbin, 1973, Depositional Environment of the Almond Reservoirs, Patrick Draw Field, Wyoming, Rocky Mountain Association of Geologists.
- Don Hallet, 2004, Petroleum Geology of Libya, Elsevier, 2<sup>nd</sup> impression, p 52-59, 125, 144-172, 277-281.
- Echikh, K. 1998, Geology and hydrocarbon occurrences in the Ghadames Basin, Algeria, Tunisia, Libya, Petroleum Geology of North Africa. Geological Society Special Publication, 132p.
- Echikh, K. 1998, Geology and hydrocarbon occurrences in the Ghadames Basin, Algeria, Tunisia, Libya. In: Petroleum Geology of North Africa, (ed. D.S. Macgregor, R.T.J. Moody, D.D. Clark-Lowes), Geol. Soc. Special Publication No. 132, p.109-130.

- Edward E., and Tawadros, 2001, geology of North Africa, Taylor & Francis Group  
6000 Broken Sound Parkway NW, Suite, 917p.
- Elfigih, O. B., 1991, The sedimentology and reservoir characteristics of the Lower Acacus Formation, NC2 Concession, Hamada Basin, NW Libya, M.Sc. thesis, Memorial University of Newfoundland, St'John's, Newfoundland, Canada, 569p.
- Elfigih, O. B., 2000, Regional Diagenesis and its relation to facies change in the Upper Silurian Lower Acacus Formation, Hamada (Ghadames) Basin NW Libya. Ph.D. thesis, Memorial University, NFLD, Canada, 399p.
- Elruemi, W., 1991, Geology of the Aouinet Ouenine and Tahara Formations, Al Hamada al Hamra area, Ghadames Basin. Third Symposium on the Geology of Libya, vol. 6 (eds. M.J. Salem, A.M. Sbeta and M. R. Bakbak), Elsevier, Amsterdam, p.2185-2194.
- Elruemi, W., 2003, Geologic evolution of Ghadames Basin; impact on hydrocarbon prospectivity. In: Salem, M.J., Oun, K.M. (Eds.), The Geology of Northwest Libya, Sedimentary Basins of Libya Second Symposium 2. Earth Science Society of Libya, Tripoli, p.327–350.
- Eni, 2005, Geological characteristics of hydrocarbon reservoirs, encyclopedia of hydrocarbon, geosciences, volume 1, exploration and transport, p. 85-116.
- Eyles C. H. & Eyles N. 1983, Sedimentation in a large lake: A reinterpretation of the Late Pleistocene stratigraphy at Scarborough Bluffs, Ontario, Canada. *Geology* 11, p.52–146.
- Eyles N., Eyles C.H. and Mail, 1983, Lithofacies types and vertical models; an alternative approach to the description and environmental interpretation of glacial diamict and diamictite sequences. Vol 30, p.393-410.
- Fisher, Q. J., Casey, M., Clennell, M. B. & Knipe, R. J. 1999. Mechanical compaction of deeply buried sandstones. *Marine and petroleum geology*, 16, 605-618.
- Folk, Robert L. 1980, Petrology of sedimentary rocks, Library of Congress Catalog Card Number 80-83557, printed in the states of America.
- Francesco Bertello, Claudio, Walter 2003, Paleozoic and Triassic Petroleum Systems in North Africa, Algeria an overview of the evolution and the petroleum systems of the eastern Ghadames (Hamra) Basin – Libya, 177p.
- Freiberg, 2003, Upper Palaeozoic bryozoans from the Carnic Alps (Austria). *Andrej Ernst, Freiburger Forschung shefte*, 499p.
- Hammuda, O.S. 1980a, Geologic factors controlling fluid capping and anomalous freshwater occurrences in the Tadrart Sandstone, Al Hamada al Hamra area,

- Ghadames Basin. Second Symposium on the Geology of Libya, vol. 2 (eds. M.J. Salem and M.T. Busrewil), Academic Press, London, p.501-508.
- Henares, 2014, Luca Caracciolo, César Viseras, Juan Fernández, and Luis M. Yeste, Diagenetic constraints on heterogeneous reservoir quality assessment: A Triassic outcrop analog of meandering fluvial reservoirs, AAPG Bulletin, V. 100, No. 9, P. 1377-1398.
- Hoang Van Tha, Anna Wysocka , Phan Dong Pha , Nguyen Quoc Cuong , Piotr Ziólkowski, 2015, Lithofacies and depositional environments of the Paleogene/Neogene sediments in the Hoanh Bo Basin (Quang Ninh province, NE Vietnam), Geology, Geophysics & Environment , vol.41 (4): p. 353-369.
- Howlett, P., 2000. Trapping style in the Ghadamis (Berkine) Basin of Algeria, Libya and Tunisia, Second Symposium on the Sedimentary Basins of Lib ya. The Geology of Northwest Libya, Book of abstracts, p. 361.
- Jones, M. E. and Leddra, M.J., 1989, compaction and flow of porous rocks at depth; Rock at great depth symposium. (ods. Maury, v. and Fourmaintraux, D.), Pau, France, 28-31 August, 1989, A. A. Balkema, Rotterdam, p.891-898.
- Katherine A. Pollard, 2013, Geological controls on geological carbon storage capacity, efficiency, and security in the Middle Devonian Sylvania-Bois blanc saline aquifer, central Lower Michigan, USA, AAPG Search, Western Michigan Un., 1903 W. Michigan Ave, Kalamazoo, MI, 49008.
- Khanin, A. A. 1965, Osnovnyeucheniya o porodakhkolektorakhneftiigaza [Main Studies of Oil and Gas Reservoir Rocks]. Publishing House Nedra, Moscow,362 pp. [in Russian].
- Khanin, A. A. 1969, Porody-kollektoryneftiigazaiikhizuchenie [Oil and Gas Reservoir Rocks and Their Study]. Publishing House Nedra, Moscow, 368 p.
- Klingbeil, R., Kleineidam, S., Asprien, U., Aigner, T., Teutsch, G., 1999, Relating lithofacies to hydrofacies: outcrop-based hydrogeological characterization of quaternary gravel deposits. Sediment. Geol. p.299–310.
- Klitzsch, E. (1970), Die strukturgeschichte der Zentralsahara. Neue Erkenntnisse zum Bau und zum Palaogeographic eines Tafellandes. Geol. Rundsch, 59/2, 459-527.
- Klitzsch, E. 1971, The structural development of parts of north Africa since Cambrian time. First Symposium on the Geology of Libya (ed. C. Gray). Faculty of Science, University of Libya, Tripoli, p.253-262.

- Klitzsch, E. 1981, Lower Palaeozoic rocks of Libya, Egypt and Sudan. In: Lower Palaeozoic of the Middle East, eastern and southern Africa and Antarctica, (ed. C.H. Holland). John Wiley, New York, p.131-163.
- Le Herisse, A., Bourahrouh, A., Vecoli, M., Paris, F., Palynological Tracers of sea-ice cover extent during the latest Ordovician on the north African margin, AAPG Search and Discovery Article #90016©2003 AAPG Hedberg Conference.
- Massa and Moreau-Benoit (1985), Biostratigraphy and paleogeography of Devonian in Libya (Ghadames Basin), sciences geologist, Vol 38, 518p.
- Massa, D. (1988), Paleozoic de Libya Occidental Stratigraphic et Paleogeography. Doctoral thesis, Univ. Nice, 520p.
- Massa, D. and Collomb, G. R., 1960, Observations nouvelles sur la regions d 'Aouinet Ouenine et du Djebel Fezzan (Libya). Proc. 21 st Int. Geol. Congr. 12, P.65-73.
- Massa, D. and Jaeger, H. 1971, Donnees stratigraphiques sur le Silurien de l'Ouest de la Libya. Mem. Bur. Rech. Geol. Min. vol. 73, p. 313-321.
- Massa, D. and Moreau-Benoit, A. 1976, Essai desynthese stratigraphique et palynologique du Systemedevonien en Libya occidental. *Rev. Inst. Fr. Petr.* vol. 31, p.287-332.
- Massa, D., Coquel, R., Loboziak, S. and Taugourdeau-Lantz, J., 1980, Essai de synthese stratigraphique et palynologique du Carbonifere en Libye occidentale. *Ann. Soc. Geol. Nord.* Vol. 99, p.429-442.
- Moreau-Benoit, A. 1988, Considerations nouvelles sur la palynozonation du Devonian moyen et superior du bassin de Ghadames (Ghadames), Libya occidental. *C.R. Acad. Sci. Paris*, vol. 307, p.863-869.
- Moreau-Benoit, A., 1979, Les spores du Devonian de Libya, PART 1 Micropaleontology. 4: p.3-58.
- Moreau-Benoit, A., 1980, Les spores du Devonian de Libya, PART 2 Micropaleontology.
- Odoh B. I, Onyeji Johnbosco, Utom A. U., 2012, The integrated seismic reservoir characterization (ISRC), study in Amboy field of Niger delta oil field – Nigeria, Department of Geological Sciences, NnamdiAzikiwe University, Awka, Anambra State, Nigeria Onyeji, Johnbosco, Ebute-Metta, Lagos, P. O. Box 1369, Nigeria.
- Remi Eschard and Brigitte Doliges, 1992, Subsurface reservoir characterization from outcrop observations, 7<sup>th</sup> IFP Exploration and Production Research Conference.
- Robert L. Folk, 1980, petrology of sedimentary rocks, hemphill publishing company Austin, Texas, p.186.

- Ruth Underdown and jonthan Redfern, 2008, petroleum generation and migration in the Ghadames Basin, north Africa: A two-dimensional basin-modeling study, AAPG Bulletin, v. 92, No. 1 (January 2008), p.53–76.
- Santa-Maria, FS, 1991, Ghadames Basin regional study analysis and evaluation. Internal report, Exploration Division, AGOCO Benghazi, Libya, p.20-46.
- Schön, J. H. 1996, Physical Properties of Rocks: Fundamentals and Principles of Petrophysics Pergamon, Oxford, UK, 583p.
- Selley, R. C. 1985, Ancient sedimentary environments. Third edition. Chapman and Hall, London, 317p.
- Selley, R. C., 1997, The Sedimentary Basins of NW Africa: Stratigraphy and Sedimentation. In: Selley, R.C. (Ed.). African Basins, Sedimentary Basins of the World 3. Elsevier, Amsterdam, 316p.
- Shahlol A. A. M. and Elmajdoub Ahmed T. A., 1998, Velocity investigations in concession NC2 Ghadames Basin, NW Libya, the geology of northwest Libya, sedimentary Basins of Libya-second symposium, volum3, p. 233-242.
- Shamah A. K., A Zalal, 1991, Biostratigraphy of the Middle Eocene succession at Gebel Mishgigah, Wadi Rayan, Libyan Desert, Egypt, Journal of African Earth Sciences (and the middle east), volume 12, Issue 3, p.449-459.
- Sikander, A. H., 2000, The geology, structure and hydrocarbon potential of the Ghadames and Murzuq Basins an overview (Abstract). Second Symposium on the Sedimentary basins of Libya. The Geology of Northwest Libya. Book of abstracts, 281p.
- Slatt, R. M., 2013, Stratigraphic reservoir characterization for petroleum geologists, geophysicists, and engineers, 2<sup>nd</sup> Edition, Elsevier Publ. Co. 671p. (First Edition published 2006, 492p.
- Trond Lien, Ruth Elin Midtb and Ole J. Martinsen, 2006, Depositional facies and reservoir quality of deep-marine sandstones in the Norwegian Sea, Norwegian journal of geology, Vol. 86, p.71-92. Trondheim 2006.
- Van der Meer, J.W., 1993, Conceptual design of rubble mound breakwaters. Delft Hydraulics Publication number 483p.
- Weber, K. J., 1986, How heterogeneity affects oil recovery, in L. W. Lake, and H. B. J. Carroll, eds., Reservoir Characterization: Orlando, FL, Academy Press, p.487–544.
- Wong T. F., and Baud P., 1999, Mechanical Compaction of Porous Sandstone. Oil & Gas Science and Technology – Rev. IFP, Vol. 54 (1999), No. 6, department of Geosciences, State University of New York, Stony Brook, NY 11794-2100 - United States e-mail: [wong@horizon.ess.sunysb.edu](mailto:wong@horizon.ess.sunysb.edu) - [pbaud@horizon.ess.sunysb.edu](mailto:pbaud@horizon.ess.sunysb.edu),



Zee Ma. Y., W.R. Moore, E. Gomez, W.J. Clark, Y. Zhang, 2016, Tight gas sandstone reservoirs, part 1: overview and lithofacies, Schlumberger, Denver, CO, USA1; University of Wyoming, Laramie, WY, USA2, Unconventional Oil and Gas Resources Handbook in <http://dx.doi.org/10.1016/B978-0-12-802238-2.00014-6>  
Copyright © 2016 Elsevier Inc.

Zuffa, G. G. 1980, Hybrid arenites: their composition and classification. *Journal of Sedimentary Petrology*, 50, p.21-29.

Zuffa, G. G. 1985, Optical analysis of arenites: influence of methodology on compositional results. Ill: ZUFFA G. G. (ed.) *Provellallce of Arellites*. Reidel, Dordrecht, p.165-190.



**جامعة بنغازي**  
**كلية العلوم، قسم علوم الارض**  
**بنغازي - ليبيا**

**تحديد السحنات و التغير في جودة المكنم لطبقة الأكاكوس السفلى،  
الأمتياز م ن 100، حوض غدامس، شمال غرب ليبيا.**

**إعداد**  
**نجم الدين إدريس الراحل**

**إشراف**  
**د. عمر بوزيد الفقيه**

**قُدمت هذه الرسالة استكمالاً لمتطلبات درجة الماجستير في الجيولوجيا بكلية العلوم  
بتاريخ 2017/12/7م**

## الخلاصة

من خلال عرض وتوصيف 215 قدم من العينات الإسطوانية المقطوعة في طبقة الأكاكوس السفلي من خمسة آبار في منطقة الدراسة (امتياز م ن 100)، حوض غدامس، شمال غرب ليبيا ، تنقسم طبقة الأكاكوس السفلي إلى خمسة أنواع من السحنات متضمنة؛ (1) سحنات الطين السلتي البحري المنقش او المثقب، (2) سحنات الحجر البحري المعاد ترسيبه ، (3) سحنات الحجر الرملي السلتي للجزء الخلفي للدلتا الأمامية، (4) سحنات الحجر الرملي الساحلي للجزء الأمامي للدلتا الأمامية، (5) سحنات الحجر الرملي للقنوات النهرية. علاوة على ذلك ، وبالأعتماد على أشكال تسجيلات اشعة جاما ، تم تجميع هذه السحنات في أربع فئات رئيسية ، وهي: (1) الفئة الأولى ممثلة بشكل تسجيلات اشعة جاما على شكل جرس وتتوافق مع سحنات القناة النهرية ، (2) الفئة الثانية علي شكل قمع لتسجيلات اشعة جاما و يتطابق هذا الشكل مع تسلسل متدرج للحجر السلتي الطيني للجزء الخلفي للدلتا الأمامية عند القاعدة إلى سحنات الجزء العلوي للدلتا الأمامية- الساحلية في اعلي التدرج او التسلسل، (3) الفئة الثالثة تتميز بالشكل المسنن العشوائي لتسجيلات اشعة جاما و التي تتطابق مع حبيبات الحجر الرملي البحري المعدلة و المعاد ترسيبها، (4) وتتوافق الفئة الرابعة مع شكل تسجيلات اشعة جاما المسنن الرقيق إلى المسنن ، و التي تمثل سحنات الحجر الطيني البحري المثقب. استُخدمت مجموعة من سرود تسجيلات الآبار لبناء مقاطع عرضية طبوغرافية لمعرفة الجغرافية القديمة لمنطقة الدراسة "امتياز م ن 100" ولتفحص العلاقات الجانبية بين وحدات الحجر الرملي أو مجموعة السحنات التي تم تحديدها في العينات الأسطوانية.

التحليل الصخري ل 18 شريحة تم الحصول عليه من وحدات الحجر الرملي المختارة من تكوين أكاكوس السفلي من خمسة آبار، سمح بتحديد التركيب الأولي والمكونات اللاحقة لتكوين الأكاكوس السفلي في الامتياز م ن 100. تضمنت التركيبات الفتاتية الأصلية سبلت- ارينايت مع كوارتز- ارينايت ونادراً لث- ارينايت. من اهم العمليات اللاحقة للترسيب و التي لوحظت في هذه الدراسة هي: ضغط حبيبات الصخر، المادة اللاصقة السيلكية بواسطة السائل المضغوط و ترسيب و نمو الكوارتز بين الحبيبات، ذوبان حبيبات الفلدسبار اللحم بالكالسايت/ و الدولومايت، الإذابة الجزئية و الكلية لبعض الحبيبات الغير مستقرة و اعادة لحم الحبيبات بمادة الكالسايت و الدولومايت خلال عملية الدفن، و تكوين النوع الثاني من المسامية و التي جزئياً او كلياً تُملأ بالطين.

أظهرت العلاقة بين مسامية قطع العينات الأسطوانية ( $\emptyset_c$ ) و النفاذية ( $k$ ) لطبقة الأكاكوس الفلي بأن العينات الممثلة لها علاقة سالبة حيث تظهر عدم تحانسها نسبياً نظراً لأنحراف نفاط العينات و تشتتها بين السحنات المختلفة. ومع ذلك ، وجد أن العلاقة الخطية والعلاقة الإيجابية موجودة بين مسامية قطع العينات الأسطوانية ( $\emptyset_c$ ) والنفاذية ( $k$ ) لنفس السحنات التي لها خصائص صخرية متشابهة. وقد تم إنشاء علاقات إيجابية خطية جيدة أخرى بين مسامية الشرائح الصخرية ( $\emptyset_{T.S}$ ) والنفاذية ( $k$ ) ، وبين مسامية قطع العينات الأسطوانية ( $\emptyset_c$ ) مقابل مسامية الشرائح الصخرية ( $\emptyset_{T.S}$ ) لمختلف نقاط السحنات المدروسة.

كما تم تعريف و تجميع السحنات المدروسة لطبقة الأكاكوس السفلي في امتياز م ن 100 وتم تصنيفها إلى ثلاث درجات لتقييم جودة صخر المكن: متوسطة و منخفضة و منخفضة جداً. تم تقييم النوعية الجيدة على أنها متوسطة وتميزت بمتوسط المسامية الكلية لقطع العينات الصخرية الإسطوانية بنسبة 18% ونفاذية 204 مل د. (md) ، مقترنة بالحجر الرملي للدلتا الأمامي -الساحلي، في حين أن الجودة المنخفضة تُظهر متوسط إجمالي المسامية الكلية لقطع العينات الصخرية الإسطوانية 7% و متوسط نفاذية 2 مل د. (md) ، حيث يرتبط مع سحنات الحجر الرملي للقنوات النهرية،

و منخفضة جدا من حيث متوسط المسامية الكلية لقطع العينات الصخرية الإسطوانية ويمثل 2٪ ومتوسط نفاذية 0.025 مل د. (md) و التي تميز سحنات الحجر الرملي السلتي للجزء الخلفي للدلتا الأمامية كما ان المسامية الكلية لقطع العينات الصخرية الإسطوانية و التي تمثل 14٪، ونفاذية 12 مل د. (md) تكون مرتبطة بسحنات الحجر الرملي البحري المعدلة و المعاد ترسيبها.

بشكل عام ، تشير النتائج التي تم الحصول عليها في تقييم جودة المكنن بأن هناك بعض العمليات الطبيعية و اللاحقة للترسيب مرتبطة بنوع السحنات و الحجر الرملي المكنني و التي قد تؤثر في تجمع الهيدروكربونات في التراكيب المدروسة لطبقة ألكاكوس في الإمتياز م ن 100.

يساعد تكامل جميع مكونات التنقيب الجيولوجية ، بما في ذلك هياكل الترسيب والخرائط الطبقيية وأنماط الكائنات الدقيقة وأنسجة الحجر الرملي والتركيب الأولي والعمليات والمنتجات الطبيعية وأنواع المسام ، على توليد بعض الخطوات الأساسية (1-8) لاستخدامها في إنشاء و فهم استراتيجية التنقيب المستقبلية في الامتياز م ن 100.